



THE MORPHOLOGY OF SALT-INDUCED
STRESS-CRAZING AND CRACKING IN POLYAMIDES.

R.P. BURFORD

B.Sc., Hons.

Department of
Chemical Engineering
(Materials Science)

Ph.D. Thesis
September 1975.

I give consent to this copy of my thesis, when deposited in the University Library, being available for loan and photocopying.

Date ..26/8/76.....

Signed

TABLE OF CONTENTS

	<u>Page</u>
SUMMARY	i.
DECLARATION	iii.
ACKNOWLEDGEMENTS	iv.
CHAPTER 1. INTRODUCTION	1.
CHAPTER 2. LITERATURE REVIEW	4.
2.1. Introduction	4.
2.2. Aspects of Crazing in Glassy Polymers	5.
2.2.1. The Initiation of crazes in Glassy Polymers	5.
2.2.2. Craze Growth	12.
2.2.3. Craze Breakdown - Crack Initiation and Growth	15.
2.2.4. Advanced Crack Propagation	20.
2.2.5. Morphology of Crazes in Glassy Polymers	22.
2.3. Theoretical Aspects of Polymer-Salt Interaction	27.
2.3.1. Polymer Properties	28.
2.3.2. Polymer Interactions with Salts and Solvents	34.
2.3.3. Salt-Model Amide Interactions	39.
2.3.4. Evidence for Cation-Polymer Interaction	44.
2.3.5. Summary - Metal Salt-Polymer Interactions	53.
2.4. Environmental Stress Crazing in Glassy Polymers	54.
2.4.1. Agent Penetration into the Polymer	54.
2.4.2. The Mechanism of Initiation of Environmental Crazing	57.
2.4.3. The Mechanics of Environmental Stress Crazing	61.

	<u>Page</u>
CHAPTER 3. MATERIALS AND METHODS	65.
3.1. Materials	65.
3.1.1. Properties of Materials Used	65.
3.1.2. Determination of Viscosity Average Molecular Weight	67.
3.2. Transmission Electron Microscopy Methods	69.
3.2.1. Thin Film Preparation	69.
3.2.2. Straining Experiments with Thin Films	70.
3.2.3. Replication Procedures	72.
3.3. Scanning Electron Microscopy	74.
3.3.1. Specimen Preparation	75.
3.3.2. Operation of the Microscope	76.
3.3.3. Energy Dispersive X-ray Analysis	77.
3.4. Tensile Testing of Polymers	83.
3.4.1. Method Used	83.
3.4.2. Interpretation of Results	84.
3.4.3. Justification for the Test Method Used	85.
CHAPTER 4. THE MORPHOLOGY OF CRAZED NYLONS	88.
4.1. Introduction	88.
4.1.1. The Fracture of Untreated Nylons	89.
4.1.2. The Morphology of Untreated Nylon Fracture Surfaces	94.
4.1.3. Morphology of Stress-Crazed Nylons	101.
4.1.4. Morphology of the Craze Surface ab in Plane AA'B'B	120.
4.2. The Morphology of Crazing in Nylons Induced by Different Agents	129.
4.2.1. Crazing Induced by Aqueous Zinc Chloride Solutions	129.
4.2.2. Crazing Induced by Cobalt Chloride	151.
4.2.3. Stress Crazing Induced by Magnesium Perchlorate	158.
4.2.4. Stress Crazing and Cracking Induced by Lithium Salts	173.

	<u>Page</u>
4.2.4.1. Crazing Induced by Lithium Bromide	173.
4.2.4.2. Crazing Induced in Nylons by Lithium Iodide	187.
4.2.4.3. The Effect of Solvent Upon Stress- Crazing Activity of Lithium Iodide in Nylons - Morphological Aspects	194.
4.2.5. The Effect of Water Content and Annealing of Nylon 6 upon Stress Crazing	202.
4.3. Transmission Electron Microscopy of Nylons Strained in the Absence of Stress-Crazing Nylons	215.
4.3.1. Direct Observation of Thin Films	216.
4.3.2. Observation of Thin Film Using Replicas	218.
4.3.3. Studies of Thick (>10 μ m) Nylon Samples, using Replicas	224.
 CHAPTER 5. MECHANICAL AND CHEMICAL ASPECTS OF ENVIRONMENTAL STRESS CRAZING	 230.
5.1. Mechanical Testing of Polymers	230.
5.1.1. Effect of Water and Salt Content Upon the Properties of Nylon 6 - Equilibrium Studies	230.
5.1.2.1. Comparison of Mechanical Behaviour of Nylons Stressed with Type I and II Salts	233.
5.1.2.2. The Effect of Water Content in Nylon 66 Upon Stress-Crazing	233.
5.1.2.3. Influence of Strain Rate Upon Stress-Crazing	
5.1.3. Influence of Solvent Type Upon Stress- Crazing Activity	237.
5.1.4. Stress-Crazing Activity of Metal Salts with Polar Polymers	240.
5.2. Chemical Analysis using Energy-Dispersive Nylon Films	251.
5.2.1. Energy Dispersive X-ray Analysis of Unstressed Nylon-Films	251.
5.2.2. The Distribution of Cations in Stress- Crazed Nylons	257.

	<u>Page</u>
5.3. Solution Studies	268.
5.3.1. The Influence of Salts Upon the Solution Viscosity of Polyamides	268.
5.3.2. Changes in the Nature of Chelates in the Coordination Shell of Cobalt Salts	272.
 CHAPTER 6. DISCUSSION	 275.
6.1. The Morphology of Agent-Induced Crazes in Polyamides	275.
6.2. Chemical Mechanism of Salt-Induced Crazing in Polyamides	287.
6.2.1. Polymer Properties	288.
6.2.2. Sorption Mechanisms	289.
6.2.3. Salt Solvent-Polymer Interactions	292.
 CHAPTER 7. SUGGESTIONS FOR FURTHER WORK	 296.
 BIBLIOGRAPHY.	

SUMMARY

The morphology of crazes induced in polyamides by salt solutions has been investigated by scanning and transmission electron microscopy. In general they resemble crazes found in glassy polymers but differ mainly in scale.

A mechanism for craze formation in polyamides was deduced from analysis of the fracture surface of spontaneously ruptured specimens. When a variety of stress-crazing agents were used it was found that two craze patterns emerged. Salts including lithium halides and magnesium perchlorate, which are known [4] to associate with amide groups using an interposed solvent molecule, produced crazes and fracture surfaces which differed from those caused by salts capable of direct cation-amide bonds (zinc and cobalt halides). Energy-dispersive X-ray analysis substantiated the existence of two types of craze mechanism.

The effects of changing experimental conditions (for example, salt and solvent identity, applied strain rate and physical state of the polymer itself) upon the morphology and mechanism of craze formation and breakdown were investigated. Conditions which favor rapid uptake of the agent into the polymer can be correlated with prominent craze and crack production.

It is now recognised that environmental stress crazing can occur in both polar semicrystalline and amorphous polymers. The disruption by salts of hydrogen bond

"crosslinks" in polyamides results in facilitating polymer flow. Under appropriate stress conditions, craze initiation results. It can be implied from this study that most polymers will, under suitable conditions, be susceptible to environmental stress crazing.

DECLARATION

To the author's knowledge and belief, the material in this thesis, except where due reference is made or where common knowledge is assumed, is original. No part of this work has been submitted for any other degree or award in any university.

R.P. BURFORD.

ACKNOWLEDGEMENTS

I wish to thank my supervisor, Dr. D.R.G. Williams, for his assistance and advice during the course of this work.

I would also like to thank my colleagues in the Materials Science Group at the University of Adelaide, in particular Dr. G. Wood and Mr. H. Bartsch, who offered every encouragement.

The work was carried out with the assistance of a University Research Grant.

CHAPTER 1.INTRODUCTION

Crazing has only been accepted as a significant and distinct form of deformation in the last two decades. The importance of crazing, however, has been reflected in recent years by the vast output of literature, which has considered many aspects in glassy polymers. Without doubt, further progress will be made, especially in explaining the effects of orientation, temperature and strain rate upon crazing in glassy polymers. However, the ultimate goal of providing a universal molecular description of craze initiation, growth and breakdown may not be achieved for some time.

The mechanism of Gent [1,2] explains many aspects of crazing and sums up what is currently understood by crazing in glassy polymers. In essence, stress-induced crazing occurs by the transformation of a small region at a tip of a chance flaw from a glassy to a soft rubbery state under the influence of a large local, dilatant stress, followed by cavitation of the transformed material. If the material at the tip region undergoes very large deformations before softening, then a transition to ductile yielding occurs. The theory has been able to predict the magnitude of tensile stress at which crazing occurs and the effect of external pressure, and can account for the dimensions of crazes, the physical characteristics of the craze matter, and the effect of loading upon the crazing process.

However, there is still some uncertainty about certain aspects of the craze process. In particular, the fracture mechanics approach which is attractive because it can offer

the possibility of measuring parameters which influence craze development, have not been totally successful; the complex relationships between intrinsic physical properties of the polymer, and the local stress, conditions which arise at the craze tip, for example, have not been fully solved. In contrast the morphology of crazes from which the greatest contribution has undoubtedly come from Kambour, is now well understood for glassy polymers.

It has been further realised that crazing was becoming the limiting criterion for the use of plastics under conditions of high stress and active environments, and so it was considered valuable to investigate the mechanism of craze initiation and development.

The discovery and substantiation of "stress-cracking" in polyamides caused by a large number of salt solutions (reported by Dunn and Sansom [3-6]) appeared to be related to environment stress-crazing in glassy polymers. The work described in this thesis has as one of its aims, to show that crazing is a significant deformation mode in polyamides under particular conditions.

The strength of secondary bonding between chains largely determines the resistance to flow in polymers. In polyamides, hydrogen bonding is the major component of the inter-chain forces, and so its disruption will greatly weaken the polymer. The complex chemical interactions between polyamides, salts and solvents such as water has been reviewed, because a knowledge of them is vital if an understanding of the fundamental mechanism of crazing is to be achieved.

Because the morphology of crazes in glassy polymers has been so well ascertained in glassy polymers, it was considered the logical criterion for verifying crazing in polyamides. The scanning electron microscope offered many advantages over other instruments for examining crazes in polyamides and so was extensively used. The morphology of crazes in polyamides is described in detail in Chapter 4 of this work.

The energy dispersive X-ray analyser presented a method of directly correlating the distribution of the stress-crazing agent with the morphology of the crazed nylon. This promised to be a valuable aid in assisting the formulation of a crazing mechanism, as the role of agent in determining the physical property of the polymer was considered to be fundamental. Further chemical evidence was also sought to supplement the X-ray analysis.

CHAPTER 2.LITERATURE REVIEW2.1. Introduction

Stress-crazing in nylons by salt solutions has been studied with particular emphasis upon characterising the morphology of crazes which are produced under a variety of conditions, and upon examining the nature of the chemical interactions which promote crazing.

In glassy polymers crazing has been extensively investigated whereas in crystalline polymers it has only recently been recognised. Consequently, the first section of the review (2.2) deals with aspects of crazing in glassy polymers which may be relevant to that which occurs in nylons.

The nature of chemical interactions between salts and amides, both in small model compounds and in polymers, is reviewed in section 2.3. An attempt has been made to indicate how significant secondary forces are in determining the mechanical properties of polymers, and how molecules and ions are able to disrupt them, weakening the polymer. Interactions between cations and amide functional groups in synthetic polyamides (nylons) and biologically important polyamino acids (proteins) are outlined.

In the last section (2.4) environmental stress crazing in glassy polymers is briefly reviewed. It is considered that this would be a basis upon which stress-crazing in nylons could be compared. A better understanding of the mechanism of stress-crazing in nylons could then be gained by analysing the differences and similarities between the two phenomena.

2.2. Aspects of Crazeing in Glassy Polymers

This section reviews the progress made in understanding how glassy polymers fail under tension, in particular, by craze formation and breakdown (with coincident fracture). It is in five parts.

The first outlines some of the theories of craze initiation. The approach taken by most workers is to define the conditions under which crazes initiate, without reference to the molecular processes involved.

The development of crazes is then discussed in section 2.2.2. In particular, the kinetics of lineal growth in crazes is described, as this subject has been extensively investigated.

Craze breakdown (or crack initiation) and crack propagation are the subjects of the next two parts (2.2.3 and 2.2.4). The growth of cracks within and outside the pre-crazed regions is mentioned, and the conditions for which crack initiation arises are outlined. The advanced stages of crack propagation are discussed and some of the problems which are not properly resolved are given.

In the last section (2.2.5) the morphology of crazes in glassy polymers is briefly reviewed.

2.2.1. The Initiation of Crazes in Glassy Polymers

The approach taken by most researchers when developing theories for craze initiation is to determine either the conditions under which crazes form, or to deduce from the geometry of the crazes what type of mechanism was responsible. The theories described below have variously used strain and strain energy, or stress or shear yield

criteria. At the present time there is no concensus of opinion, and in any event, Kambour states [7] that in most cases a critical stress may be interchangeably defined with a critical strain in terms of an elastic modulus. Molecular theories of craze initiation are predictably absent; the present crude models of the structure of amorphous solids (entailing "chain end" and "loop" levels, etc.) lack credibility. As a first step towards the ultimate goal of a universally applicable molecular model, the experimental difficulties which exist in resolving the molecular structure of amorphous polymers need to be overcome.

Haward [8] has estimated the hydrostatic stress required to nucleate a cavity in a polymeric liquid and has found it to be much lower than the bulk yield and crazing stresses, at temperatures well under the glass transition temperature. For an elastic-plastic solid, a cavity with radius r is in equilibrium with a hydrostatic tension p , as given by

$$p = \frac{2\sigma_y}{3} \left(\ln \frac{E}{3\sigma_y(1-\delta)} \right) + \frac{2\alpha}{r}$$

where σ_y = yield stress

δ = Poisson's ratio

α = interfacial tension of the void

E = elastic modulus.

The first term represents the stress necessary to expand the void against the resistance to plastic flow, and depends upon solvent content and temperature. It appears

that if cavitation proceeded from a single void, and p represents the hydrostatic cavitation stress, then the necessary condition for initiation,

$$p < \sigma_y$$

would not be met. By suggesting cooperative nucleation at a number of voids occurs, Haward explains how this predicament can be overcome [8a].

Andrews and Bevan [9], use a similar theory in explaining craze initiation in solvent crazing. The stress-dilated tip region in this instance is swollen by the solvent, so that σ_y at the tip is lower than σ_y of the bulk polymer, and now $p < \sigma_y$ (bulk). They were able to combine the cavitation theory of Haward with the equations for the surface work of craze formation, and obtained good correlation with experimental results.

The theory of Gent [1,2] proposes that a critical stress at the tip of a chance nick or flaw is required to bring about a "glass-to-rubber" transition. This transition is considered equivalent to the normal glass to rubber transition, which takes place at a stress-dependent transition temperature $T(D)$; $T(D)$ reaches the test-temperature at a critical dilatant stress, D_c . The molecular model is that molecular motion becomes possible when the free volume increase (from the dilatant stress) exceeds a critical value. The critical dilatant stress is given by Ferry [132], when the free volume is increased by volume expansion in excess of that characteristic of the glassy state only, by

$$D_c = (T_g - T) (\alpha_r - \alpha_g) (C_r - C_g)$$

where α_r , α_g are the coefficients of thermal expansion in the rubbery and glassy states, and C_r , C_g are the corresponding compressibilities.

By observing that the hydrostatic pressure has a lineal dependence upon the glass transition temperature [2], Gent obtains an equation relating the tensile stress needed for development of a thin band of softened material;

$$\sigma_c = [\beta (T_g - T) + P] / k$$

where σ_c = critical value of the applied tensile stress
 β = a coefficient related to the pressure dependence of T_g
 T_g = glass transition temperature
 T = test temperature
 k = stress intensity factor at the flaw.

When the local stress at the flaw tip is maintained at $\bar{\sigma}_c$, the transformation of more polymer from the glassy to the rubbery state will occur, but when σ_c is sufficiently high to cause deformation of the glassy polymer ($\approx E/3$) then the craze matter can no longer be considered to be restrained between two rigid regions, so that the dilatant stress is no longer enhanced at the tip. Under these conditions general plastic yielding occurs. The critical glassy-to-rubbery transition described above, is a step in the total sequence of craze development, which Gent proposes to be:

- (a) production of a large dilatant stress at a chance nick or flaw
- (b) transition from a glassy to a soft rubbery state
- and (c) cavitation of the transformed material.

The effect of both compatible and incompatible stress crazing agents is then discussed. Compatible liquids cause swelling in the absence of stress, and the degree of swelling increases with dilatant stress [10]. The glass transition temperature is effectively reduced, and so the value of $\bar{\sigma}_c$ is lowered. Of interest is the finding that the swelling ability of incompatible liquids is greatly enhanced by dilatant stress; and so material at a flaw tip will selectively undergo softening. The crazing mechanism is able to account for the powerful stress-induced crazing effect of weakly swelling liquids.

Experiments using poly (methyl methacrylate) (PMMA) under biaxial stress conditions have enabled Sternstein et al [11] and Bowden and Oxborough [12] to develop craze initiation criteria in terms of a stress bias. Sternstein showed that a finite hydrostatic tensile stress was required; Bowden and Oxborough developed the equation for initiation.

$$\sigma_1 - \nu\sigma_2 = \frac{A}{\sigma_1 + \sigma_2} + B$$

where ν = Poissons ratio

A = temperature dependent constant

B = a time and temperature dependent constant

σ_1, σ_2 = major, minor principal stress, respectively

and $\sigma_1 - \sigma_2$ = stress bias

When

$$E\epsilon_c = \sigma_1 - \nu\sigma_2 \text{ is true,}$$

then a strain criterion for crazing,

$$\epsilon_c = A'/P + B'$$

can be proposed.

P is the hydrostatic tension, and A', B' are dependent upon the environment. The dependency of craze initiation upon stress is not clear in this theory, although it is known that the first stress invariant, I (the sum of the three major stresses) needs to be greater than zero. There may also be a critical value of the major principal tensile stress for craze initiation to arise.

A "two-dimensional equilibrium model" is used by Knight [13] to explain stress-crazing in thermoplastics. It is based on a number of assumptions; stresses must remain finite because linear mechanics equations have been used, and significantly, it is assumed that all stresses at the craze surface are perpendicular to the long axis of the craze (a condition which clearly fails at or near the craze tip). The non-normal stresses which are required at the craze tip are ignored. Internal and external stress distributions are determined for the model, which assumes that craze matter comprises "tenacious elongated fibrils". When the fibrils of the craze material are elongated, "orientation hardening" causes stress intensification to occur at the craze bulk interface, preventing general elongation; instead crazes propagate.

In this paper, Knight admits that no allowance has been made for stress or temperature criteria for the size of crazes, and whilst the assumptions used cannot be ignored, the concept of orientation hardening as a process which promotes craze growth rather than normal yielding is valuable.

More recently, Knight [14] has attempted to relate molecular structure with fracture toughness in polymers. It is considered that the initiation of a "craze-fracture" (the formation of a craze, followed by rupture of the low-density craze material) is related to the "stress-deformation function" of the material. The paper appears to be a preliminary attempt to correlate brittle ductile behaviour with stress-deformation parameters, taking into account the reality of craze formation before fracture. It is unsubstantiated by a thorough mathematical analysis.

A very different approach has been used by Matsuo and coworkers [15,16]. They have embedded soft and hard balls into a polystyrene matrix, and have studied the effect of altering the distance between balls upon stress crazing. With rubber balls, crazing initiates at the equator (predicted by all theories), but when steel balls were used, crazing developed at an angle of 37° from the applied stress direction, suggesting that a maximum strain or maximum strain energy is the correct criteria to use (dilatation proposes maxima at 0° , principal stress at 25° and shear stress at 44°). The later paper [16] shows how by using different spacings, the correct criteria is maximum strain. The dilatation mechanisms of Gent [1,2] and Kambour [17] are therefore rather suspect, although the evidence of Matsuo

requires further verification, particularly in the absence of molding artifacts (orientation, stresses etc.).

Clearly there remains a great deal of controversy about the mechanism of craze initiation. Ultimately, the relevance of "inherent flaws", the real criteria for crazing, and the fundamental reasons for crazes to exist at all, may only be known when the molecular structure is more clearly defined. One should be aware, however, that when metallurgists who wished to determine the mechanism of fracture in metals expended large amounts of effort into developing an atomic-level understanding, they met with little success. (The breakthrough came instead from a continuum approach where the stress field was recognised as the important parameter.)

2.2.2. Craze Growth

Crazes enlarge by simultaneous areal development and thickening.

Thickening of Crazes

This aspect is experimentally more difficult to study and the kinetics have not been thoroughly investigated.

Thickening may occur in any of three ways:

- (a) in the early stages transformation of bulk material above and below the craze to craze matter,
- (b) viscous drawing of the craze substance
- and (c) viscoelastic deformation of craze filaments [2].

In glassy polymers with no hostile environment, Kambour [18] considers that crazes thicken by extension of craze material already present. Only near the craze tip is new craze matter created. The interface between the craze zone

and the bulk polymer is very narrow, suggesting that the transformation from bulk polymer to filaments is sudden.

When long filaments are seen in environmentally stress crazed polymers, for example, it appears that flow must continue from the bulk polymer into the craze region. A "vaulted arch" configuration at the interface, associated with lateral tensile components (which may assist void formation) is proposed [19].

Kinetics of Craze Growth

No adequate experiments have been documented which correlate areal craze growth with time or temperature. The kinetic studies of craze elongation under restricted test conditions (discussed below) are of limited usefulness, because quantitative analysis is complicated by an ever-changing stress-field at the leading edge of the craze.

Regel [20] found two elongation rates when he measured craze growth versus the applied body stress of polystyrene at room temperature. Whilst the first rate was immeasurably fast, the second rate was slow and constant. It was later shown that shear band arrest competed with craze growth in the second stage. Ultimately, craze growth decelerates because of homogeneous creep near the craze tip. When conditions near the craze tip favor normal ductile yielding craze growth ceases.

Higuchi [21] found with PMMA and a constant strain rate that the length of the craze increased linearly with increased log strain rate,

$$\text{i.e.} \quad \frac{d(c)}{dt} = \beta \dot{\epsilon}$$

where $\dot{\epsilon}$ is the strain rate normal to the growth plane of the craze and β is a constant.

This equation allows for the observation that with increasing strain rate, the density of crazes at fracture increased. The dependence of both craze initiation and growth on temperature and strain rate needs to be known so that craze density can be predicted. Apparently initiation is more sensitive to strain rate than is craze growth).

Sternstein and Sims [22] conducted experiments under very different conditions. When straining a prenotched PMMA test-piece in ethanol-water mixtures, they measured environmental stress crazing with a second growth rate faster than the first. They include the commonly observed induction time, t_0 , in the equation for constant load conditions,

$$l_c = K \log \left(\frac{t}{t_0} \right)$$

where l_c is the craze length
 t is the elapsed time
 and K is a rate constant.

When the stress is increased, both K and t_0 decrease exponentially.

The changing molecular conditions at the craze tip as growth proceeds is acknowledged by Knight [13]. As elapsed time increases, molecular orientation (and so craze tip

blunting) inhibits areal craze growth. This bulk flow has a greater temperature dependence than has craze growth, so that lower temperatures favor long, thin crazes and high areal growth rates. At high temperatures, areal growth is slower, and the tip is blunter. Consequently, thick, short crazes usually form.

2.2.3. Craze Breakdown - Crack Initiation and Growth

When a craze in a polymer is no longer stable, because either it has become so thick that the elongated craze matter finally fractures, or the mechanical properties of the craze matter have become adversely affected by the environment, then crack initiation and propagation occur. The two processes, craze breakdown and crack initiation, are one and the same thing. Only at cryogenic temperatures can true brittle fracture, the formation of two fresh surfaces without plastic deformation, occur [23]. The following aspects of craze breakdown will be discussed:

- (a) the conditions for crack initiation
- (b) the growth of cracks within crazes,
- and (c) the propagation of cracks beyond precrazed regions.

Craze Breakdown - Crack Initiation

Most theories which apply to craze breakdown are unsubstantiated in molecular terms, because the micromorphology is not known. The practical difficulties of observing such rapid changes have yet to be overcome.

Murray and Hull [24,27] have proposed the sequence: craze thickening, with small void regions developing about relatively macroscopic heterogeneities, enlarging and finally coalescing to form a cavity within the craze. At

a critical stage the cavity develops into a crack which moves through the centre of and parallel to the craze material; cavities which form in front of the crack merge into it as the crack grows.

Four types of molecular processes are implicated in craze breakdown and crack propagation [28,29]. They are the formation of cavities, plastic flow, viscoelastic breakdown, and molecular rupture. Viscoelastic breakdown requires the most energy, whereas rupture has only a small requirement [30].

Conjecture exists about the nature and importance of "inherent flaws". If a very small flaw is able to initiate fracture, then it is expected that every crazed material would be very susceptible to cracking, and would superficially fracture at low elongations. If large flaws are required for crack initiation, then foreign inclusions or other macroscopic heterogeneities may be necessary before craze breakdown will occur. While it might be possible that the ultimate strength of the material is limited by intrinsic flaws, which can develop into plastic and viscoelastic flaws, the estimation of strength and energy requirements to propagate cracks using intrinsic flaw theories is beset with problems.

Growth of Cracks in Precrazed Material

When the work required to fracture a glassy polymer is measured, it is found to be greater than would be expected just to form two new surfaces, but less than that needed to sever every bond which initially passed through the fracture plane. It is now accepted that a crack passing through a polymer is preceded by a zone of crazed material, so that

much of the surface work is consumed in the formation and disformation of craze matter. When it is assumed that a large craze already exists, it is possible to adapt crack growth theories to allow for the presence of the craze. Growth of a small crack in a large craze is much easier than in a small craze, because not only is the craze matter already extended in the large craze, but no new craze material needs to be created [31,32].

The model for a crack is modified by incorporating a craze zone, which is shown in Fig. 2.1 [33,34], where the length of the crack is $2a$ and that of the craze is $2a_p$.

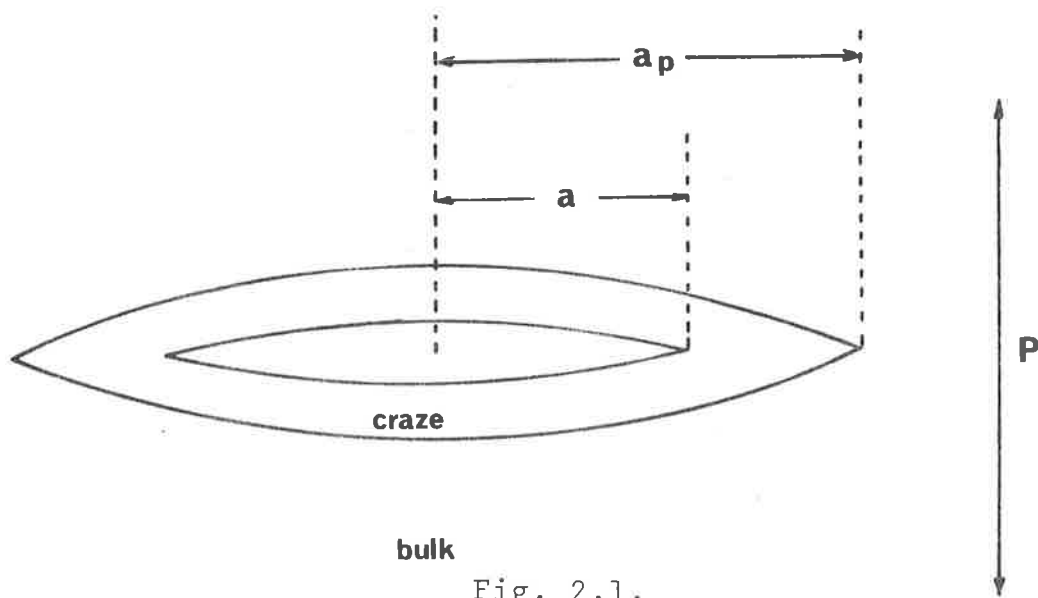


Fig. 2.1.

When uniaxial stress p is applied and the yield stress is p_y , then the values of a and a_p are related by the equation

$$\frac{p}{p_y} = \frac{2}{\sigma_y} \cos^{-1} \frac{a}{a_p}$$

It can be shown that under adiabatic conditions, a craze of constant thickness should proceed a running crack.

By analogy with fracture theory in metals, a criterion for fracture which may be used is the critical crack opening displacement δ_c is a measure of the separation of the fracture faces at the tip of a crack; if σ exceeds a certain value, then the crack grows. It is defined by the equation

$$\delta_c = \frac{K^2}{\rho_y E}$$

where K is the stress intensity factor
and E is Young's Modulus.

A linear fracture mechanics approach can be used [35] if it is assumed that test temperatures are much less than the glass transition (T_g), and that only low stresses are applied. For fracture to occur, the crack must be above a critical length, C_0 , for each set of test conditions. If a crack pre-exists, then propagation will occur only if δ is above a critical value, or if the stress intensity factor, K_I , existing at the tip, is above the critical value, K_{IC} . For fracture mechanics to be used it is necessary to assume that the "energy losing zone" about the craze tip is small compared with the overall crack length (not valid for a small crack in a large craze). The elastic non-linearity of glassy polymers also casts some doubt upon the validity of these criteria.

Another theory which has been adapted from "brittle solid" studies is the energy balance approach [36]. When the strain energy released by the body is greater than or equal to the energy required to cause crack extension, a crack propagates.

i.e.
$$-\frac{\partial \epsilon}{\partial A} \geq \tau$$

where A is the interfacial area of the crack,
and ϵ is the total elastic energy.

The surface work, τ , in glassy polymers, is always much greater than the true surface energy, because of plastic deformation at the tip, and viscoelastic extension of craze material. Kambour [14,20] has calculated that the contribution made to the total surface work are:

surface energy of the holes in the craze	1.5%
plastic work in craze formation	16%
viscoelastic extension of craze matter → rupture	82.5%

At low temperatures, the crack is initiated at the surface step and passes through only a very thin craze zone; very little viscoelastic deformation occurs, so that the surface work is much closer to the true surface energy [37].

Other theories have been proposed which rely on two assumptions; that no new craze matter is created during crack growth in the craze, and that all work done is viscoelastic in nature, even at low elongations [38]. These restrict the theories to particular situations only, such as early crack growth in a large, mature craze.

2.2.4. Advanced Crack Propagation

The transition from a crack growing within a preformed craze to one continuing to grow beyond the craze is accompanied by a change in the morphology of the craze layer seen on the fracture surface. This is the result of a transition from rupture of well-developed craze filaments, to rupture of the very restricted craze which precedes the crack. Craze formation in front of a crack with high velocity is particularly hindered. Other complications such as secondary crack initiation, make analysis of fracture surfaces complicated; some of the different phenomena which may arise, with their effect upon the fracture surface morphology, are described below.

Cracks enlarge slowly at first, through the midplane of the craze [32]. As the velocity increases, fracture may occur along the craze-bulk polymer interface [24], until at very high velocities the crack can oscillate from one interface to the other [25,39], or jump over to a secondary craze [40,41]. In nylons, electron microscopy has revealed "sub-microcracks" in strained filaments, which may interact with the main crack front [42].

When the craze matter is highly elongated, crack propagation is relatively slow; as the crack proceeds through a narrow crazed zone, or into initially uncrazed polymer, the crack velocity increases. The extent of craze development when slow crack growth changes to crack propagation is determined by the viscoelastic deformation dependence upon molecular weight and other material properties [43].

When a crack passes through a polymer, with localised crazing occurring in front of the crack tip, the stress

intensification may be sufficiently high to enable crazing to initiate above and below the main crack trajectory [40]. This "secondary craze formation" often occurs when craze initiation is favored over craze deformation (for example, in high molecular weight polymers, or at low test temperatures). When the crack velocity is high, "craze jumping" can occur [44,45]. It is possible to determine an optimum crack velocity for minimal secondary craze formation.

At room temperature, the craze area in polystyrene is large before cavitation to initiate a crack begins. Consequently slow crack growth occurs through precrazed material [26], and so "patchy" surfaces are produced by secondary fracture as described by Murray and Hull [24]. When slow crack growth involves generation of new craze matter (as occurs in PMMA at room temperature) a smooth surface is produced.

The residual craze layer on the fracture surface has been shown using a variety of methods [28, 46-49] to be similar in nature to whole craze matter. For example, polystyrene has craze filaments between 0.01 and 0.05 μm in diameter [50-52] and from 0.1 to 2.8 μm long [53]. The stability of such filaments depends upon the polymer type, the temperature and the nature of the environment.

At low temperatures, the crack always initiates at the surface of the specimen although it is difficult to discern a heterogeneity at the origin. There appears to be no slow-growth stage, because viscoelastic deformation is inhibited. Stresses associated with the surface steps are considered to cause crack initiation [16,37,54].

Three aspects of advanced failure in polymers are poorly understood. First, the influence of flaws and orientation upon secondary crazing and fracture is not known; second, how the crack velocity and strain rate changes the fracture morphology has not yet been precisely determined, and finally, no qualitative work has been carried out on semibrittle (low temperature) fracture in glassy polymers.

2.2.5. Morphology of Crazes in Glassy Polymers

The morphology of crazes in glassy polymers is relatively well known and has been extensively reviewed by Rabinowitz and Beardmore [31] and Kambour [55]. The more important features of crazes in glassy polymers will be discussed with the thought in mind that any differences or similarities between crazing in semicrystalline polymers will help in the elucidation of environmental stress crazing.

Crazes in most materials resemble cracks in that they are narrow zones caused by heterogeneous strain behaviour. The material within the zone has different physical properties from the surrounding polymer. For example, crazes have different refractive indices which make them discernable in transparent polymers. The major observable difference between cracks and crazes is that the crazes are filled with highly voided and elongated matter which still has a load-bearing capacity [56,57]. In isotropic polymers, crazes elongate at right angles to the major principal stress axis. The initiation of crazing, and the transition from uncrazed to crazed polymer is poorly understood; some current theories will be discussed in a subsequent section. The structure of plastically deformed polymer within the craze is, however, well characterised, and appears to be similar for

all glassy polymers over a wide range of conditions.

An indication of the geometry of a craze is shown in Fig. 2.2.

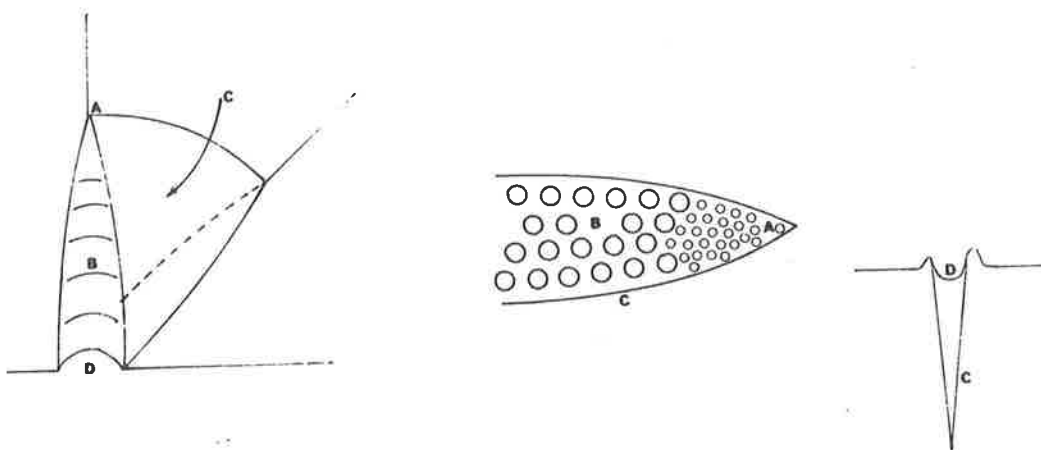


Fig. 2.2.

Each craze comprises nascent craze matter at the tip (A), mature craze material (B), a bulk-polymer-craze interface region (C), and a surface discontinuity (D). A well developed craze may be as thick as $4\mu\text{m}$ and have an area of about 10^2 mm^2 .

Tip Region (A)

This region is narrow, generally having a thickness of no more than $0.01\mu\text{m}$ [17,58]. The "fresh" craze is sponge-like, with interconnected [17], spherical voids, shown by transmission electron microscopy and X-ray diffraction to also be about $0.01\mu\text{m}$ in diameter. The production of the new craze matter and the uniformity of the voids are both incompletely understood. The angle formed by the

craze walls near the tip is very small (from 2 to 10^0) [7,59]; at a distance of from 10 to 50 times the eventual craze thickness, the sides of the craze are parallel [60].

Craze Matter (B)

Craze matter has been characterised using transmission and scanning electron microscopy, X-ray diffraction and numerous other physical methods [7,17,19,24-26,28,61,62]. The density of the dry craze matter can be determined [17,63] using the Lorenz-Lorenz equation:

$$p = \frac{\eta_c^2 - 1}{\eta_c^2 + 2} \cdot \frac{1}{\rho_c}$$

where p = the specific refraction of the polymer

η_c = the craze refractive index

and ρ_c = the density of the craze

When stresses are low, newly formed crazes have been shown from density measurements to contain 50 to 60% polymer, whereas the fracture surface of polystyrene (after extensive elongation) contains only 35% polymer [18]. The factors which determine the coarseness of the craze matter are not known. Transmission electron microscopy of a variety of amorphous polymers has revealed that the void diameter of mature craze material is about 0.02 μm , at low elongation [e.g. 7,17,19,61,63]. Although the polymer within the craze zone may be strain-hardened and so have a higher true modulus than the unoriented bulk polymer, when the large void content is taken into account, the craze is compliant,

as shown in Fig. 2.3 [29,44].

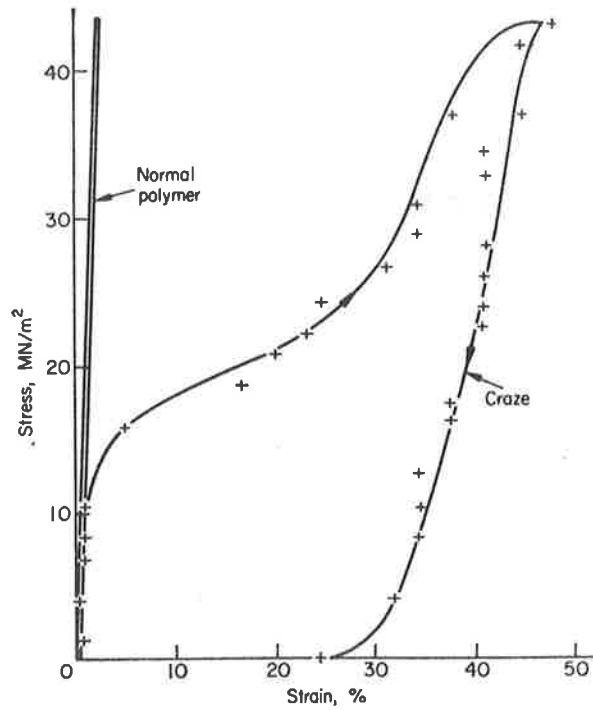


Fig. 2.3.

At large elongations, Beahan and coworkers [64] have observed the microstructure of crazes in solvent-cast and bulk polystyrene. Five fibril structures can be seen and they propose that craze development occurs as shown in Fig. 2.4.

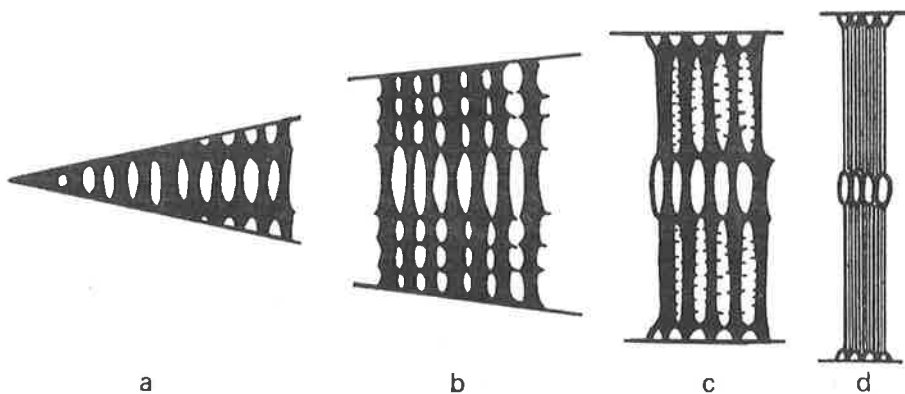


Fig. 2.4.

The transition from crazed to uncrazed polymer is always found to be abrupt. The interface (C) is considered to be no thicker than $0.002 \mu\text{m}$ [69]; further progress is restricted by the resolution limit of replicas and scanning electron microscopy. The thin sections used in transmission electron microscopy give no three-dimensional information about the structure of the interface.

Surface Discontinuities (D)

Crazes initiate at the surface of a specimen, unless a suppression agent is present [65]. As the craze grows, surface discontinuities (D) develop. They may exist as lips of uneven height [66], which are associated with crazing under most conditions, or as sharp steps which form when narrow crazes are produced at low temperatures [67]. Each type is represented in Fig. 2.5.

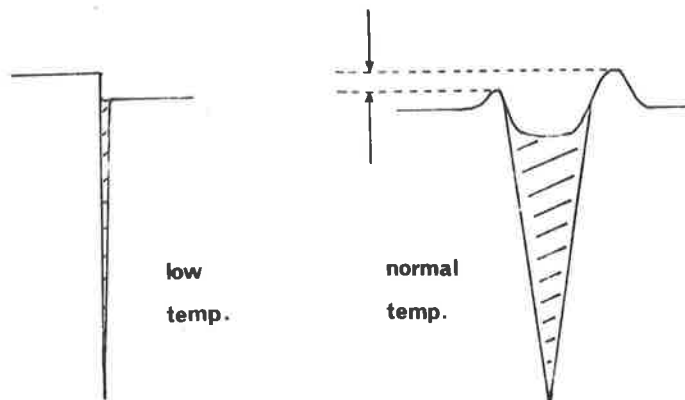


Fig. 2.5.

The edge groove results from constrained Poisson contraction as the material within the craze extends [28]; the size of the surface discontinuity can give an indication of the size of the craze [18]. The step seen at low temperatures may behave as a stress-intensifying notch, which can

promote crack growth in the thin craze [37,68]; this explains why craze matter only experiences low elongation before fracture. It is not understood why the heights of the lips are unequal, nor why step production occurs.

2.3. Theoretical Aspects of Polymer-Salt Interaction

The approach adopted in this part of the review is outlined below.

Stress-crazing in polyamides is a consequence of the weakening of secondary forces between adjacent polymer chains. It is important to recognize the forces which exist before treatment, and to be aware of the ways in which salts and solvents may interfere with the secondary forces.

The physical properties of polyamide and related polymers is outlined first, as a knowledge of them is fundamental to the comprehension of their behaviour in a hostile environment. In particular, synthetic polyamides and polyamino acids have been selected as being representative of two classes of polymer having a similar primary structure (in that both have amide groups), but different secondary structure.

In addition, much interest has centred around the latter group, because of their biological significance, with the advantage that many studies of cation-polyamino acid interactions have been reported.

Some of the theoretical aspects of polymer - small molecule interactions are then discussed. The factors which determine whether a solvent is taken up by a polymer, and the types of interactions which may occur between salt, solvent and polymer, are given. Predictions are made about

the conditions which would favor uptake of salts and solvents into the polymer.

The next section examines more closely the evidence for amide - salt interaction which is provided by model compound studies. The experiments cited have repercussions for both synthetic and biological polyamides. The results are often less complicated than those obtained for macromolecules, but can be applied to polymers, if the additional influence of the size of the polymer is acknowledged.

Finally, review of the literature describing interactions between polyamide-type polymers and a variety of salts, both anhydrous and in solution is given. These results have particular relevance to the stress-crazing of polyamides which is to be described at length in the remainder of the thesis.

2.3.1. Polymer Properties

Polymers which are strongly affected by salts and salt solutions are those in which the polymer molecules are attracted together by polar secondary forces. In other words, ion-dipole, dipole-dipole and hydrogen bonding forces are those most affected by highly polar or ionic environments. A list of some polymers which can have polar interchain secondary forces is given in Table 2.1. along with the types of secondary forces which are most important for each polymer.

Many of these polymers may have their interchain forces (and consequently their secondary structure) modified when subjected to a highly ionic environment. It will be convenient, however, to discuss the possible interactions

Name	Structure	Secondary Bond Type
Polyamino-acids	$-\text{NH}-\overset{\text{R}}{\text{CH}}-\overset{\text{O}}{\underset{\parallel}{\text{C}}}-\text{NH}-\overset{\text{R}'}{\text{CH}}-\overset{\text{O}}{\underset{\parallel}{\text{C}}}-$	H-bond
Polyamides	$-\text{R}-\left[\text{NH}-\text{CO}-\text{R} \right]_n \text{ or } \left[\text{CO}(\text{CH}_2)_x-\text{CO}-\text{NH}(\text{CH}_2)_y\text{NH} \right]_n$	H-bond
Polyurea	$\left[\text{NH}-\text{R}-\overset{\text{O}}{\underset{\parallel}{\text{C}}}-\text{NH}-\text{R}'-\overset{\text{O}}{\underset{\parallel}{\text{C}}}-\text{NH} \right]_n$	H-bond
Polyurethane	$\left[\overset{\text{O}}{\underset{\parallel}{\text{C}}}-\text{NH}-\text{O}-\text{R}-\text{O}-\overset{\text{O}}{\underset{\parallel}{\text{C}}}-\text{NH}-\text{R}' \right]_n$	H-bond
Polyester	$-\text{R}-\text{O}-\left[\overset{\text{O}}{\parallel} \text{C}-\text{R}'-\overset{\text{O}}{\parallel} \text{C}-\text{O}-\text{R} \right]_n$	dipole-dipole
Polyacrylonitrile	$\left[\text{CH}_2-\overset{\text{CN}}{\text{CH}}-\text{CH}_2-\overset{\text{CN}}{\text{CH}}-\text{CH}_2-\overset{\text{CN}}{\text{CH}} \right]_n$	dipole-dipole
Poly (methyl methacrylate)	$\left[\text{CH}_2-\overset{\text{CH}}{\text{C}}-\text{O}-\text{CH}_3 \right]_n$	dipole-dipole

TABLE 2.1.

between only a few polymers and the environment. Polyamides and polyamino acids (the latter occurring in nature as proteins) have been selected to represent polar polymers, and it is assumed that comments made about them can apply, in general terms, to the other polymers.

Polyamides (or nylons) are a family of synthetic polymers in which non-polar, hydrophobic methylene segments are linked by the amide group, $-NH-CO-$ (polar and hydrophilic). The $-CH_2-$ segments are flexible whilst the amide group potentially has the ability to form hydrogen-bonds with neighbouring chains. The amide groups can therefore be regarded as being able to reduce the flexibility of the chain. Hence the spacing of the amide groups (or the length of the methylene segments) will affect both the overall flexibility and polar nature of the polymer. The effect of increasing the spacing of polar groups upon the crystalline melting point is shown in Fig. 2.6 [69].

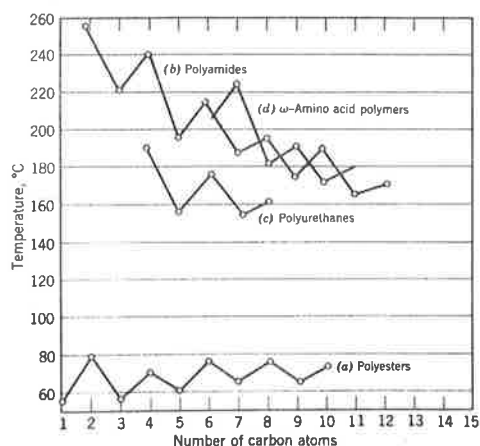


Fig. 2.6.

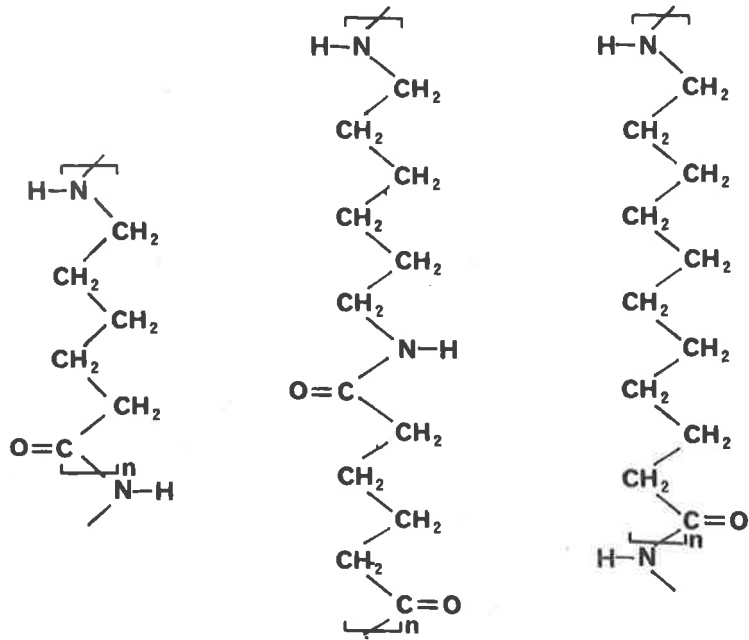
Nylons which have amide groups closely spaced together are able to absorb larger quantities of polar molecules than when the amide groups are wide apart. In the three

commercially important polymers depicted in Fig. 2.7, the spacing of amide groups in nylon 11 is larger than in the other two polyamides, and it is found to absorb smaller quantities of water than nylon 6 or 66.

Some nylons may assume different crystallographic forms. Adjacent chains may in some cases have the same order of appearance of functional groups ("parallel"), or in other cases the order may be reversed in each consecutive chain ("antiparallel") (Fig. 2.8). The potential for hydrogen bonding, and the interchain spacing are affected, and so it is important to distinguish between these forms of nylon.

Within the context of this discussion, the most important facet of nylons is the interchain hydrogen bonding, the geometry and strength of which will be determined by the relative position of adjacent chains. Van der Waal's forces and other non-polar interactions are not relevant to polar-ionic interactions and will not be considered further.

In polyamino acids, there are two important structural differences from nylons. The first is that intramolecular hydrogen bonding occurs, parallel to the molecular "axis" (in nylons interchain bonding perpendicular to the molecular "axis" occurs). A stabilized helical molecule is produced, which is shown diagrammatically in Fig. 2.9 [70].



NYLON 6

NYLON 6.6

NYLON 11

Fig. 2.7.

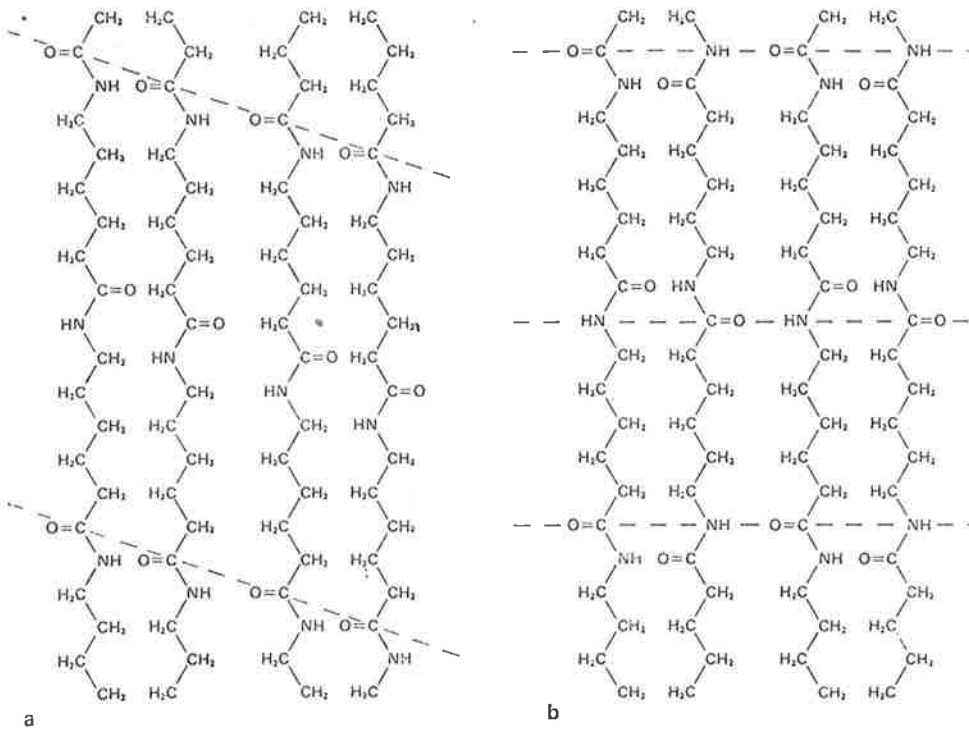


Fig. 2.8.

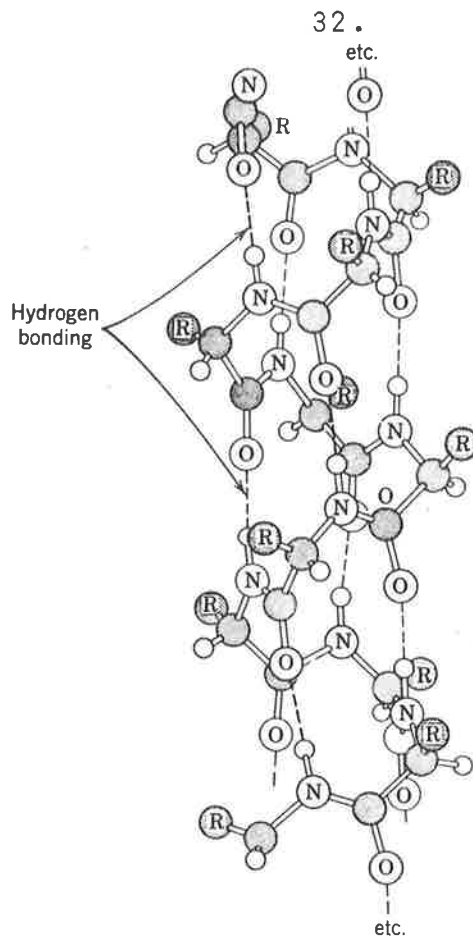


Fig. 2.9.

The other major difference is that the side-groups may be one of twenty or more different structures. In synthetic polyamino-acids, it is usual for one side-group to be repeated along the chain, but in proteins a complex structure is inevitably encountered. Some of the side-groups are highly polar, and so will affect not only the conformation of the protein molecule, but also strongly influence interactions between the protein and its environment. Examples of side-groups encountered in proteins are shown below (Fig. 2.10).

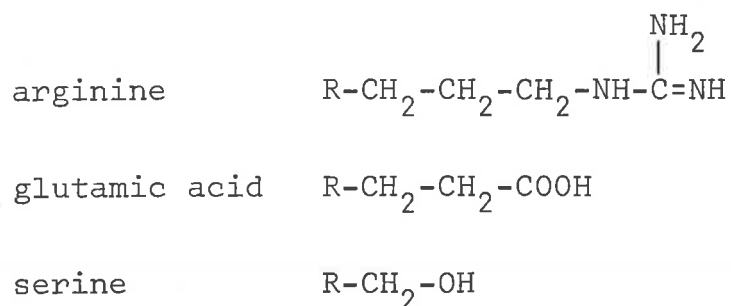


Fig. 2.10.

Most significant is the disruption by salts of hydrogen bonds (similar in both polyamides and polypeptides, with a bond energy of approximately 30KJ/mole and a spacing (x in Fig. 2.11) of 0.295 nm [71].). In polypeptides the hydrogen bonding may be slightly modified when larger sidegroups are attached to adjacent carbon atoms (marked C*).

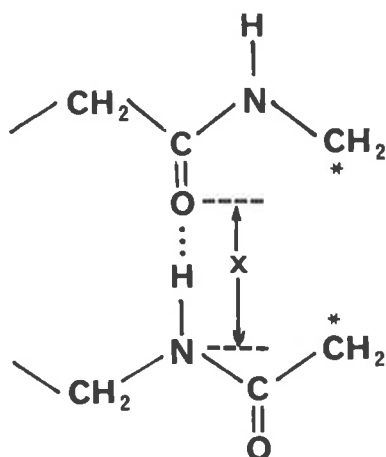


Fig. 2.11.

Strong hydrogen bonding is possible in polyamides because the amide oxygen may readily reduce its bond order. An electron pair on the nitrogen can transfer towards the carbonyl oxygen, so that the tautomer shown in Fig. 2.12 is possible. The atoms -NH-CO- are coplanar, making the delocalisation of the electrons possible.

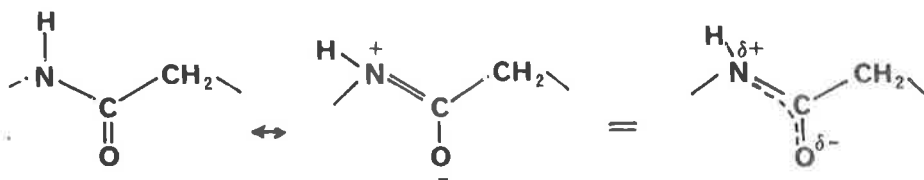


Fig. 2.12.

N-alkylation inhibits hydrogen bonding with the result that only weaker dipole-dipole forces remain; the polymer is less crystalline, and has a reduced melting point and

yield point. (Alkyl groups attached to the nitrogen will also sterically hinder chain alignment and so also be a contributing factor.)

2.3.2. Polymer Interactions with Salts and Solvents

An empirical system has been developed for predicting the compatibility between solvents and polymers, which had originated from work by Hildebrand and Scott [72]. A solubility parameter, δ , which originally was related only to the cohesive forces between molecules, was assigned to each polymer and solvent.

It was then proposed that solvents would interact strongly with polymers having the same δ value, and a solution would result. When small differences of δ existed, the solvent was only capable of swelling the polymer.

The values of solubility parameters for non-polar polymers have generally proven to be satisfactory when interaction with non-polar solvents are considered. Modified solubility parameters which include the effects of polar groups in polymers have however not been satisfactory, indicating that interaction of polar groups is somewhat more complex than that suggested by Hansen [73,74]. The concept of solubility parameters is discussed further in section 2.4.

It can be predicted that small polar molecules capable of penetrating the bulk polymer would be most likely to disrupt hydrogen bonding between polyamide chains. This is confirmed by noting the known solvents and molecules absorbed by nylons shown in Table 2.2.

	NAME	FORMULA
SOLVENTS	m-cresol	$C_6H_4(OH)_2$
	phenol	C_6H_5OH
	formic acid	HCO_2H
	2,3 tetrafluoro- propanol	$CHF_2-CF_2-CH_2-OH$
	Chloral hydrate	$CCl_3-CHO+H_2O$ $\rightleftharpoons CCl_3-CH(OH)_2$
ABSORBED BY NYLON	methyl alcohol	CH_3OH
	water	H_2O
	other aliphatic alcohols	$R-CH_2OH$
	methyl cyanide	CH_3CN
	benzyl alcohol	$C_6H_5CH_2OH$

Table 2.2.

Molecules absorbed by nylons.

All the liquids listed are capable of interfering with hydrogen bonding. In addition, the solvents for polyamides have a deshielded proton, resulting from electron withdrawal away from the O-H bond. The enhancement in the acidity of this hydrogen enables each of these compounds to dissolve the polymer.

Small protic molecules including water and methyl alcohol are absorbed into the polyamide matrix when the length of the hydrophobic methylene segments in the chain is small (for example, in nylon 6 or 66). Hydrogen bonding can occur between the solvent molecules and polyamides, as shown in Fig. 2.13 (alcohols may only hydrogen bond as in A and not as in B, because they are not diprotic) [75].

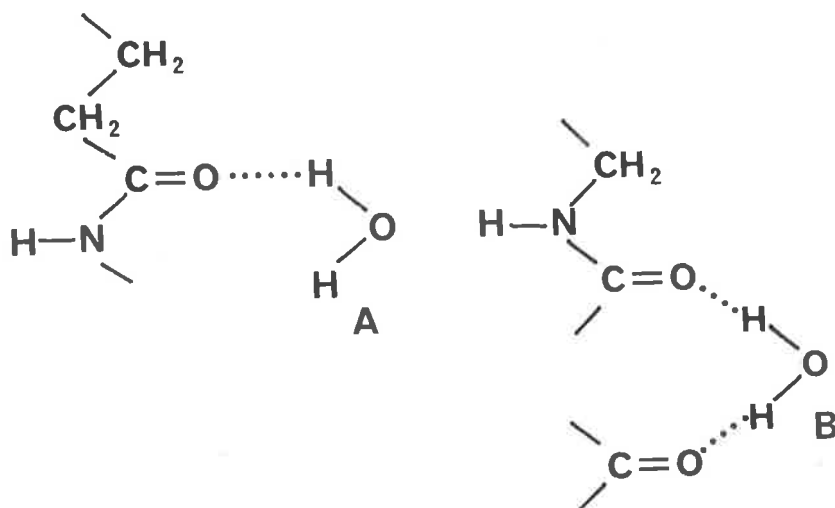


Fig. 2.13.

Interactions between π electrons in some solvent molecules and the polymer amide group also appears to be significant. Concentrations of benzyl alcohol, much higher than cyclohexanol, can be absorbed into nylon 6 [76]. Even when the difference in the dimensions and shape of the two cyclic compounds is taken into account, it remains clear that the aromaticity in the ring promotes increased uptake.

Salt-solvent interactions are well understood; only a brief summary is given below.

Cations have unfilled electronic orbitals into which electron pairs from solvent molecules may be accommodated. The coordinate bonds between small molecules such as water or methyl alcohol and cations are strong and in dilute solutions the maximum possible number of solvent molecules will be bound to the cation. Many cations, such as most of the first period transition metals, will have six solvent molecules surrounding each cation in an octahedral structure. Zinc complexes are an exception and usually form tetrahedra (Fig. 2.14).

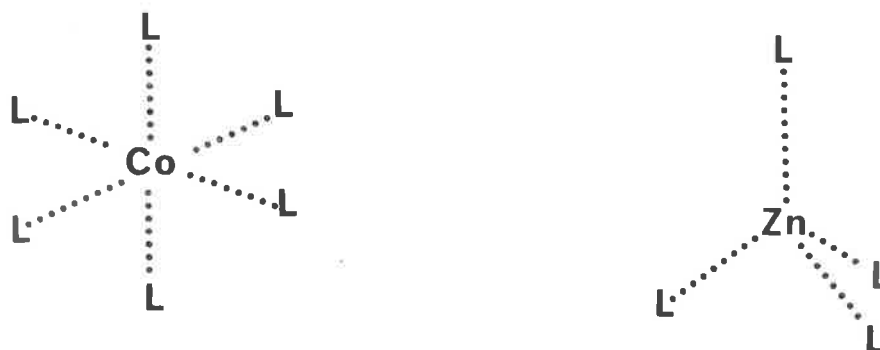


Fig. 2.14.

In dilute solutions, all the ligands will be solvent molecules but at high concentration, there may be insufficient solvent molecules to satisfy the coordination requirements of the cations, and in this case, anions will also coordinate to the cation. An example is shown in Fig. 2.15.

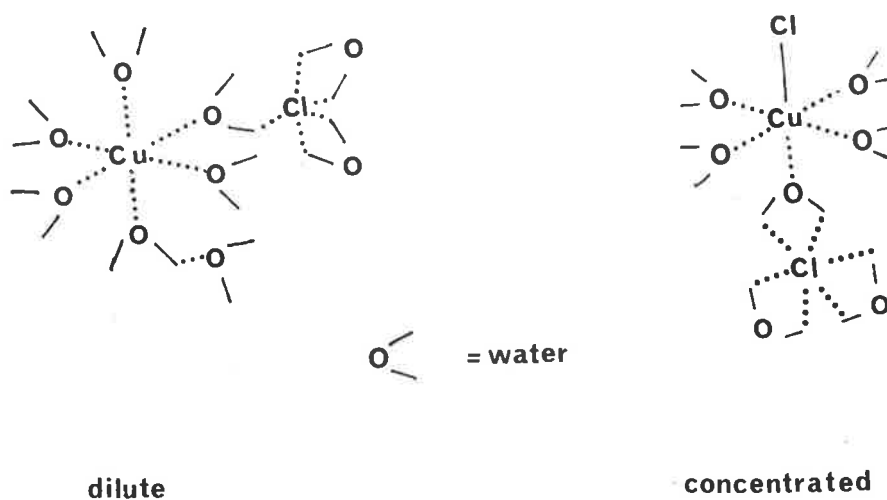


Fig. 2.15.

Cations may interact with appropriate acceptor molecules to produce molecular adducts. Lindquist [77] defines the "donor-acceptor" bonds in these adducts as "the interaction between donor and acceptor molecules leading to the formation of an adduct molecule which exhibits an increased coordination and an associated gain in energy". Donor molecules have one or more lone pairs of electrons which form the bond with the acceptor; the electrons often come from oxygen. Examples of donor molecules are urea, simple aliphatic amides and esters; polyamides and polypeptides also qualify as donors.

Acceptor species must be able to increase or improve coordination, by reducing the number of shared bonds. The energy density about the acceptor will increase, and about the donor, decrease. It has been established [77] that when a donor molecule has two different elements both capable of reducing their electron density, then oxygen predominates, when present. In an amide complex, for example, the donor-

acceptor bond will be between the cation and the carbonyl oxygen instead of the nitrogen [78].

Interactions between Polymer, Salt and Solvent

When solvent is absent, it is possible that cations may form donor-acceptor bonds with carbonyl groups existing in the polymer. When solvent is present, a number of alternatives are possible.

When the concentration of both salt and solvent is low compared with polymer, then only a small number of secondary bonds between the polymer chains can be disrupted.

When the concentration of solvent is high compared to salt, then salt-solvent complexes will form, and the carbonyl donors in the polymer chain will be unable to compete with the excess solvent for the cationic coordination shells. Although no direct cation-polymer interactions are predicted, the secondary forces between the polymer chains may still be modified by solvent.

When cations form strong donor-acceptor bonds and the concentration of solvent molecules is relatively low, then direct interaction between cation and polymer is possible. When the cation forms very strong bonds with solvent molecules, then it may be possible for the salt-solvent aggregate to interact with the polymer.

2.3.3. Salt-Model Amide Interactions

The study of the interaction of salts with monomolecular amide-containing molecules is helpful in unravelling the more complicated interactions of salts with polyamides.

An advantage in using such compounds is that there exists no macromolecular superstructure which might mask the

evidence of cation-amide binding. In addition, complexes which are derived from model amides are easier to isolate and characterise, and interpretation of physical measurements (such as infra-red spectra), are often less ambiguous. Once the nature of the binding itself has been determined, the additional consequence of the large size of polymers (and the complexity of proteins) can then be attempted to be taken into account.

Changes in the physical chemistry of small protein analogues which occur when treated with both aqueous and non-aqueous solutions of alkali and alkali-earth metal salts have been measured. Lithium and calcium salts appear to change the properties of the model amides most, and so have been the most extensively studied.

Anhydrous lithium perchlorate was shown by Diorio and coworkers [79] to form a complex with N-methyl propionamide (a model compound for keratin and other proteins). In this complex a direct donor-acceptor bond between the lithium ion and the carbonyl oxygen was shown to exist. However, in aqueous conditions, water molecules competed successfully with the carbonyl group for the hydration shell of the lithium ion.

In a similar experiment Bello and Bello [80] observed the interaction of aqueous lithium bromide with N-methyl acetamide (N.M.A.) and other simple amides. They isolated a molecular adduct in which lithium cations were surrounded by four carbonyl oxygens (from the amides) and two water molecules. The bromide anions were each coordinated to four amino-hydrogens and two water molecules, the latter bridging lithium with bromine.

When 10M aqueous lithium bromide was used, participation of the water molecules in complex formation was verified using deuteration experiments [80]. The agglomeration of amides, water and lithium ions caused an increase in the viscosity of the solution. It was proposed by Bello and Bello that the aggregate now behaved like a very large molecule. They consider that the lithium ion increased the hydrogen bonding potency of the water molecules by de-shielding the proton. Lithium bromide appeared to cause a larger viscosity increase than lithium chloride, indicating that the anion has a secondary but significant role in salt-amide interactions.

This work was extended by Bello, Haas and Bello [81] by using a variety of alkali and alkali-earth metal salts. Viscometry, calorimetry and crystallography were used to show that only lithium and calcium salts interacted strongly with the model-amide compounds. When 6M aqueous salt solutions were used, it was found that calcium chloride complexed to the amide in a similar way to lithium bromide and lithium chloride. For the lithium: 4 N.M.A. complex, crystallographic studies confirmed the identity of the ligands which had been earlier proposed.

The lithium bromide - N.M.A. complex had a greater enthalpy of formation than the corresponding lithium chloride analogue. This was explained by suggesting that bromine interacts more strongly with the amino hydrogen than chlorine, as reflected by the N-H...Br distance in the crystal lattice. The authors also agree with Robinson and Jencks [82], who consider that denaturing salt anions, upon interaction with amide groups, lost some coordinating water molecules.

Balasubramanian and Shaikh [83] isolated 4:1 molecular adducts of N.M.A. and dimethyl formamide with lithium bromide and chloride. They confirmed Bello and Bello's observations that lithium coordinates directly with few carbonyl oxygens, under anhydrous conditions, and showed amino hydrogen-anion binding. Infra-red spectroscopy revealed that the frequency of the carbon-nitrogen absorption peak had increased, and so the resonance hybrid shown in Fig. 2.16 was proposed.

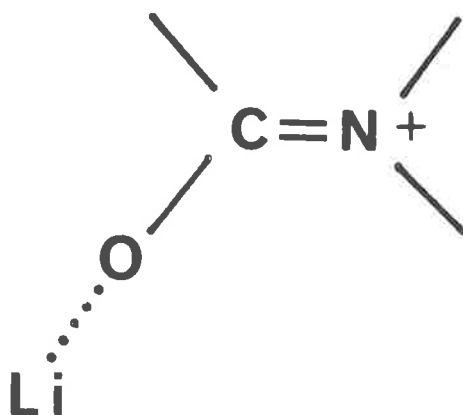


Fig. 2.16.

When water was present, no amide spectral shifts were observed, showing the absence of direct cation-carbonyl oxygen bonds.

Lithium salts were found to interact most strongly with amides in the order tertiary amides > secondary > primary, as measured by heats of reaction under anhydrous conditions. When a variety of lithium salts were dissolved in liquid amides, the heat of reaction was greatest for the perchlorate, and decreased in the order perchlorate > bromide > chloride > acetate.

Solution studies using water, salts and the liquid amides were less easy to interpret. For example, N.M.A. in

dilute aqueous solution was shown to hydrogen bond preferentially to water; only at concentrations as high as 12M did the interamide hydrogen bonding exceed 50% [84]. Viscosity increases which were noticed when concentrations up to 3M lithium chloride were used, were caused by "fixing" of water molecules. Only when the concentration was increased to 5M did strong lithium-water-amide associations cause the viscosity to increase further. Using calorimetry and solubility measurements it was shown that lithium salts bind much more strongly than either sodium or potassium salts to water and amides.

The generality of cation-carbonyl complex formation was shown by Bull and coworkers [85] when they prepared twenty six adducts of N,N-dimethylacetamide (D.M.A.), with salts of fourteen different metals. Apart from the infrared spectral shift (approximately 50cm^{-1}) which showed metal-oxygen association in every case, there was also evidence that halide ions or water molecules often coordinated to the cation at the same time as the amide. Significantly, the only adduct prepared using a Group I or II metal salt was lithium perchlorate: D.M.A.

When investigating the mechanism of stress "cracking" in nylons, Dunn and Sansom [4] used three model compounds (N-ethyl acetamide, t-caprolactam and N-methyl-2-pyrrolidone). The salts which were active could be put (using spectroscopic evidence) into one of two categories; type I salts; in which cations bind directly to the carbonyl oxygen when in concentrated aqueous solution, and Type 2 salts, which modify the solvent, thus allowing solvent stress cracking. In the latter case, water molecules bridge the cation with the amide

group. Proposed structures for each type of binding are reproduced in Fig. 2.17 [4].

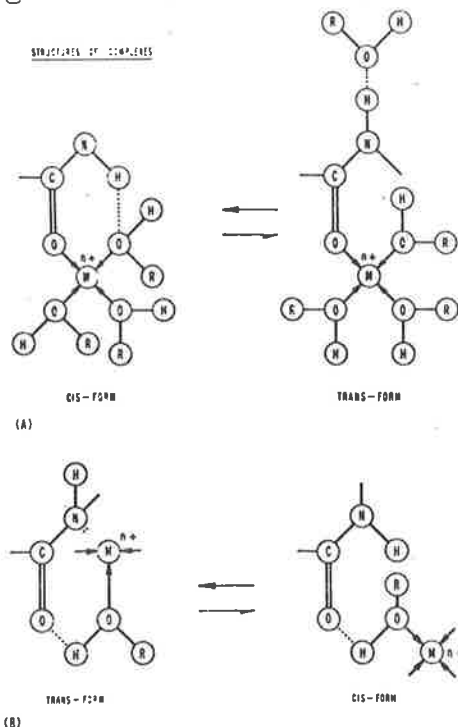


Fig. 2.17.

Salts of Group I and II elements of the periodic table (including lithium halides, calcium chloride and magnesium perchlorate) were Type 2 agents. Salts of the transition elements were in the Type 1 category. This nomenclature will be adopted in the remainder of this thesis.

2.3.4. Evidence for Cation-Polymer Interaction

Proteins are macromolecules which comprise a large number of amino acids linked by amide bonds. They are structural analogues of synthetic polyamides, containing polar regions which, like polyamides, may associate with cations. Their biological activity may be modified as particular tertiary structures are destroyed and previously hidden or shielded groups are made available for interaction with the environmental species. The change in protein activity has widespread biological repercussions and has therefore stimulated considerable research.

There are two commonly occurring conditions under which protein structure may change. Having localised sites of high polarity, proteins are more discriminating towards cations than synthetic regular polymers. As a consequence of the peculiar arrangement of the large number of different amino acids which make up the protein; low concentrations of cations may affect the properties of the polymer.

The second effect is a result of variations in high concentrations of salt. When the ionic strength of the medium surrounding the protein alters, the tertiary structure of the protein may change. This phenomenon is relevant to the properties of synthetic polymers under conditions of high salt concentration, and so is reviewed.

Regular polyamino acids and synthetic optically active polyamides have been used as models for proteins; they may with equal validity be used as models for nylons.

Changes in the helical conformation of poly-L-proline can be brought about by lithium bromide in the absence of water [86]. It is considered that under saturated aqueous or anhydrous conditions, lithium bromide binds directly at the peptide linkages, lowering rotation about the peptide bonds. Reversible mutorotation from a right-handed to a left-handed helix was induced by solvents such as m-cresol, and chloroethanol, as well as the lithium salts such as lithium bromide and perchlorate decreased the value of η_{sp}/c for polyproline, by producing a globular protein-salt mixture, from which a five to one complex of proline to lithium salt could be isolated. They acknowledge that modification of the poly-L-proline could be the result of:

- i. changes in the polypeptide-solvent interaction,
- ii. by the lithium salts altering the properties of the solvent,

or iii. salt-binding directly to the peptides.

The isolation of lithium-proline complexes from mixtures containing low levels of water indicates direct binding.

Optical rotatory dispersion (O.R.D.) and viscosity measurements were used by Lotan [87] to examine the effect of lithium chloride-methanol solutions upon poly-N⁵-(4-hydroxybutyl)-L-glutamine. When the concentration of lithium chloride was increased from 2 to 4M, a decrease in the viscosity indicated a conformational change from semi-rigid rods to disordered chains. As the concentration of lithium bromide was further increased from 4 to 6M, an increase of the viscosity of the mixture was attributed to lithium binding between the peptide chains. Lotan proposes that the chloride anion is solvated by methanol molecules and the lithium ion-amide complex forms as suggested by Balasubramanian [83].

Hamoud and coworkers [88,89] have also used O.R.D. to measure the changes in the physical properties of optically active polyamides. Of the Group I and II salts tested, only calcium chloride was found to bind significantly with the amides, and further it was shown that direct binding rather than conformational changes occurred. A solid-state preparation of an adduct comprising calcium chloride and a diamide in a molar ratio of 1:1 was carried out; it had a melting point of 225°C compared with 138°C for the pure amide.

The interactions which were observed between amide

groups and salt, as measured using O.R.D., were said by Hamoud to explain the solubilisation of polyamides in alcoholic solutions of potassium and calcium chloride.

The depression of the melting point of nylon 6 by lithium salts was measured by Valenti et al [90], but these results were later found to be ambiguous because of thermal degradation of the unstabilised nylon. Bianchi and co-workers [91] made a more intensive study of the bulk properties of nylon 6 in the presence of lithium bromide and chloride. They found that the melt viscosity of the nylon 6 was increased when quite low (up to 4% w/w) levels of salt were added, but that the morphology of the solid was not significantly altered. The crystalline state of the treated nylon was complicated by the presence of both α and γ forms of nylon 6. In the later experiments intrinsic viscosity values were found to be unaltered with fusion time (cf Valenti et al [90]) showing that now molecular degradation did not occur.

When Bianchi proposed a mechanism for salt interaction with nylon 6, the observation that the T_g of nylon 6 was not greatly affected by salts and that lithium chloride depresses the T_m of nylon 6 more than lithium bromide [92] was cited. (The concentrations used by Ciferri [92] were given in % w/w and not as molar ratios, so that the molar concentration of lithium chloride would be higher than lithium bromide). Bianchi considers that the salt binds to amorphous regions, but during crystallisation the bound salt can dissociate as ordered regions develop. When long annealing times were used, highly crystalline samples of salt containing nylon 6

were prepared.

This compares with the results of Valenti [90]; when 8% lithium chloride or 12% lithium bromide was used, the nylon 6-salt mixture was not crystallisable. Salts were found to depress the T_m of nylon 6 in the order lithium bromide > lithium chloride > potassium chloride (c.f. Ciferri [92]).

Kaplan and Kelleher [93] studied the effects of potassium and lithium chloride upon the fusion temperature and crystallinity of nylon 6, under anhydrous conditions. Lithium chloride was found to reduce the crystallinity of the nylon, as the mole fraction of the salt was increased, and the fusion temperature is depressed. Both the α and γ modification of nylon 6 was detected using X-ray diffraction. In contrast, potassium chloride produced no changes in the nylon, and only the α type of nylon was present. The authors explain these results (in part) by suggesting that lithium chloride can enter the crystalline region of the nylon better than potassium chloride.

Melting properties of nylon 66 and spectroscopic properties of formylamide (n-phenyl formamide), in the presence of chlorides, thiocyanates, stearates and acetates of zinc, lead and copper were observed by Kargin et al [94]. Acetates and stearates of all salts, and lead salts in general, had no effect upon the melt properties of nylon 66. Zinc thiocyanate and chloride (25% w/w) prevented crystallisation of nylon 66, and localised amorphous regions were observed adjacent to introduced copper salts. Copper chloride slowly dissolved in nylon 66; copper thiocyanate caused no structural change until abrupt dissolution occurred. Infra-red

spectroscopy revealed that the carbonyl stretch frequency was lowered and the N-H deformation frequency was altered in the presence of active zinc salts. The π bonds of the thiocyanate were shown to interact with the amino proton, forming a type of hydrogen bond. Acetates and stearates were shown not to associate with the nylon.

The sorption of some hydroxylic solvents by nylon 6 has been measured by Addy and Andrews [95]. They used aliphatic alcohols, benzyl alcohol and phenol (in carbon tetrachloride). For simple monoalcohols, uptake ranged from 0.40M of methyl alcohol, to 0.10M of hexan-1-ol, for each molar quantity of nylon 6. The uptake increased as the molecular size of the alcohol decreased. Diols and triols, and cyclohexanol were also absorbed to about the same levels, but benzyl alcohol and phenol showed very high uptakes. Because they are absorbed much more than cyclohexanol (having a similar molecular size), it can be concluded that aromaticity has an important role in binding to the polyamide. Although the nature of the interaction was not discussed by the authors, presumably some type of π electron interaction must occur which favors uptake of the aromatic alcohol. (There are no conjugation effects between the oxygen and the benzene ring in benzyl alcohol).

A different range of swelling agents for nylon 6 was examined by Andrews [96]. The effects of phenol, iodine-potassium iodide, and concentrated aqueous solutions of zinc chloride upon the mechanical and thermal properties of nylon 6 were investigated. Whilst the phenol was found to act as a plasticiser, reducing the glass transition temperature from

70°C to -23°C in the highest levels used, zinc-chloride was shown to act as an anti-plasticiser, increasing both the size (indicating a higher amorphous content) and the position (to higher temperatures) of the α -peak.

When nylon 6 was treated with up to 3M aqueous zinc chloride, swelling occurred, caused by the change in the crystallographic form of the nylon from α to γ . This was accompanied by an increase in the yield stress of the still-highly crystalline nylon. When treated with aqueous zinc chloride in concentrations increasing from 3 to 6.5M, a reduction in the crystalline content was observed, and the yield stress of the nylon decreased.

Finally, at very high concentrations (greater than 6.5M), the crystalline content began to increase. These results require further explanation.

Sarda and Peacock [97] were among the first to recognise the interaction of metal salts with nylon 66. Infra-red measurements of thin nylon 66 films treated with concentrated (50, 100% w/v) aqueous solutions of magnesium and lithium perchlorate and lithium bromide indicated that a new peak at $3,390 \text{ cm}^{-1}$ and a broadening of the amide bonds in the $1,400$ to $1,600 \text{ cm}^{-1}$ region were the only changes to occur. The new band was attributed to a modified N-H bond, and the cation was thought to bind directly to the nitrogen atom, as indicated in Fig. 2.18.

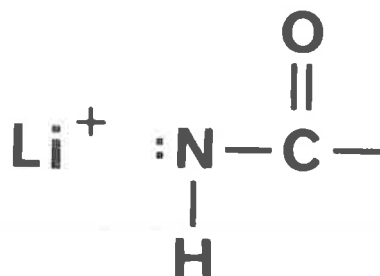


Fig. 2.18.

The solubility of polyacrylonitrile fibres in aqueous lithium bromide was suggested as supporting evidence with the cyanide nitrogen interacting with the lithium ion. Other proposals were also somewhat conjective.

Dunn and Sansom [3-6] have investigated interactions between salt solutions and nylons. They made a systematic study of the stress-cracking of (mainly) nylon 6, caused by metal halides, thiocyanates and nitrates.

In the first paper [3] it was noted that stress cracking was favored by high temperature, moisture content, concentration of the agent, and stress. Chain scission and hydrolysis were absent. An abbreviated list of the most active halides in water and methanol are given in Table 2.3.

Water as solvent	
Highly active	LiBr, $Mg(ClO_4)_2$, $ZnCl_2$, ZnI_2
Moderately active	$CoCl_2$, $InCl_3$
Methyl alcohol as solvent	
Highly active	LiBr, $ZnCl_2$, ZnI_2
Moderately active	$CoCl_2$, $InCl_3$, $CaCl_2$, LiI, LiCl

Table 2.3.

Anhydrous nylons and nylons which absorb very little water (such as nylon 11), were generally more resistant to stress-cracking, although even nylon 11 could be stress-cracked after conditioning in methyl alcohol for one week. Similar treatment with water did not affect the resistance

of nylon 11 to environmental stress cracking. Nylons conditioned in hydroxylic liquids such as ethylene glycol, methyl alcohol and isopropanol were also found to be more susceptible to cracking, and in general, methanolic salt solutions had enhanced cracking activity over the aqueous equivalent solutions.

At concentrations less than 30% w/v, no cracking was observed, even with long exposure times and at high stresses. Cracking appeared at concentrations higher than 30%, and the activity of the solution increased with increase in concentration. Above a concentration of 50% w/v, however, no further increase in cracking activity was observed (the activity of 80% w/v zinc chloride was not significantly higher than at 50%).

These results show how solvent molecules can compete with carbonyl groups for the hydration shells of the cation. When an excess of solvent (in practical terms, when the concentration of zinc chloride is less than 30%) is present, complexing of cation with amide is inhibited. Above 50% w/v, all possible cation-amide associations are present.

Dunn and Sansom propose that the cracking agents can swell the polymer, causing micro- and gross plasticisation, with the solvent acting as a swelling agent and transport medium for the salt. Initiation of cracks often occurred at the agent-air-polymer interface, but the reason for this was not given.

When the activity of thiocyanates were measured using a stressed film method [5], lithium, cobalt and zinc salts, as well as cobalthiocyanates, were found to be highly

active. The lithium salts were the most active, and caused the nylon to become highly amorphous. The cobalt and zinc salts complexed with the nylon and subsequently transition from the crystalline to the amorphous state occurred. Deuteration experiments showed that water molecules could only enter non-crystalline regions.

When nitrates were tested [6], it was found that only copper and zinc salts were active in aqueous solution, with copper nitrate having a cracking activity comparable with zinc chloride. All nitrates possessed some degree of cracking activity in methyl alcohol, but those nitrates which were bound by the Type 1 mechanism [4] and had the highest activity, were more active in water. Salts which were found to be inactive were all acetates and sulphates.

2.3.5. Summary - Metal Salt-Polymer Interactions

It has been established that under appropriate conditions, it is possible for cation-carbonyl associations to occur. The associations are strong with calcium, lithium, magnesium and many transition element salts. In the absence of solvent, direct binding alters the physical properties of both small and large donor molecules. Changes in the spectroscopic and viscosity values can be readily explained by direct donor-acceptor bonds.

Some cation-amide bonds are more sensitive to the presence of solvent than others. It has been shown by infra-red spectroscopy, in particular, that solvent molecules compete strongly for the hydration shells in lithium, calcium and magnesium salt complexes. Solutions of these salts will complex indirectly with carbonyl oxygens, through interposed solvent molecules.

Transition metal salts bind directly to the carbonyl oxygen, even when good solvents such as water and methanol are present. When the solvent is in high concentration, there is little evidence for cation-carbonyl interaction, with the solvent molecules now being able to compete successfully for the vacant hydration shells of the cation.

2.4. Environmental Stress Crazeing in Glassy Polymers

Environmental stress crazeing (e.s.c.) may be defined as crazeing initiated at abnormally low stresses by a hostile environment. For glassy polymers, the environment is often an organic liquid or vapour. It will be shown later that e.s.c. may arise under a wide range of conditions, with substances as diverse as liquid nitrogen and aqueous salt solutions behaving as hostile environments for some polymers.

Historically e.s.c. has been associated with glassy polymers, and many aspects have been studied. Of interest are:

- (a) penetration of the agent into the polymer
- (b) the types of association between agent and polymer
- and (c) the structural and mechanical consequences of such associations.

2.4.1. Agent Penetration into the Polymer

There needs to be intimate contact between agent and polymer for environmental stress crazeing to occur. Diffusion and other types of transport of molecules into polymers are extensively discussed by Crank and Park [98] and Hopfenberg and Stannett [99]. Of particular interest are two

uptake processes, known as Case I and Case II transport [100].

Case I Transport

The simplest type of diffusion in isotropic polymers is Case I or Fickian transport, where the rate of transfer of the diffusing substance through unit area of a section is proportional to the concentration gradient measured normal to the section;

$$\text{i.e.} \quad F = -D \frac{\partial C}{\partial x}$$

where F = rate of transfer per unit area of section
 C = concentration of diffusing substance
 x = space coordinate normal to the section
 and D = diffusion coefficient.

When diffusion occurs in one direction only (e.g. a concentration gradient in the x axis), then

$$\frac{\partial c}{\partial t} = D \frac{\partial^2 c}{\partial x^2}$$

i.e. the rate of diffusion is proportional to the concentration gradient. Frisch [101] has identified type A and B Fickian transport, each applying to molecules of a particular size.

Type A transport is observed with small penetrants, such as diatomic gases, and may be significant in the early stages of liquid nitrogen and argon e.s.c. of polymers [102].

Type B Fickian diffusion, observed with larger organic molecules, is characterised by;

- (a) non-dilute penetrant-polymer mixture
- (b) markedly concentration-dependent diffusion coefficients

and (c) temperature dependent energies of activation.

Case II transport allows for the difference in concentration of agent between the outer, swollen layers and the unpenetrated central core. The rate determining step is osmotically induced polymeric relaxations at the boundary. When the two types of transport are superimposed, apparent time dependent anomalies result. The relationship between the different types of uptake for hydrocarbons in polystyrene has been determined for different temperature and penetrant activity conditions [103].

From this work it is apparent that both the activity and temperature must be known before the absorption behaviour of a penetrant-polymer pair can be specified.

Peterlin [104] considers that a Fickian diffusion front precedes the advancing convection front manifest by the boundaries between the swollen shell and the partially penetrated core (see Fig. 2.19).

In relaxation controlled transport, a linear relationship exists between initial weight gain in the film and time, ($T \ll T_g$), and a sharp boundary, advancing at constant velocity, separates the inner glassy core of essentially zero penetrant activity from the outer swollen shell of uniform

concentration [100]. The parameters affecting relaxation (such as temperature and polymer orientation) also affect the transport of molecules into glassy polymers.

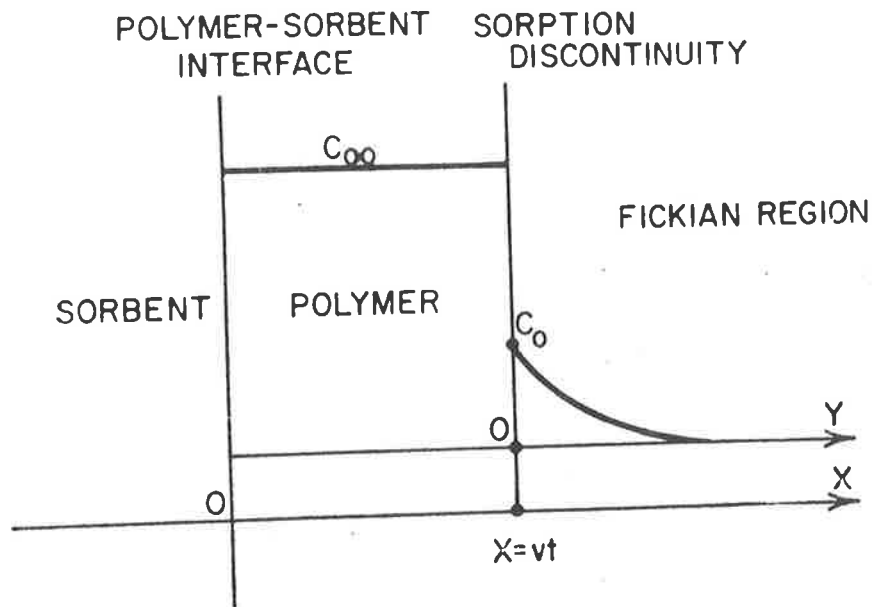


Fig. 2.19.

2.4.2. The Mechanism of Initiation of Environmental Crazeing

In glassy polymers, a number of proposals have been given for the initiation of environmental crazeing.

The first is based on "domains", which in Robertson's [105] view are approximately $0.01 \mu\text{m}$ in diameter and are regions of imperfect alignment of chains. Nielsen [106] considers domains to be imperfections or inhomogeneities in which high stresses are relieved by crazeing.

The second proposal, by Rosen [107], is that the vapour or liquid is accommodated when differential expansion of the polymer occurs during swelling. Diffusion is considered to be relaxation-controlled; internal tensions

arising from the swelling may cause internal fracture or crazing. The swollen layer must presumably be thin, because most crazes initiate at the surface. Similar theories [108, 109], emphasise "crystallisation stresses" which initiate solvent crazing in polycarbonate.

The absorption behaviour of agents is modified by the presence of voids and oriented polymer in crazed samples. There is evidence that the voids in craze matter are interconnected [17], so that the active agent may move rapidly by a capillary action. The transport of liquid at or near the craze tip has not been described in molecular terms, but it appears that the passage of agent keeps up with the elongation of the craze.

As well as the domain and swelling-crystallisation theories, two other theories have been developed to explain how crazing can be promoted by the environment.

Stabilization of Newly-Created Surfaces

This theory assumes stabilization of nascent voids just prior to and during craze initiation and growth. It is assumed that the agent is absorbed onto the internal surface of the void, lowering the surface free energy and thus stabilizing the void. This theory suggests that the agent stabilizes new surfaces and does not modify the internal inter-chain attractive forces. It does explain how non-solvents can act as crazing agents, but each of the examples used to support it (such as crazing of polymers in liquid nitrogen) has recently been refuted (see [102] for example).

Plasticization

It is now widely accepted that plasticization is the significant step which leads to environmental stress crazing in polymers.

A plasticizer molecule must be able to interpose itself between polymer chains, but interacting with the forces which hold the chains together (dispersion and inductive forces, dipole-dipole interactions, hydrogen bonding and chain entanglements). As the plasticizer allows increased segmental movement of the polymer new mechanical properties of the polymer will result.

In non-polar glassy polymers dispersion forces are dominant. They arise from electrostatic interactions between atoms resulting from perturbation of electronic clouds. To predict which substances may behave as plasticizers for a particular polymer, the concept of solubility parameters has proven useful in establishing compatibility between agent and polymer.

The Solubility Parameter

The solubility parameter (δ) of Hildebrand and Scott [72], is defined as

$$\delta = \left(\frac{\Delta E}{V} \right)^{\frac{1}{2}}$$

where E is the energy of vaporisation
and V is the volume.

i.e. δ is the square root of the energy of vaporisation per unit volume. $\Delta E/V$ may be considered equivalent to the

"cohesive energy density", as it is a measure of all the cohesive forces holding the substance together. If the δ values of two substances are similar, then the entropy of mixing will be low and so they are likely to be miscible.

Hansen [73,74] has been able to measure δ values for a large number of polymers and liquids, and has partially been successful in predicting the behaviour of non-polar polymers in the presence of non-polar liquids. The relevance of solubility parameters to environmental stress crazing is as follows: when the overall value of δ of the polymer is the same as that of the liquid possible stress cracking is predicted. When the values of δ of solvent and polymer are close, then swelling and e.s.c. are considered possible.

In polar polymers, allowances have to be made for the presence of strong dipole-dipole and hydrogen bonding forces. The success in assigning δ values which can realistically predict cracking and crazing in these polymers is small.

The importance of hydrogen bonding was demonstrated for e.s.c. in PMMA, PVC and polysulphone by Vincent and Raha [110]. Using a "two-dimensional" solubility parameter, they succeeded in accounting for the occurrence of crazing and cracking using a variety of agents.

Recently Henry [111] has developed "three-dimensional" solubility parameters, which allow for dispersion, polar and hydrogen bonding forces. They were used to predict crazing in styrene-acrylonitrile copolymers, in particular, but it was indicated that such parameters could be applied to a large range of polymers and solvents.

2.4.3. Mechanics of Environmental Stress Crazeing

The fracture mechanics approach to e.s.c. has been used successfully to indicate how environmental crazing occurs in glassy polymers. In particular, the work of Andrews and coworkers [112-114] and Marshall and coworkers [33,115] with solvent crazing in PMMA, is noteworthy.

Andrews and Bevan [112] found that for each temperature a minimum surface work, τ_0 , equivalent to the work of craze formation at a crack tip, could be defined. The value of τ_0 for PMMA stress-crazed in a particular solvent decreased as the temperature was increased until at a certain temperature, T_c , the value of the surface work τ_0^* remained constant.

The value of this temperature-independent minimum surface work could be related to the difference between the solubility parameters of solvent and polymer. The variation of τ_0 at $T < T_c$ was attributed to a yield stress effect, and the value of τ_0^* was attributed to a polymer-solvent interfacial energy effect. Fig. 2.20 shows τ_0 as a function of temperature for PMMA in methanol, isobutanol and carbon tetrachloride [112].

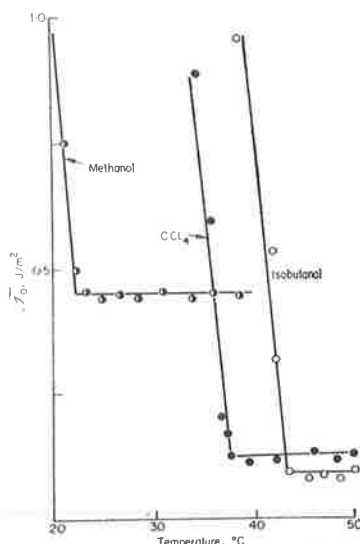


Fig. 2.20.

The dependence of T_c with solubility parameter for PMMA is shown in Fig. 2.21. T_c is considered to be the effective glass transition of the solvated polymer at the craze tip.

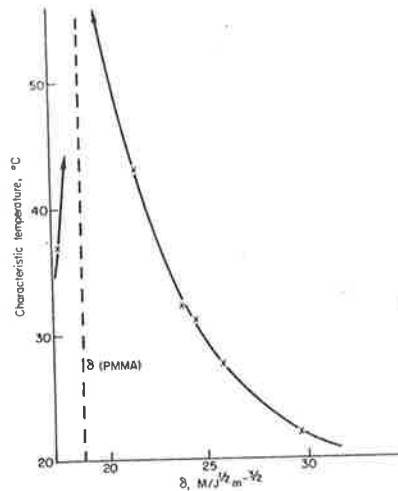


Fig. 2.21 from [112]

Andrews, Levy and Willis [113] investigated swelling of PMMA using different solvents over a range of temperatures. They were able to calculate values of ϕ_2 , the equilibrium polymer fraction, and show how each value influenced the yield stress, and glass transition temperature. They confirmed that stress accelerates the uptake of solvent in the craze tip region.

The fracture mechanics approach has been used by Andrews and Levy [114] and Marshall and coworkers [33,115] using single-edge-notched tensile specimens of PMMA and low density polyethylene.

For PMMA it was shown [33,114] that the craze propagation velocities were not determined by the applied stress level alone, but rather by the stress intensity factor K_O , given by

$$K_o = Z \sigma_o C_o^{\frac{1}{2}}$$

where σ_o = applied tensile stress

C_o = length of the starter crack

and Z = a constant

Surprisingly, it was shown that the length of the starter crack was critical, even when it was much less than the craze, in which it was inserted.

Andrews and Levy [114] extended their work by measuring craze lengths and propagation velocities when

(i) low stresses were applied and craze arrest occurred after limited growth,

(ii) craze growth occurring at constant velocity under a steady applied stress, after the "break-away point",

and (iii) constant velocity growth continues after removal of the original "starter" crack and reapplication of the load.

They introduce l , the equivalent crack length, "equal to the length of a true crack which would give rise at its tip to a stress concentration equal to that actually existing at the tip of the craze".

The physical model which can be used incorporates a crack at the craze tip. The interdependence of C_o , l and K can then be analysed using fracture mechanics analysis. The value of l is very sensitive to strain hardening in the craze. A framework has been set up to determine stress

requirements for environmental crazing.

When Marshall and coworkers used fracture mechanics analysis on environmental cracking in low density polyethylene [115], they found that the stress intensity factor was related to the crack velocity; presoaking and specimen thickness differences had no effect upon the velocity.

Environmental crazing of polystyrene and polycarbonate has been measured in alcohols and hydrocarbons [116]. When the activation energies for yielding and crazing were estimated using the Eyring treatment, it was discovered that crazing occurs by a lower energy molecular rearrangement. This correlates with the observation that crazes occur before fracture or yielding (high activation energy processes).

CHAPTER 3.MATERIALS AND METHODS3.1. Materials3.1.1. Properties of Materials Used

Nylon 6 and 66 were used extensively throughout the study. Two types of nylon 66 and three types of nylon 6 were received from commercial suppliers and specifications for each type are given in Table 3.1.

The crystallinity of each sample was determined from the measurement of densities, and the nomograms of Miller [117]. For this purpose it was shown by wide angle X-ray analysis that the "as received" nylons were essentially of the α crystallographic form. The values of \bar{M}_v were found by viscosity measurements, as outlined in Section 3.1.2.

Compression molded and solution cast films of nylon 6, 66 and 11 were produced from granules of Maranyl F.103, Maranyl A.100 (both I.C.I., England) and Rislan Grade B.M.N.O. (Fisons, France), respectively. Compression molded films were generally prepared by melting granules between glass slides treated with release agent, and applying a pressure of approximately 25 to 50 MPa (depending upon the desired film thickness). The film was then allowed to cool slowly, or was quenched, as required.

Thin films were usually cast onto water from a dilute (0.5 to 5.0% w/v) solution of the nylon in formic acid or molten phenol, as described in Section 3.2.

Salts used in stress-crazing experiments were laboratory grade or better. For the viscometry experiments, reagents were analytical grade. Solvents used for all experiments were analytical grade, and water was triply distilled over glass.

Nylon Type	Dimensions as received	Standard testpiece	\bar{M}_v	\bar{X}_m (%)	ρ as rec'd
Maranyl A-100 nylon 66	cross-section of neck = 12.9 x 3.1 mm.	ASTM D638 Type I	18,000	47	1.145
Polymer Corpora- tion Nylatron - G.S.	extruded film 125 x 0.16 mm.	ASTM D 638 Type IV	35,000	43	1.139
Nylon 6 sheet	extruded sheet, thickness range 0.97 to 1.00 mm.	ASTM D 638 Type IV	87,000	15	1.129
nylon 6 strip	extruded strip, area of cross- section 3.3 x 13.2 mm.	Standard not used.	94,000	17	1.131
nylon 6 film	extruded blown film, thickness = .04 mm.	ASTM D 638 Type II, IV	33,000	not deter- mined.	not deter- mined.

Table 3.1.

Specifications of Nylon 6 and 66.

3.1.2. Determination of Viscosity-Average Molecular Weight

Solutions of the nylon were prepared with concentrations of 0.25, 0.50, 0.75 and 1.0% w/v, in formic acid using the concentrations given in Table 3.2.

Polymer	Solvent	Temperature	K	a	Ref.
nylon 6	85% aqueous formic acid	20.0°C	0.75×10^{-3}	0.70	[118]
nylon 66	90% aqueous formic acid	25.0°C	1.1×10^{-3}	0.72	[119]

Table 3.2.

Measurements were carried out in a Ubbelohde suspended-level dilution viscometer, which had a flow time for water at 25.0°C of 80.0 seconds. Flow times were recorded for each concentration until agreement within 0.2 seconds was obtained for three readings. Care was taken to ensure that no solid matter entered the capillary, that residues from previous samples were not carried over, and that the temperature of the solution had reached equilibrium. The water bath was kept to within 0.1°C of the required temperature. From the values of the election times of each solution of polymer, and that of the solvent alone, it is possible to determine the molecular weight of the polymer, using the procedure given below.

$$\eta_r = \frac{\eta_s}{\eta_o} \eta \frac{t_s}{t_o}$$

where η_r is the viscosity ratio,
 η_s is the viscosity of the solution,
 and η_o is the viscosity of the solvent.

The specific viscosity, η_{sp} , is given by

$$\eta_{sp} \approx \frac{t_s - t_o}{t_o} = \eta_r - 1$$

The viscosity number (η_{red}) can be determined by dividing the specific viscosity by the concentration of the solution. The relative viscosity of polymer solutions is concentration dependent, so the useful value is the limiting one when η_{red} is extrapolated to zero concentration. This value is known as the limiting viscosity number ($= [\eta]$), and is defined by

$$[\eta] (\eta_{sp}/c)_{c \rightarrow 0} = [\ln \eta_r / c]_{c \rightarrow 0}$$

The viscosity number is plotted against the concentration, for solutions of different concentrations, to give a line which indicates the limiting viscosity number when c is zero. Values of η_{red} ($= \eta_{sp}/c$) were plotted against c for at least three different concentrations. A typical graph is shown in Fig. 3.1 for 1.00 mm thick nylon 6.

The increase in viscosity due to a polymeric solute is a function of the volume of the polymer molecule, and so is not a direct measure of its molecular weight. The limiting viscosity number can still be associated with the

absolute measured molecular weights, M , for a series of homogeneous, linear polymers, by the Mark-Houwink equation [120,121],

$$[\eta] = KM^a$$

When the appropriate values of K and a are used (see Table 3.2) it is possible to determine the viscosity-average molecular weight of the polymer.

3.2. Transmission Electron Microscopy Methods

Observation of thin coated and uncoated polymer films, and replicas of thick samples, was carried out using a Philips E.M. 200. transmission electron microscope. The preparation of thin films, the methods used for straining them, and the replication procedures used for other samples are described below.

3.2.1. Thin Film Preparation

Most thin films which were studied were of nylon 6, and nylon 66. The first films were cast onto water from 0.5 to 1.0% w/v solutions of the nylon granules in 99% formic acid. It was found that with practice reasonably uniform films with a thickness of about 0.1 to 0.2 μm (as estimated by interference colours) could be cast on water at a temperature of about 50°C, although water at room temperature was sometimes found satisfactory. When a large shallow pool of mercury (anhydrous, inert and level) was used instead of water, films were produced which were not uniform in thickness, and in which traces of mercury persisted; this alternate method, which has proved satisfactory in other

studies of polymer film, was therefore relinquished. It was soon realised that nylon films cast from phenolic solutions were more satisfactory; highly spherulitic films of uniform thickness could be routinely produced by allowing a few drops of a 1.0 to 5.0% w/w solution of the nylon in phenol to come into contact with water at elevated temperatures (usually approximately 50°C). These films were refloated upon distilled water to remove traces of residual phenol. Nylon 6 films of high quality were more easily produced than those of nylon 66 (also observed when cast from formic acid), and so these were used more often.

Nylon films were cast from solution onto glass slides and the solvent removed at elevated temperatures. The dry film could then be floated onto water or some other liquid. These films were generally no better than those cast directly upon water. Films which were to be shadowed or replicated were dried upon glass slides coated with a release agent. The coated film could then be scored, refloated upon water, and then collected on electron microscope grids.

3.2.2. Straining Experiments with Thin Films

Studies of the structure and mechanical properties of polymers frequently require a thin polymer film (1 μm thick) to be deformed in a controlled manner and held under stress for a sufficient period of time. An apparatus was constructed which enabled this to be done and, by using magnetic clamps, the risk of accidental damage to the film in the neighbourhood of the clamps has been minimised.

An overall view of the device is given in Fig. 3.2. Two arms (J), each with a clamp, are pivotted at a common point (A); the distance between the clamps can be regulated

Fig. 3.2. Straining device used with very thin nylon films.

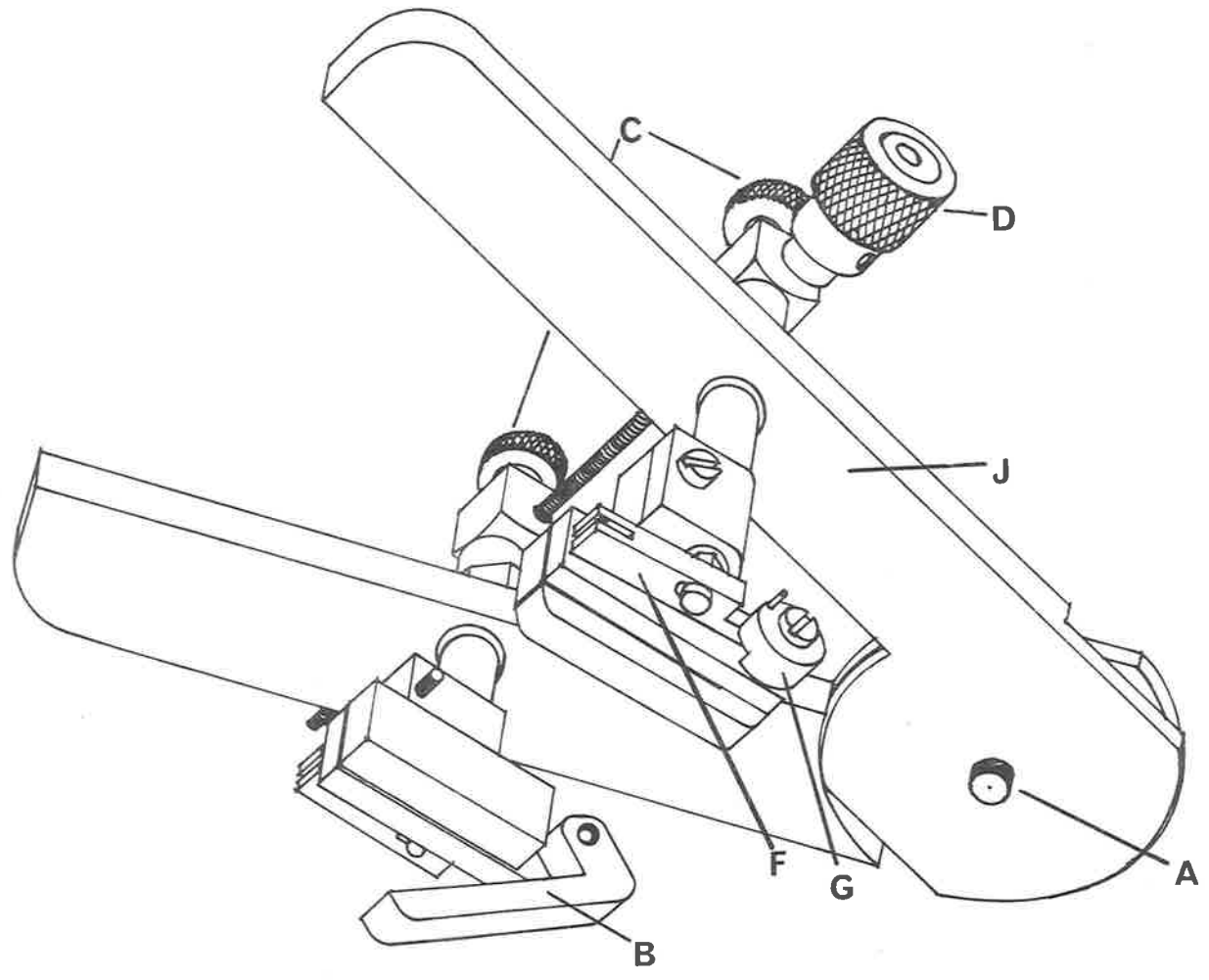


Fig. 3.2.

by turning the large thumb-screw (D).

The mechanism for opening and closing the clamps is described with reference to the cross-sectional view shown in Fig. 3.3. The top of each grip (I), is a corrosion-resistant permanent magnet, which has a polished bottom face. The lower hinged jaws (B), are made from martensitic stainless steel. Each jaw is opened or closed by turning screw (C). A centre rod (H) moves the arm (F), which in turn acts upon disc (G), operating a lower jaw. The arm (F) is pinned to the disc (G) in an elongated hole so that ultimately magnetic forces bring the jaws of each grip together. The advantage of this method is that thin, fragile polymer films are not subjected to excessive forces at the grip region, which would result in localized fracture.

The film to be transformed was transferred, after trimming, to the surface of the desired liquid (usually water or aqueous metal halide solutions). With the arms of the tensile device resting on the lip of 250 or 400 cc beaker and the jaws of the grips open, the film was positioned under the magnets. By turning thumbscrews (C), the jaws were closed: the arms were then opened using knob (D). After the deformation has been completed, the jaws were reopened and the device removed.

3.2.3. Replication Procedures

Three methods were used successfully for which brief details are given.

The most direct method was to shadow the specimen with platinum, and then coat with a support film of carbon. The coated nylon specimen was then trimmed and immersed directly

Fig. 3.3. Sectional diagram showing mechanism of the thin film straining device.

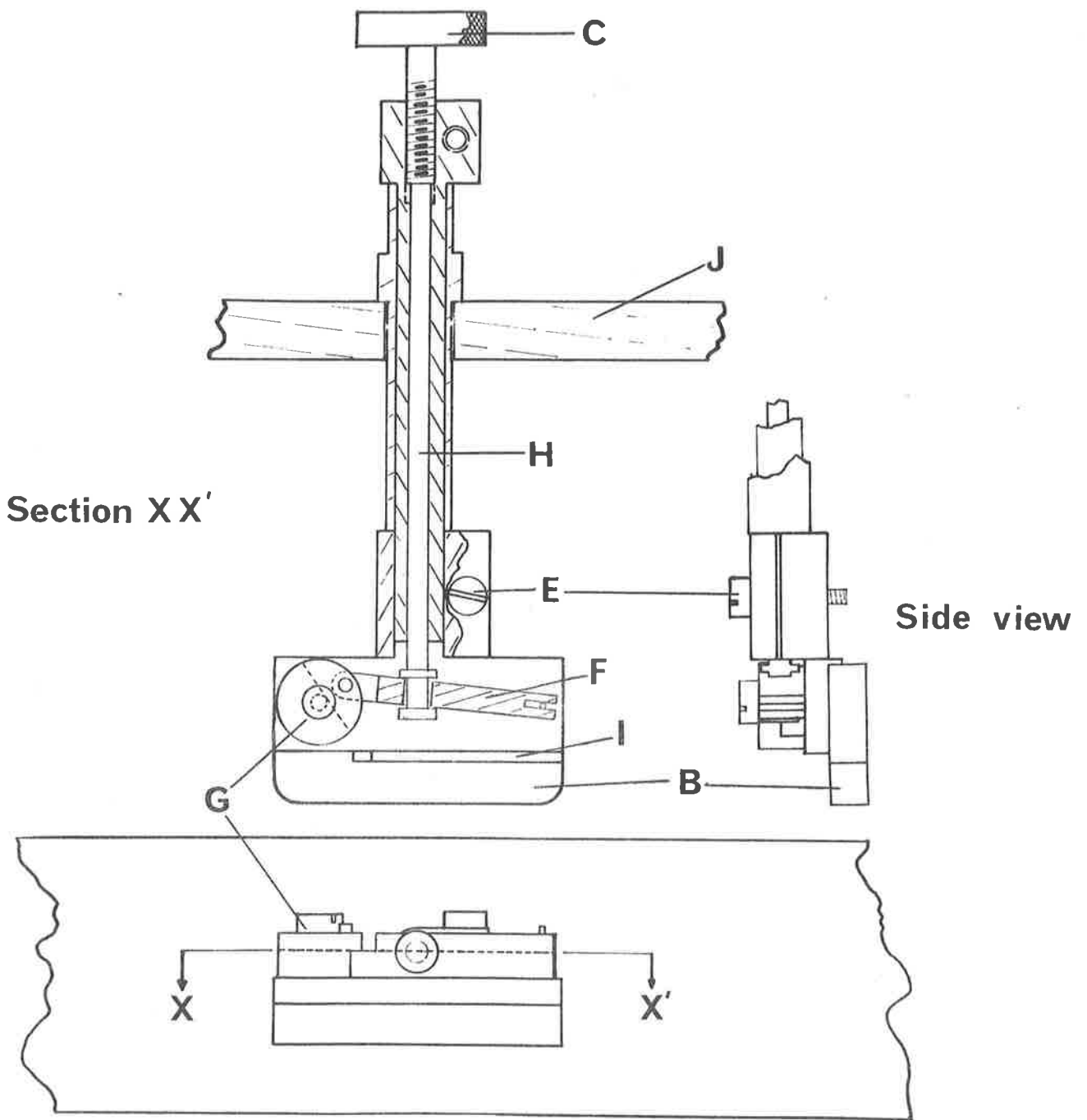


Fig. 3.3.

in 99% (w/v) formic acid. The metal-carbon film can be separated from the swollen polymer, and carefully transferred to fresh formic acid using an electron microscope grid. After multiple washes with formic acid, the film was then flattened on the surface of distilled water, and examined under the optical stereomicroscope for traces of residual polymer. Clean replicas were then observed on grids without a support film. Although this method was most successful for thin nylon 6 and 66 substrates, very thick (> 3 mm) specimens could also be replicated.

When the surface of the specimen was very rough (for example, in stress-crazed polymers), single stage replication using Formvar[®] was found necessary. Several drops of a 1% (w/v) solution in ethylene dichloride were allowed to dry on the region of interest. The stripped replica film was then coated with platinum and carbon in the normal way, and the Formvar then redissolved in ethylene dichloride. Occasionally the replica with Formvar intact was viewed in the scanning electron microscope; the advantages over looking directly at the crazed specimen were better contrast and reduced charging.

A multi-stage replication method, as described by Geil [122], was also investigated. It proved to be a time-consuming procedure, and because results were not significantly better than the other two methods, it was not adopted.

3.3. Scanning Electron Microscopy

The scanning electron microscope was used extensively to investigate the morphology of stress-crazed polymers because it offered a number of distinct advantages over other

techniques. Sample preparation was usually simple, specimens were able to be observed over a wide magnification range, images possessed a great depth of focus, and signal processing could provide further information.

3.3.1. Specimen Preparation

Two types of samples were most commonly examined. Fractured testpieces presented no problem - they were simply trimmed, washed when necessary, and glued onto an S.E.M. stub. Finally, the dry specimen was coated with gold. The most uniform coating was obtained when the sample was simultaneously rotated and gyrated. Usually a thick coating of gold was used to reduce charging within the specimen; the small decrease in ultimate resolution was not a problem as normally very high magnifications were unnecessary. Very thick layers of gold were avoided, because the metal flaked off, causing artifacts and an unstable image.

Crazed testpieces which were not broken were clamped in small frames to maintain strain. The frames were designed so that specimens could also be observed in the optical microscope.

Each specimen was stress-crazed to the extent desired, and then immediately clamped in the frame. The stress-crazing agent was then removed by irrigating the craze region with solvent and then the ends of the testpiece were trimmed. The dried specimen was then made conductive by painting areas of contact between polymer and frame, and frame and stub, with silver dag. Finally the specimen was coated with gold in the usual way. Sometimes elements in the frame (such as aluminium, copper and zinc) gave high emissions of X-rays

upon irradiation with the electron beam, and so reduced the efficiency of X-ray analysis. This problem was overcome by precise alignment of specimen and detector.

3.3.2. Operation of the Microscope

Polymers, including nylons, are not ideal subjects for S.E.M. because they are non-conductive and unstable to high levels of energetic electrons. Some of the steps taken to reduce the severity of these problems are given below.

(a) Unabsorbed stress-crazing agents were normally removed from specimens; when present they cause deterioration of the specimen after coating, and instability of the image.

(b) The conductive coating was made as uniform as possible. While it is inevitable that deep crevices and the like could not reasonably be coated, every effort was made to spray the metal slowly whilst the specimen was rotated and gyrated. This reduces variations in the thickness of the coat and so misleading contrast.

(c) High tilt angles were used so that the geometry of the surface of the specimen relative to the electron beam and X-ray detector enabled high contrast images and efficient X-ray collection.

(d) When the specimen did not require X-ray analysis, a fine electron beam spot size was used to reduce specimen damage and enhance resolution. This was achieved by using a high condenser lens current. The poor signal to noise ratio was overcome when photographs were taken, because of the slow raster rate.

(e) Slow travel of a high energy beam over a small area produced etching of the polymer surface, and sometimes further decomposition. As this was unavoidable when some

types of X-ray analyses were conducted, the procedure adopted was to photograph the area of interest using low energy, small spot size electron beams first; then limited destruction of the sample was of less consequence.

(f) Voltages of 10 and 20 KV were found satisfactory for most purposes. Rarely a lower voltage was necessary; lower resolution and contrast resulted.

Scanning electron microscopy was carried out using an "Autoscan" instrument, equipped with an eucentric focussing stage, and a Nuclear Chicago energy-dispersive X-ray detector with Packard Multichannel analyser. Operation of the microscope did not require deviation from normal procedures, except for the precautions listed above.

3.3.3. Energy Dispersive X-ray Analysis

When electrons of high energy impinge upon a specimen, X-rays with energies characteristic of the irradiated elements are produced. When the voltage used is 20KV, and a high flux of electrons reach the specimen, X-rays are produced which are collected by a silicon X-ray detector. For reasons which need not be mentioned here, it is possible to measure only X-rays characteristic of elements with an atomic number greater than or equal to 11 (sodium).

Each count is registered in a single channel representative of the energy of the X-ray. When a large total number of counts have been collected, a "histogram" is produced, with each channel containing counts from X-rays of the appropriate energy. The resultant spectrum will have peaks located at energies which can be read directly on the analyser. By referring to tables of prominent line energy values for all elements, it is then possible to deter-

Fig. 3.4. A typical energy dispersive X-ray spectrum of a nylon sample with absorbed zinc chloride.

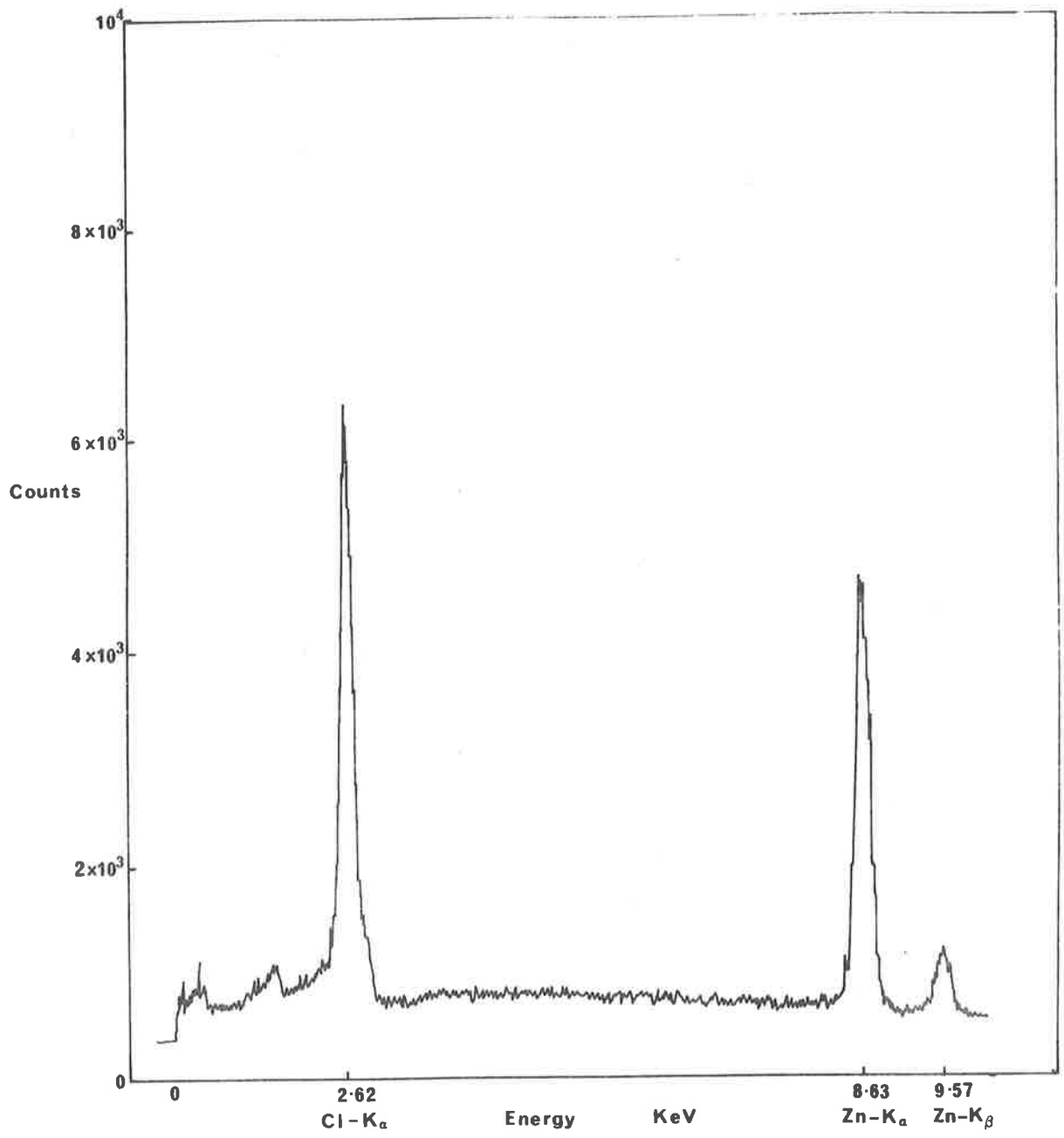


Fig. 3.4

-mine which elements (with $Z < 11$) are present.

In a nylon sample which has been treated with aqueous zinc chloride solution, for example, and then made conductive with carbon, only zinc and chlorine will produce X-rays which are registered in the spectrum (all elements in the nylon have $Z < 11$). An example of such a spectrum is shown in Fig. 3.4.

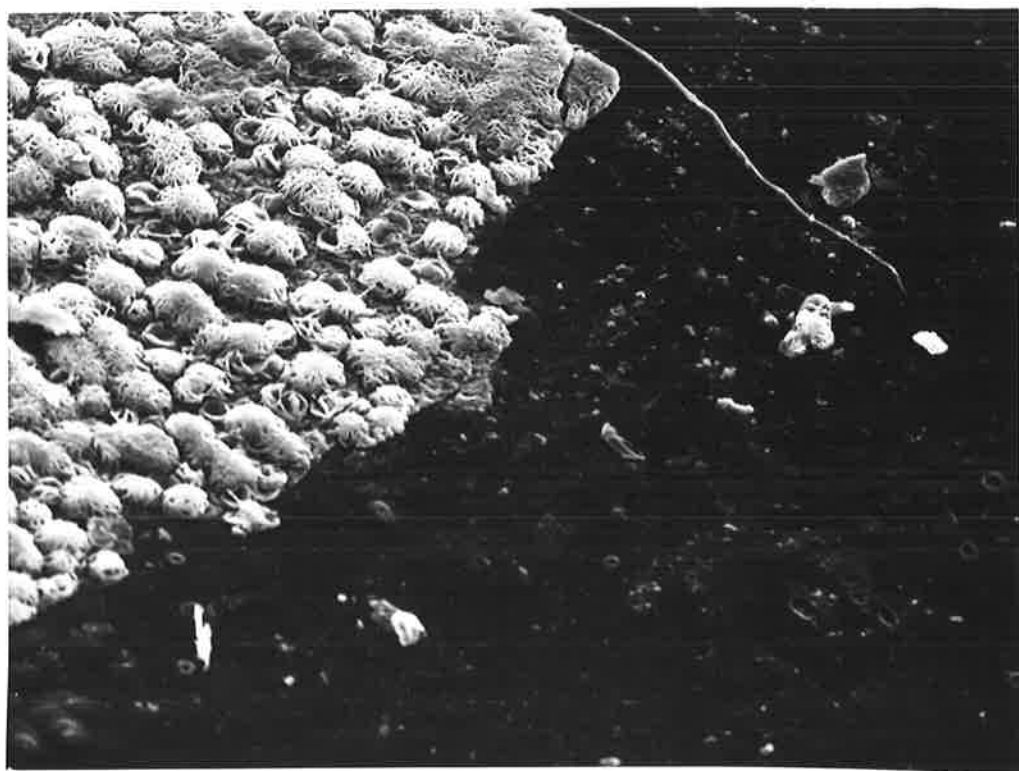
The analyser used was only able to give semi-quantitative results, but was still invaluable because not only could a spectrum of elements be recorded, but other related information modes could be used.

For example, when the electron beam slowly rasters across the specimen in the photographic recording mode, X-rays of many energies will usually be produced (depending upon the elemental composition). All the counts received from each "micro region" (a small element corresponding to the area upon which the beam "dwells" for a small fraction of a second), are transmitted to the analyser. The analyser is adjusted to retain all counts which fall in channels corresponding to the element of interest; all other counts are electronically erased (by adding an equal number of "negative counts" to each channel). The counts which remain are returned to the microscope where they are recorded on the viewing screen. In this way, an "X-ray map" of a particular element is produced which correlates with the normal image of the specimen.

An example of an X-ray map is shown in Fig. 3.5 next to the normal image. In this instance, X-rays with an energy of about 8.6 KeV (Zn $K\alpha$ emission) have been selected. The sample is a thin nylon 6 film dosed with zinc chloride (seen at top left).

Fig. 3.5.a. An ultra-thin nylon 6 film with zinc chloride treated region at top left (white).

Fig. 3.5.b. Associated "X-ray map", produced with 8.6 Kev (Zn K_{α}) X-rays.



Another display mode reveals the concentration of an element as the beam traverses the specimen once only. A high intensity electron beam is made to traverse the region of interest slowly. The multichannel analyser is adjusted to discriminate for a particular element (as before), so that there appears on the screen of the analyser a histogram of "element counts" versus cross-section. When conditions are set for a very slow scan rate, the total counts received will be high, making the background counts less significant. A "line-scan" for a nylon specimen containing zinc chloride, with the analyser discriminating for zinc, is shown in Fig. 3.6.

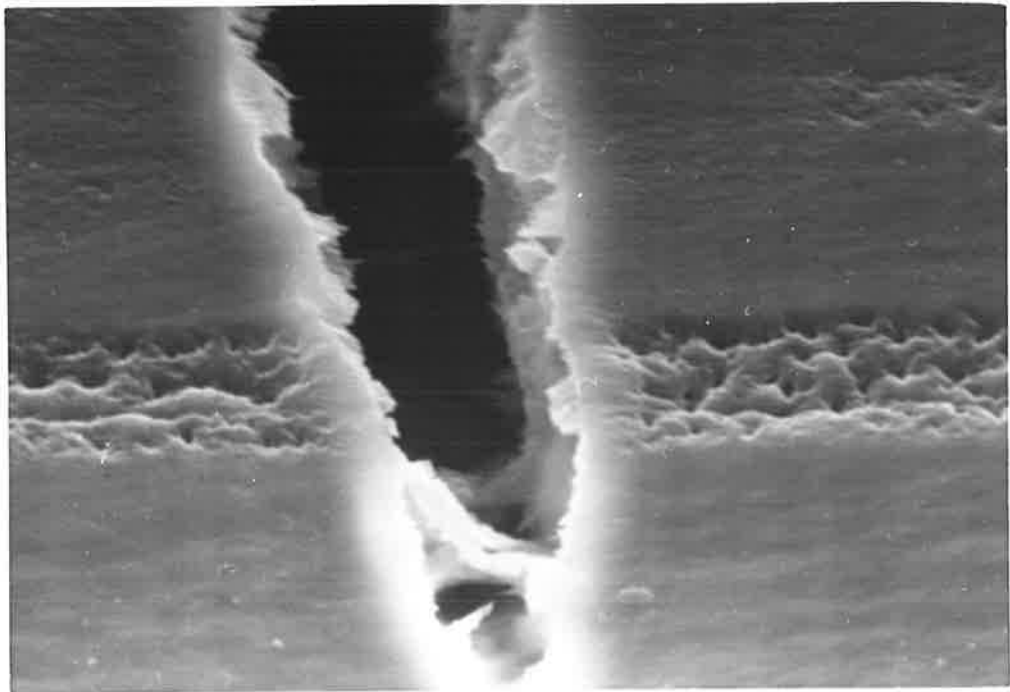
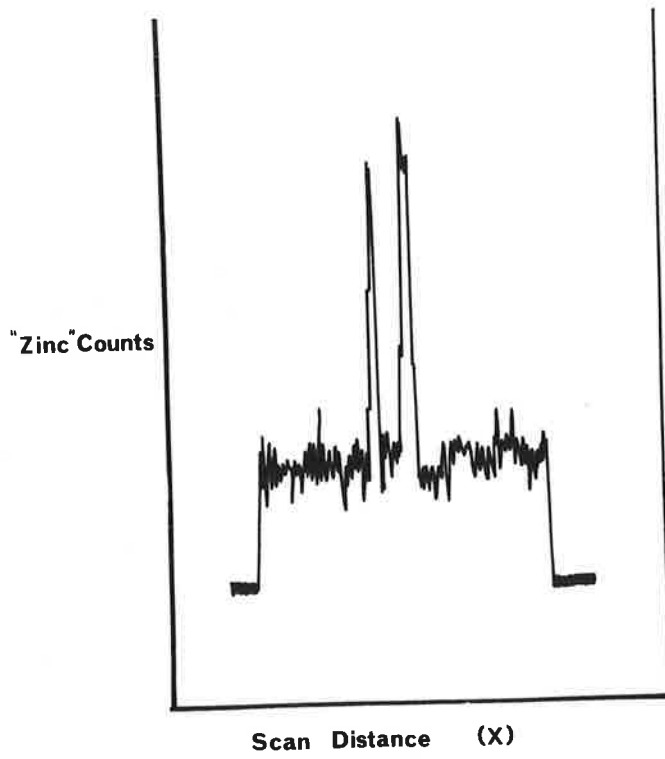
One of the disadvantages of this technique is that large electron beam spot sizes and high voltages are required to give a sufficiently large number of counts. When the energetic beam remains on a small area for a long time (which commonly occurs, especially at high magnification), specimen damage invariably results. The "imprint" of the beam as it has passed over the nylon 6 specimen, to give the line-scan, is shown in Fig. 3.7.

The problem of localised melting of polypropylene has been noted by Way and coworkers [123] and they compromised by using lower voltages and accepted lower resolution as a consequence. Breedon and coworkers [124] and Grubb and Keller [125] found that topographic features in polyethylene (such as spherulites) were accentuated after short exposures to the electron beam.

The resolution for X-ray analysis was limited to approximately 1 μm (point to point), so that high resolution studies were not conducted. At high magnifications it was

Fig. 3.6. Representation of a "line-scan" across zinc chloride cracked nylon 6 (discriminating for Zn $K\alpha$ radiation).

Fig. 3.7. Morphology of specimen which the intense electron beam used to give Fig. 3.6 has traversed. The etching of the nylon was deliberately made excessive to show the beam path.



important to recognise that volatile compounds within the nylon could be vaporised and so abnormally low X-ray readings would result from an area that had previously been subjected to a slow scan.

The scanning electron microscope has proved to be of great assistance in discovering the morphology of crazed nylons. Further improvements and a larger range of accessories are continuously increasing the ability of the S.E.M. to analyse materials [126].

3.4. Tensile Testing of Polymers

3.4.1. Method Used

Quantitative tensile testing was performed using an Instron floor model, type TT-DM machine, which was un-modified, except that for small specimens (with thickness less than 0.20 mm), small brass screwdown grips were used. All tensile tests were performed at $20 \pm 2^{\circ}\text{C}$. Tensile curves relating time elapsed (proportional to distance between the grips at constant crosshead speed) with load (in Kg) were obtained. The strain was then determined knowing the gauge-length. Some polymer samples were also strained in a simple testing device which could be mounted in an optical microscope, enabling direct observation of changes in the morphology of the specimen. As the main purpose of the work was to study morphological changes during stress crazing, the device was often used when no mechanical data was required.

Simple tensile machines and clamps were constructed so that films could be strained, and then coated (whilst

still in tension) with gold or carbon in preparation for examination in the S.E.M.

3.4.2. Interpretation of Results

The procedure adopted for carrying out stress-crazing experiments with nylons was to apply a small droplet of the crazing-agent to the specimen, usually just prior to straining. A discussion of the reasons for using this method, and for not using others, is given in Section 3.4.3. Rather, the purpose of this section is to introduce the method used to describe craze morphology.

The whole craze which forms cannot be viewed in its entirety, because nylons are not transparent, and so it is necessary to use indirect methods of observation.

The surface enlargement of a craze can be easily observed and so is a valuable indicator to the overall development of the craze. Another advantage is that it can be directly viewed at high magnifications, but coupled with this are two disadvantages. Information relevant to the total structure of the craze which can be derived from surface features is limited, and furthermore, interpretation may be misleading, because the conditions at the surface are different from those within the bulk polymer, where areal growth occurs.

Knowledge of the cross-section of the craze, passing through plane abc in Fig. 3.8, adds another dimension to the understanding of the mechanics of craze growth.

Either the natural progression of a crack can be allowed through the crazed zone, until separation occurs, or alternatively, the straining process can be stopped at a particular stage in craze development, and then separation

can be effected by using very rapid strain rates and/or liquid nitrogen temperatures to promote brittle fracture. Whilst both these methods are commonly used by workers investigating crazes in glassy polymers, it is necessary to bear in mind the possibility of misinterpretation. Retraction of highly strained filaments, limited ductile yielding at low temperatures [102] and other artifacts can make fractographic conclusions ambiguous.

Two aspects of crazing: surface morphology (through plane AA'B'B) and fracture morphology (through plane abc) with an indication of the progression of events in the crazing process, will be given generally in Section 4.1.

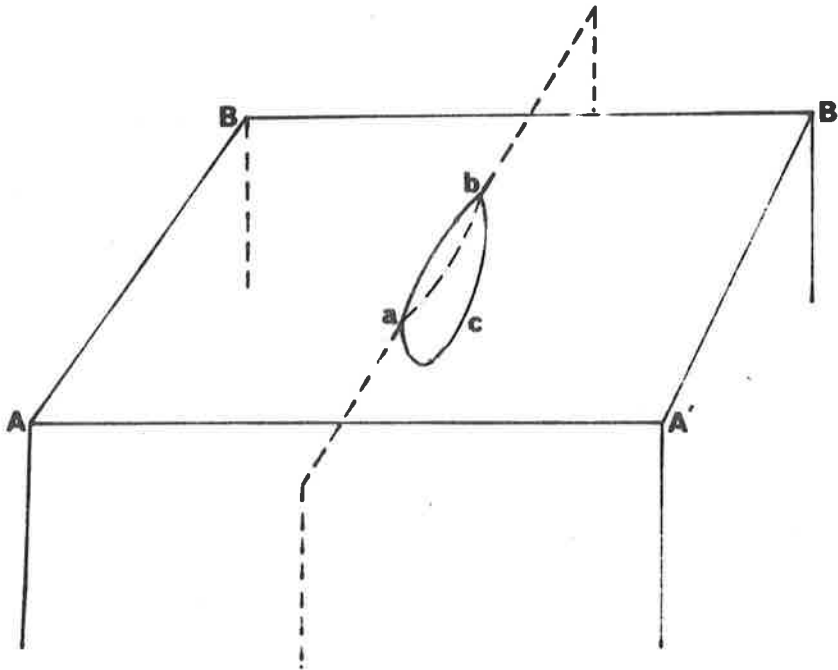


Fig. 3.8 .

3.4.3. Justification for the Test Method Used

The method of inducing crazing which was selected, namely placing a drop of solution on the specimen and loading at a fixed strain rate, can be criticized for lacking in precision, so it is appropriate to examine alternative methods

and discuss the reasons for rejecting them.

- (a) Complete immersion of the specimen in the active solution and application of a fixed strain rate or fixed stress.

There is little to be gained in complete immersion of the specimen. Firstly, craze and crack growth will occur at the point of maximum stress concentration, and so will give no more valuable or informative data than the adopted method.

Secondly, it would be difficult to remove the specimen from the solution quickly, after the advent of crazing. The preservation of crazed specimens which are free from artifacts (caused by subsequent modification with the residual agent) would be practically impossible if this method were used.

- (b) The application of a variable strain along the length of the specimen to determine the critical strain for crazing, and

- (c) The application of constant loads to the specimen to determine the critical stress for crazing.

The principle behind methods (b) and (c) is that there exists either a strain or stress criterion for crazing. As pointed out by Kambour [55], there still remains uncertainty as to which criterion is valid. The reason for the lack of agreement undoubtedly lies with the very nature of crazing, in that the process is complex, with a number of physical processes being operative simultaneously, both across the length of the craze, and at the crack tip. (This problem is currently being approached by trying to isolate each

process and determining the effect of varying test conditions upon it.).

(d) The application of a fracture mechanics approach related to (i) the stress intensity factor, K

(ii) the strain energy release rate, G

or (iii) some modification of a linear elastic fracture mechanics theory incorporating the Dugdale model or the crack opening displacement theory which takes into account the non-linear elastic behaviour of polymers.

These methods have been applied with some success to explain the behaviour of "brittle" polymers such as polystyrene or P.M.M.A., in the absence of a hostile environment. However, in "semiductile" or "ductile" polymers such as rigid PVC, [143] or when active environments are present, these methods are not as successful.

The method was discarded, then, because it did not appear to contribute readily to the understanding of basic deformation mechanisms.

The droplet test method gave results which were internally consistent and reproducible, when efforts were made to keep test conditions constant (for example, the droplet size was kept uniform by using a micro-syringe). Once deformation had commenced, deformation is extremely localised and so this contributes to the consistency of the results obtained. In the context of the work it was considered that the approach taken was preferable to the alternatives listed above.

CHAPTER 4.THE MORPHOLOGY OF CRAZED NYLONS4.1. Introduction

In this section the mechanism of craze and crack development will be described in general terms, for both treated and untreated nylons. There are three parts;

- (i) a description of the conditions which lead to fracture in untreated nylons,
- (ii) an account of the morphology of the fracture surface of untreated nylons, and
- (iii) the morphology of agent-induced crazed nylons.

One of the problems which needs to be outlined at this stage is that of nomenclature. It is difficult to distinguish precisely between three separate events,

- (a) the passage of a crack through agent-induced craze, which existed before the crack initiated,
- (b) the passage of a crack through well-developed craze matter, which has again been agent-induced, but which has been produced subsequent to crack initiation, and
- (c) the passage of a crack through a craze, in the absence of agent; in particular, where the crazed zone is confined to a localised, highly stressed region near the craze tip.

Although it is realised that some compromise is being made at the expense of scientific precision, the following convenient expressions will be used to distinguish between each of the three phenomena. The first (a) will be called

crack propagation through "preformed mature craze", the second (b) will be called crack propagation through "mature craze" and the third (c) will be designated "ductile fracture".

The third example is considered justified, because of the evidence provided by Hull and Owen [127], for example, (which will be discussed later) which shows that viscoelastic deformation precedes fracture in polymers.

4.1.1. The Fracture of Untreated Nylons

To provide, as it were, a datum for analysis of environmental stress crazing of nylon specimens it will be helpful to appreciate the fracture morphology of nylon specimens that have been fractured in the absence of the aggressive environment.

Assuming that a notch defect exists at the surface of the specimen then the fracture mechanism can best be understood by considering the two extremes of stress field conditions as depicted schematically in Fig. 4.1.1, namely plane strain and plane stress conditions.

Plane strain conditions will be prominent in situations where

- (a) a notch defect is present
 - (b) the specimen is relatively thick
- and (c) the yield stress is relatively high (at high strain rates or at temperatures well under T_g).

At the tip of the crack the stress distribution arising from elastic strains will be as shown in Fig. 4.1.2. (If plastic strains are considered the stresses will be magnified ahead of the plastic zone, but the resultant effect will be similar.

Fig. 4.1.1. Plane Strain Vs. Plain Stress Conditions

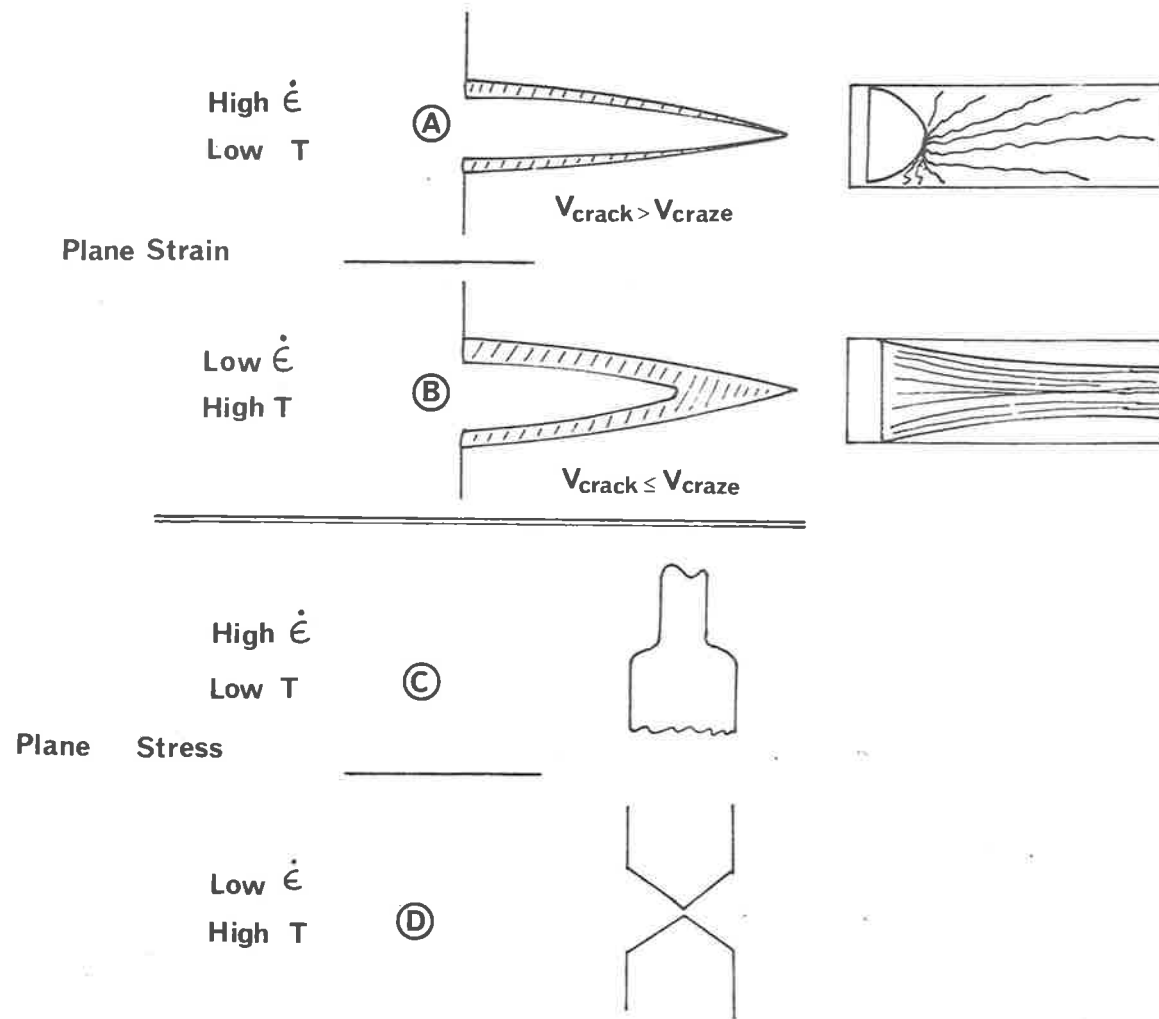


Fig. 4. 1. 1.

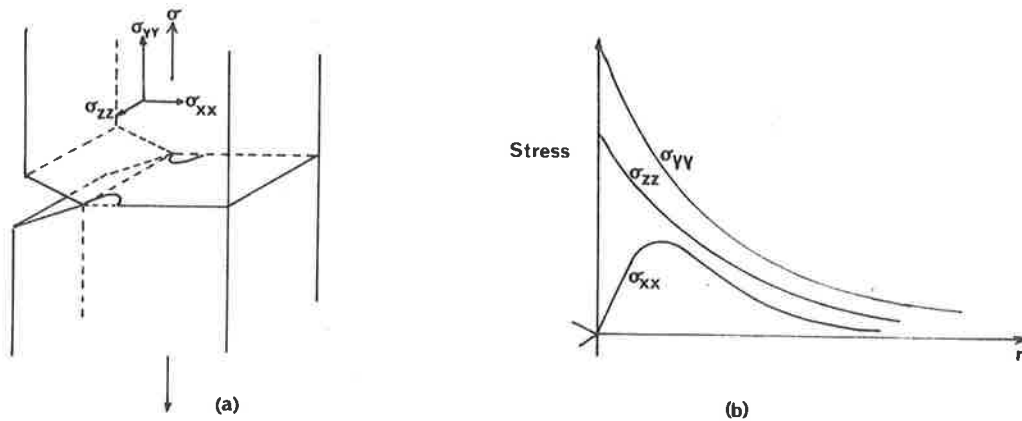


Fig. 4.1.2.

When the principal tensile stresses σ_x , σ_y , σ_z are approximately equal then a condition of equal triaxial stress distribution exists and the only available mode of deformation will be by rapid crack growth, with cleavage of primary bonds.

If the yield stress is lowered by reducing the strain rate or by lowering the temperature, or by reducing the sharpness of the notch, then the condition of approximately equal triaxiality will not exist. Under these conditions net shear stresses are present and plastic deformation by sliding of chain segments is possible. When this occurs, formation of microvoids, and associated limited plastic deformation may occur, to produce a crazed area.

The production of cavities in the presence of certain defects is facilitated by dilatant forces, but the molecular sliding motion which then occurs requires a localised reduction in the flow stress. Gent [1,2] considers that the glass transition value of the polymer is effectively reduced because the increase in free volume during dilation facilitates movement of chains. At some stage after craze formation a crack will initiate within the craze, and begin to propagate.

To assist in the analysis of events during fracture, the velocity of propagation across the specimen of three entities will be considered:

- (a) the velocity of the craze, v_{craze}
- (b) the velocity of the crack propagating within the craze, $v_{\text{crack-craze}}$ (both in preformed and other "mature" craze) and
- (c) the velocity of the crack propagating within the bulk polymer, v_{cleavage} .

It is proposed that at a constant strain rate, the velocities have the relative values shown in Fig. 4.1.3.

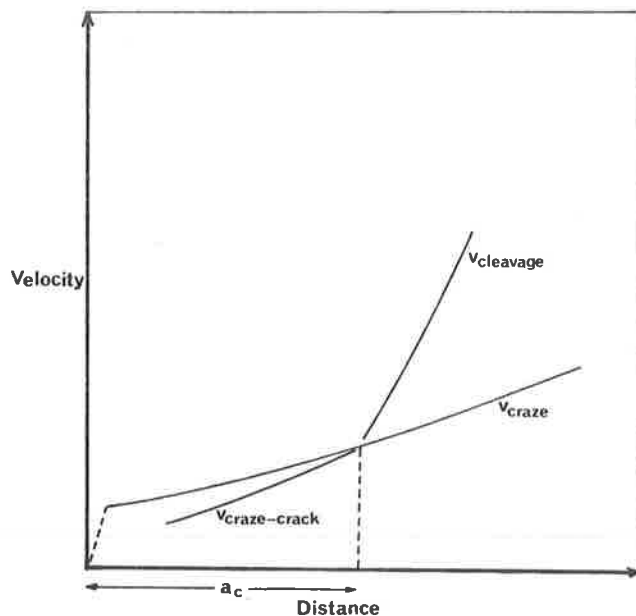


Fig. 4.1.3.

The only relevant information on craze velocities is that obtained by Higuchi [21], who found that for a constant strain rate the craze growth velocity was constant,

$$\text{i.e.} \quad \frac{dlc}{dt} = \beta \dot{\epsilon}$$

The process of crack initiation and growth in the preformed craze appears to be controlled by very similar parameters to those which control craze growth. Kambour [55] has stated that the evidence suggests that "both craze growth and breakdown are time dependent processes with marked viscoelastic features, but that these processes, while similar, are not identical." However, the craze is capable of carrying a load whilst of course the crack is not and so the velocity of the crack will increase as the stress intensity increases. Thus a point will be reached where the crack overtakes the craze front and the possibility exists that a crack will then initiate free of preformed craze material.

If the strain rate is reduced or the temperature raised, then the viscoelastic processes in the craze region will be allowed to occur although the elastic constraint of the undeformed bulk polymer will prevent large scale deformation (see section 2.2.1.). In this case the crack velocity will be less than or equal to the craze velocity.

The other extreme stress condition is that of plane stress, which is favoured by

- (a) the absence of a notch
 - (b) a relatively thin specimen
- and (c) a yield stress which is relatively low (for example, when the strain rate is low or the test temperature $\geq T_g$).

Plastic instabilities occur with the formation of a neck. If the work hardening rate is high and intermolecular colusion is maintained, then cold drawing will result. If the work hardening rate is too low then the instability will continue and failure soon follows (Fig. 4.1.1).

4.1.2. The Morphology of Untreated Nylon Fracture Surfaces

The fracture morphology of nylons having

- (a) a brittle fracture surface
 - (b) a "ductile" fracture surface
- and (c) a fracture surface containing both brittle and "ductile" fracture zones, is given.

The brittle fracture was induced by straining an anhydrous test-piece which had been immersed in liquid air, at a crosshead speed of 50 cm/min. The fracture surface appears in Fig. 4.1.4, and the initiation zone at higher magnification in Fig. 4.1.5. At the magnifications used, no fine structure indicative of viscoelastic deformation can be seen although other workers have reported that limited deformation (resolved at very high magnifications) can be detected at temperatures as low as 20°K. During the fracture process only small amounts of energy are absorbed.

In this specimen the crack is not passing through a precrazed region, nor is crazing preceding the crack tip. The stored elastic energy is being released at a much greater

Fig. 4.1.4. Brittle fracture surface of nylon 66.
Magn. = 25x

Fig. 4.1.5. Same surface showing initiation zone.
Magn. = 980x

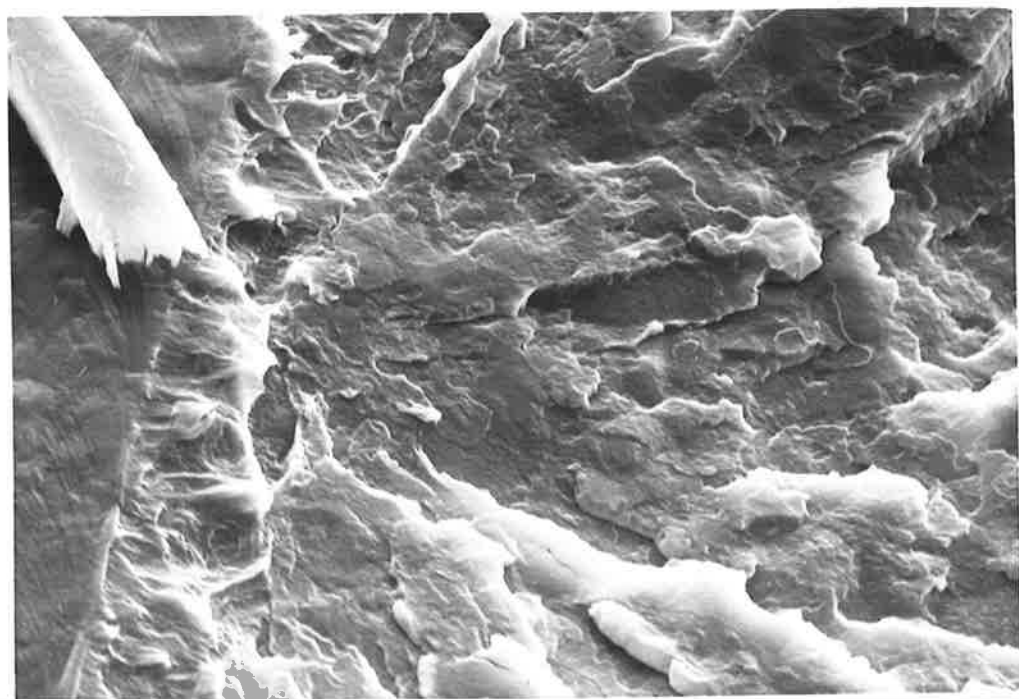
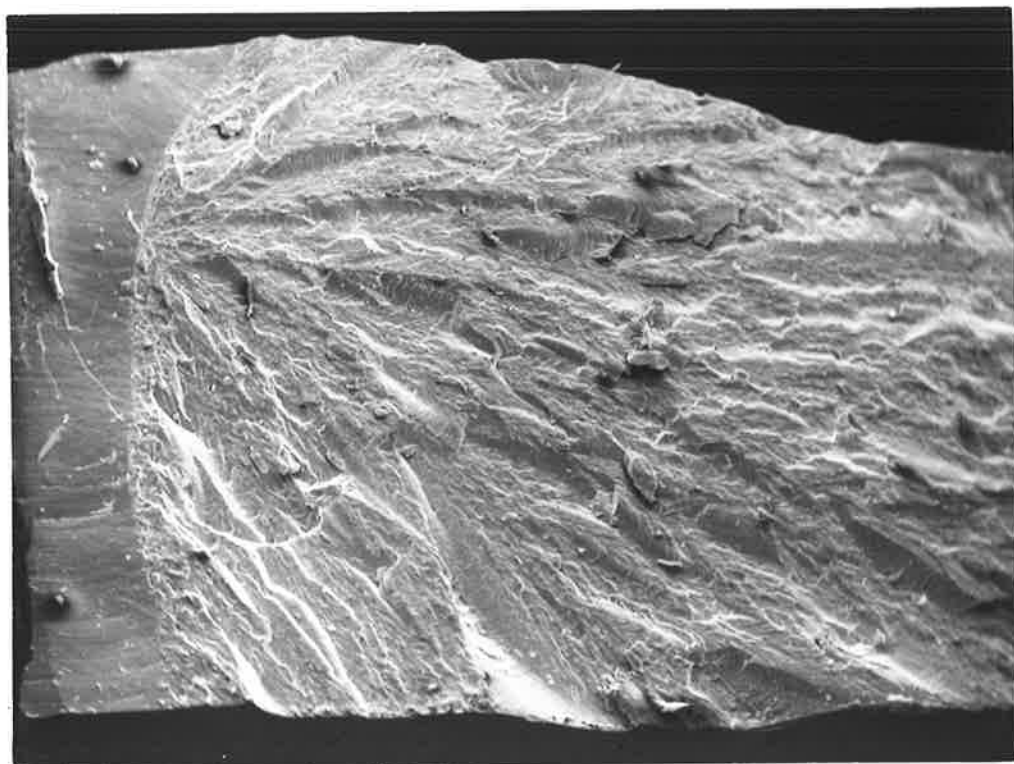
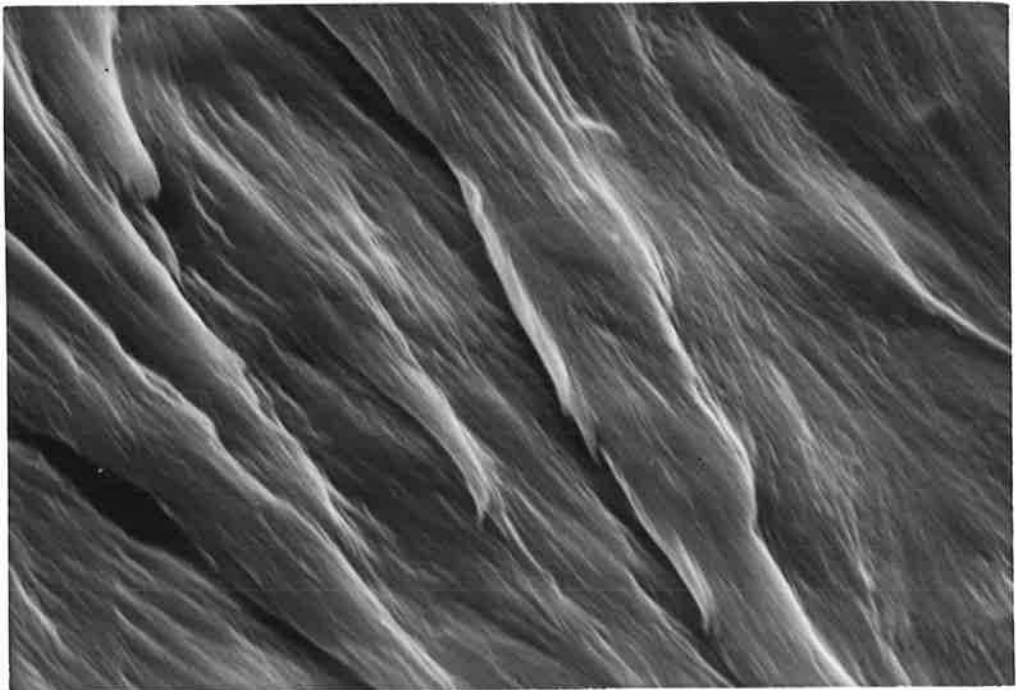
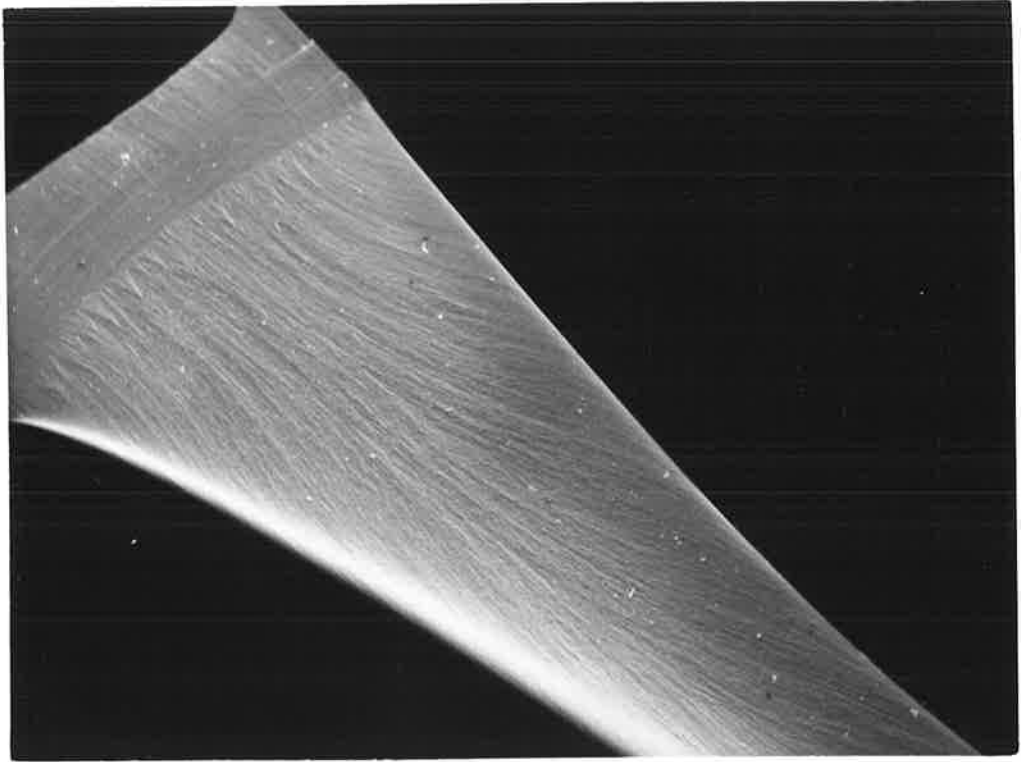


Fig. 4.1.6. "Ductile" fracture surface of nylon 66.
Magn. = 20x

Fig. 4.1.7. Fine detail of surface at centre of
specimen shown in Fig. 4.1.6. Magn. = 2040x



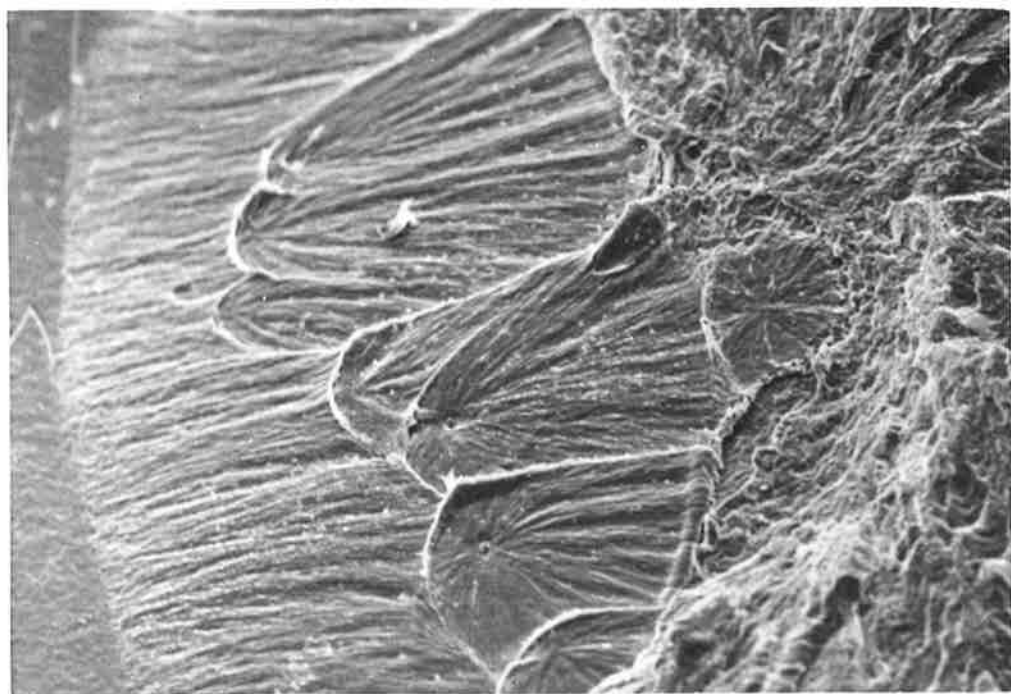
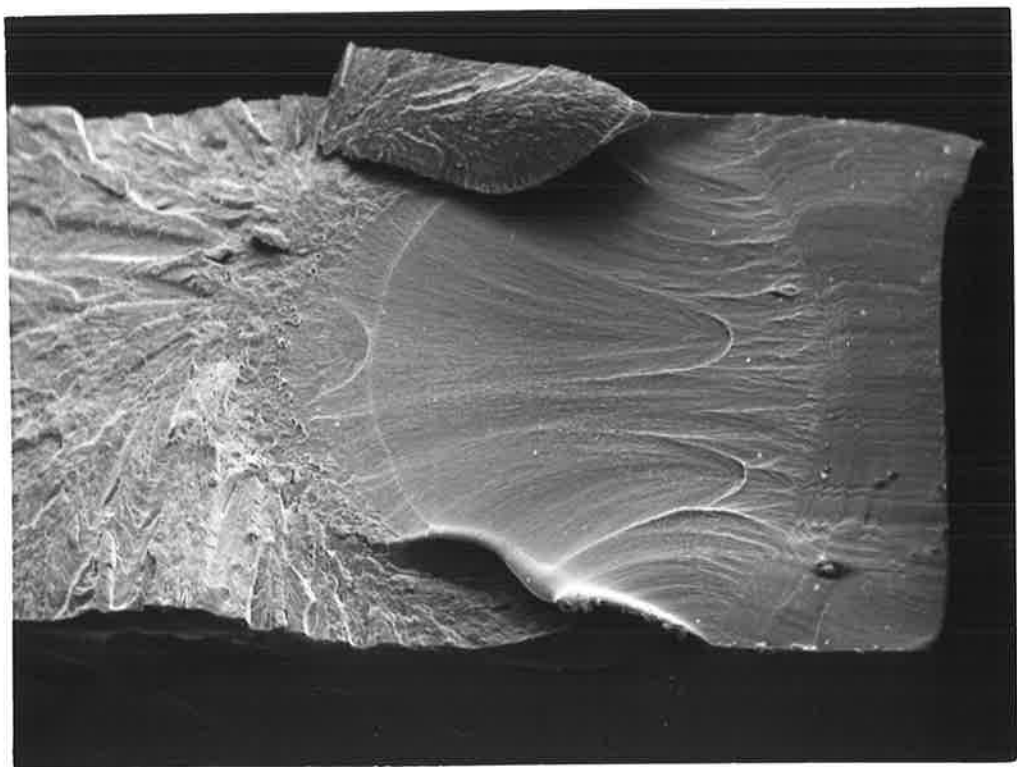
rate than that which is required to supply the surface energy requirements of the new faces and any viscoelastic energy absorption process at the crack tip. The excess energy is converted into kinetic energy and the crack accelerates to a high velocity, and may begin to fork. The stress field apparently becomes unstable, and oscillates about the horizontal plane, to give ridges and steps. Although the crack does not propagate along crystallographic planes, the general faceted structure may be compared with that found in glasses and metals.

When a notched, "as received" nylon 66 testpiece is strained at room temperature with a crosshead speed of 1.0 cm/min., a "ductile" fracture, as shown in Fig. 4.1.6, is produced. The highly drawn microstructure of the fracture face, shown in Fig. 4.1.7, is from the centre of the region shown in the previous photograph. The exact processes which are occurring cannot be determined from the morphology of the surface, but by analogy with the results carried out on amorphous thermoplastics by Hull [127] and Kambour [63], it is proposed that craze formation precedes fracture. In this particular specimen the texture is relatively uniform, across the fracture face, suggesting that the crack velocity has remained relatively constant.

When a notched nylon 66 specimen was strained using a crosshead speed of 50 cm/min. at room temperature, both "ductile" and brittle fracture faces are seen in the specimen [Fig. 4.1.8]. The explanation is similar again to that used to describe fracture in glassy polymers.

Fig. 4.1.8. Fracture surface of nylon 66 showing transition from ductile to brittle fracture. Magn. = 23x

Fig. 4.1.9. Secondary fracture, characterised by hyperbolae, initiated by visible inclusions of foreign matter. Fracture proceeds from left to right. Magn. = 47x



At first the crack propagates at a low to medium velocity, with limited viscoelastic deformation occurring in front of the crack tip. As the velocity increases, the amount of deformation at the tip decreases (as reflected by a "fining down" of the surface texture as the distance from the notch is increased).

The stress intensity factor will be high, so that it is possible that stresses greater than the fracture stress may arise at heterogeneities in front of the tip, and so initiate secondary fractures. The interaction between the crack-front from the heterogeneity, and the main crack front (each travelling at different velocities), gives rise to characteristic hyperbolae which can be seen in the ductile fracture zone in Fig. 4.1.8. They are readily observed, because secondary fracture is not on the same plane as the main crack front. Presumably limited crazing precedes secondary fracture as well, so that in effect two highly localised craze zones interact at the interface between primary and secondary fracture (as suggested by Hull and Owen for polycarbonate [127]).

Easily resolvable inclusions have initiated secondary fracture in the nylon 66 specimen shown in Fig. 4.1.9. (X-ray analysis showed that they contained calcium and silicon, and so are traces of dirt, which must have contaminated the nylon before or during the molding process.)

As the crack velocity increases during the test, crazing in front of the accelerating crack tip diminishes. Brittle fracture ensues in the central region where plane strain conditions are optimized.

The two distinctive morphological types occur in the fracture surfaces of many of the environment stress-crazed specimens and are designated regions 3 and 4. When they occur, it is considered that they are characteristic of the untreated polymer, and cannot be attributed, per se, to the presence of stress-crazing agent.

4.1.3. Morphology of Stress-Crazed Nylons

The study of the morphology of craze and crack growth is quite complex both in relation to position and time of events, and so to facilitate discussion, the following mechanism is proposed. Discussion of the validity of these stages and the various exceptions will be properly dealt with in later detailed descriptions.

Failure occurs by craze initiation at the surface followed by areal development of the craze (Fig. 4.1.10). A crack subsequently commences and follows the craze path, and depending upon the conditions, the possible extremes of behaviour are:

- (a) the craze continues to expand across the specimen and the crack size remains relatively small
- or (b) craze growth is interrupted by the rapid crack growth which will overtake the craze and propagate through the bulk.

From the observation of fracture surfaces of a large number of nylons stress-crazed in the presence of salt solutions, it has become clear that there are many analogies with surfaces of crazed glassy polymers, so that it is inevitable that much of the terminology used will be the same. The pattern of craze morphology as indicated by fracture surfaces is represented in Fig. 4.1.11.

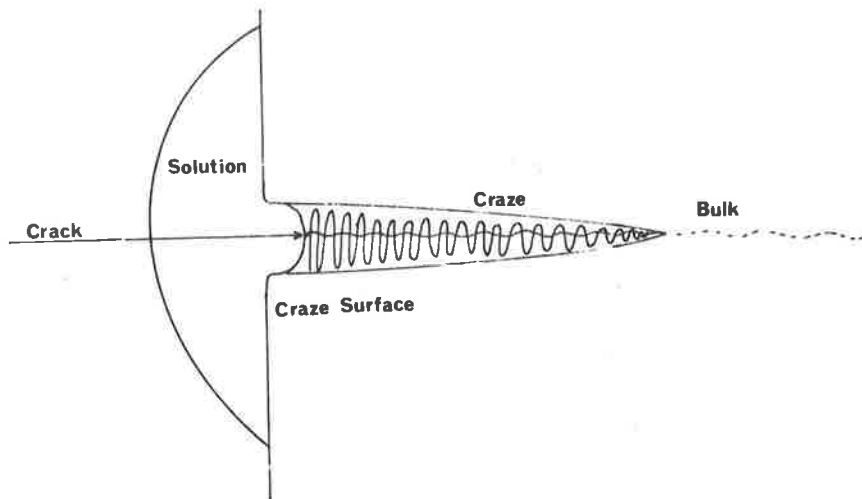


Fig. 4.1.10.

The four regions which are shown in the fracture surface of nylon 66 crazed with 4M zinc chloride are typical of many specimens.

Region 1 is the initiation site.

Region 2 is the region of agent-induced craze development.

Region 3 is the slow-medium crack velocity zone, where crazing precedes the fracture tip, but where no mature agent-induced craze has pre-existed.

Region 4 is the brittle fracture zone.

Regions 1 and 2 will now be discussed in more detail.

Region 1 - The Initiation Site

Crazing in semicrystalline polymers initiates at the surface, where there is an abundance of crazing agent. The exact source of initiation in homogeneous polymer is not known, but from evidence obtained from the internal crazing

Fig. 4.1.11. Montage of fracture surface of nylon 66 stress crazed with zinc chloride, showing Regions 1-4. Magn. = 505x



4



3



2



1

of rubber modified polymer [15,16] and from the effect of sharp mechanical notches on the surface [144], it appears that conditions which favour a triaxial stress state are necessary. In proposing a mechanism for craze initiation, it is generally agreed that a "flaw" or inhomogeneous region is required, but there is still little agreement about the nature of the "flaw". For the uptake discussion given below, it is assumed that a microscopic scratch has resulted in a V-cut into the surface of the sample, which produces a triaxial stress state, as shown in Fig. 4.1.12. Further, it is assumed that should heterogeneities (such as holes and foreign matter) exist in the polymer, that they will cause anomalies in the uptake of crazing agents.

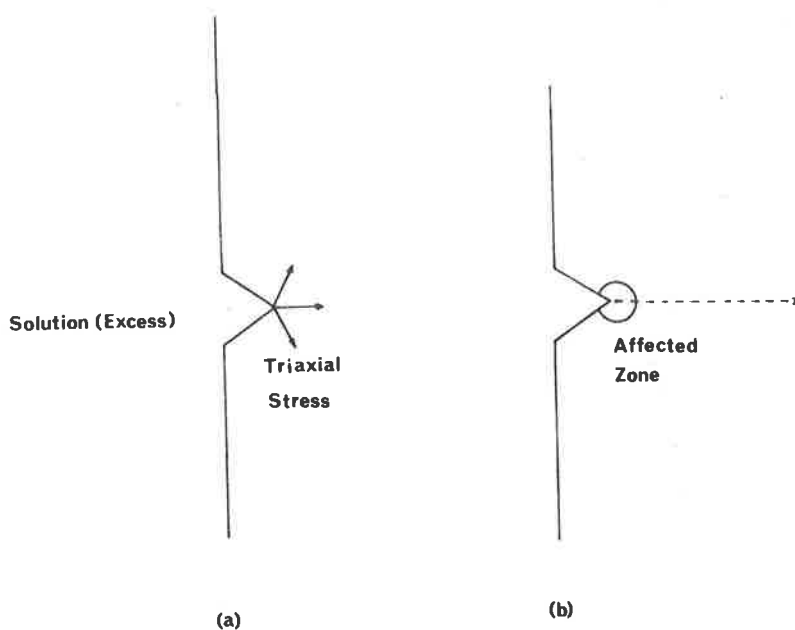


Fig. 4.1.12.

At the flaw two solution uptake processes may occur.

They are

(a) normal Fickian diffusion of the agent through the polymer

and (b) accelerated Case II transport as described in

Section 2.

Both uptake mechanisms will be modified by the incidence of pre-existing cavities and similar heterogeneities. If it is assumed that the uptake is confined to the zone where the stresses are concentrated (Fig. 4.12b), then a situation for craze growth exists, which is different from that shown in Fig. 4.12a.

We now have a zone of polymer which has been altered by cavitation and agent uptake. Complex modified triaxial stresses remain in this "new" polymer, which can cause the following changes:

(a) If it is assumed that the concentration of agent in the polymer is high, then the polymer will extend at low stresses and will rupture at a low elongation (see Fig. 4.1.18) in the discussion of the type II region).

(b) There will be continuing cavitation processes occurring in the direction indicated in Fig. 4.12b.

It is notable that the strain incurred in the initiation of a craze will allow some stress relief elsewhere so that further craze formation is in fact discouraged and one observes, under say slow strain rate conditions, relatively few crazes per unit area.

The morphology of the initiation zone is predicted to be relatively featureless, for three reasons. The initial flaw may be very small, elongation of the polymer in the presence of large amounts of agent will be limited and swelling and retraction of drawn material will blunten any discontinuities.

Figs. 4.1.13 and 4.1.14 show a typical region 1 morphology. At low magnification (Fig. 4.1.13) this region can be readily contrasted with the highly fibrillated and voided region 2. At high magnifications, (Fig. 4.1.14) apparent swelling is evident, but still no microdrawing or flaws are obvious.

If the agent is a particularly good solvent for the polymer then an extreme case for the extent of region 1 is predicted. Crazes formed will rupture at very low elongations and rapid retraction of fibrils will produce an almost entirely featureless fracture. The morphology and stress strain properties of nylon 66 "solvent cracked" with 99% (w/w) formic acid are shown in Figs. 4.1.15 and 4.1.16. This surface shown in Fig. 4.1.15 is similar to the initiation zone of some stress-crazed nylons.

A very weak stress crazing agent would be expected to produce little type 1 region. The amount of swelling and the reduction in the mechanical properties of the nylon would both be less extensive (see Fig. 4.1.18, this section). The nylon would be predicted to be able to sustain high strains (elongating to produce long filaments) even when the agent was abundant. Consequently, initiation is expected to occur at higher stresses, and the initiation zone (Region 1) to be poorly represented.

Fig. 4.1.13. Region 1 morphology - nylon 66 fractured in the presence of 4M aqueous zinc chloride solution. Magn. = 330x

Fig. 4.1.14. Same specimen surface at higher magnification. Traces of agent can be discerned at bottom left of photograph. Magn. = 670x

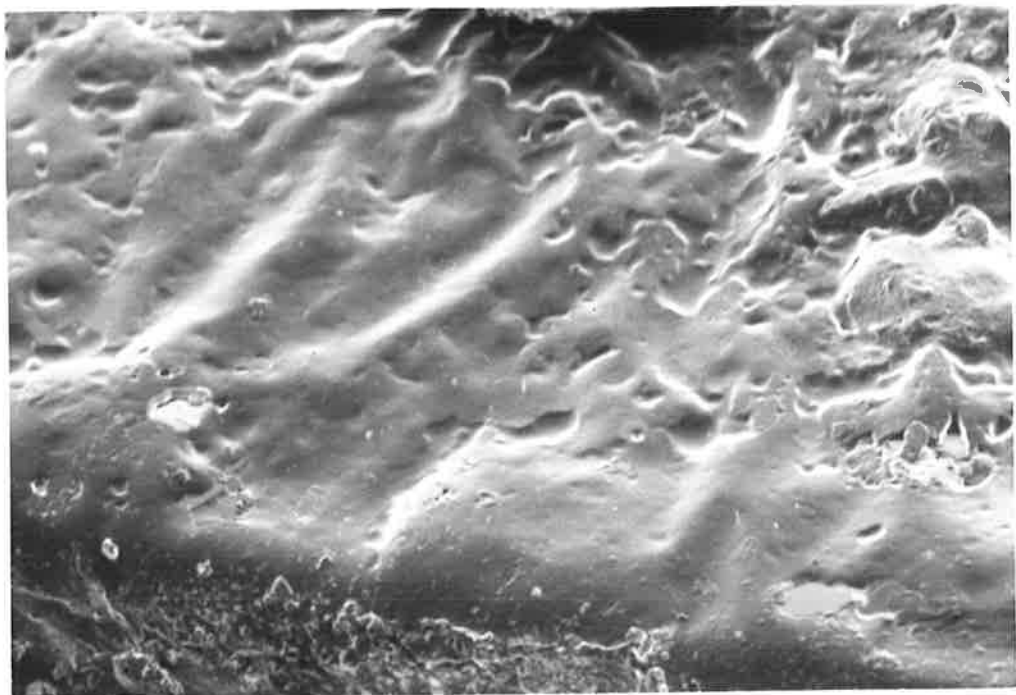
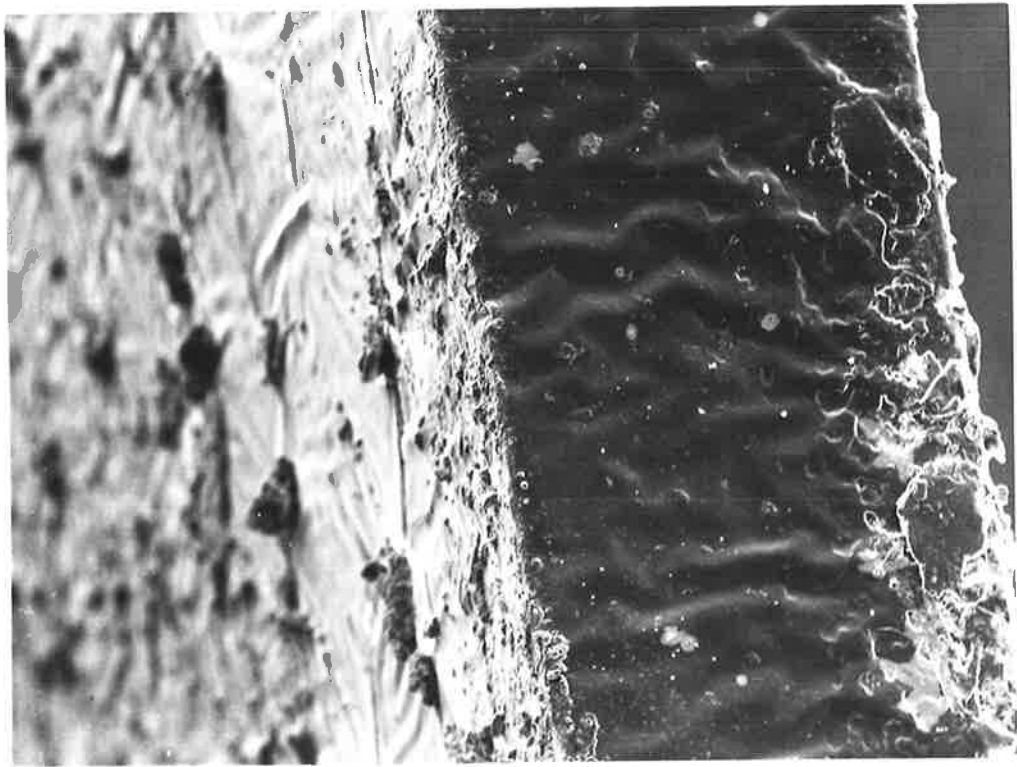
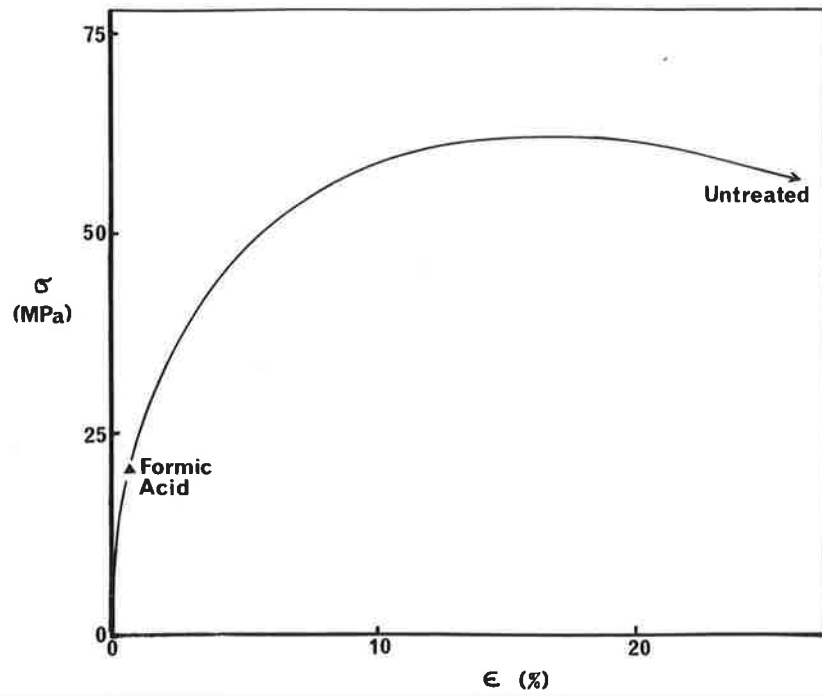
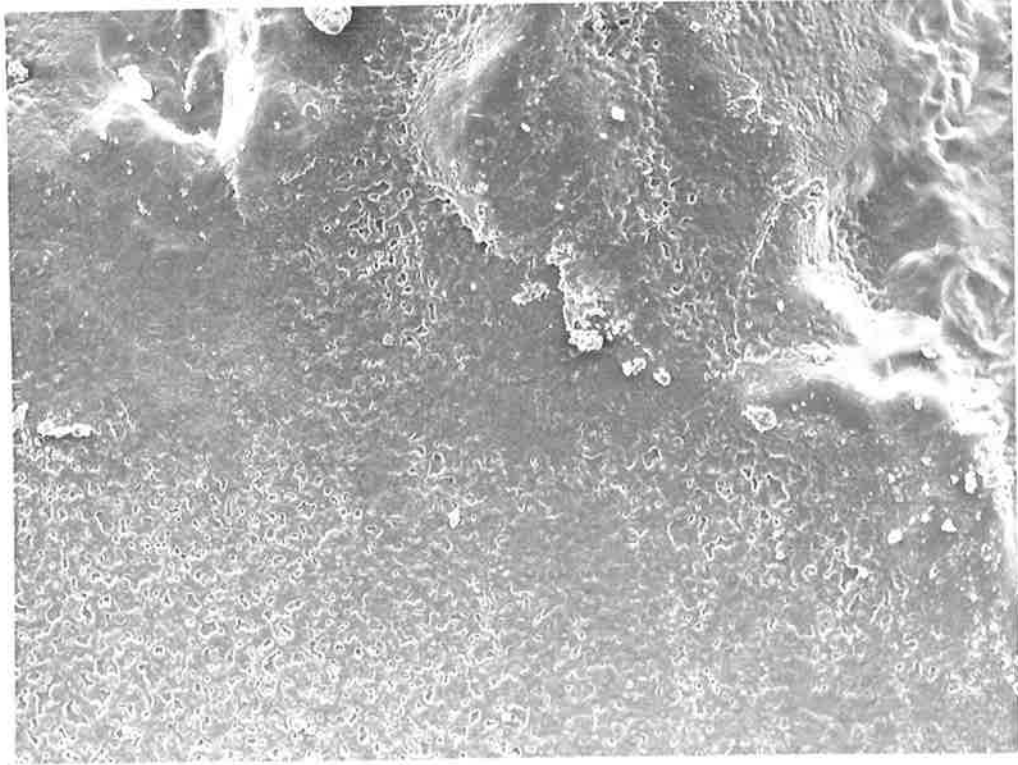


Fig. 4.1.15. Fracture surface of nylon 66 resulting from stress cracking with formic acid.
Magn. = 375x

Fig. 4.1.16. Mechanical behaviour of nylon 66 stressed with and without formic acid present.



Region 2 - The Craze Zone

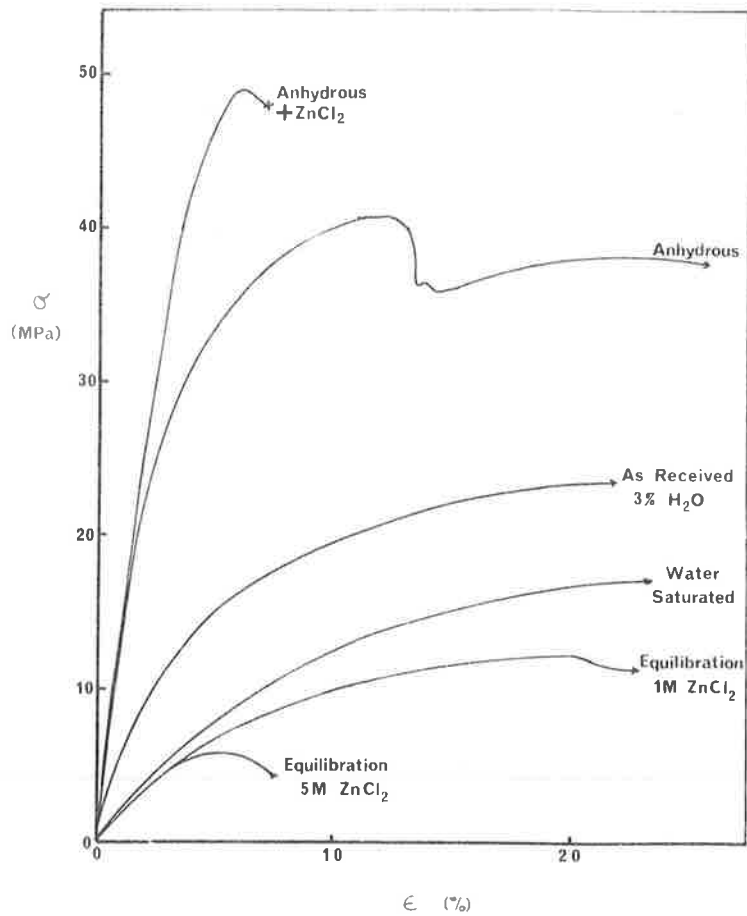
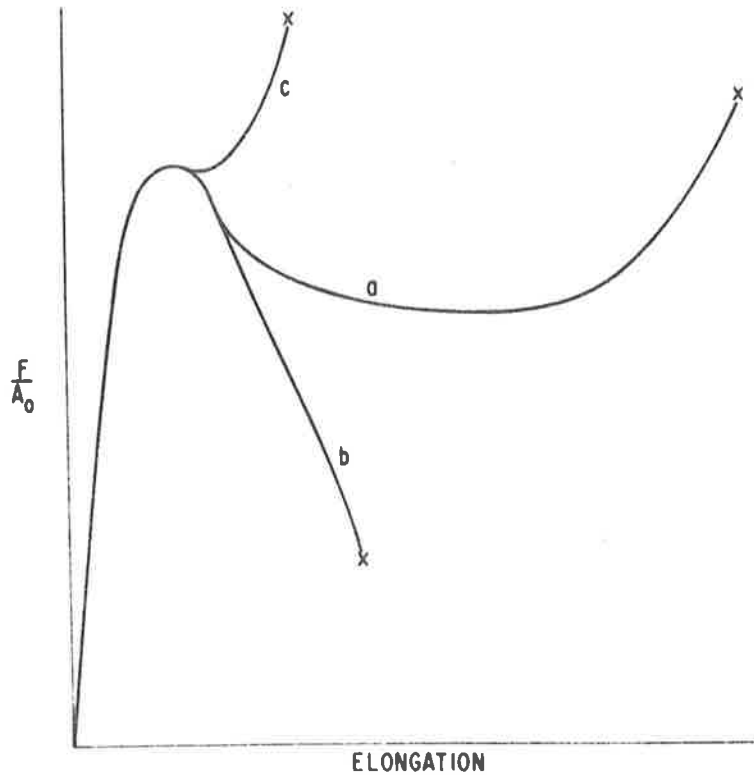
The marked transition from a smooth featureless region (1) to a highly filamented, voided region (2) reflects both the change in the micromechanical properties of the polymer, and the stress conditions which exist in each region.

Kambour [55] considers that two requirements exist for prominent crazing. The first, which is discussed earlier in this chapter, is "cavity nucleation at frequent intervals under uniaxial applied load". The second requirement is the appropriate type of stress-strain behaviour.

Fig. 4.1.17 illustrates three possible types of stress-strain behaviour for materials having the same yield point [55]. They were originally proposed to explain the presence or absence of crazes in resins of different molecular weights. Curve (a) represents the ideal mechanical behaviour for stable craze filaments to coexist. If strain hardening does not occur (curve (b)), then as the polymer necks, the instability continues, causing rapid fracture. This behaviour is typical of low molecular weight resins, and Kambour explains the absence of craze growth by saying that the stresses maintained above and below the deformed zone are insufficient to cause cavity nucleation ahead of the craze tip. The behaviour of cross-linked resins, is explained by stating that orientation hardening is too rapid (curve (c)) causing stresses above and below the deformation zone to become so high that fracture occurs before craze matter can undergo extensive elongation, giving a fracture surface devoid of craze filaments.

Fig. 4.1.17. Three possible types of stress strain behaviour for materials with the same yield point (from [55]):

Fig. 4.1.18. Change in the tensile characteristics of nylon with various levels of absorbed water and zinc chloride.



In an endeavour to provide a model for the behaviour of polymer in the craze, where the concentration of stress-crazing agent will be high, a series of tensile tests were conducted on nylon 6 films which had equilibrated in zinc chloride solutions with different concentrations. If a nylon was shown to have type (b) behaviour in the presence of high levels of zinc chloride, then fracture at low elongations with no well developed craze would be predicted. However, if type (a) behaviour is displayed by some of the specimens containing zinc chloride, large crazes are predicted.

The experimental results are shown schematically in Fig. 4.1.18. When nylon had equilibrated with aqueous zinc chloride, only low elongations, at low stresses, were recorded before fracture. This corresponds to type (b) behaviour (except that σ_y is lowered in this instance). These conditions would apply to initiation of crazing in nylons, where the surface concentrations of agent are very high. As reported previously, the fracture surface morphology confirms that in this region only low elongation to break has occurred (region 1). As the local concentration of agent at or near the craze tip decreases to the equivalent of 2M zinc chloride, for example, type (a) behaviour is observed. High elongations to break are now possible, but drawing occurs at reduced stresses. These conditions are ideal for large, stable craze production.

If it is assumed that the local concentration of agent near the craze tip decreases as the craze grows across the specimen, the graphs shown in Fig. 4.1.18. suggest that the

deformation behaviour of the nylon will change.

With exhaustion of agent, large craze development ceases, as shown by the transition from region 2 to region 3 in Fig. 4.1.11.

Regions 3 and 4 - Crack Propagation Beyond the Agent-Induced Craze Region

It is proposed that the regions 3 and 4 shown in Fig. 4.1.11 are identical to the "ductile" fracture and brittle fracture regions discussed in detail in Section 4.1.2.

No further comments are considered necessary.

Typical Examples of the Morphology of Fracture Surfaces of Stress Crazeed Nylons

Example 1.

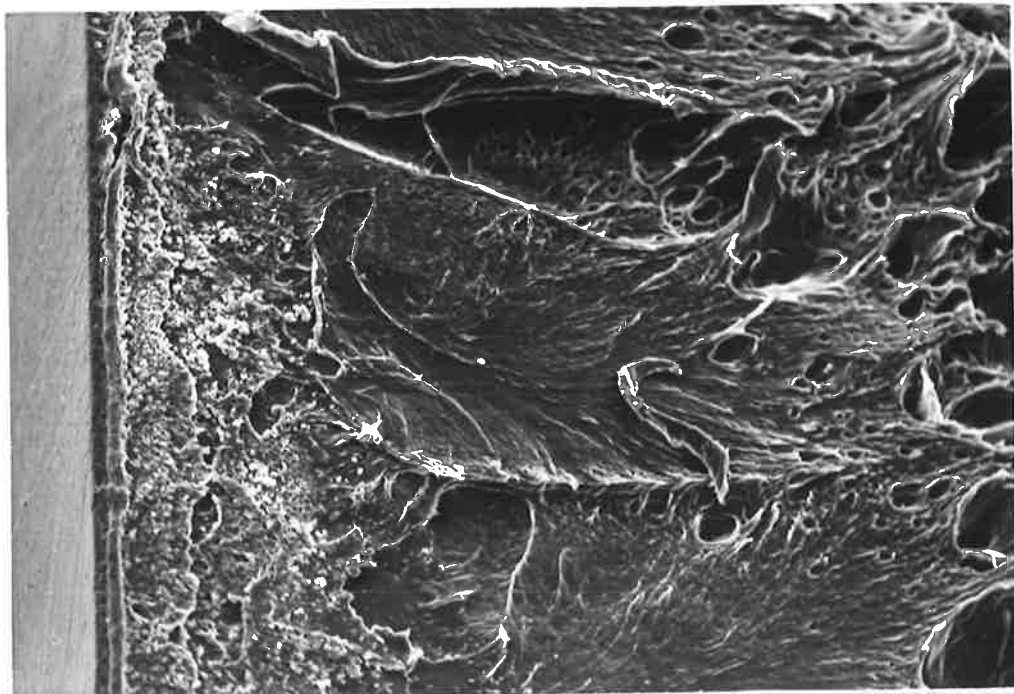
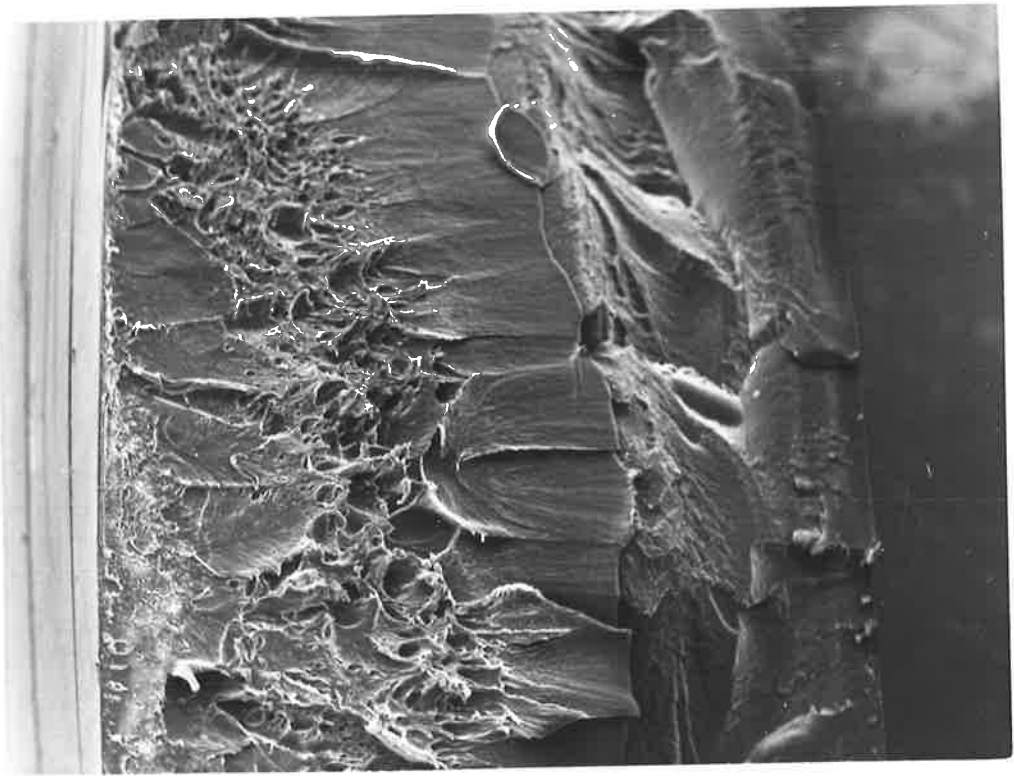
A constant load was applied to a nylon 66 specimen so that the initial stress was 61 MPa ($\sigma_y \approx 85$ MPa). When a droplet of 4M aqueous zinc chloride was applied it took 20 min. for the specimen to fracture. (Crazing began after 19 min.).

Regions 1 to 4 are shown in Fig. 4.1.19. At higher magnification regions 1 and 2 can be seen more clearly (Fig. 4.1.20). The initiation zone is contaminated with residual zinc chloride, which has been incorporated into the nylon (details are given in Chapter 5, of salt uptake into nylon at various stages of stress-crazing). The fibrous ruptured craze region is also clearly recognisable (region 2).

Although precise interpretation of the features in region 2 is difficult, it appears that there is a gradual increase in the ability of the nylon to elongate across the

Fig. 4.1.19. Fracture surface of nylon 66 showing regions 1 to 4 (from left to right). Magn. = 31x

Fig. 4.1.20. Region 1 (contaminated with zinc chloride) at left, and region 2 at right : same specimen as above. Magn. = 123x



sample. This is influenced by the local concentration of agent (which is expected to decrease as the crack progresses) the stress concentration at the craze tip, and the crack velocity compared with craze growth rate.

When the stage of high polymer elongation is reached (as shown at the right hand side of Fig. 4.1.20) a network of filaments and voids are produced. The complex nature of the fracture surface in this region can be attributed, in part, to interaction between the radiating leading edges which have initiated from a broad initiation site. The crazed zone gives way, as the level of agent diminishes, to a region of more rapid crack growth outside of the precrazed zone (region 3), Fig. 4.1.21. Finally, the fracture velocity increases until brittle fracture occurs (region 4, Fig. 4.1.22).

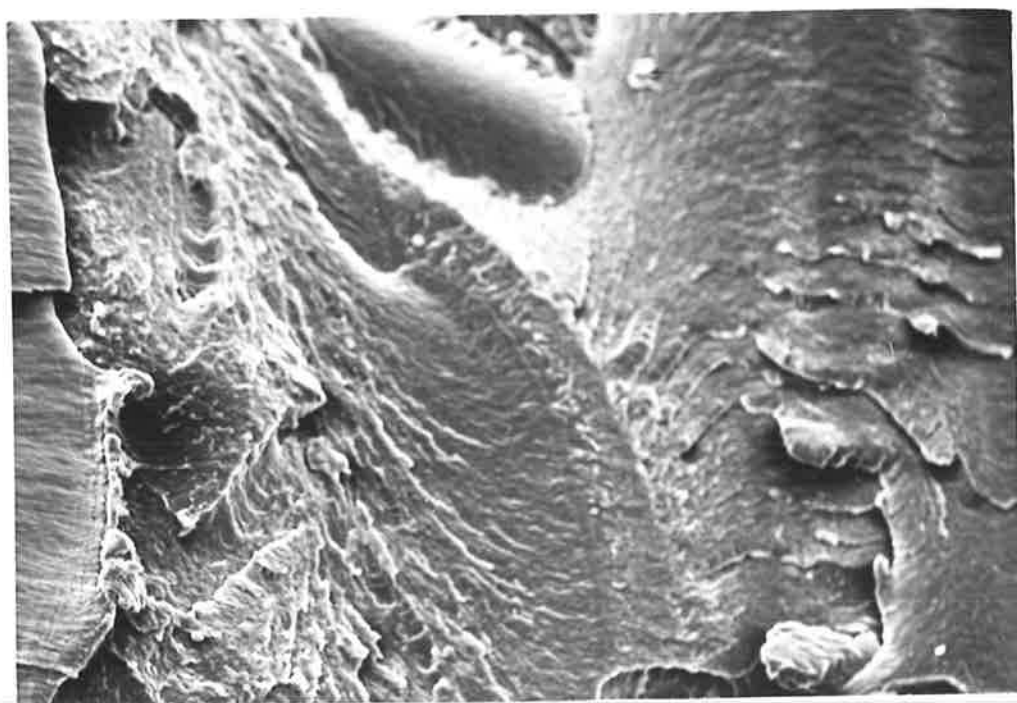
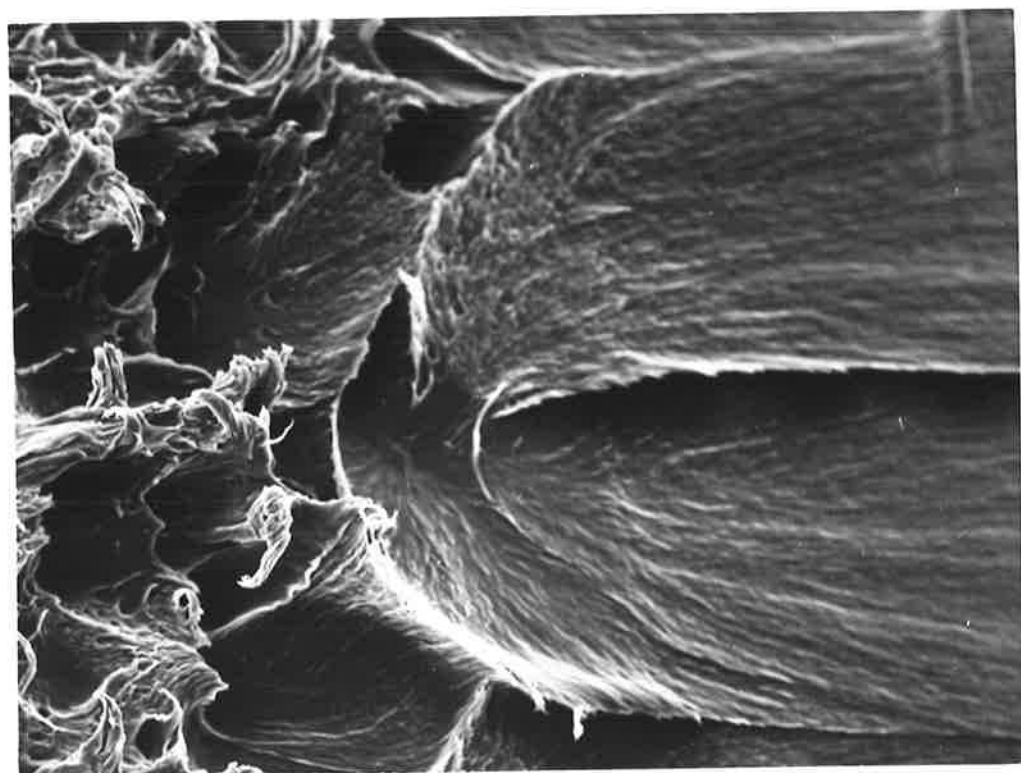
Example 2.

In this example a nylon 6 specimen was slowly strained (crosshead speed = 0.1cm/min.) in the presence of copiously applied 5M aqueous zinc chloride. The conditions have been made so that extensive formation of regions 1 and 2 is favoured; the slow strain rate and large quantity of agent, coupled with the higher sensitivity of nylon 6 over nylon 66 all contribute to considerable uptake of the zinc into the polymer.

The surface seen at low magnification (Fig. 4.1.23) shows crazing to have occurred on both sides of the specimen (where agent had been applied), and that no brittle fracture (region 4) is present. This is expected, in view of the conditions of low strain rate and ambient test temperature.

Fig. 4.1.21. Region to right of that shown in Fig. 4.1.20, showing transition from type 2 to type 3 morphology. Magn. = 123x

Fig. 4.1.22. Brittle fracture (region 4) of same specimen. The sharply defined boundary from ductile region 3 can be seen at left. Magn. = 123x



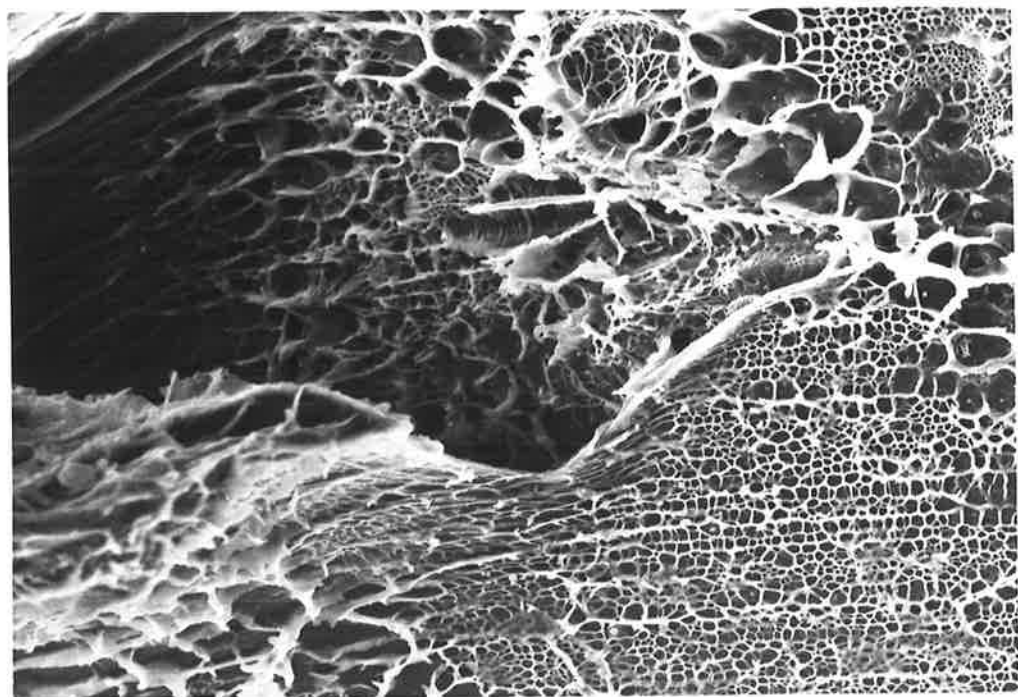
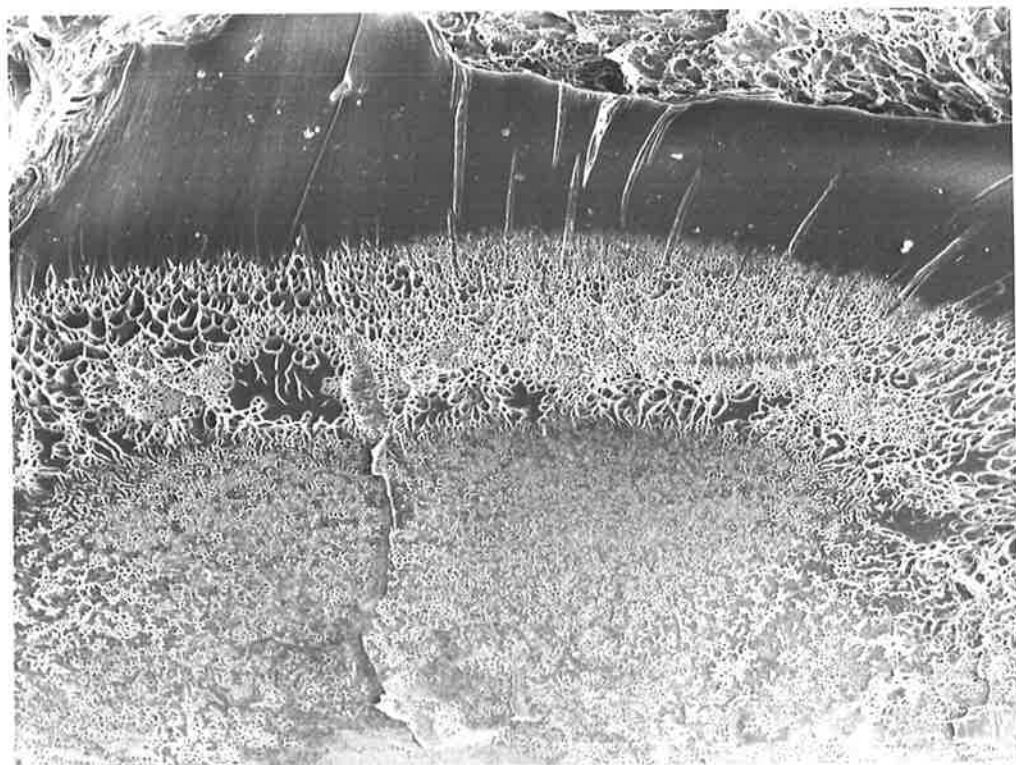
Three regions may be identified. At the bottom, a morphology which is intermediate between region 1 and 2 can be seen. There is a very small strip of region 1 material out of view; however, most prominent is the region where void formation and a small amount of elongation of polymer has occurred. The level of agent taken up by the polymer causes the polymer to fracture soon after necking, to give the interconnected filamental stumps.

The effective concentration of agent taken up by the nylon decreases across the specimen (verified in experiments described in Chapter 5), until it falls to a level which, coupled with the stress concentration at the craze tip, allows extensive drawing to occur. The polymer now behaves as in curve (a) of Fig. 4.1.17. This region (region 2) is shown at higher magnification in Fig. 4.1.24. In this region the voids range in size, and are interconnected, as if in an irregular honeycomb. The voids and interconnected filaments are similar to those seen in polystyrene, near the initiation zone.

Mann [128] shows voids which are larger than expected from the fracture of craze matter (Fig. 4.1.25). Similarly, in high molecular weight polystyrene fractured at liquid nitrogen temperatures, Haward [129] also showed interconnected "modular forms" (Fig. 4.1.26); the voids were once again at least an order of magnitude higher than expected from the simple rupture of voids in craze matter (with a diameter of no more than $.02\mu\text{m}$). The mechanisms leading to the formation of these structures have not been fully explained. In metals plastic fracture, giving a surface similar to that seen in polymers, is thought

Fig. 4.1.23. Fracture surface of nylon 6 strained slowly in the presence of copiously applied zinc chloride solution. Craze and crack growth proceeded from both edges of specimen (top and bottom of photograph) simultaneously. Magn. = 35x

Fig. 4.1.24. Honeycomb region 2 morphology of same specimen. Magn. = 285x

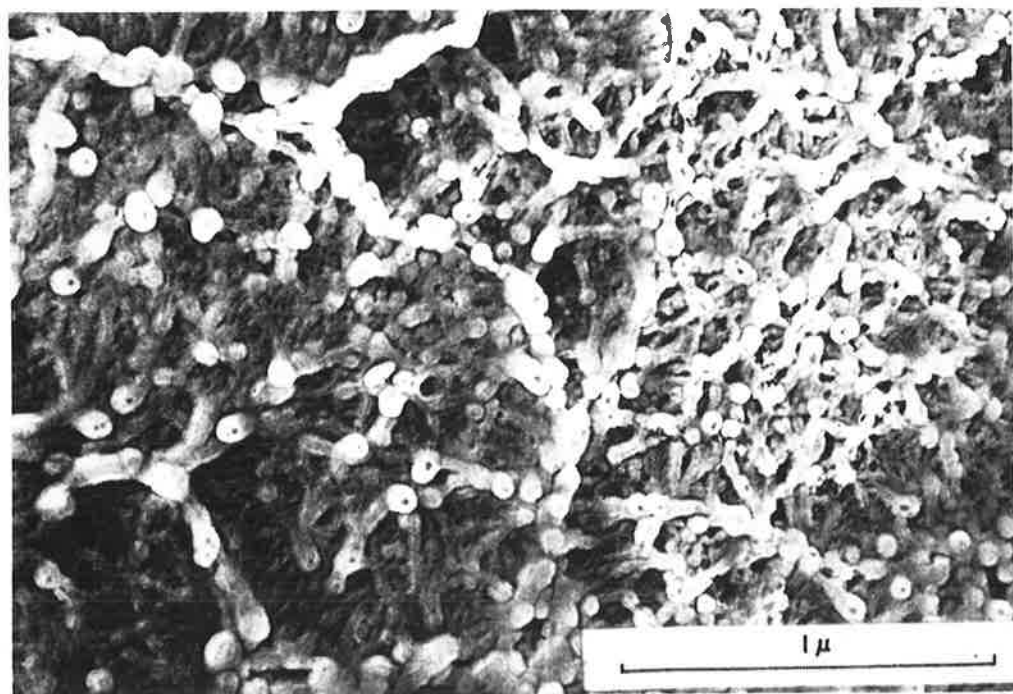
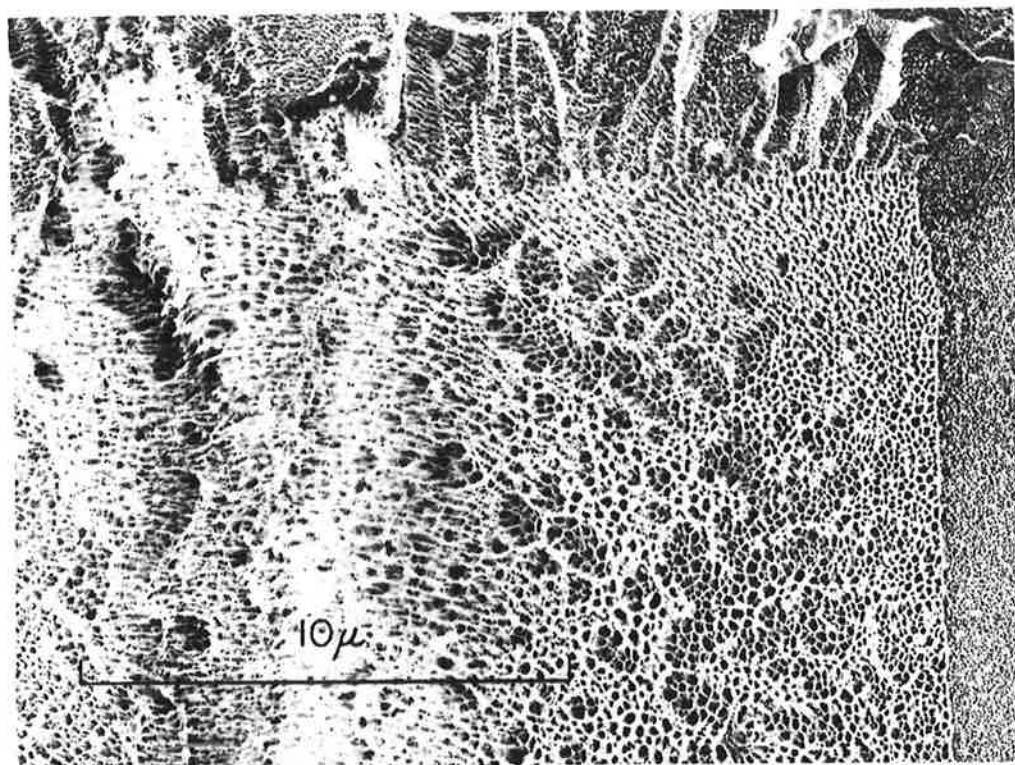


to occur by the coalescence of microvoids; "dimples" are produced by deformation processes resulting from differences in the elastic and plastic properties of the metal [130].

The crack velocity increases relative to the rate of craze growth, until the crack overtakes the main craze. This is indicated by the transition from voided region 2 to smooth "ductile fracture" region 3 in Fig. 4.1.23.

Fig. 4.1.25 Honeycomb structure of ruptured craze matter in polystyrene (from [128]).

Fig. 4.1.26. Interconnected "nodular forms" in the fracture surface of high molecular weight polystyrene (from [129]).



4.1.4. Morphology of the Craze Surface ab in Plane AA'B'B.

When nylons are stressed in the presence of an active crazing agent, long narrow strain inhomogeneities resembling crazes in amorphous polymers are observed.

The first evidence of crazes is their appearance at the surface because internal areal growth cannot be readily detected in non-transparent polymers such as nylons.

The dimensions and distribution of crazes in nylons vary greatly, depending upon the experimental conditions. When the polymer in the craze is capable of large visco-elastic deformation, broad crazes are formed, whilst at low temperatures or when high concentrations of stress-crazing agent are taken up, narrow crazes are produced before fracture occurs.

Unlike crazes in glassy polymers, those in nylons appear to have no lip or step surface-discontinuity. Instead, an abrupt depression forms, as represented in Fig. 4.1.27. The height of the wall, x , depends upon the maturity and size of the craze.

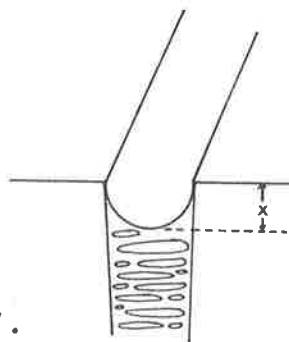
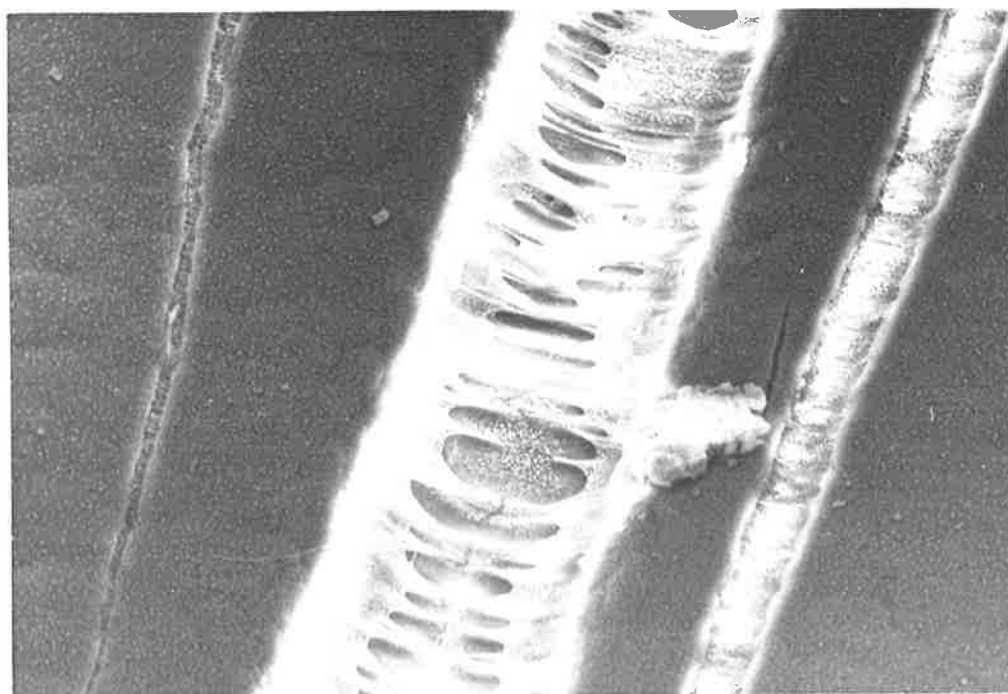
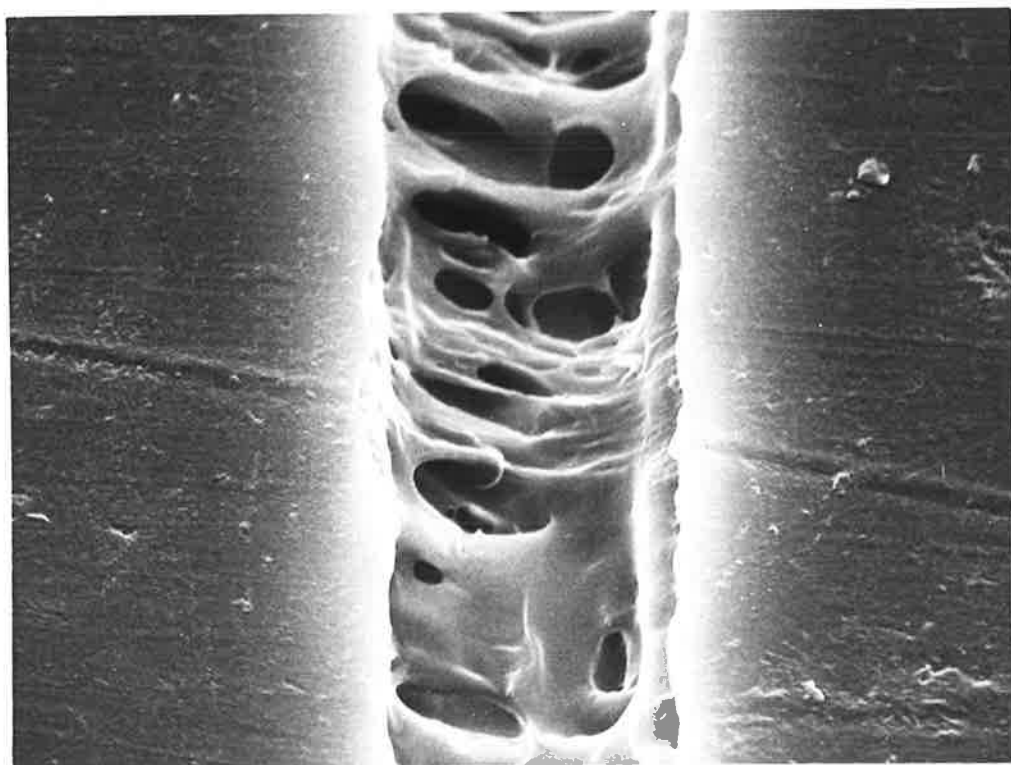


Fig. 4.1.27.

Craze matter near the surface may take many forms; experimental factors such as type of agent and polymer, stress conditions and time will all affect the surface morphology. Four examples of the surface of crazes, in order of maturity, are shown in Figs. 4.1.28-31.

Fig. 4.1.28. Surface morphology of an immature craze.
Magn. = 2290x

Fig. 4.1.29. Highly drawn filaments and elliptical voids
at the craze surface. Magn. = 2350x



Stage 1

Material near the craze tip is shown in Fig. 4.1.28. The polymer has not been highly elongated, as evidenced by the thick fibrils. The voids in this region are approximately 10 μm in diameter, compared with about 0.02 μm in a typical glassy polymer. The craze in this photograph is outside the treated region. Craze agent has moved with the advancing craze tip through the bulk polymer.

Stage 2

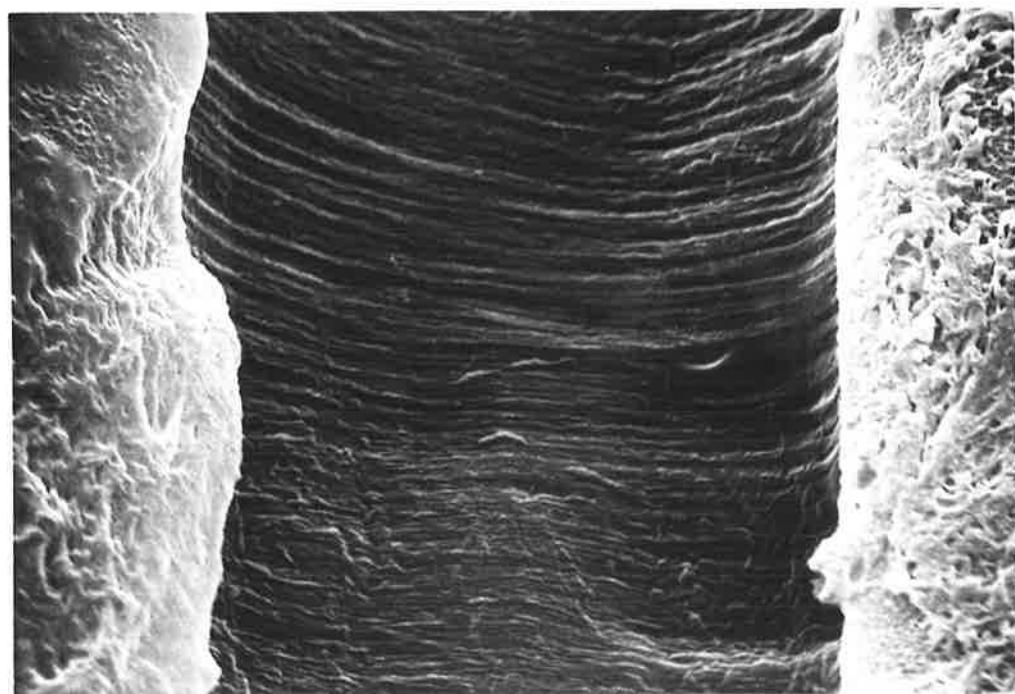
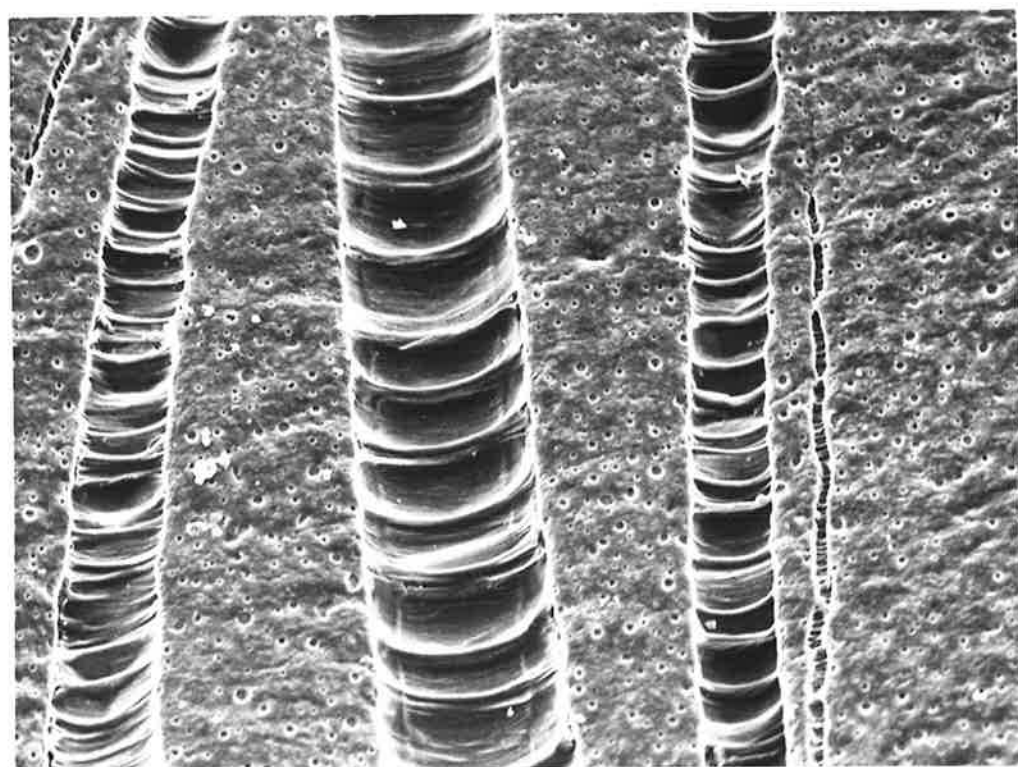
The next stage in the development of a craze is commonly the extension of thick fibrils to produce highly drawn filaments. In the craze shown in Fig. 4.1.29, voids are now aligned and elliptical. The arrow points to where some of the filaments have ruptured; when the craze broadens and cracking occurs remnants of these filaments will remain on the crack wall.

Stage 3

Often ribs or ridges of polymer are associated with the craze surface. Those in Fig. 4.1.30 appear to be curved but this is an illusion resulting from the specimen being tilted in the microscope. Y-modulation or rotation of the image indicates that the ribs are straight and perpendicular to the long axis of the craze. The regular spacing between the ribs increase as the craze grows. They result from contraction occurring both along and across the craze. crazes on the surface often possess a "skin", which is because of contraction. At the surface there is only biaxial constraint, compared with triaxial constraint in the interior of the craze. Even in narrow crazes ribs

Fig. 4.1.30. Ribbed craze morphology caused by the change from a triaxial to a biaxial stress distribution at the surface. Porous, swollen polymer between crazes can also be seen. Magn. = 820x

Fig. 4.1.31. Mature craze morphology. The "skin" may not be truly representative of the interior structure of the craze. Magn. = 2350x



spaced close together can be seen. In the specimen shown, polymer between the crazes has swollen, resulting in a porous appearance.

Stage 4

If the craze matter is capable of large viscoelastic deformation without rupture (for example, when the local concentration of agent is not excessive), the craze surface will appear uniformly and highly oriented (Fig. 4.1.31). At higher magnifications the microstructure resembles that of polymer in a ductile neck. It is considered that this morphology may be superficial and not useful in providing information about the interior of the craze.

When a crack begins to grow within a craze, without complete rupture, some of the elements of a craze can be detected by tilting the specimen (Fig. 4.1.32).

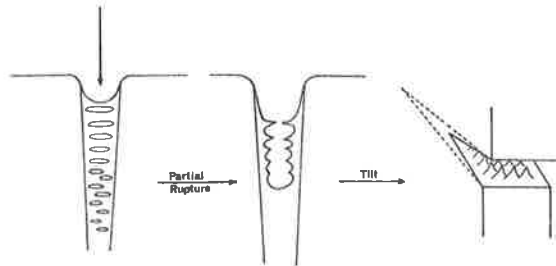


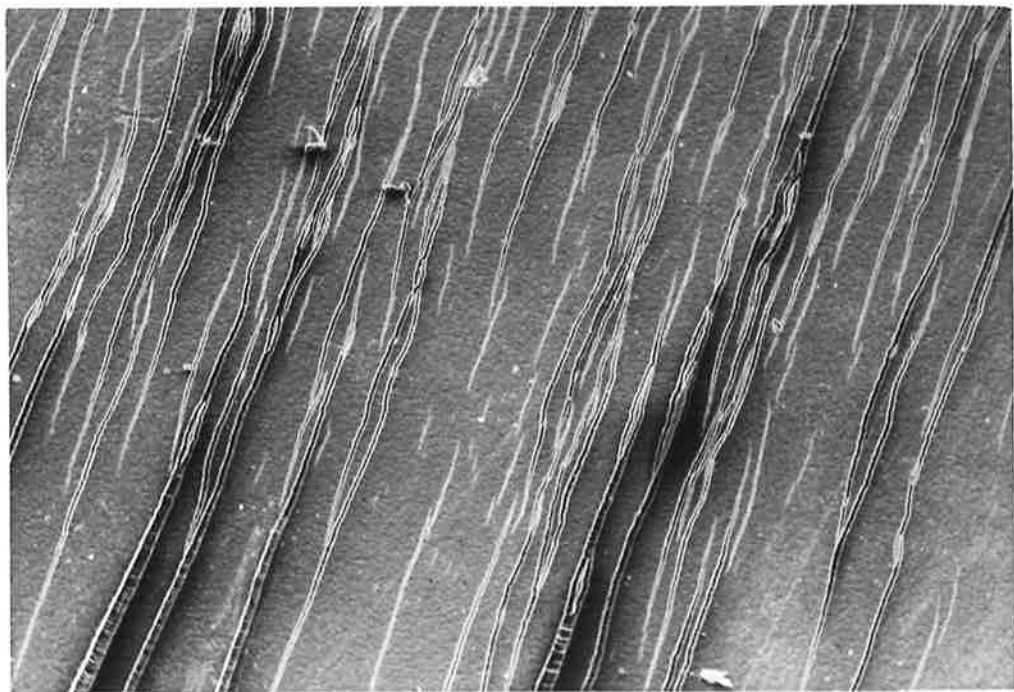
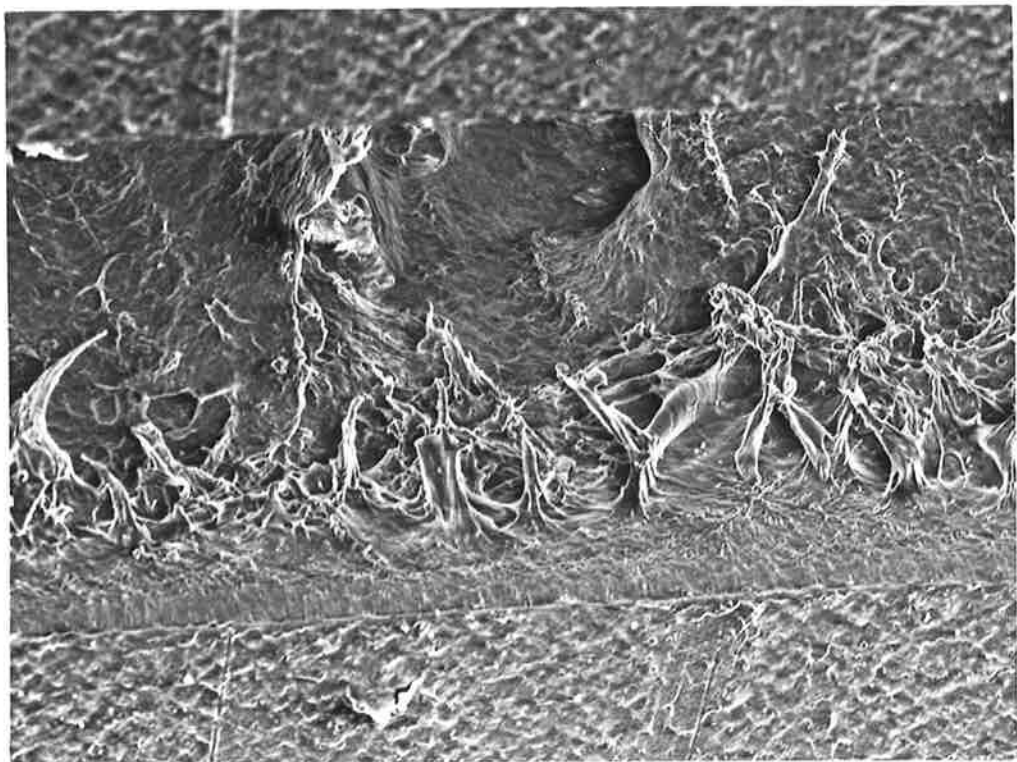
Fig. 4.1.32.

Three interesting aspects of the specimen which has been tilted in this way (Fig. 4.1.33) are the sharp and well-defined interface between bulk polymer and the craze, the featureless region nearest the specimen surface, and the sharp, apparently unaltered filament remnants.

Craze matter which is morphologically different from that described here will be encountered later; the crazing process will be analysed in each case, then the conditions

Fig. 4.1.33. Interior of a crack showing remnants of craze matter. Specimen tilted as described in Fig. 4.1.32. Magn. = 358x

Fig. 4.1.34. Narrow crazes which have terminated by interaction of stresses at the craze tip. Magn. = 164x



which have resulted in such variations discussed.

Crazes may terminate in one of two ways. In specimens where a high number density of short crazes exist, a gradual and continuous reduction of the dimensions of the craze matter will occur. Small crazes which are aligned but not quite in the same plane may grow until interaction of stresses at the craze tip results in a reduction in the stress component which favors craze growth. They can be seen in Fig. 4.1.34.

Bifurcation may occur at the ends of large crazes, producing a large number of narrow radiating crazes. This is presumably a manifestation of the changing stress conditions; the stress intensity factor changes just before the onset of divergence. This type of termination is illustrated in Figs. 4.1.35-36.

When a specimen is stressed in the presence of only a small volume of crazing agent, some crazes may extend outside of the area where the agent has been applied. Generally no abrupt change in the morphology of the craze surface is detected at the treated-untreated interface (Fig. 4.1.37). This is consistent with rapid transport of the agent with the voided craze tip.

The fine structure of the craze may be obscured by some polymer crazing adduct, which might remain in the crazed zone, or separate to form a crust at the edge of the craze. An extreme example is shown in Fig. 4.1.38. The specimen has been allowed to retract causing the complex to be extruded from the craze region. It can be differentiated from the bulk polymer by its porous, amorphous appearance.

Fig. 4.1.35. Bifurcation of the craze tip outside of the treated zone (dark ellipse in centre of photograph). Nomarski interference optical micrograph. Magn. = 164x

Fig. 4.1.36. Termination of a craze induced by magnesium perchlorate solution in spherulitic nylon 66. Magn. = 2860x

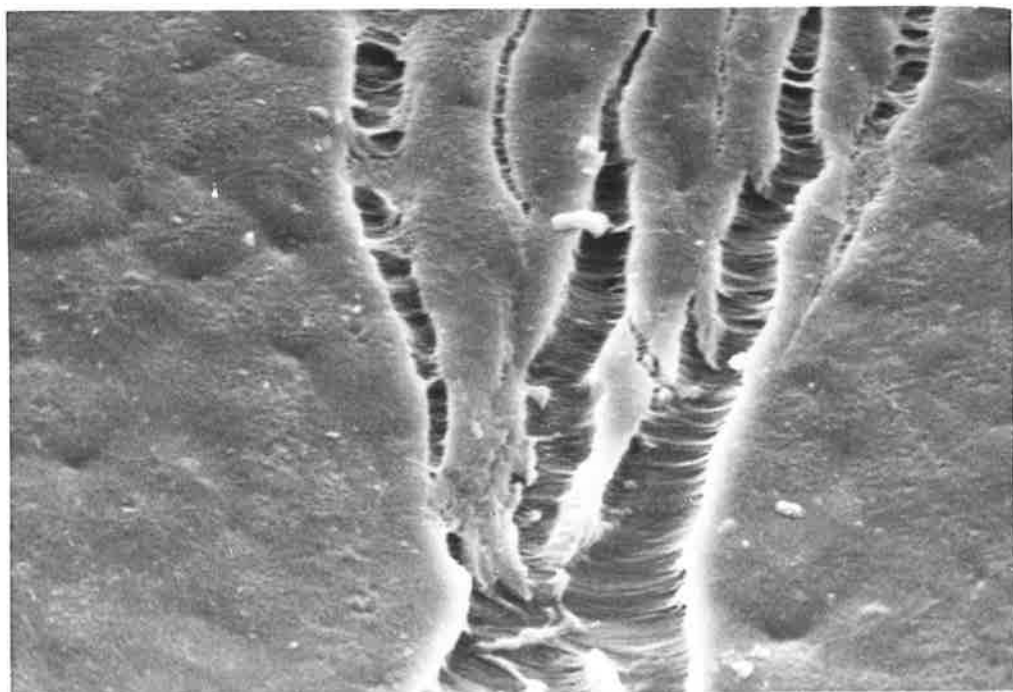
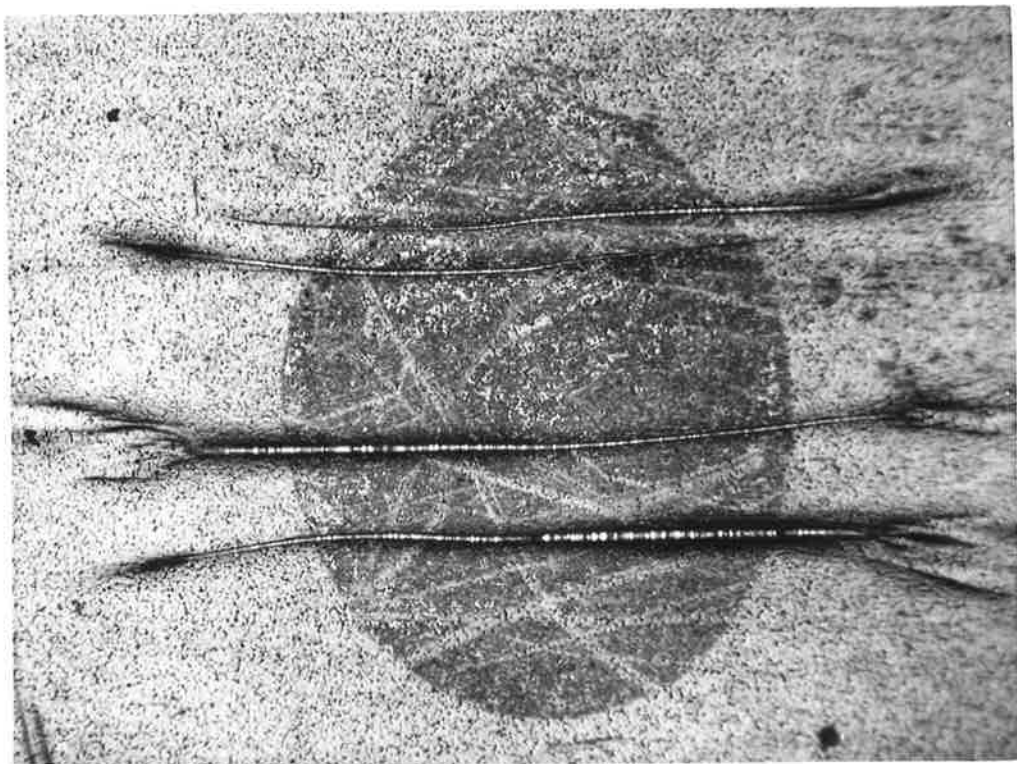
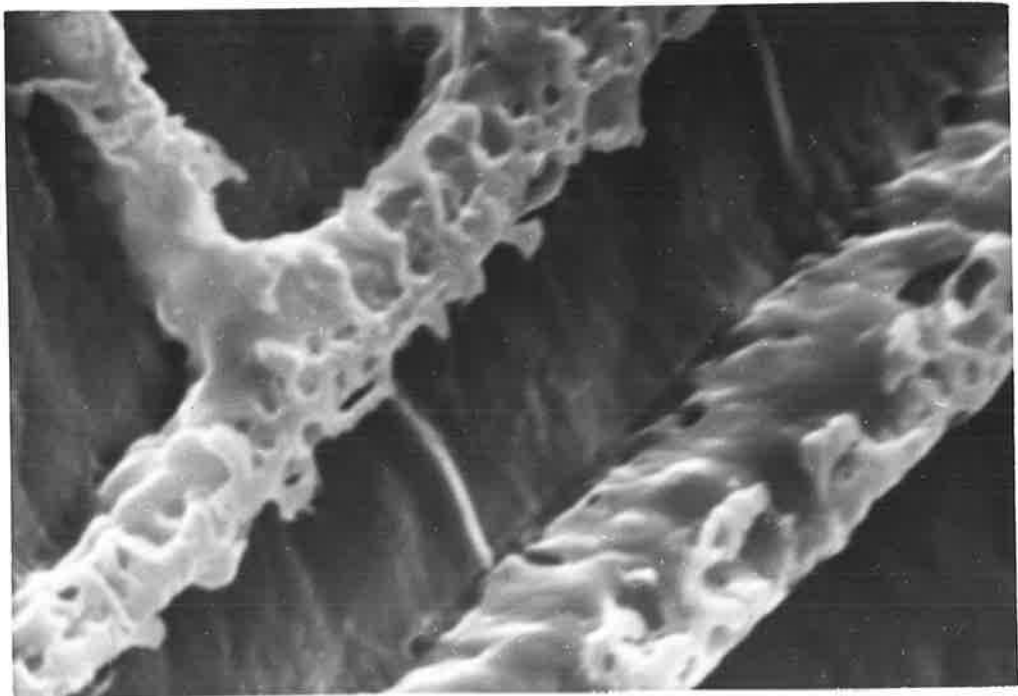
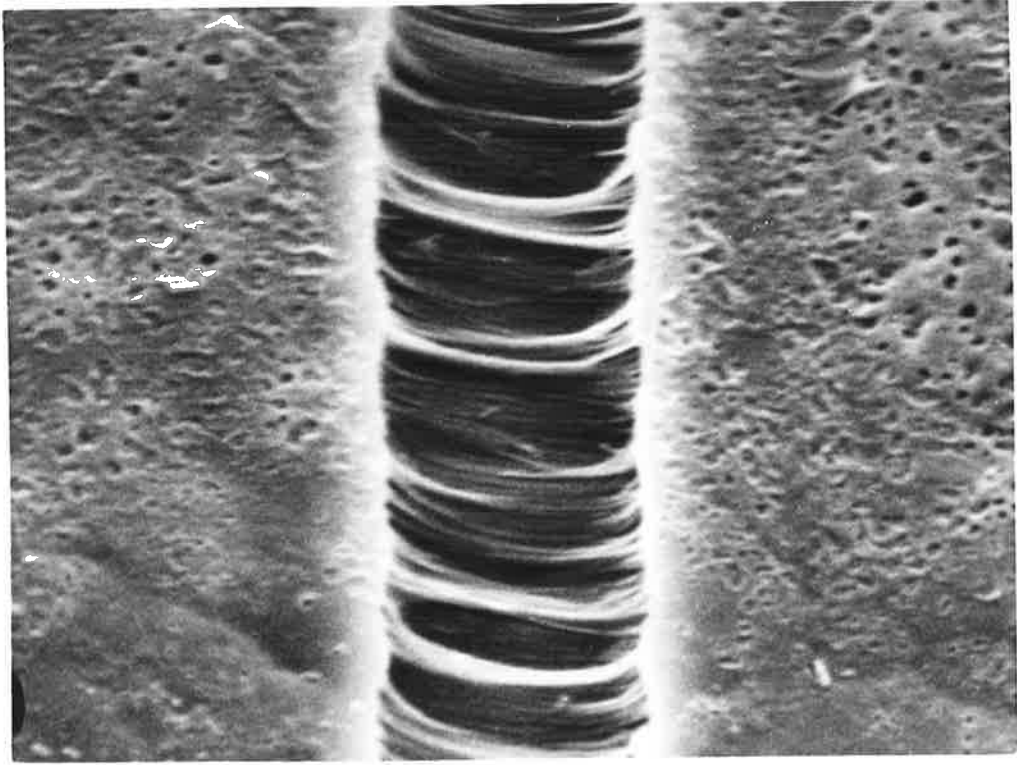


Fig. 4.1.37. Craze passing from salt-treated polymer (at top) through untreated polymer (at bottom) with no apparent change in morphology. Magn. = 5720x

Fig. 4.1.38 Nylon 66 - magnesium perchlorate complex extruded from craze zone. Magn. = 5010x



4.2. The Morphology of Crazing in Nylons Induced by Different Agents

In this section the morphological results of uniaxial tensile testing of nylons in the presence of solutions of five different salts will be discussed. Each agent was found by Dunn and Sansom [3] to have high "stress-cracking" activity, and this was confirmed in the present work, when brief tests were carried out on a large number of salts.

The first two subsections (4.2.1 and 4.2.2) will discuss results obtained with zinc and cobalt chloride, which are Type I salts [4]. The other two sections (4.2.3 and 4.2.4) deal with Type II salts, the first being magnesium perchlorate, and the bromide and iodide of lithium being discussed together. The differences in craze and fracture morphology which can be attributed to a change in anion size can then be ascertained.

This section will be confined to a discussion on morphology alone. Other aspects of the interaction between salts and nylons will be discussed in Chapter 5.

4.2.1. Crazing Induced by Aqueous Zinc Chloride Solutions

Nylon 66

Analysis of the fracture surface of zinc chloride-induced crazed nylon 66 has been discussed in Section 4.1.3 and will also be described in Chapter 5 (in a correlation with agent levels), so that this aspect of crazing need only be briefly described in this section.

It will be remembered that, using Fig. 4.1.11 as a guide, four regions could be distinguished. There was a flat, featureless initiation region (region 1), and if uptake

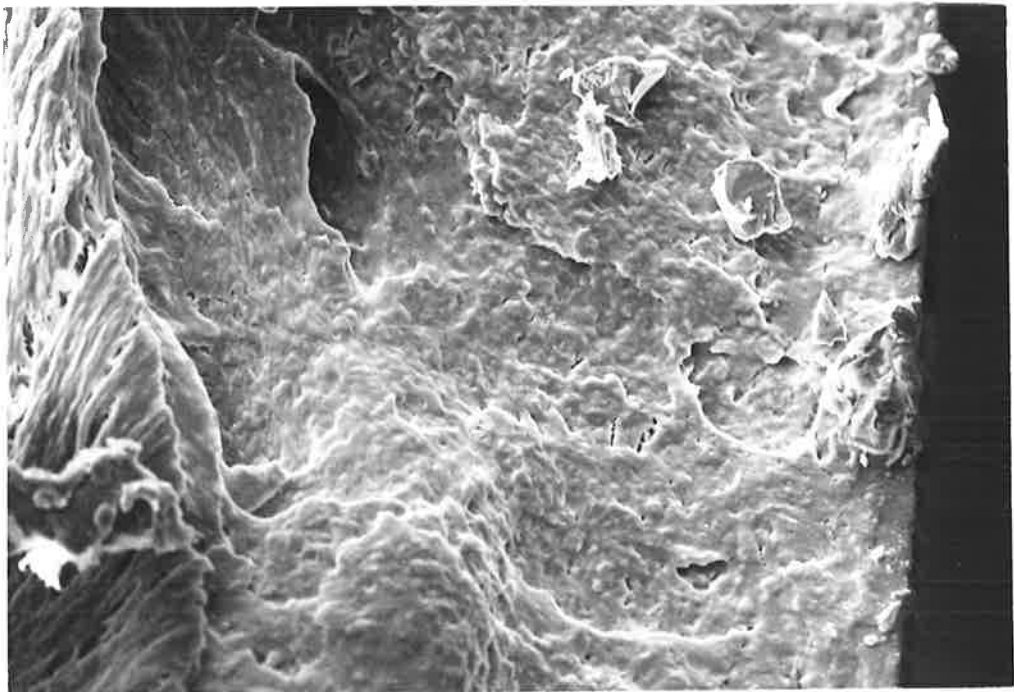
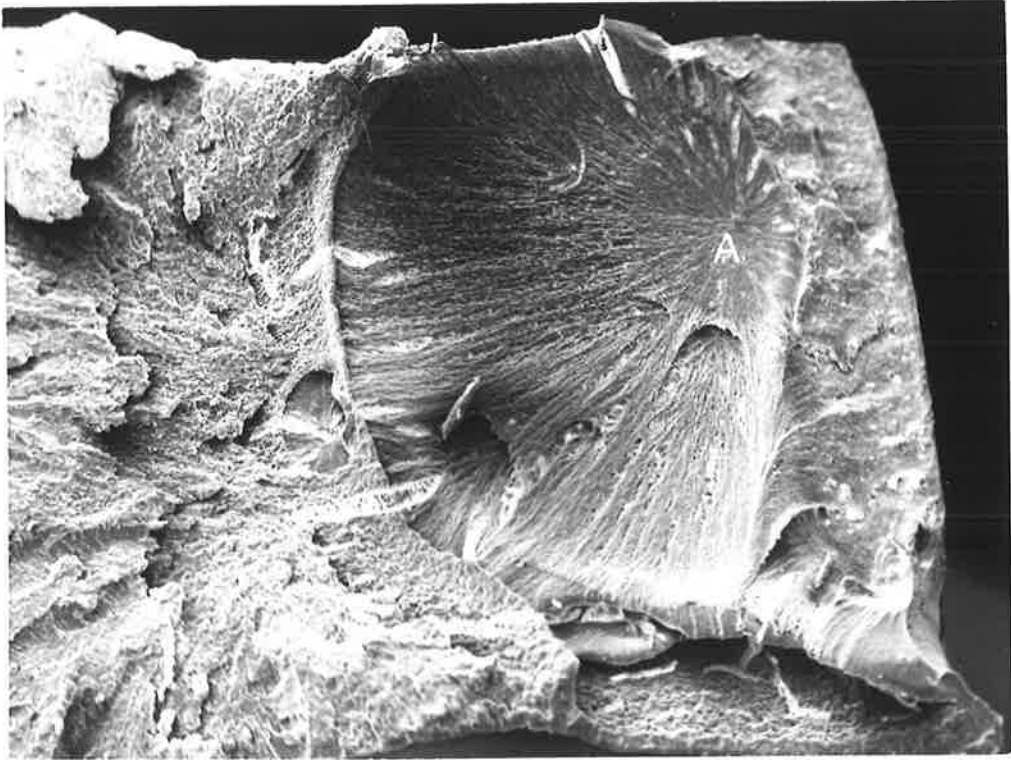
of the agent and subsequent salt-induced crazing was able to occur before fracture, remnants of the craze could be identified as region 2. Crack propagation beyond the salt-induced craze gave region 3 at low velocities and region 4 (brittle) at high velocities.

The variations on this model which are encountered, and which depend upon the test conditions, are often most prominent in regions 1 and 2. For example, the fracture surface of un-notched anhydrous nylon 66 (ASTM type 1 test-piece) strained with a crosshead speed of 10 mm/min., shows no region II (Fig. 4.2.1.). Under the conditions of the test, uptake of the zinc chloride has been confined to near the surface of the specimen. The flat featureless zone (at the right in Fig. 4.2.1), which is shown at higher magnification in Fig. 4.2.2, contains high levels of absorbed zinc (see Chapter 5). Fracture has then initiated from point A, and "ductile fracture" of un-modified nylon has occurred. No absorbed zinc was found in this region. Presumably the tip of the craze-crack which occurred at the edge intensified the stress so that at a "flaw" in front of the tip, catastrophic fracture initiated. The crack has accelerated until ultimately brittle fracture occurred. The "ductile fracture" has pre-empted the development of region 2 material.

The fracture surface of most specimens previously crazed with zinc chloride conforms with the pattern outlined in the introduction. It is nevertheless often difficult to distinguish between regions which have been produced by the rupture of preformed, agent-induced crazes, and the voided regions which can arise when the complex stress

Fig. 4.2.1. Fracture surface of un-notched fracture surface of anhydrous nylon 66 stressed with zinc chloride present. Fracture initiation point is designated "A".
Magn. = 29x

Fig. 4.2.2. Zinc rich craze initiation zone of specimen shown above. Magn. = 188x



field is present. For example, a fracture surface of the complexity shown in Fig. 4.2.3 is often encountered. It is possible to see, at higher magnification, small voided regions which are surfaces in line with other cracks on the side of the specimen. By looking at the sample in toto, it is possible to determine whether the voiding has been a consequence of the agent being present.

The surface shown in Fig. 4.2.4 also illustrates the ambiguities which can arise. Superficially, part of the fracture face appears to fit the proposed model, with regions 1, 2 and 3 present. However, viscoelastic deformation preceding rupture in both x and y directions presumably causes shear forces, and the formation of voids in the nylon may be a consequence of this complex stress field.

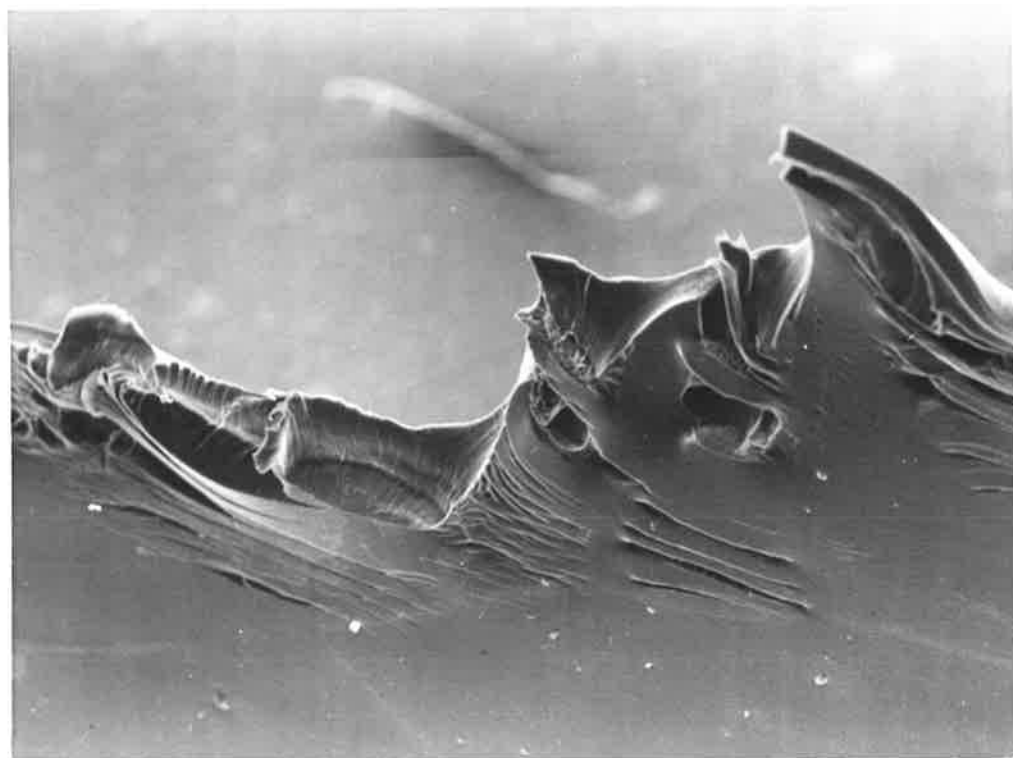
In relatively thin specimens (say < 1mm thick) development of crazes is limited to two dimensions once the craze has grown to the full thickness of the test-piece. For this reason, the morphology of the fracture surface of crazed films often needs to be interpreted differently from thick specimens, although it is often still possible to identify the four regional types (regions 1-4).

The Morphology of the Crazed Surface - Through Plane
AA'B'B.

The distribution and dimensions of crazes in nylons depends largely upon the conditions of strain rate and agent activity. When the agent is highly active and strain rates are low, high uptake of the agent into the polymer can occur, and so, depending upon the mechanical properties of the treated nylon, either rupture at low elongation, or production of well-developed crazes can result.

Fig. 4.2.3. Fracture surface of nylon 66 showing interaction of many cracks and crazes. Magn. = 50x

Fig. 4.2.4. Another part of fracture surface of same specimen, showing complicated structure. Interpretation of failure mechanism is ambiguous (see text). Magn. = 170x



The morphology of nylon 66 which has been strained in the presence of zinc chloride until surface perturbations are first observed is shown in Fig. 4.2.5. The discontinuities are similar to those seen in glassy polymers, and possibly arise from short-term localised swelling. The resolution is low in this photograph because low voltages have been used to reduce charging.

With further craze development, surface discontinuities tend to disappear. Narrow crazes are seen in Fig. 4.2.6; the edge of the craze does not rise above the plane of the uncrazed surface. Swelling can also be discerned away from the craze.

Well-developed crazes are seen in Fig. 4.2.7. In this experiment the nylon 66 film was strained slowly until crazes were seen; rapid irrigation with water prevented further craze and crack growth. No clear correlation between the onset of craze rupture and craze thickness can be made, because there appear to be highly elongated craze filaments still intact in the broadest region of the craze, whilst rupture has occurred in some of the narrower parts.

The fine structure of part of the craze is seen in Fig. 4.2.8. Prominent are the sharp interface between the craze and the bulk polymer, and the regular spacing between the craze filaments. The pattern is strikingly similar to that observed in polystyrene by Beahan, Bevis and Hull [62] (Fig. 2.4). The striations observed parallel to the strain direction in Fig. 4.2.7 and the apparent breaks in the craze filaments in Fig. 4.2.8 are both artifacts which have been

Fig. 4.2.6. Narrow craze in nylon 66 induced by zinc chloride - residual salt can be seen at top centre of photograph as a pale zone. Surface etching of uncrazed nylon surface can also be detected. Magn. = 392x

Fig. 4.2.5. Surface ridges observed in early stage of craze formation. Magn. = 2,615x

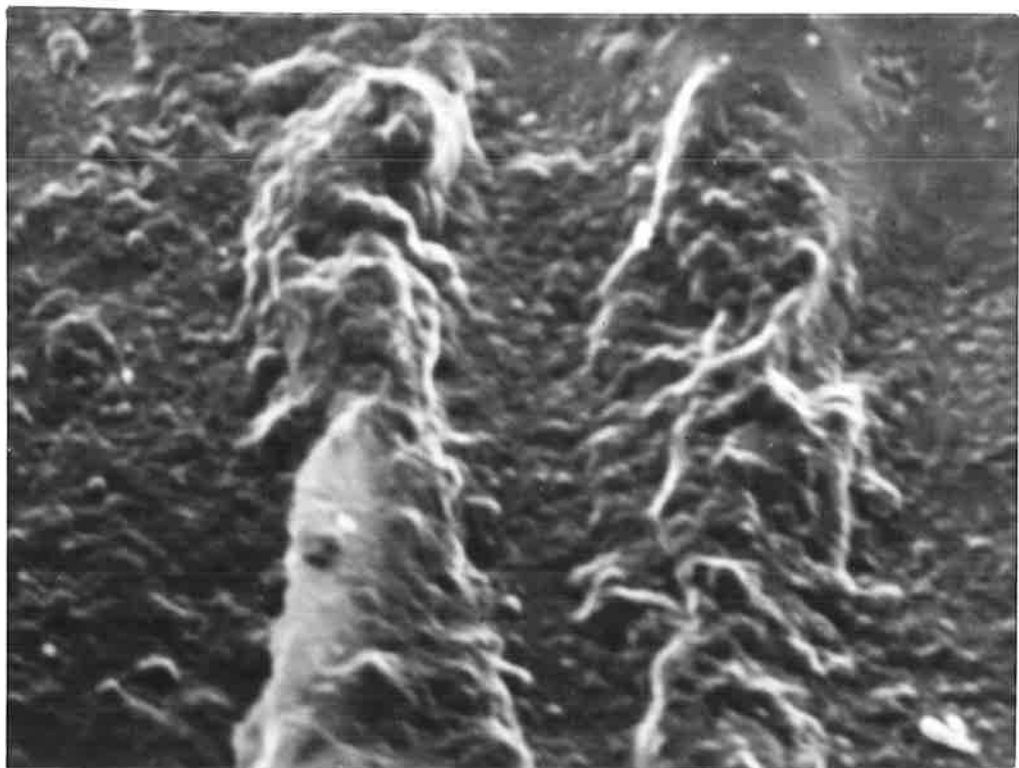
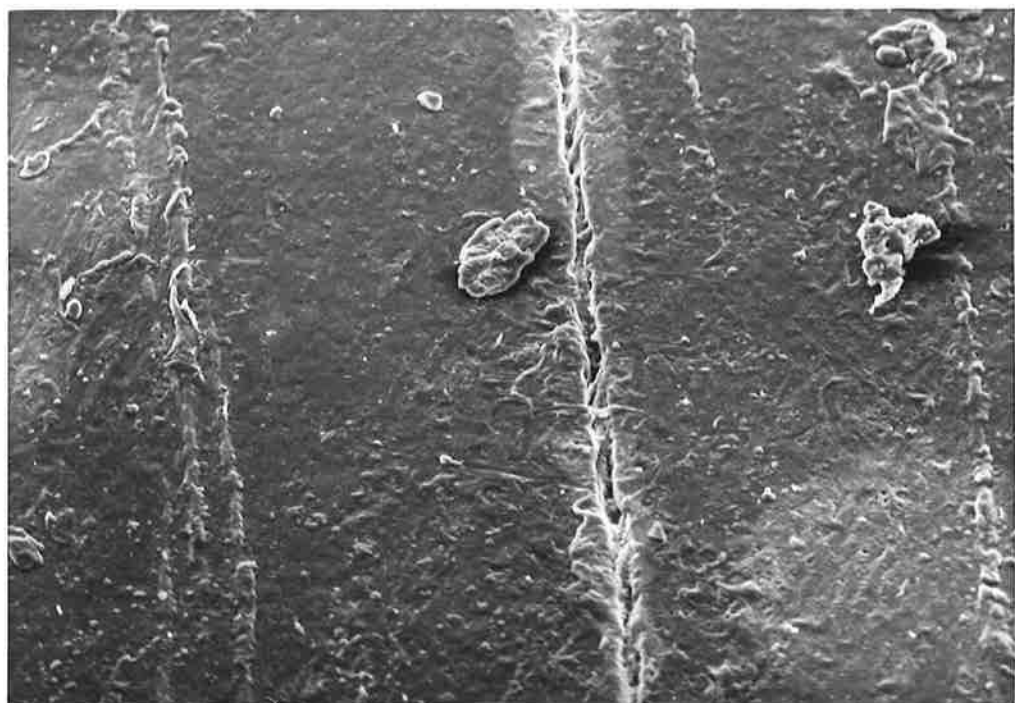
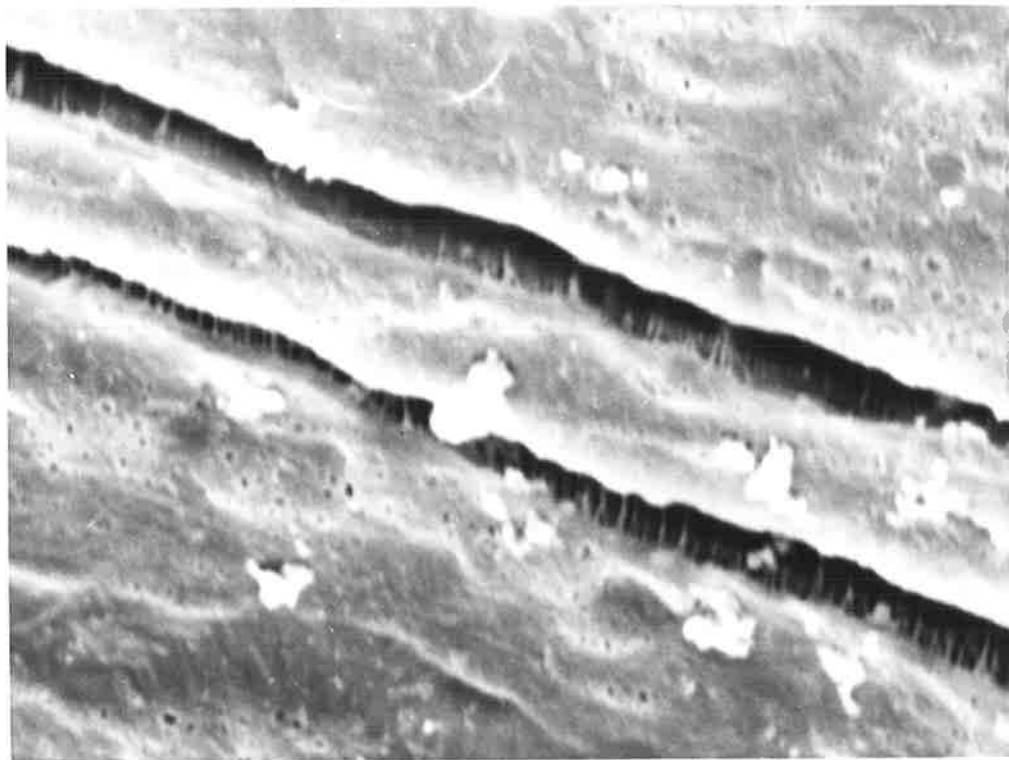
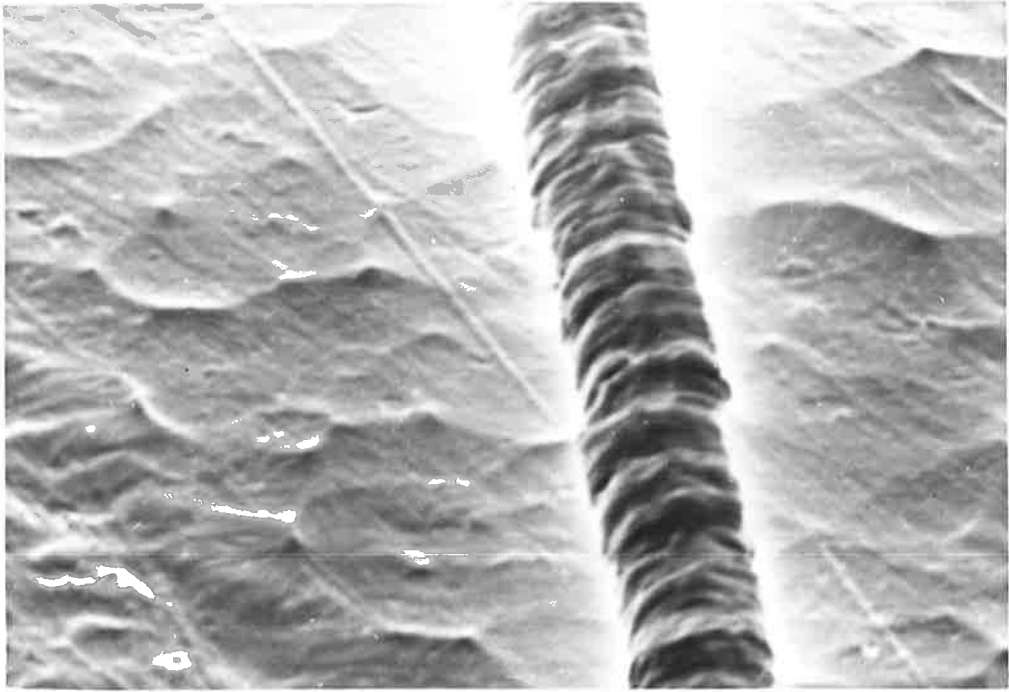


Fig. 4.2.7. Broad crazes in nylon 66. Fine striations perpendicular to craze axis are artifacts from conductive coating on specimen.
Magn. = 26x

Fig. 4.2.8. Fine structure of craze surface showing regular void distribution. Magn. = 590x



caused by movements of the thick gold coating.

It appears from Fig. 4.2.9, where crazes have deviated from a straight trajectory, that inhomogeneities in the bulk polymer will strongly influence the direction and shape of the crazes. Local changes in the stress field, which can determine the growth rate of a craze, may be brought about by other crazes nearby.

When the specimen is tilted so that the fracture face above the drawn craze filaments can be seen (Fig. 4.2.10), it is obvious that very little evidence of previously highly drawn filaments exists. This zone corresponds to region 1, where crazing and cracking both initiate in the presence of high concentrations of agent.

The interior of a ruptured craze can be determined by using a Formvar replication technique. The nylon sample was crazed, and straining was continued until cracks passed through the agent-induced craze region, without completely fracturing the specimen. The advantages in preparing such replicas is that the surface of the interior of the crack can be observed without having to break the sample. This would be impossible to carry out by direct observation of the specimen in the S.E.M.

The first replica reflects the morphology of the surface (through plane AA'B'B) of the polymer, as well as the fracture face (Fig. 4.2.11). The former is rough, as a result of interaction between salt and polymer, which has produced swelling and a white adduct. The ridge, representing the crack, can be divided into three sections. Nearest the surface, regions 1 and 2 appear (a), although from this

Fig. 4.2.9. Deviation of craze paths suggesting craze interaction. Magn. = 82x

Fig. 4.2.10. Interior of crack above craze matter, showing flat crack wall, in contrast to the highly oriented craze fibrils.
Magn. = 256x

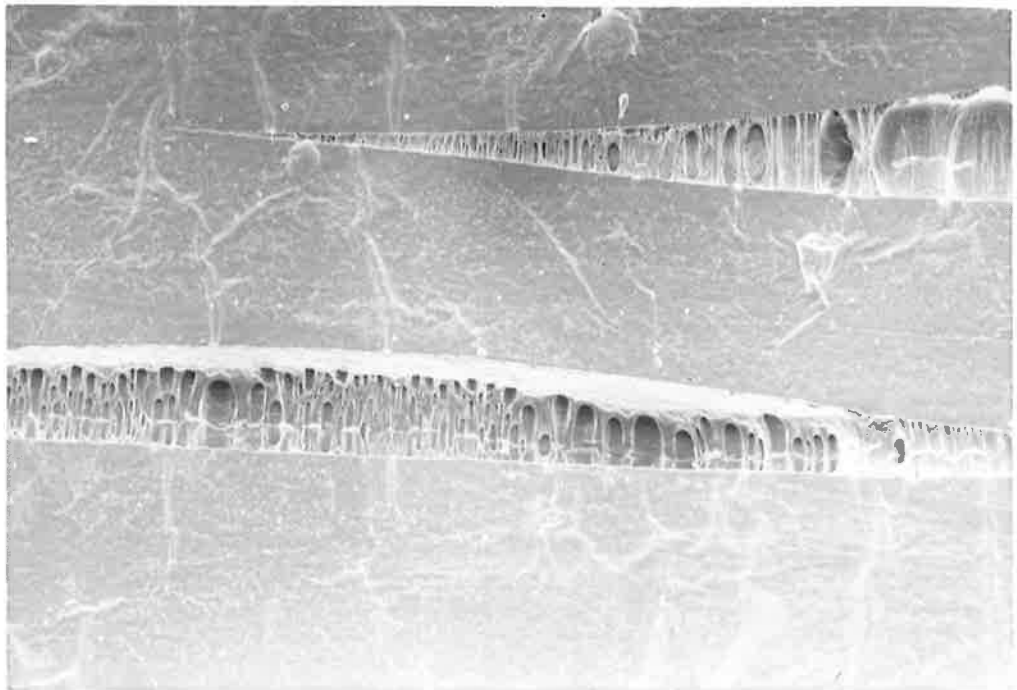
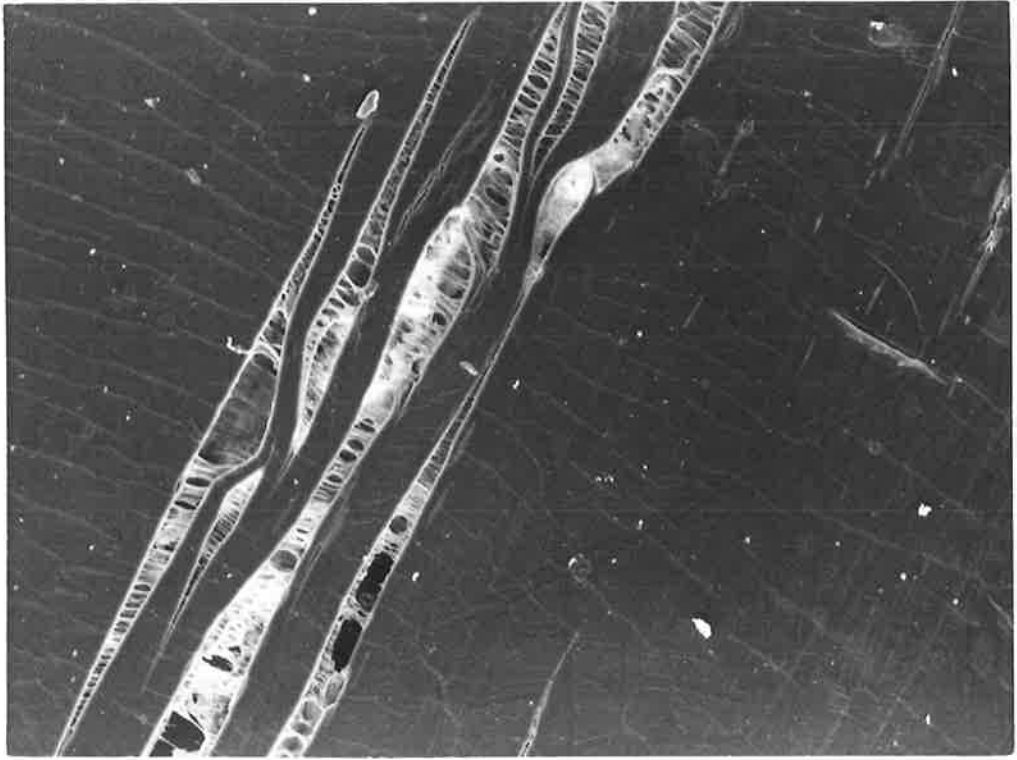
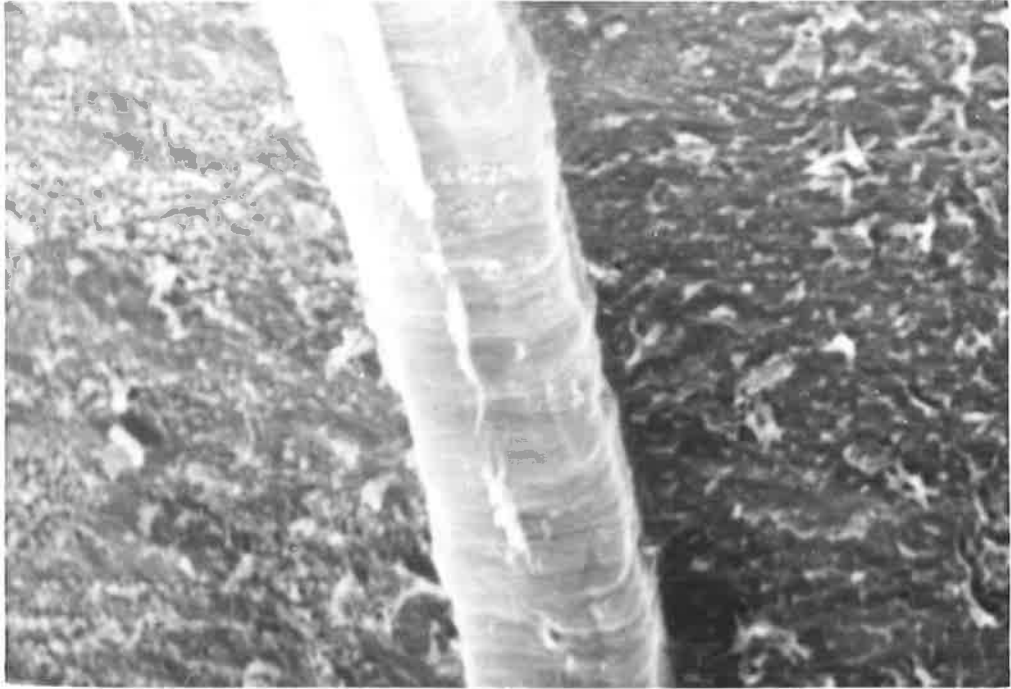


Fig. 4.2.11. Replica of zinc chloride cracked nylon 66, showing regions 1, 2 and 3 (shown as a, b, and c). Magn. = 615x

Fig. 4.2.12. Replica of craze surface, with etching of uncrazed nylon also revealed. Magn. = 4,910x



photograph no closer identification can be made. There is a transition between the two ductile fracture regions (b,c) which reflects a change in the fracture velocity.

A replica of the surface of a craze which has not fractured (Fig. 4.2.12) provides no new information. The normal biaxially oriented "skin" of the craze, with characteristic "ribs", corresponds exactly to the morphology of crazes viewed directly.

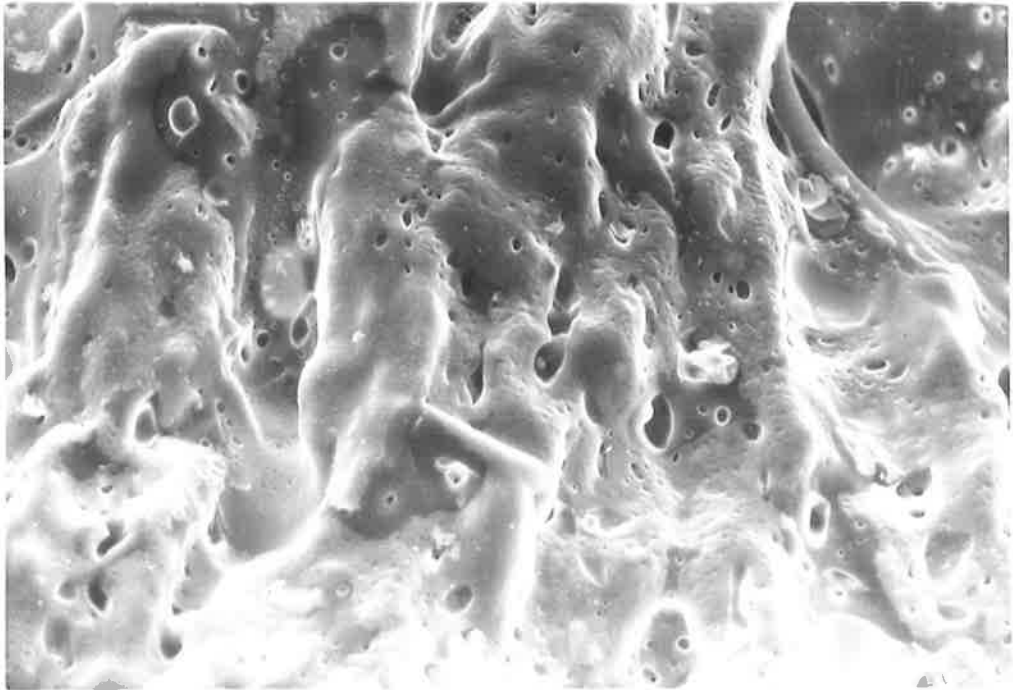
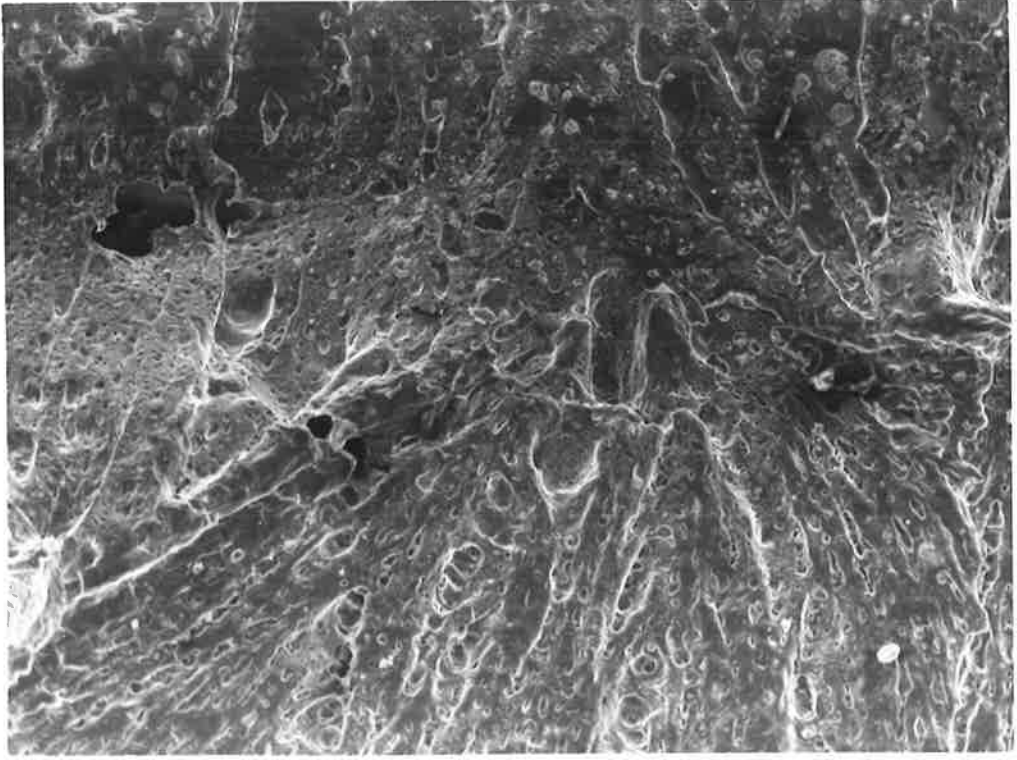
Some experiments using notched nylon 66 test-pieces (ASTM type 1) were carried out using a variety of conditions. It was considered that by localising stresses in this way, a less ambiguous assessment of the mechanism of stress-crazing could be made.

Only localised swelling was found at the notch (region 1), with ductile fracture (region 3) occurring over most of the specimen. The morphology of the swollen matter (region 1) can be seen in Figs. 4.2.13,14. The notch inhibited craze formation by causing crack velocity to exceed agent uptake, and so agent-induced craze development (for which the presence of region 2 in the fracture surface would have been sufficient evidence) is unable to precede fracture.

This result was found for the crazing of all notched specimens. Even when exposure to zinc chloride was long (12h) and the strain rate low (1.0mm/min), agent-induced craze formation was very restricted. The fracture surface in the last case (Fig. 4.2.15), for example, has very few region 2 craze remnants. Only a featureless region (a), (region 1), near the notch at left (b), and some traces of zinc chloride (c) carried over subsequent

Fig. 4.2.13. Swollen region 1 near notch of nylon 66.
Magn. = 110x

Fig. 4.2.14. Porous texture of region 1. Magn. = 480x

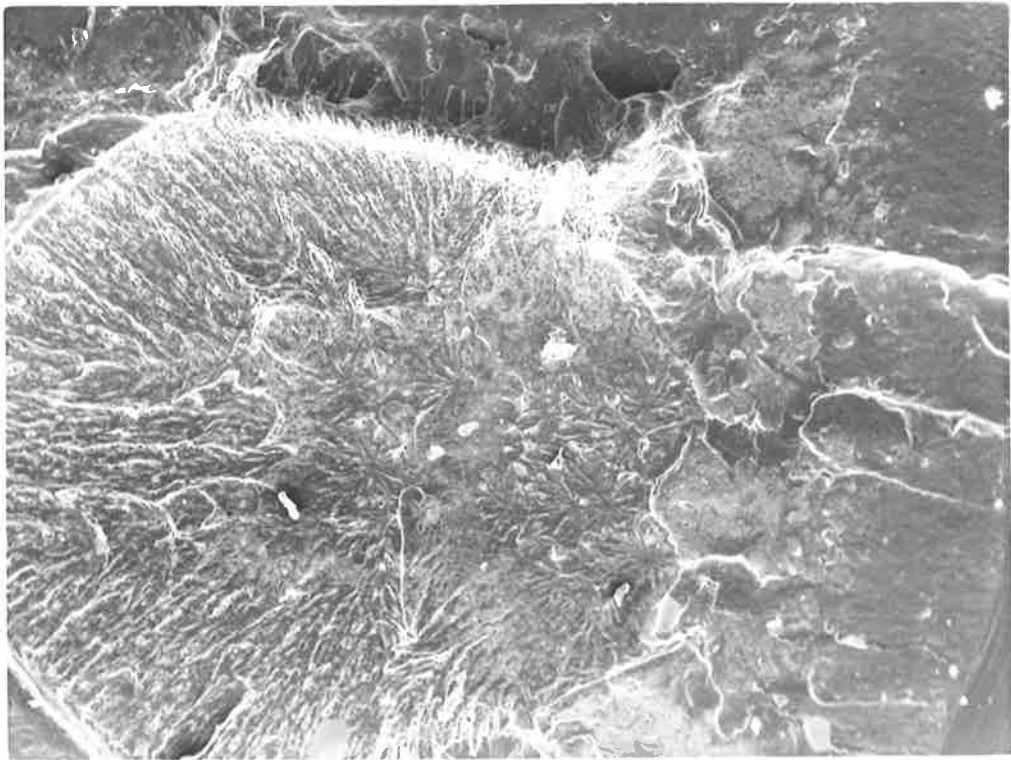
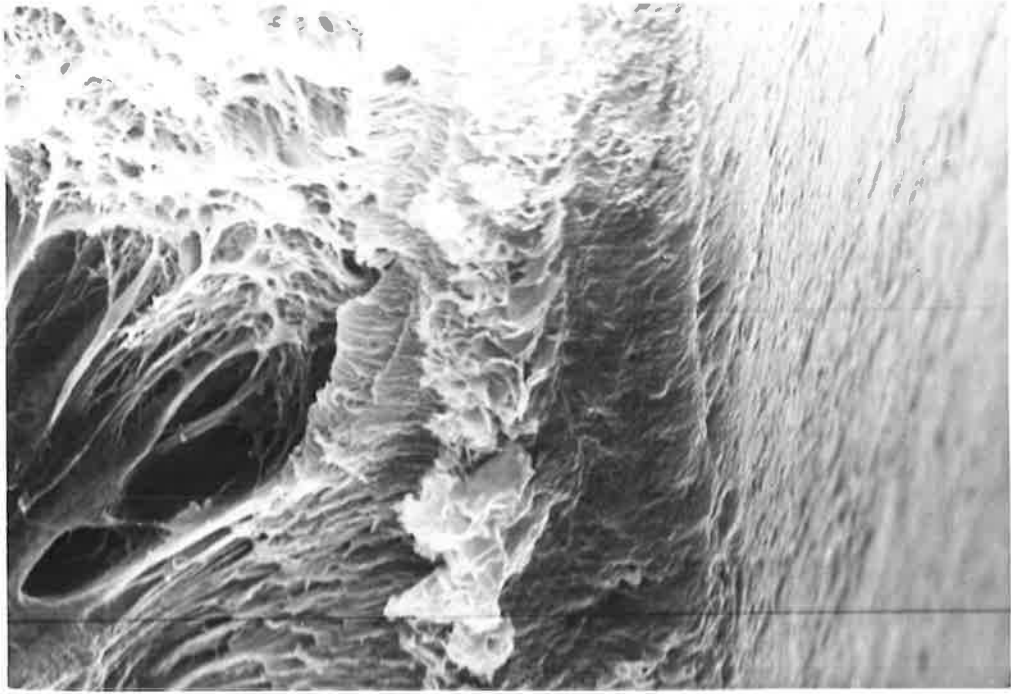


to fracture, provide evidence for the presence of zinc chloride. Apparently the salt was taken up too slowly by the nylon 66 for environmental crazing to compete with ductile fracture at the strain rates used.

Sometimes a crystalline adduct was seen in specimens near the initiation zone (region 1). This zinc-rich substance is unusual, because the adducts normally encountered appear amorphous. This material can be seen in Fig. 4.2.16.

Fig. 4.2.15. Nylon 66 fracture surface with zinc chloride contamination (pale regions) and narrow agent-induced craze zone.
Magn. = 35x

Fig. 4.2.16. Crystalline zinc chloride - nylon 66 adduct near craze initiation zone.
Magn. = 2,330x



Nylon 6

Nylon 6 undergoes more extensive damage than nylon 66 when tested under similar conditions with zinc chloride. Fig. 4.2.17 shows a nylon 6 testpiece which has been strained with a crosshead speed of 0.1 cm/min. The extent of the damage and the complexity of the morphology of the surface are immediately apparent.

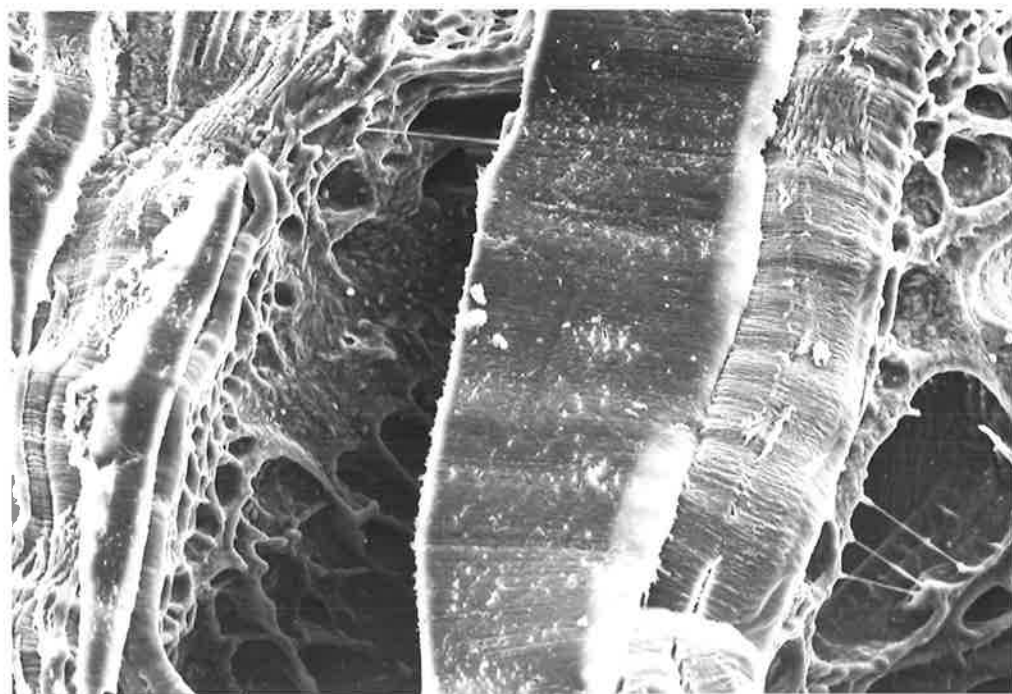
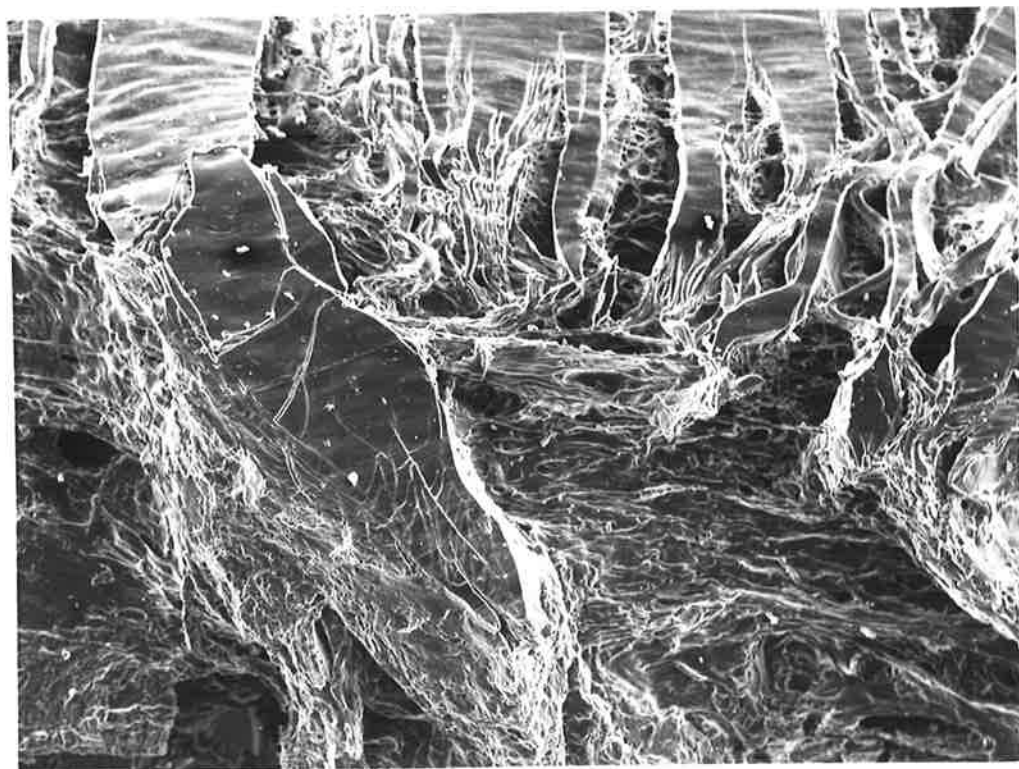
The stressed nylon 6 appears to take up zinc chloride more rapidly than nylon 66, because the regions of highly elongated and plasticized polymer (containing the salt) are more extensive. In Fig. 4.2.18 large areas of polymer, modified by salt, appear. The plasticization which occurs is extensive, even away from the surface, because swollen filaments with nodules (caused by retraction and subsequent swelling) can be seen.

Large blocks of uncrazed polymer appear at low magnification to be unchanged by the salt (Fig. 4.2.17), but at higher magnification (Fig. 4.2.18) very small voids and other evidence (such as charging) of salt uptake can be discerned. The conclusion drawn from this sample is that the extent of salt-induced crazing in this sample of nylon 6 appears to be more extensive than for nylon 66. It is suggested that the velocity of solvent induced craze propagation is more rapid than for nylon 66 under similar test conditions.

When test conditions are suitable, (such as slow strain rate and removal of agent, just after craze initiation) it is possible to isolate discrete crazes. These crazes are similar in appearance to those seen in nylon 66.

Fig. 4.2.17. Extensively cracked nylon 6 specimen -
slow strain rate and excess zinc chloride.
Magn. = 35x

Fig. 4.2.18. Fine detail from above specimen, showing
swollen and retracted craze matter, and
evidence of salt uptake in undeformed
block at centre of photograph.
Magn. = 230x



A well developed craze which was produced by straining nylon very slowly in the presence of zinc chloride, can be seen in Fig. 4.2.19. The craze initiated in the treated region and propagated into the untreated region. The bulk polymer on each side of the craze is swollen with salt; the "skin" of the craze surface is highly oriented, and as the X-ray map below (Fig. 4.2.20) indicates; this craze region is rich in zinc cations (the analyser discriminated for zinc- K_{α} counts). High counts of both zinc and chlorine were recorded on the surface of the craze, but this can be attributed to geometrical effects.

Under similar test conditions, well defined crazes containing extended filaments near the tips can be produced. Those shown in Fig. 4.2.21 have ruptured along most of the length (cracking has rapidly followed craze formation). Near the tip highly extended craze matter can be observed (Fig. 4.2.22), which near the surface has fractured. The "dimpled" fracture face of the craze, and the very high void content are also shown.

Thin Formic Acid-cast Nylon 6 Film

A nylon 6 film was formed by casting a drop of formic acid solution onto water. Drops of 5M zinc chloride were then placed on the surface of the film and stretched using the tensile straining device described in Chapter 3. Surprisingly, no crazing was observed.

This can be explained by suggesting that the excess of zinc chloride effectively plasticizes the film through its entire thickness, with the result that localised deformation (crazing) cannot occur.

Fig. 4.2.19. Mature zinc chloride induced craze and swollen nylon 66 to left and right.
Magn. = 2,290x

Fig. 4.2.20. Corresponding X-ray "map" showing distribution of zinc. Magn. = 2,290x

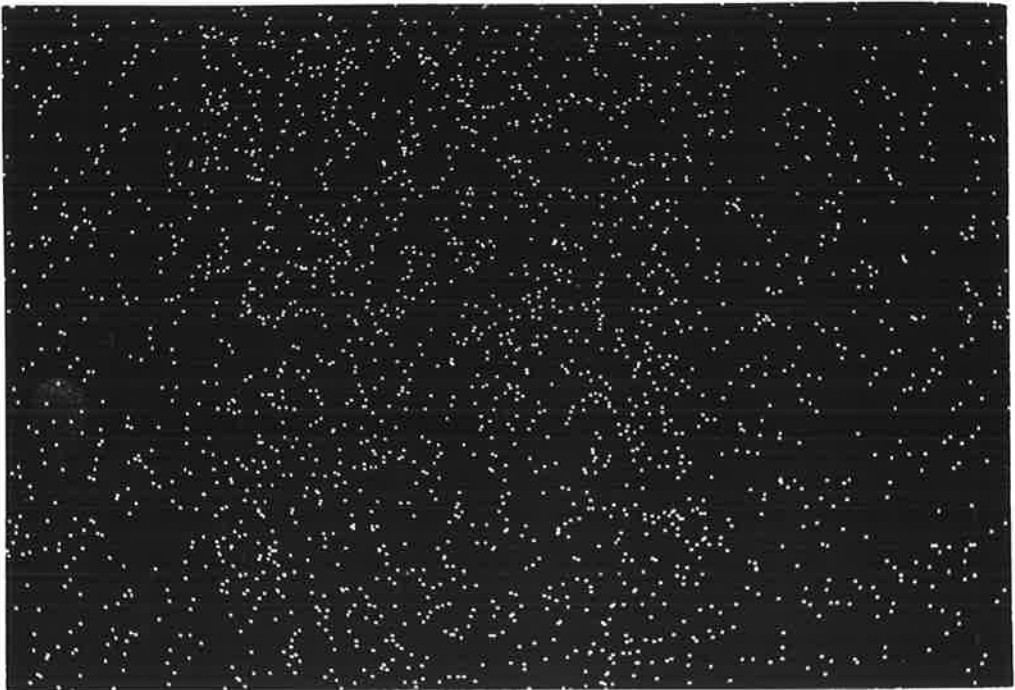
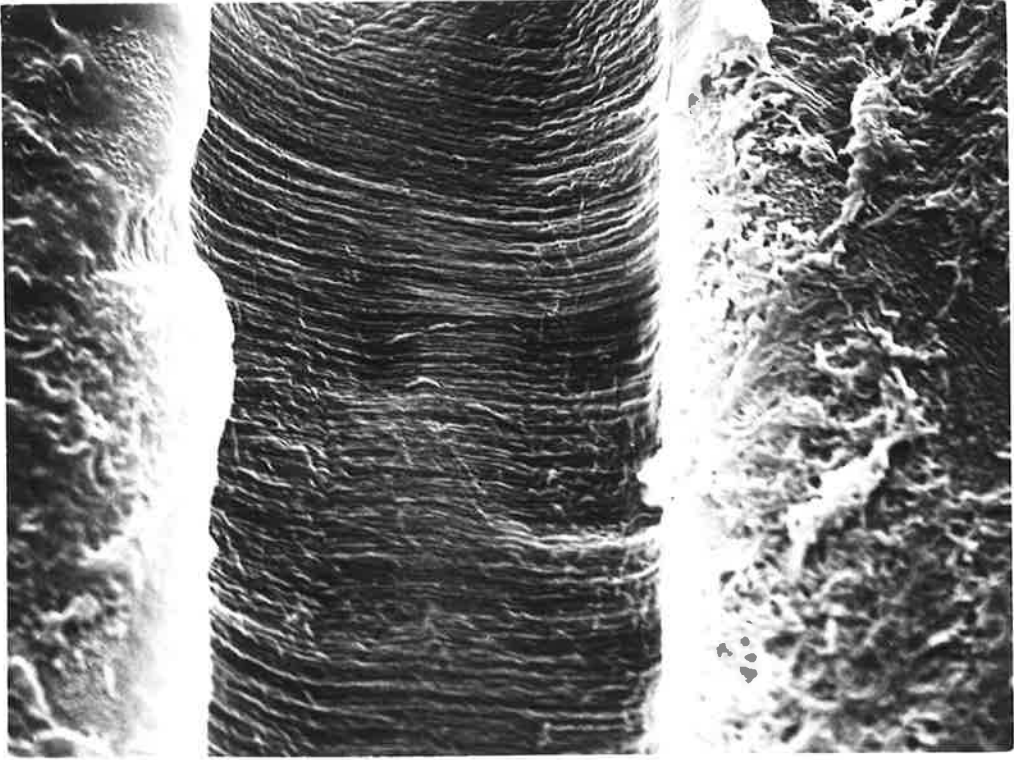
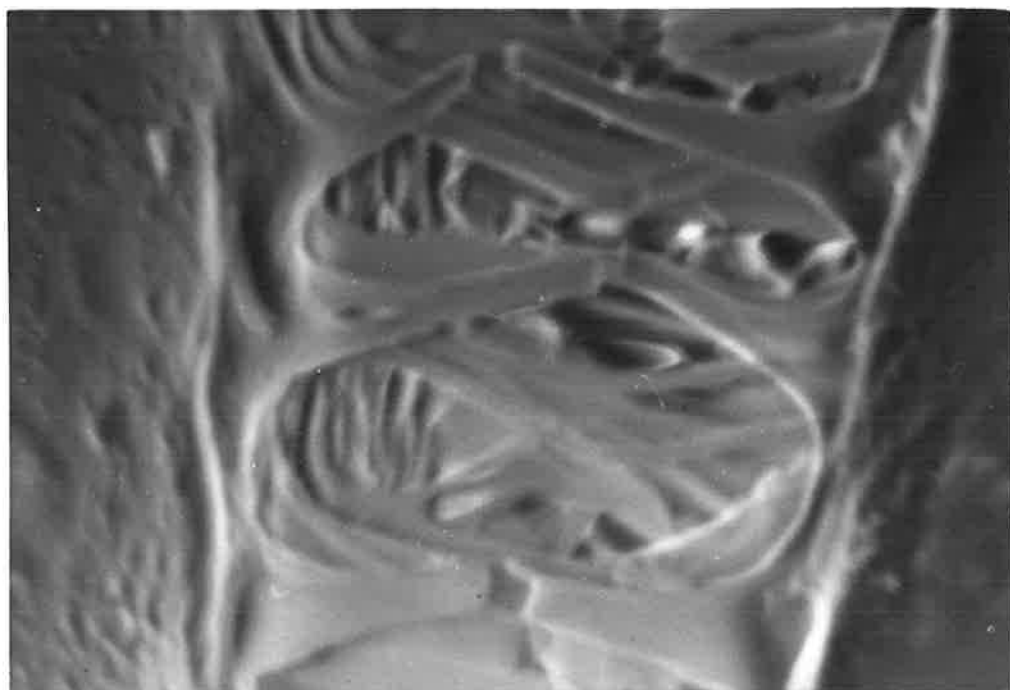
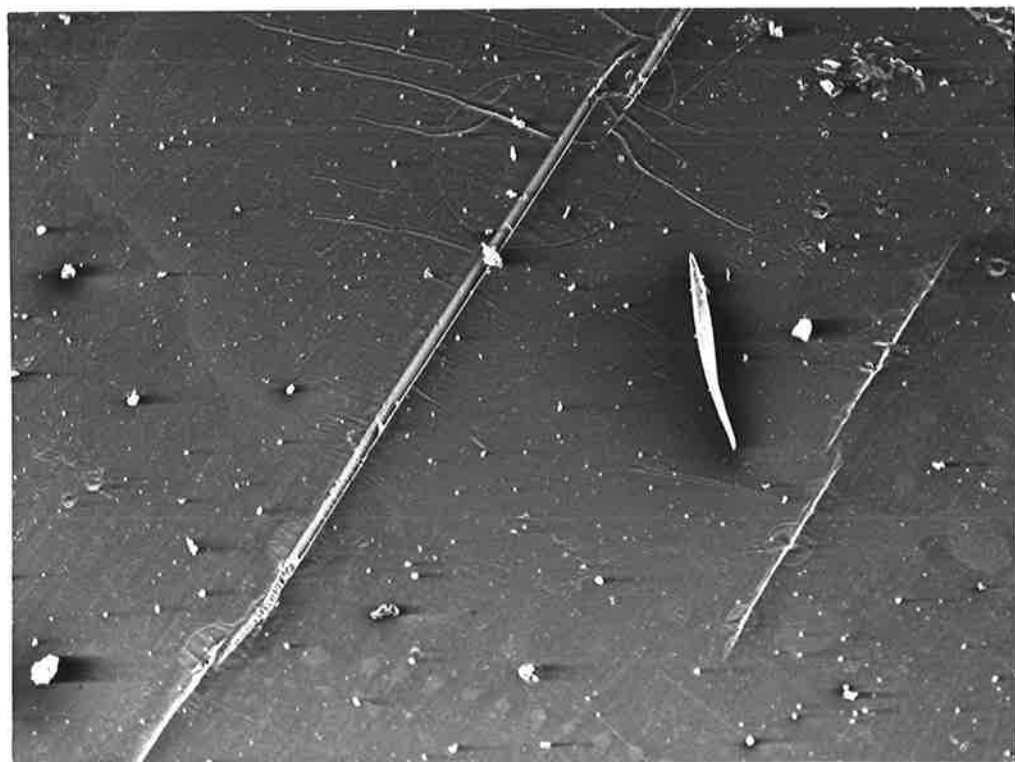


Fig. 4.2.21. Cracks in nylon 6 with craze filaments near crack tips. Magn. = 49x

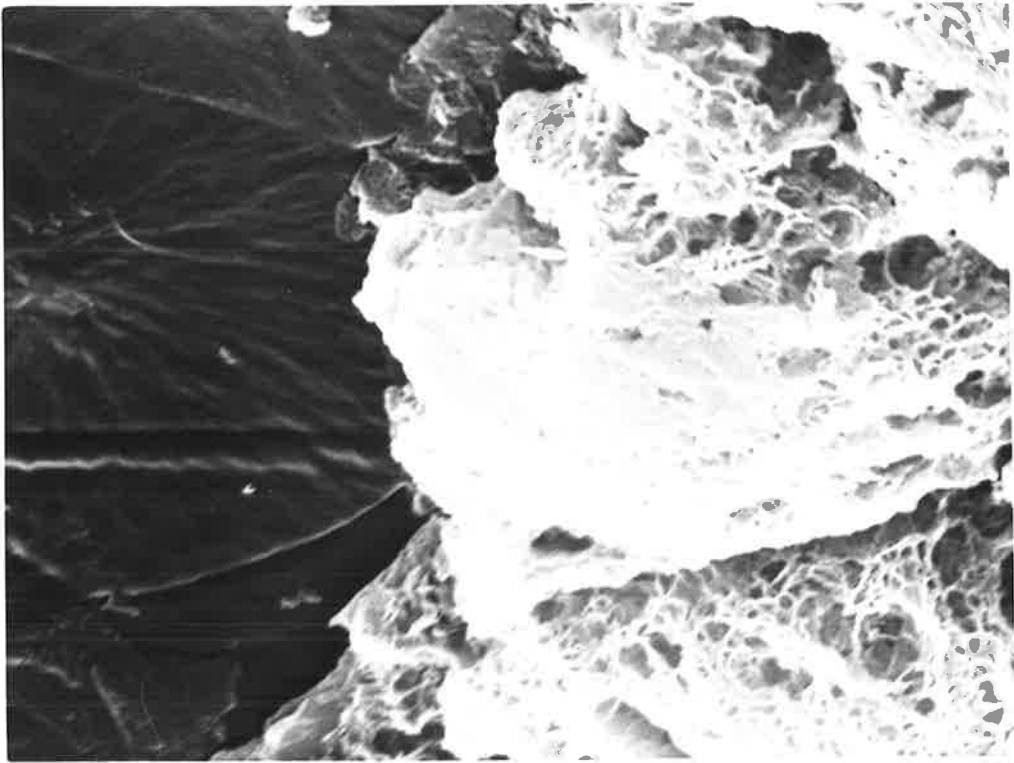
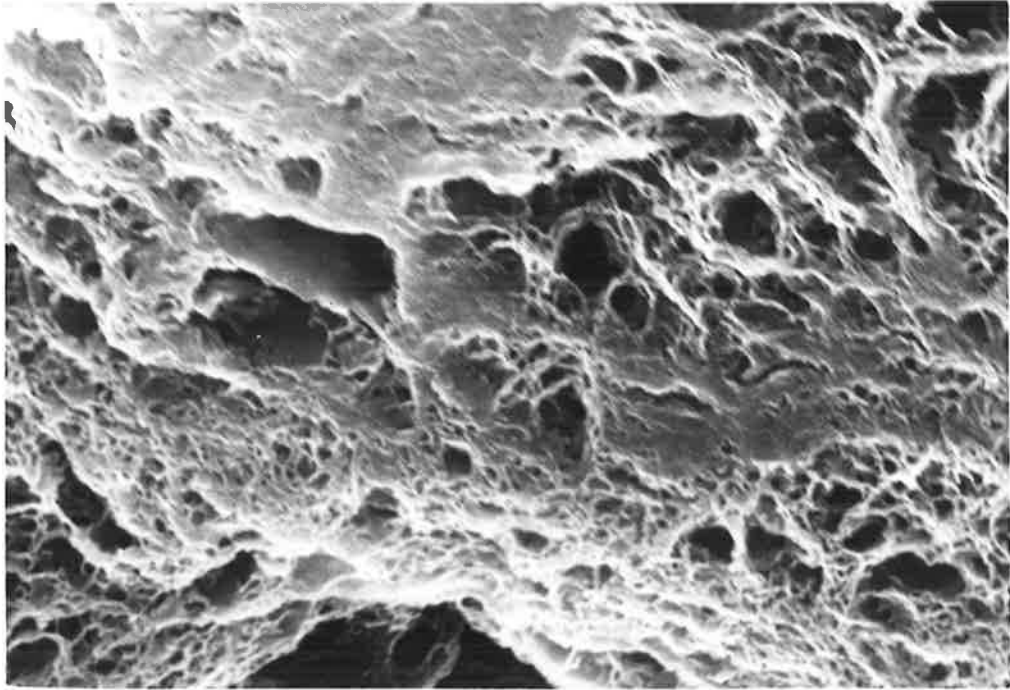
Fig. 4.2.22. Fine structure at crack tips, showing highly extended and ruptured filaments. Magn. = 2,300x



The film was collected onto a stub, carefully washed with water, and examined when dry. The formation of an amorphous adduct contrasts strongly with the spherulites observed in the untreated film. The complex is shown adjacent to the untreated film at low magnification in Fig. 4.2.23, and the adduct is shown at higher magnification in Fig. 4.2.24. Mechanically, the film has behaved in a similar way to anhydrous bulk nylon 66 which has been treated with concentrated zinc chloride for long periods of time (> 1 day). Plasticisation and swelling, and suppression of craze formation, occur in the treated region instead of premature fracture.

Fig. 4.2.23. Zinc chloride - nylon 6 complex (at left) supported on a thin, spherulitic nylon 6 film (at right). Magn. = 4,910x

Fig. 4.2.24. Complex at higher magnification showing porous, amorphous appearance. Magn. = 9,850x



4.2.2. Crazing Induced by Cobalt Chloride

Cobalt salts were shown by infra-red spectroscopy [4] to interact with nylons by forming a direct cation-carbonyl oxygen donor-acceptor bond, in much the same way as zinc salts. Using Dunn's classification, they are Type I salts.

Indirect evidence presented in Chapter 5 also indicates that the colour change observed when pink, aqueous solutions of cobalt chloride turn blue when applied to nylon and then strained, is associated with a replacement of some of the solvation shell molecules (water), which suggests direct bonding between the cation and the amide group.

Two reasons for investigating stress-crazing with cobalt chloride are the colour change associated with substitution of ligands for the cobalt ion and that unlike zinc salts, aqueous cobalt salt solutions are relatively inactive compared with methanolic solutions. It was considered of interest to compare the behaviour of nylons with both aqueous and methanolic cobalt chloride solutions.

Three examples of stress-crazing with methanolic cobalt chloride (saturated) will be discussed. (The reagent was prepared by mixing excess anhydrous cobalt chloride with dry methyl alcohol to give a deep blue solution.) The crazing activity of the solution was found to be roughly comparable to that of 5M aqueous zinc chloride (see Chapter 5).

In the first type of experiment, an un-notched nylon 66 testpiece (A.S.T.M. type I) was stressed to 55 MPa ($\approx 80\%$ of σ_y) and a drop of methanolic cobalt chloride solution was applied. A small single craze rapidly formed, through which cracking quickly developed. The fracture

surface revealed in Fig. 4.2.25 suggests that agent-induced crazing is confined to the bottom edge of the specimen, and that crack propagation has been rapid compared to craze growth. The coarse, oriented texture shown in Fig. 4.2.25 is considered to be characteristic of rapid crack growth, in the absence of crazing agent. The smoother central region is probably (by analogy with glassy polymers) a slow crack zone. The two "ductile fracture" zones are collectively designated region 3.

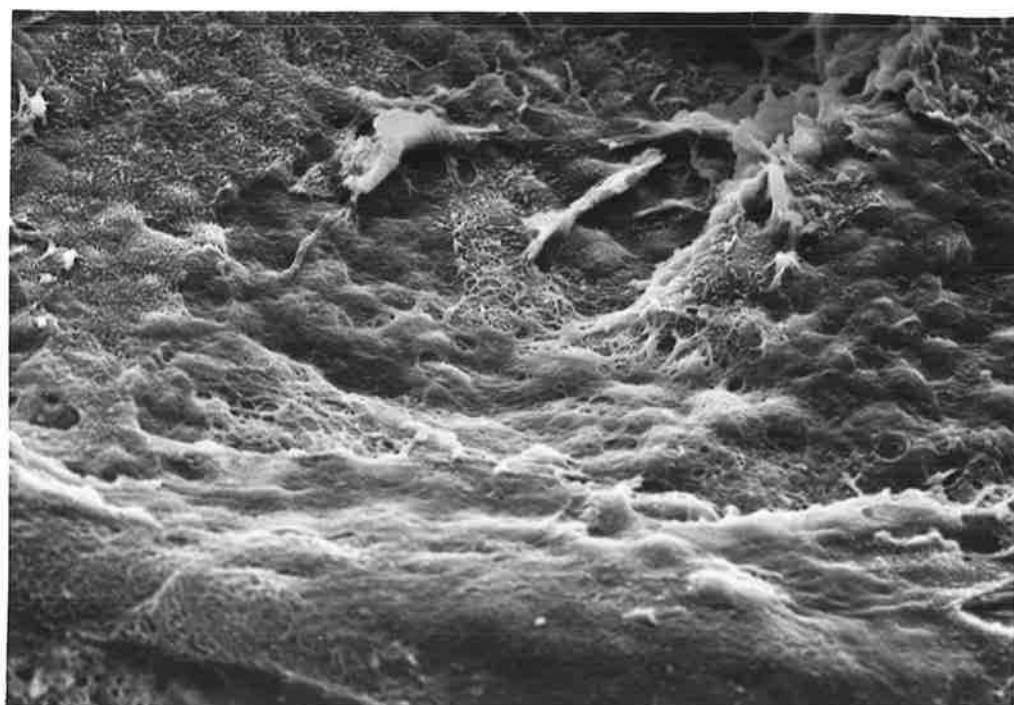
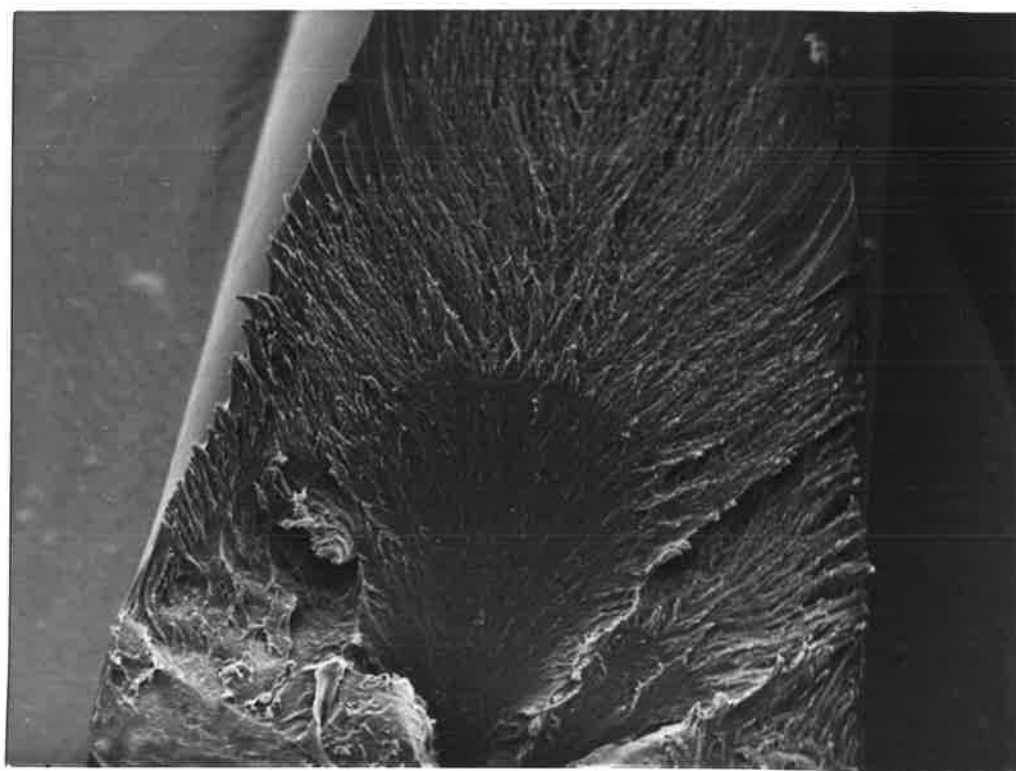
The initiation area is shown at higher magnification in Fig. 4.2.26. A swollen and porous surface (region 1) can be identified at the bottom of the photograph, whereas at the top the polymer has appeared to have drawn, producing short filaments before rupture (region 2).

It appears under the conditions of the experiment that application of the agent has caused highly localised crazing; the craze matter is incapable of extensive elongation and in the presence of high surface levels of the active agent has ruptured. The stress concentration at the resultant narrow crack tip is sufficiently high for rapid crack propagation through the specimen. This mode of failure is also commonly observed in nylons stressed in the presence of zinc chloride (Section 4.2.1), and the role of agent is elaborated upon in Chapter 5.

Under rather different test conditions results of another kind were obtained. A nylon 66 testpiece (A.S.T.M. Type IV) was treated with a drop of methanolic cobalt chloride solution applied, and was then slowly strained. The significant difference is that absorption of some of the agent can occur at stresses less than the critical craze stress, and so modify the mode of crazing.

Fig. 4.2.25. Fracture surface of nylon 66 which was prestressed and methanolic cobalt chloride treated. Magn. = 28x

Fig. 4.2.26. Craze initiation zone of above specimen. Magn. = 705x



Extensive crazing and cracking occurred about the perimeter of the drop, and swelling of the film ensued in the remainder of the treated region (Fig. 4.2.27). There are three factors which need to be considered for this result to be adequately explained.

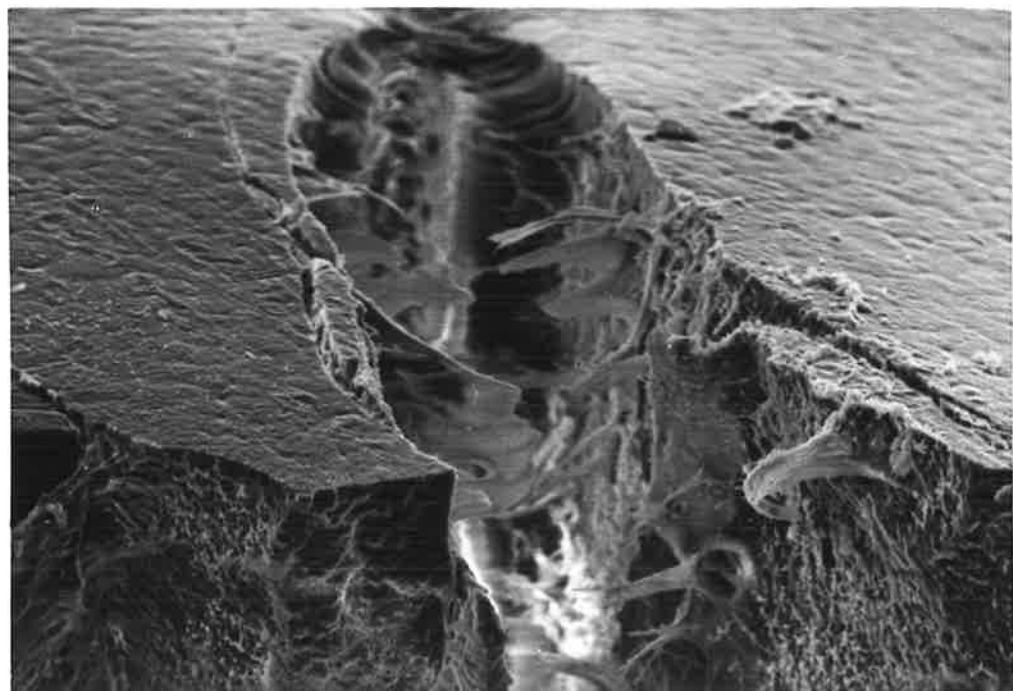
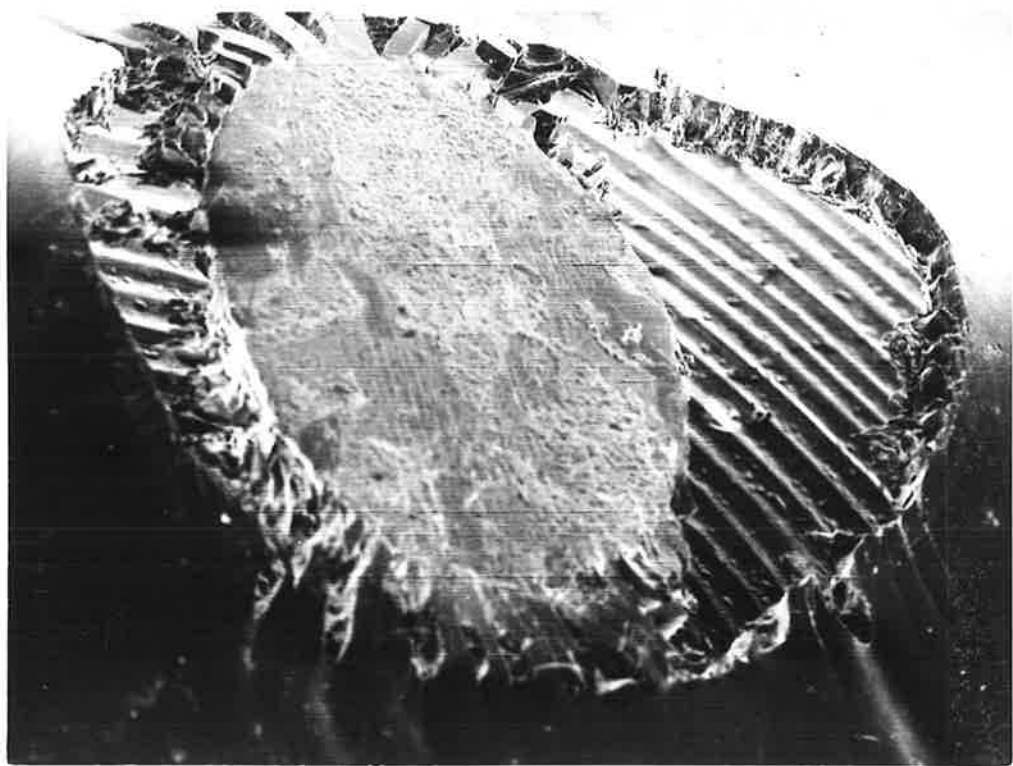
Firstly, photoelastic studies using a nylon film stressed in the presence of a droplet of water indicates that higher stresses exist at the edges of the droplet, nearest the edges of the specimen. In other words, stresses are not evenly distributed in the sample. Secondly, during the experiment, some absorption of water into the reagent, with simultaneous evaporation of methanol was observed, particularly near the edges of the droplet. When a stress-crazing experiment was performed in an atmosphere of methanol, however, the same results were obtained as in air. The third and most significant factor is that the region under the droplet has been subjected to a high rate of plasticisation, giving a swollen surface resistant to craze initiation.

The third factor is considered most important because of the following evidence. When nylon testpieces are treated for long periods of time, with active stress-crazing agents, the agent removed and the specimen strained, no crazes initiate. When one drop of the agent is applied to the treated zone and another to previously untreated polymer nearby, crazing rapidly ensues in the latter region only.

The crack walls have a very complex morphology. Long, isolated filaments can be seen adjacent to short, ruptured material in Fig. 4.2.28. The complexity of the morphology

Fig. 4.2.27. Nylon 66 stress-cracked with cobalt chloride - cracks form at the perimeter of uncracked but swollen polymer. (centre of photograph). Magn. = 24x

Fig. 4.2.28. Cracks in above specimen, with craze remnants visible as ruptured filaments. Magn. = 510x



of the specimen is exemplified in Fig. 4.2.29, where whole filaments traverse the fracture faces, which are covered with swollen, porous material. Analysis of the actual mechanism of failure in this specimen from the morphology of the fracture region is too difficult.

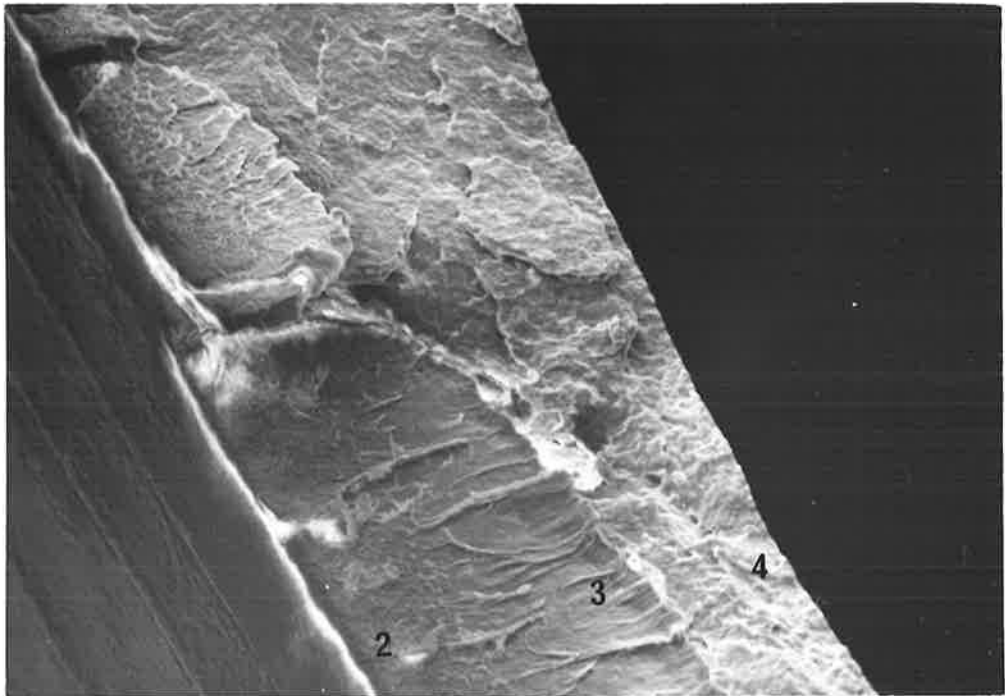
Analysis of the fracture surface (Fig. 4.2.30) resulting from nylon 66 being strained with a crosshead speed of 0.5 cm/min., with methanolic cobalt chloride is more straightforward. Where the agent was applied (to the left of the fracture face) the fracture remnants of the agent-induced craze (region 2) can be identified. Ductile drawing (region 3) occurs next, and the strain rate was sufficiently high to produce brittle fracture (region 4).

As was observed in the first example, fracture of the specimen has occurred before solvent induced crazing could develop completely across the sample. The fracture surfaces suggest that either the agent has a low mobility or the supply is rapidly exhausted, but that it has high activity; i.e. when absorbed in the polymer the mechanical properties are severely weakened.

By comparison, saturated aqueous cobalt chloride was found to induce crazing in nylon 66 only at stresses very near the yield stress of the polymer. Unlike methanolic solutions, this reagent caused a large number of small discreet crazes, which were confined to the treated region. Clearly suppression of craze initiation by swelling at the surface has not occurred, and in fact when observed at high magnifications, surface alteration was negligible.

Fig. 4.2.29. An example of the complicated morphology occurring in cobalt chloride crazed nylon. Magn. = 900x

Fig. 4.2.30. Fracture surface of nylon 66 in which regions 2,3 and 4 can be distinguished. Agent = methanolic cobalt chloride. Magn. = 330x



There appear to be differences in detail between the morphology of crazes produced by zinc chloride and those resulting from cobalt chloride, but the general mechanism of crazing seems to be comparable. The particular morphology which occurs in any one experiment will be the result of the complex interplay between the applied stress, the condition and type of polymer, the concentration and "inherent activity" of the agent, as well as other experimental parameters.

4.2.3. Stress-Crazing Induced By Magnesium Perchlorate Nylon 66

Example 1.

A 0.16 mm thick nylon 66 testpiece was strained under the stereomicroscope in the presence of saturated aqueous magnesium perchlorate (referred to in future as "magnesium perchlorate"). A large number of small crazes formed under the droplet at small strains, and a smaller number of broader crazes were produced at the treated untreated interface. Rupture of one of the largest crazes occurred before the specimen could be irrigated with water (to remove the magnesium perchlorate). The crack did not sever the specimen completely, so that the sample which was observed in the S.E.M. contained both crazes in tension as well as a fracture surface (Fig. 4.2.31).

More information can be gained by tilting the specimen to the position shown in Fig. 4.2.32. The treated surface, covered with many small crazes, and swollen uncrazed polymer (region a) is in sharp contrast to the unswollen bulk polymer

Fig. 4.2.31. Nylon 66 cracked with magnesium perchlorate. Crazes can be seen above and below the crack. Magn. = 44x

Fig. 4.2.32. Same specimen tilted to reveal various craze and crack morphologies. Regions a-f are discussed in text. Magn. = 115x



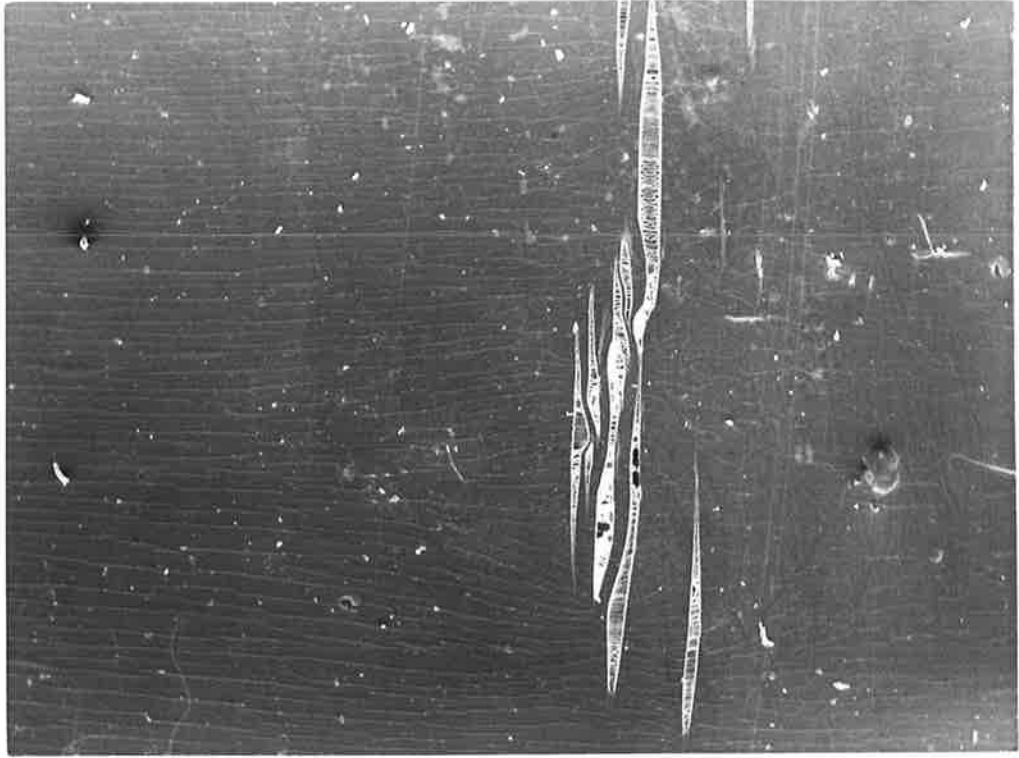
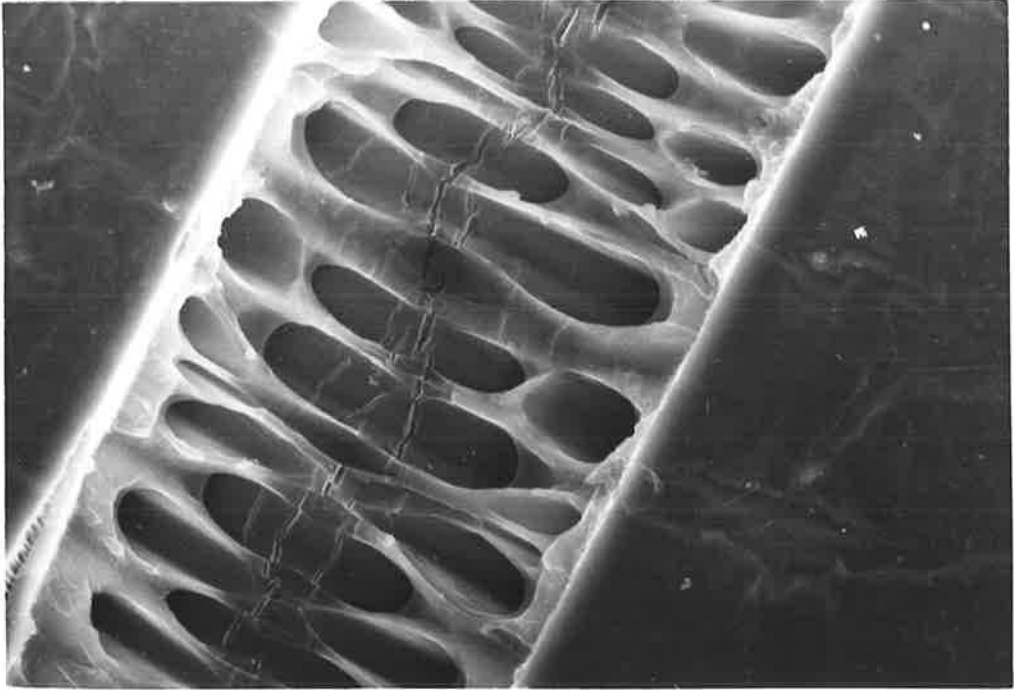
interspersed with fewer larger crazes (region b). The fracture surface of the craze at the treated-untreated boundary (region c) is where fracture was seen to initiate. Where the crack has passed along the broad craze, a surface containing very large voids and a few very large filaments can be seen (region d). Where the crack has passed through a number of previously unconnected small crazes, tearing has occurred, so that layers of polymer protrude from the fracture face (region e). At the end of the fracture surface (out of view) the crack has extended beyond the craze, and the porous craze remnants give way to a smoother, ductile-yielded surface (region f).

The fine surface structure of the crazes both within and outside the treated region is similar to that observed for nylons treated with type I agents. The porous, swollen surface of region a is seen in Fig. 4.2.33, and by contrast a craze passing through untreated bulk polymer is depicted in Fig. 4.2.34. The spherulitic microstructure of the nylon has not caused deviation of the path of the craze away from the usual direction (normal to the applied stressed direction). This was commonly observed using a variety of test conditions, and it is concluded that the orientation of lamella, for example, appears to have no significant effect upon the direction of craze growth.

No entirely featureless initiation zone (region 1) can be detected in the fracture face. Instead, a flat craze zone with many voids is seen (Fig. 4.2.35). The mechanism for crazing in this instance appears to differ from that

Fig. 4.2.33. Porous specimen surface and fine crazes characteristic of region a (from Fig. 4.2.32). Magn. = 5630x

Fig. 4.2.34. Craze passing undeviated through untreated spherulitic nylon 66 (region b). Magn. = 5210x



proposed for type I salt-induced crazing. Long narrow crazes in which the craze matter, containing fine voids, remains constant in texture over the whole length suggests that conditions for craze formation at the tip of the craze are approximately constant. This is compatible with the chemical model, which implicates solvent molecules (with high mobility) in the salt-amide bond, and is supported by X-ray analysis (Section 5.1).

During the fracture process, the crack tip passes from one small craze across to another nearby. Where there has been a craze, the fine porous texture is seen on the fracture surface, but when the crack has had to traverse the bulk polymer, discontinuities and protruded layers of polymer arise (Fig. 4.2.36).

The craze appears to be the preferred medium for crack propagation (as observed in glassy polymers [55]), so that in regions where a high number density of small crazes exist, the crack will pass from one craze to another. In the untreated region, where long, broad crazes with a coarse texture occur, the cracks propagate continuously through the one craze; local heterogeneities within the craze matter can cause small deviations in the crack path.

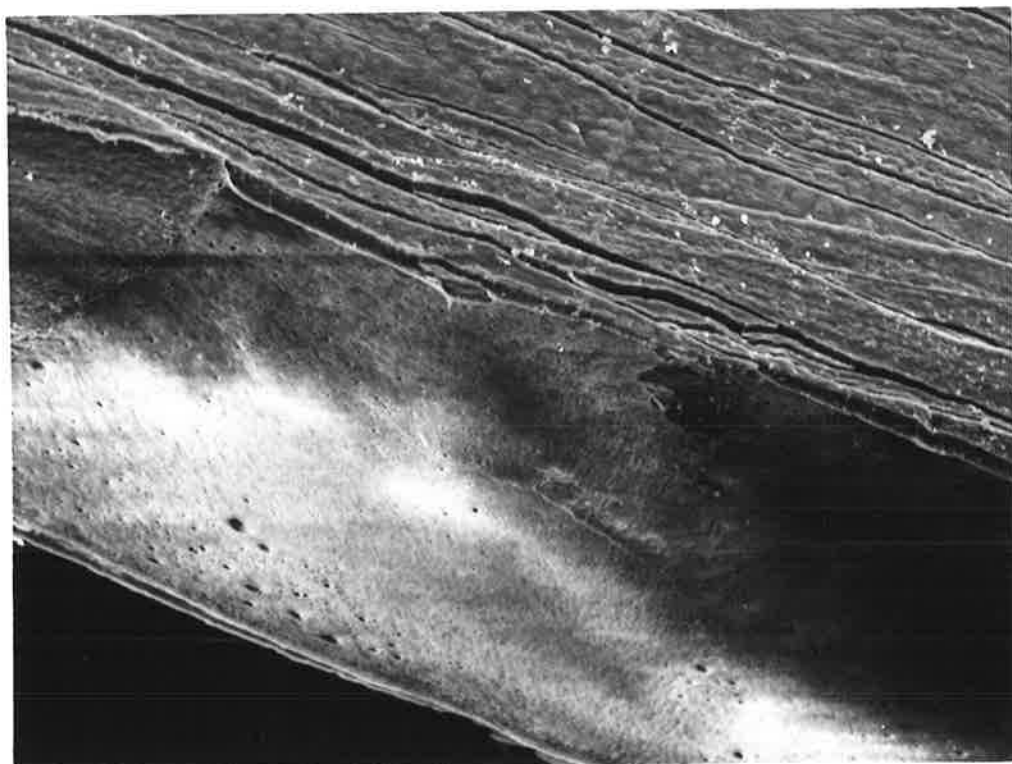
Example 2.

The test conditions used in this example were similar to those described above, except that the agent was applied 10 minutes before straining the specimen.

A small number of large crazes were produced in the treated polymer only; they were found to extend beyond the treated region; where presumably a change in the stress

Fig. 4.2.35. Flat voided craze region (region C) of magnesium perchlorate treated nylon 66.
Magn. = 575x

Fig. 4.2.36. Lamellar fracture surface (region E) caused by crack path deviation as it passes discontinuously through small non-aligned precursor crazes.
Magn. = 515x



conditions has resulted in small crazes radiating from the craze tip. Rupture of the largest crazes had occurred before the sample was washed with distilled water. Some small crazes have also formed, usually adjacent to the largest examples. In Fig. 4.2.37 the most prominent crazes and cracks are seen to be confined to the treated zone.

As observed in other stress-crazed nylons, many crazes are narrow and contrast sharply with the swollen bulk polymer through which they pass (Fig. 4.2.38). The surface of the craze is covered with ribs which are perpendicular to the long axis of the craze, and it is suggested that these arise from the partial biaxial contraction of the surface craze matter. The constraints at the surface differ from those in the interior of the craze (triaxial). As the craze lengthens and thickens, contraction in both directions may occur on the surface.

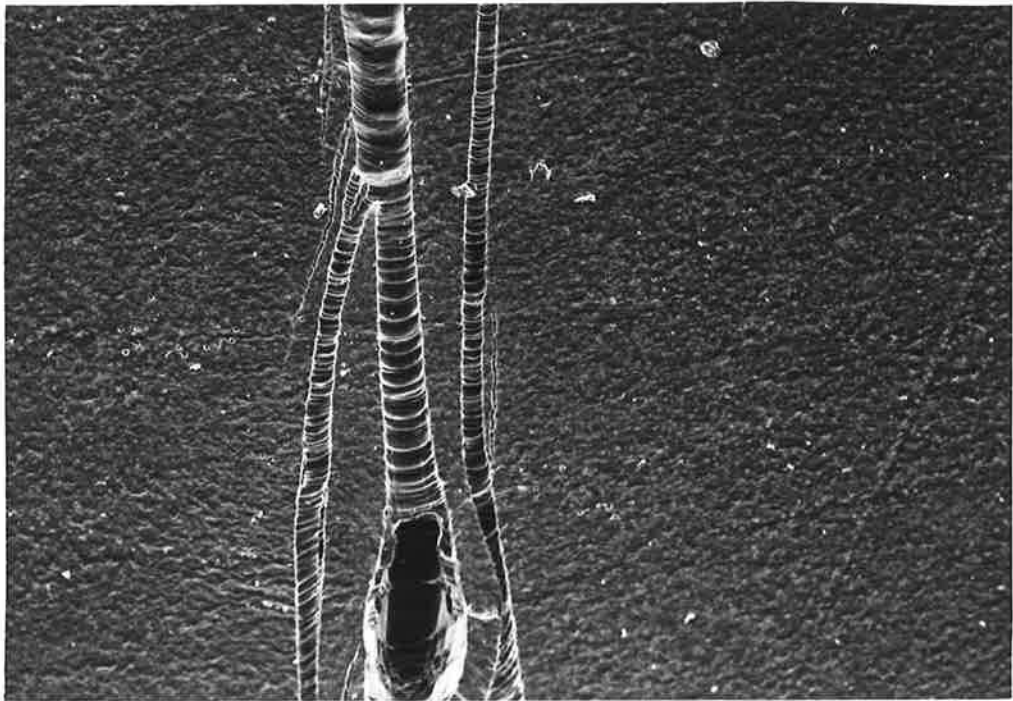
Where rupture of the craze has occurred, the morphology of the fracture surface appears too complex to be analysed. Initiation and highly drawn craze remnant zones (regions 1 and 2) can sometimes be identified.

Example 3.

Sometimes when nylon 66 is stress-crazed in the presence of magnesium perchlorate, and not washed rigorously, a white craze substance can be seen coating the fracture surface (Fig. 4.2.39). This material has been shown by X-ray analysis to contain high levels of salt, and it is proposed that it is nylon-salt complex which has precipitated in the presence of water, and resembles in texture synthetic adducts prepared by melting salts with nylons or model amide

Fig. 4.2.37. Large magnesium perchlorate induced crazes and cracks sparsely distributed in nylon 66. Specimen treated with agent before application of stress. Magn. = 18x

Fig. 4.2.38. Narrow crazes passing through porous polymer. Same specimen as above. Magn. = 200x



compounds. It appears to be craze matter which contains large amounts of agent, and forms as a separate phase from the nylon, but optimal conditions for the formation of the substance have not been determined. (The lobe which is prominent in the centre of the fracture face has resulted from the crack crossing over from one craze to another, as described previously.)

The underlying bulk polymer interface appears to be devoid of any swollen material. This surface type occurs in many specimens where washing subsequent to crazing has been so extensive that the craze-agent crust has been removed. The fracture surface shown in Fig. 4.2.40 is very similar to that which underlies the complex in Fig. 4.2.39.

Effect of Different Strain Rates upon the Morphology
induced by Magnesium Perchlorate

Nylon 66 testpieces were tested in the presence of magnesium perchlorate using crosshead speeds of 1.0, 5.0 and 20.0 mm/min. Extensive crazing occurred each time, and the morphology of the fracture surfaces were similar in type, so that it will only be necessary to consider one example. The mechanical aspects of the experiments are discussed in Chapter 5.

Nylon 66 which has been strained with a crosshead speed of 5.0 mm/min. is shown in Fig. 4.2.41. Large numbers of crazes can be seen on the side of the specimen, and the ends of the fracture face, which have necked (to \approx 40% of the original thickness) indicate that "ductile fracture" has occurred, subsequent to fracture through the craze.

It can be seen from the morphology of the centre of the fracture face that the crack has propagated through a

Fig. 4.2.39. Magnesium perchlorate - nylon 66 adduct
(white) overlying fracture surface.
Magn. = 138x

Fig. 4.2.40. Adduct-free surface of nylon 66 similar
to that shown in Fig. 4.2.39. Magn. = 485x

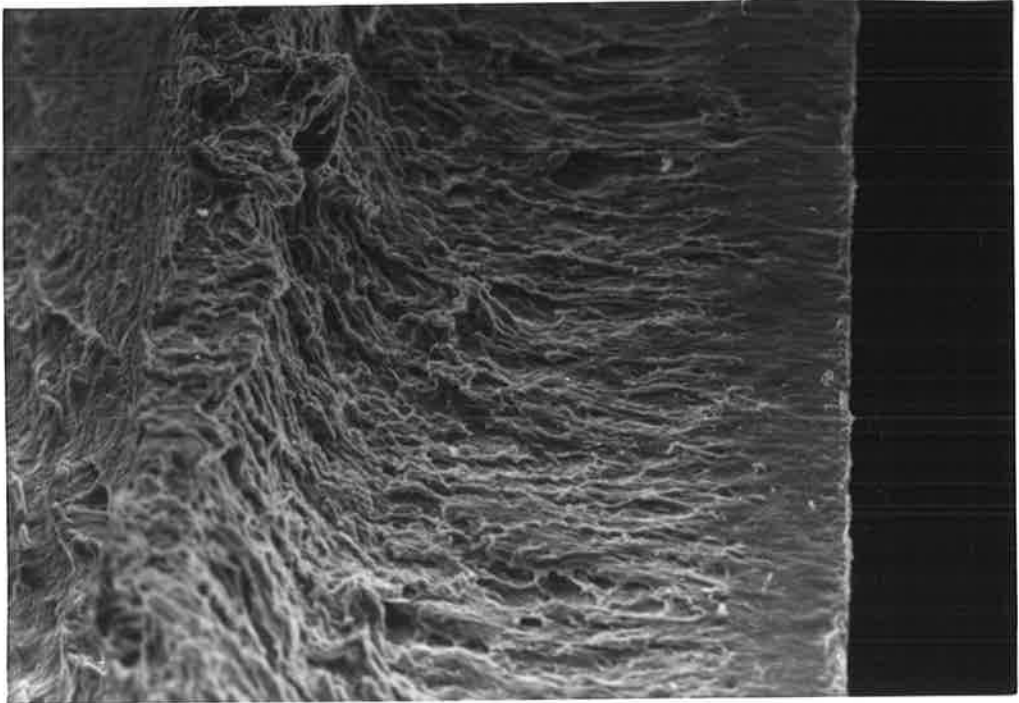
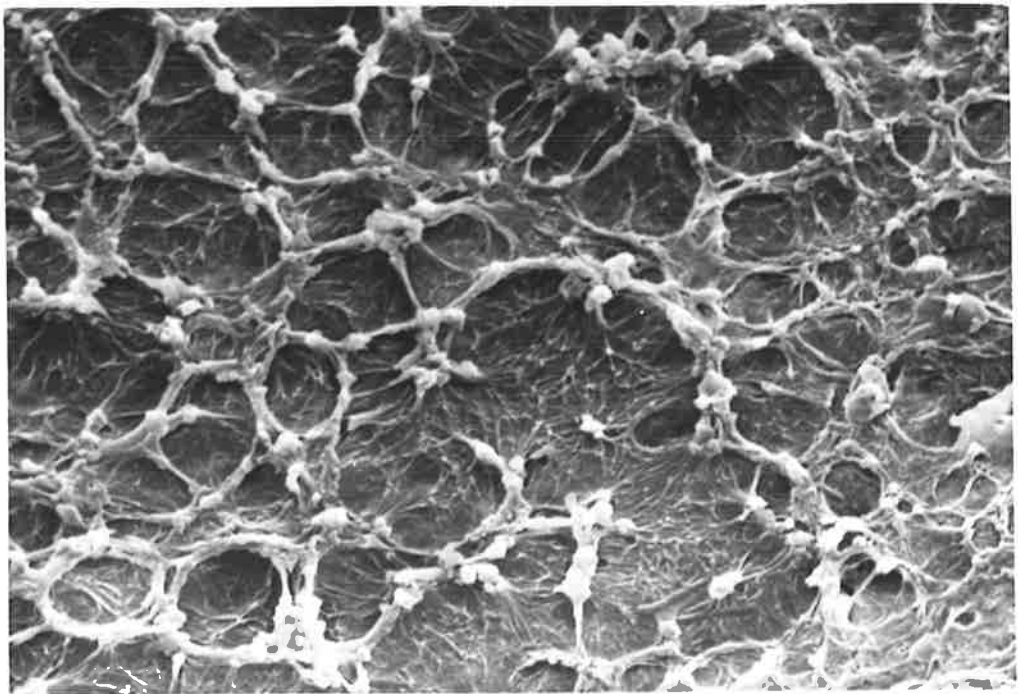
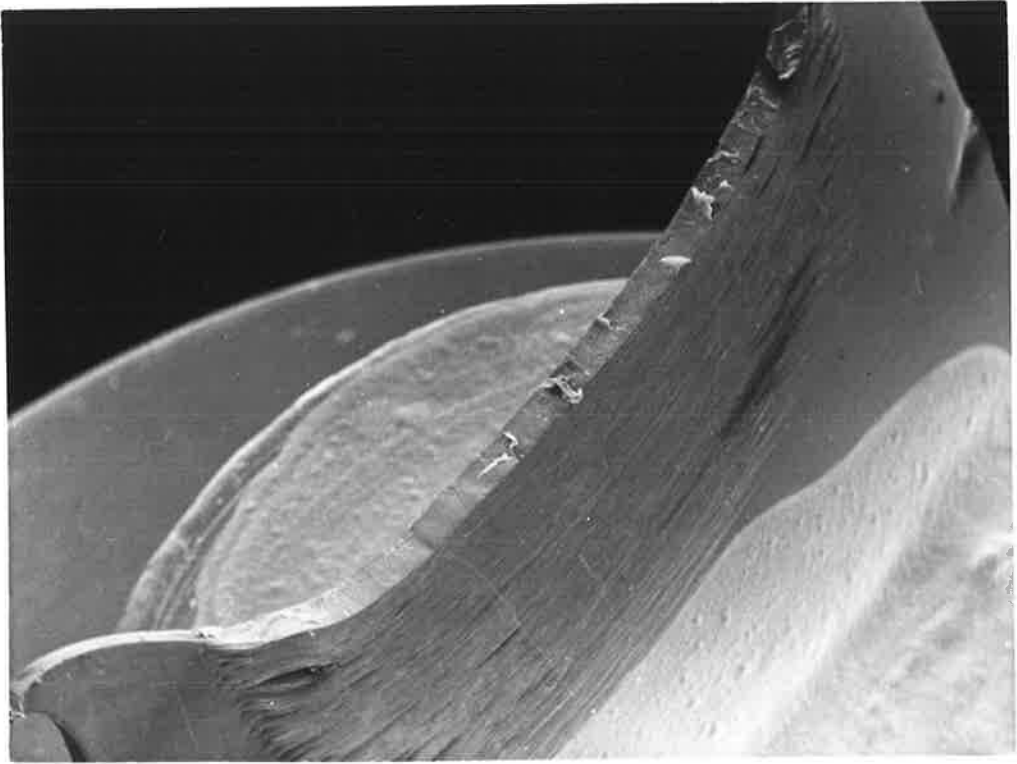


Fig. 4.2.41. Nylon 66 strained in presence of magnesium perchlorate - crazes can be seen below fracture surface. Magn. = 28x

Fig. 4.2.42. Interconnected network of craze filaments and "nodular forms" on fracture surface of magnesium perchlorate treated nylon 66. Magn. = 2045x



number of small, interpenetrating crazes, to give a uniform texture, except where discontinuities arose from the crack jumping from one craze to another nearby.

The texture of the craze is unusual, however. The coalescence of filaments surrounding large voids which is seen in Fig. 4.2.42 is strikingly similar to that observed for polystyrene by Haward [129], (Fig. 4.1.26). Nodules which can be seen in the nylon sample at the tips of the filaments are also observed in polystyrene; Haward considers that the diameter of the nodules corresponds approximately to the expected statistical length of the unperturbed random polymer [129].

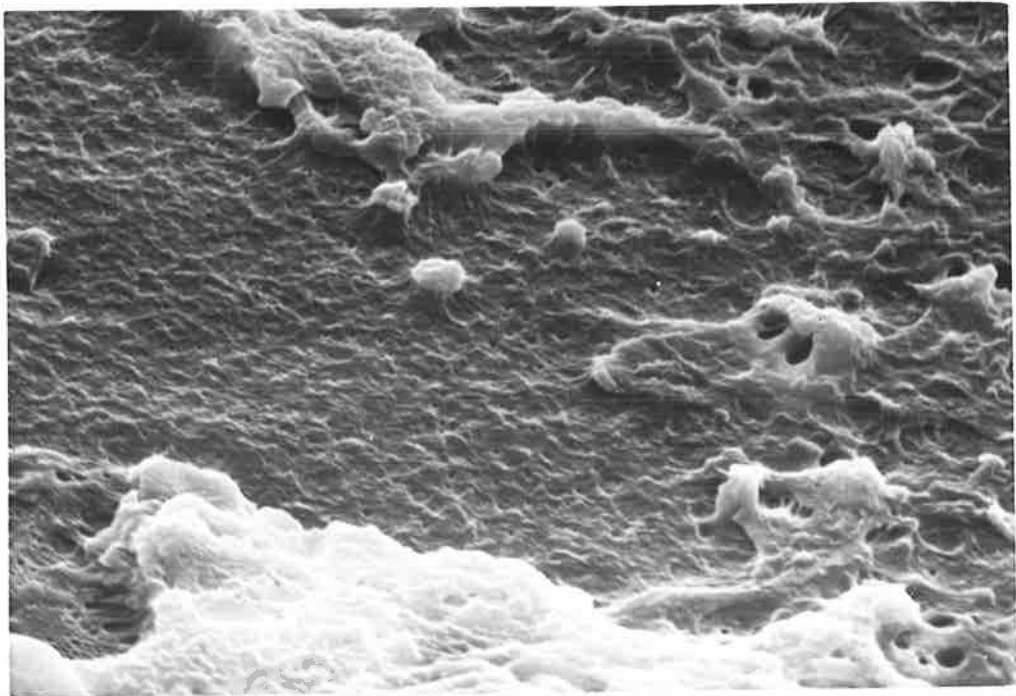
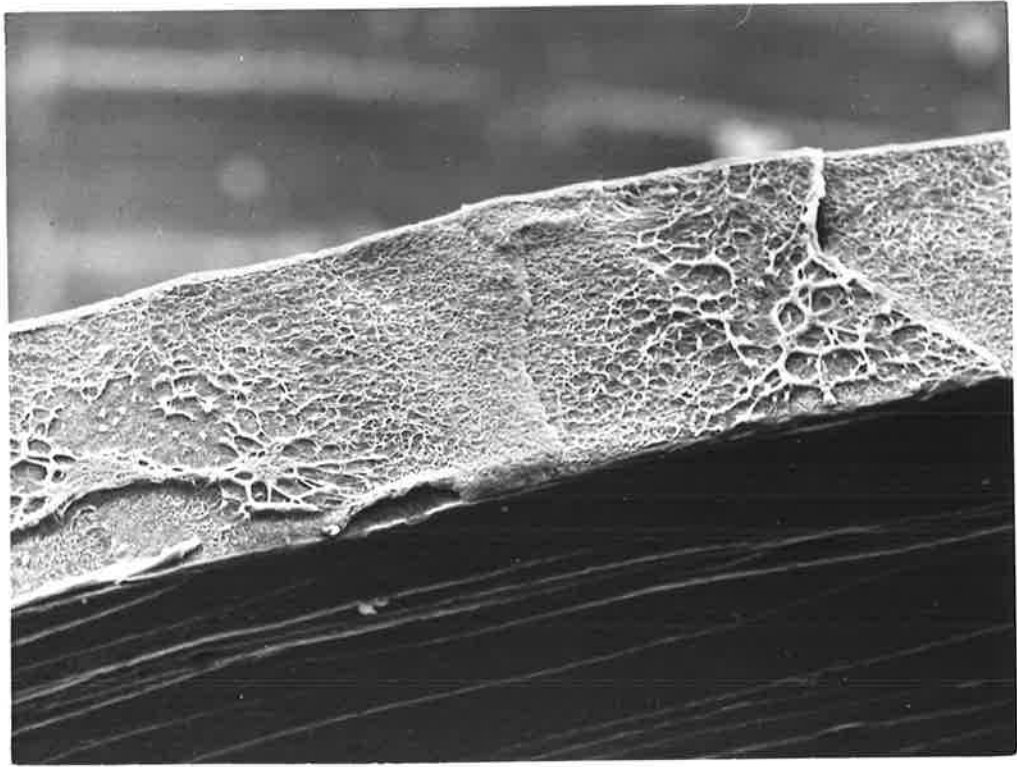
This fine structure also appears extensively in specimens strained at higher and lower strain rates. For example, the fracture surface of nylon 66 strained using a crosshead speed of 1.0 mm/min. contains identical aggregates, but interspersed with more discreet, ruptured filaments (Fig. 4.2.43). At high strain rates the craze remnants have a different appearance; the bulk-craze interface has fine holes, and there are particles of craze matter as well as many small peaks (Fig. 4.2.44). Networks of aggregated filaments are also observed, which have the same appearance as the other two fracture faces.

Cellophane

Cellophane is a transparent film which is prepared by chemically reconstituting cellulose. The polymer chains are composed of β -linked glucose molecules, which contain a large number of aliphatic alcohol groups. The mechanical properties of the film are strongly influenced by the level

Fig. 4.2.43. Similar fracture surface to that shown in Fig. 4.2.42, but with discrete filament peaks interspersed amongst networks.
Magn. = 225x

Fig. 4.2.44. Discrete nodules (light) appearing upon a finely porous template (dark). The craze mark at bottom resembles amorphous salt-polymer adduct. Magn. = 2450x



of water present, because the water molecule can interfere with secondary forces between the polymer chains by hydrogen bonding.

It is important to recognise that the mechanical strength of cellophane is severely reduced in the presence of water, with cellophane fracturing at low stresses. Magnesium perchlorate solution causes fracture at lower elongations, but of interest in the context of this chapter is the morphology of the fracture surface. (The mechanical results are shown in Chapter 5.)

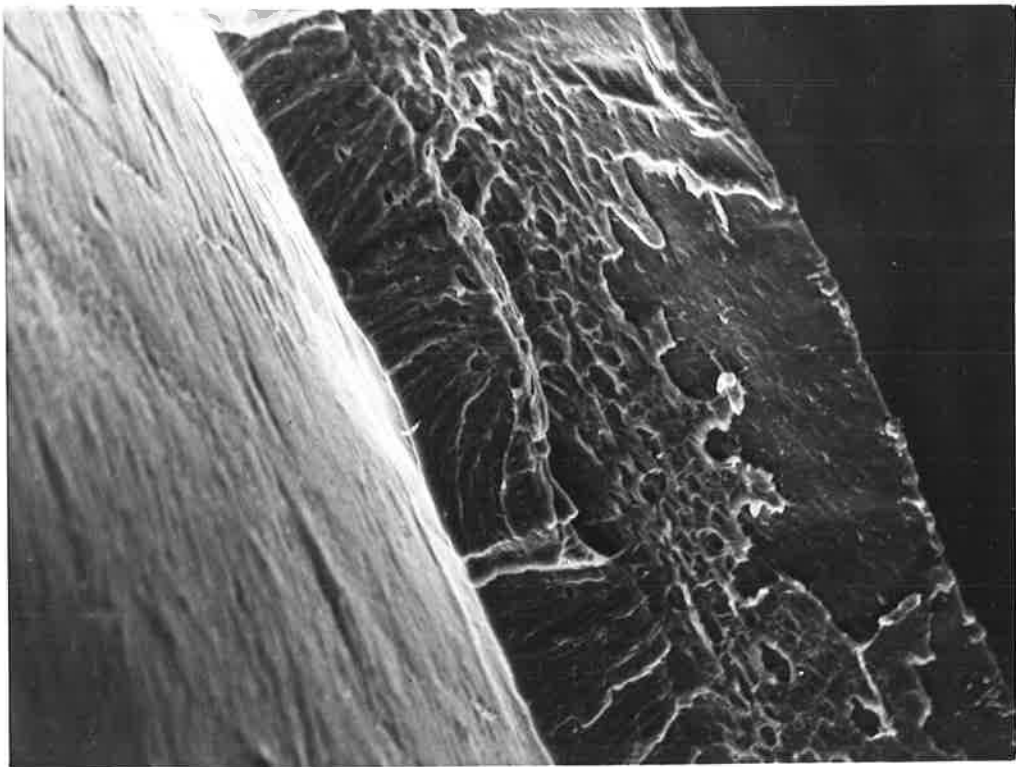
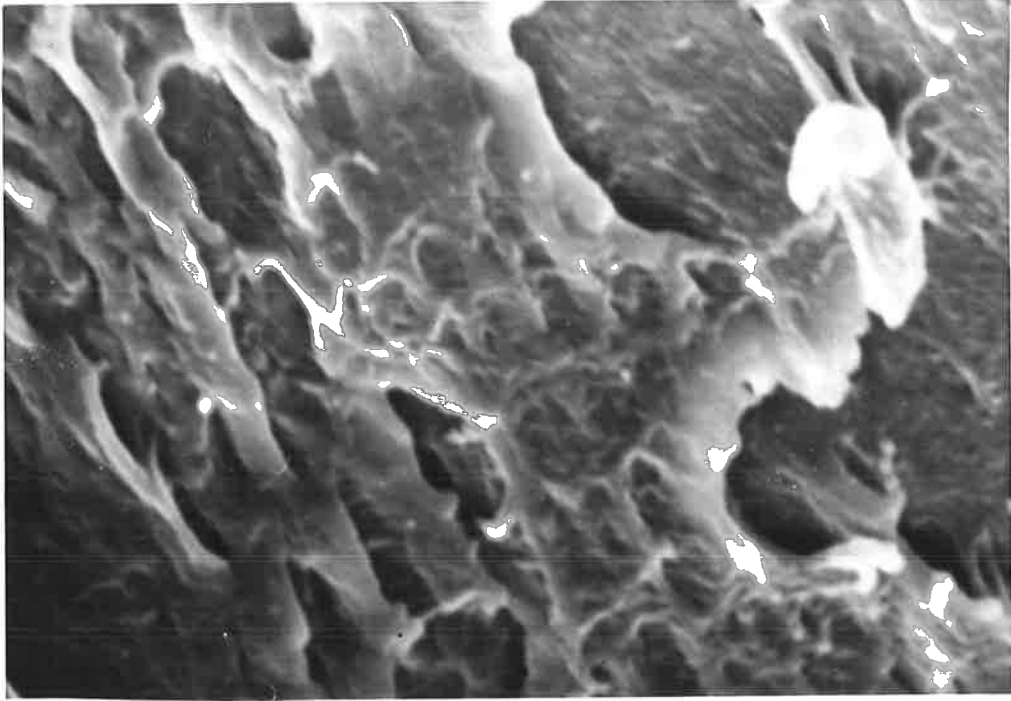
It was difficult to observe the formation of crazes before fracture (which occurred at low strains), presumably because they are very narrow and form just prior to fracture. When the fracture surface was observed however (Fig. 4.2.45) characteristic craze material was found in the vicinity of the treated region, which bears a striking resemblance to craze layers in nylons. To the right of the fracture face in Fig. 4.2.45, there appears to be a brittle fracture zone.

The craze matter in the centre of Fig. 4.2.45 is seen at higher magnification in Fig. 4.2.46. It extends over a large part of the fracture surface and appears patchy because of the oscillation of the crack from one craze matter-bulk boundary to the other.

The results of this experiment suggest that non-crystalline polar polymers such as cellophane can stress-craze in a similar way to polar, semi-crystalline polymers such as nylons. The susceptibility of polymers to crazing is primarily a function of the chemical characteristics of the polymer (such as polarity), rather than the degree of organisation of the chains.

Fig. 4.2.45. "Brittle" fracture surface of cellophane stressed with magnesium perchlorate solution present. Magn. = 1045x

Fig. 4.2.46. Craze material from fracture surface shown above. Magn. = 5230x



4.2.4. Stress-Crazing and Cracking Induced by

Lithium Salts

Concentrated aqueous and methanolic solutions of lithium iodide and lithium bromide were both found to be highly active stress-crazing agents. Lithium chloride was found to be much less active. In experiments where a droplet of lithium iodide and lithium bromide were applied side-by-side on nylon 66 test-pieces, and constant, low, strain-rates used, crazing initiated at the lithium iodide first. The crazing activities under these conditions were therefore $\text{LiI} > \text{LiBr} > \text{LiCl}$.

To investigate further the influence of anion type upon crazing activity, the morphology of crazes induced by both lithium bromide and iodide were each examined. The aim was, with the assistance of X-ray analysis, to determine the role of anion type in the mechanism of crazing.

Lithium iodide was found to turn brown in the solvents used, with the evolution of iodine. It was recognised that iodine can effect crystallographic changes in nylons (from α to γ), but it was considered that the concentration of lithium iodide far exceeded the concentration of iodine and so this secondary effect would be insignificant. Freshly prepared reagents were used to minimise iodine levels.

4.2.4.1. Crazing Induced by Lithium Bromide

Crazes which arise when nylons are stressed in the presence of aqueous or methanolic lithium bromide have many characteristics in common with magnesium perchlorate induced crazes (described in Section 4.2.3.). For example, craze

matter salt complex could be distinguished. This type of material cannot be detected in nylons crazed with Type I agents.

Nylon 66

When a droplet of saturated aqueous lithium bromide was applied to a nylon 66 test-piece stressed at approximately $0.8 \sigma_y$ craze initiation occurred at many sites to produce a high density of small crazes. A few crazes which initiated near the polymer air-agent interface developed into large crazes by extending into the untreated region (Fig. 4.2.47).

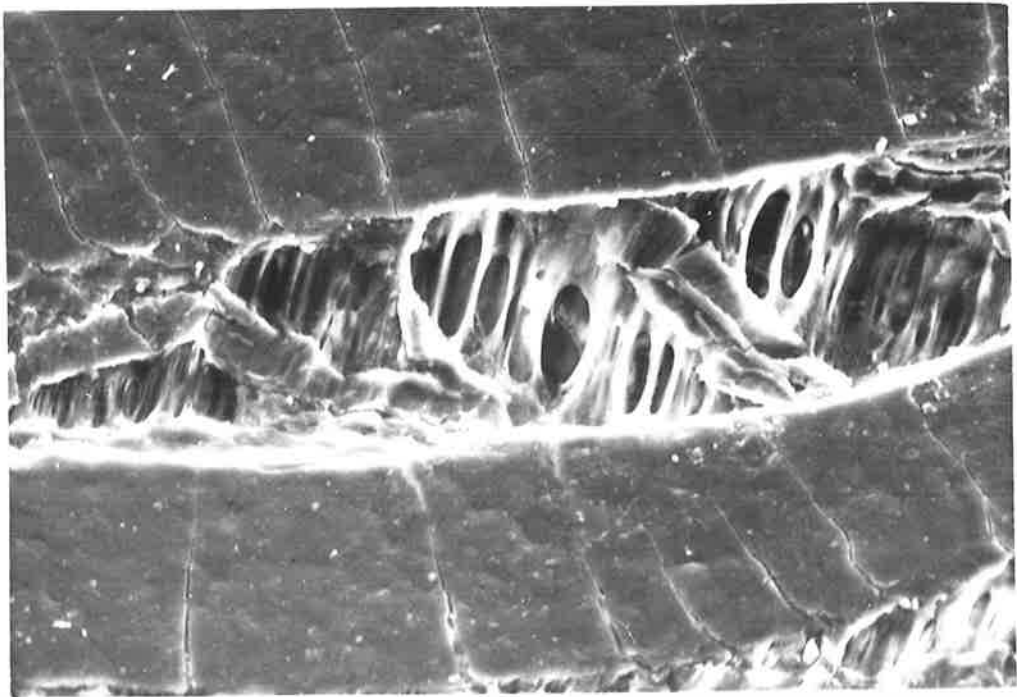
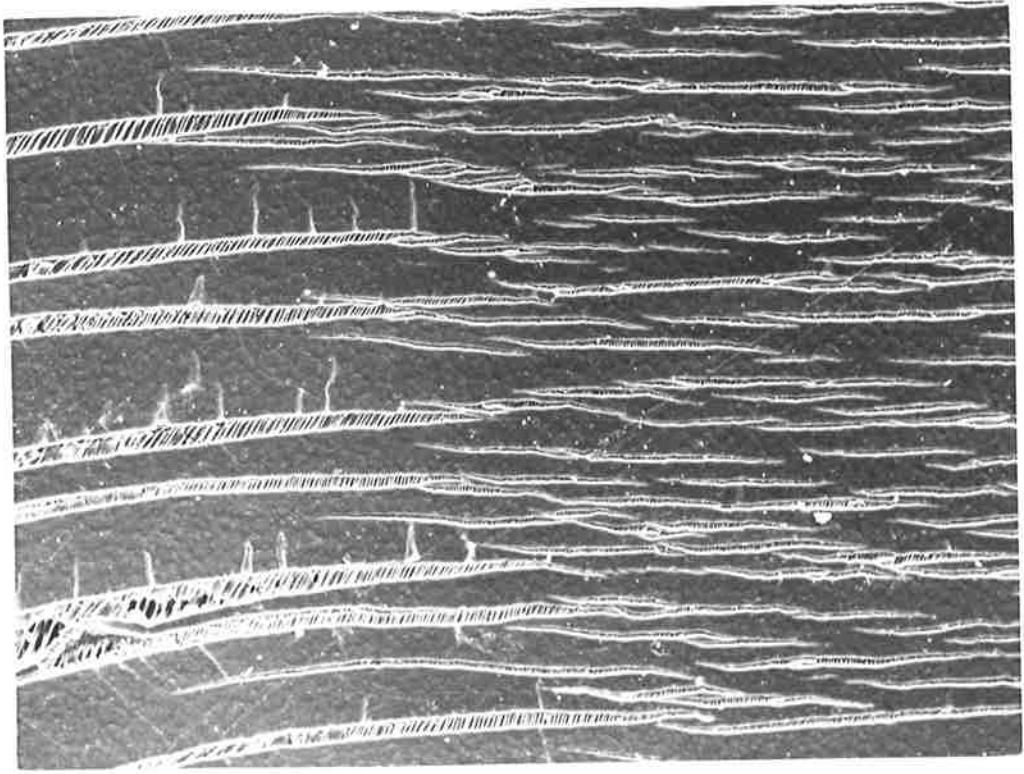
The following mechanism presumably operates. Assuming lithium bromide acts as a plasticiser, the stress level everywhere under the droplet exceeds the yield stress and so a large number of crazes initiate simultaneously. The two processes of stress relief and interaction of shear bands (which emanate from the tip of each craze) inhibit extensive craze growth, so that under the treated region many small crazes are seen.

Whilst crazes which initiate at the agent-air-polymer interface may fail to extend far into the treated region, for the reasons outlined above, it is observed that extensive craze development occurs in the untreated region. X-ray analysis indicates that levels of agent at or near the craze tip are sufficient to enable craze formation. Because no initiation sites exist in this region, a low number of large crazes (craze arrest forces being absent) are produced.

The fine structure of a well-developed craze in the untreated zone appears in Fig. 4.2.48. The direction of the long axis of larger crazes in particular deviates from being

Fig. 4.2.47. Lithium bromide induced crazes in nylon 66. Large crazes (at left) are outside the treated zone and small crazes (at right) are in the treated zone. Magn. = 205x

Fig. 4.2.48. Microstructure of a large craze outside treated zone, showing block tilting and craze filaments non-parallel to the applied stress direction. Magn. = 825x



perpendicular to the applied stress direction. In addition, craze filaments also appear to be tilted, and blocks of uncrazed polymer are also found inside the craze walls, indicating shear stresses. Otherwise, the micromorphology of the craze matter is similar to that observed in nylons stress-crazed using other salts.

The fracture surface of a nylon 66 test-piece which slowly was strained to rupture, in the presence of a droplet of saturated aqueous lithium bromide is shown in Fig. 4.2.49. Three distinct morphological zones can be distinguished (designated A, B and C).

Region A was shown to be the craze initiation region by studying the uptake of dye under the optical microscope. It can be distinguished from the rest of the fracture region by the absence of craze matter. The left hand edge of region A is smooth and resembles the walls of crazes below the fracture surface.

The fibrillated region adjacent to region A can be seen more clearly in Fig. 4.2.50. By analogy with other fracture morphologies, this can be classed as Region II. Emanating from this area are two types of craze material; truncated, discreet peaks on one side (region B) and continuous, porous craze complex on the other (region C).

Both types of craze matter (B and C) may coexist, together with apparently craze-free regions, depending upon which path the crack follows. Crazes in this specimen were well developed when cracking initiated, so that large discontinuities caused by cracks crossing from one small craze to

Fig. 4.2.49. Nylon 66 fractured in the presence of lithium bromide.

Region A = craze initiation zone

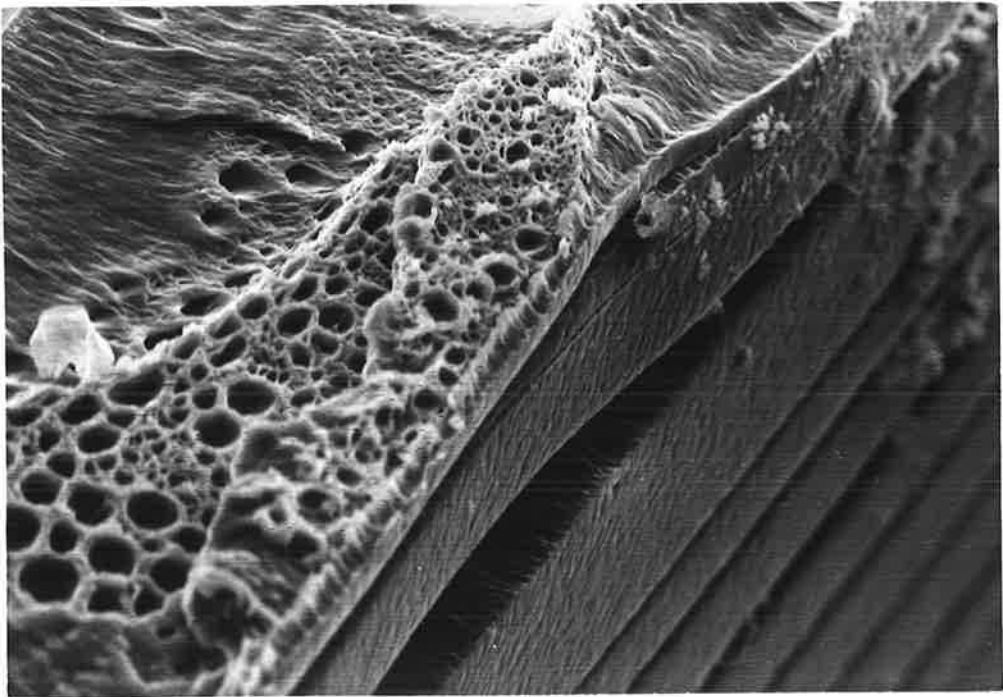
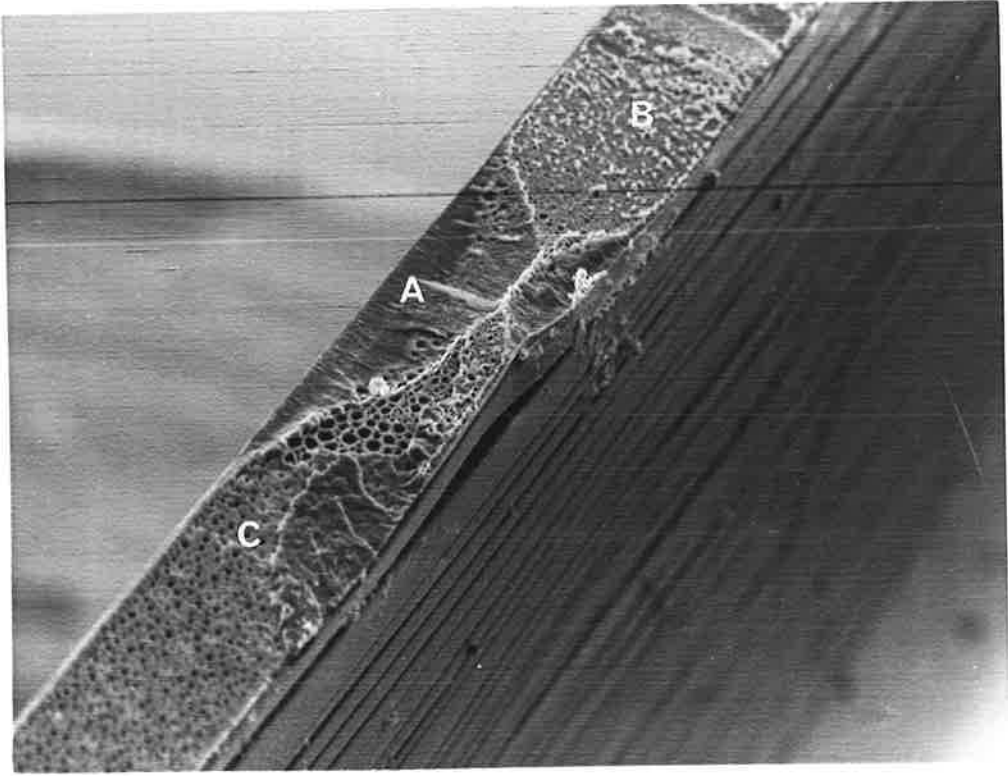
Region B = truncated craze material

Region C = porous craze complex

Magn. = 83x

Fig. 4.2.50. Ruptured craze matter near region A.

Magn. = 330x



another, cannot be seen. As observed in magnesium perchlorate crazed nylons, highly elongated craze filaments were absent (Fig. 4.2.51) and appears to be a common characteristic of fracture surfaces where "highly active" Type II salt solutions are present.

The short peaks in region B (Fig. 4.2.52) have been produced by viscoelastic deformation which has been terminated by premature rupture. The morphology of region C is quite different, having the habit of a porous layer, representative of a separate craze matter-salt complex (Fig. 4.2.53). This material covers the majority of the fracture surface, extending the whole length (Fig. 4.2.54). X-ray analysis indicates that it contains high levels of salt, and it can be seen from the last photograph that it contrasts strongly with the bulk polymer underlying it. Region C correlates with the passage of a crack through long crazes outside of the treated region. The uniform texture of the region suggests that conditions at both the craze and crack tip were approximately constant.

The salt-craze matter complex may often be removed by mechanical separation or by washing prior to preparation for S.E.M., to give a denuded, bulk polymer surface. For example, the specimen shown in Fig. 4.2.55 appears superficially to have fractured with no apparent craze formation. When examined at higher magnification (Fig. 4.2.56), fine vesicles can be discerned, and the appearance of the surface corresponds to that of the previous specimen. It is therefore important to examine specimens immediately upon fracture of the specimen, to ensure that the correct mechanism of

Fig. 4.2.51. Region B of lithium bromide-ruptured nylon 66, with patchy appearance and discrete peaks. Magn. = 178x

Fig. 4.2.52. Truncated peaks of region B at higher magnification. Magn. = 3,560x

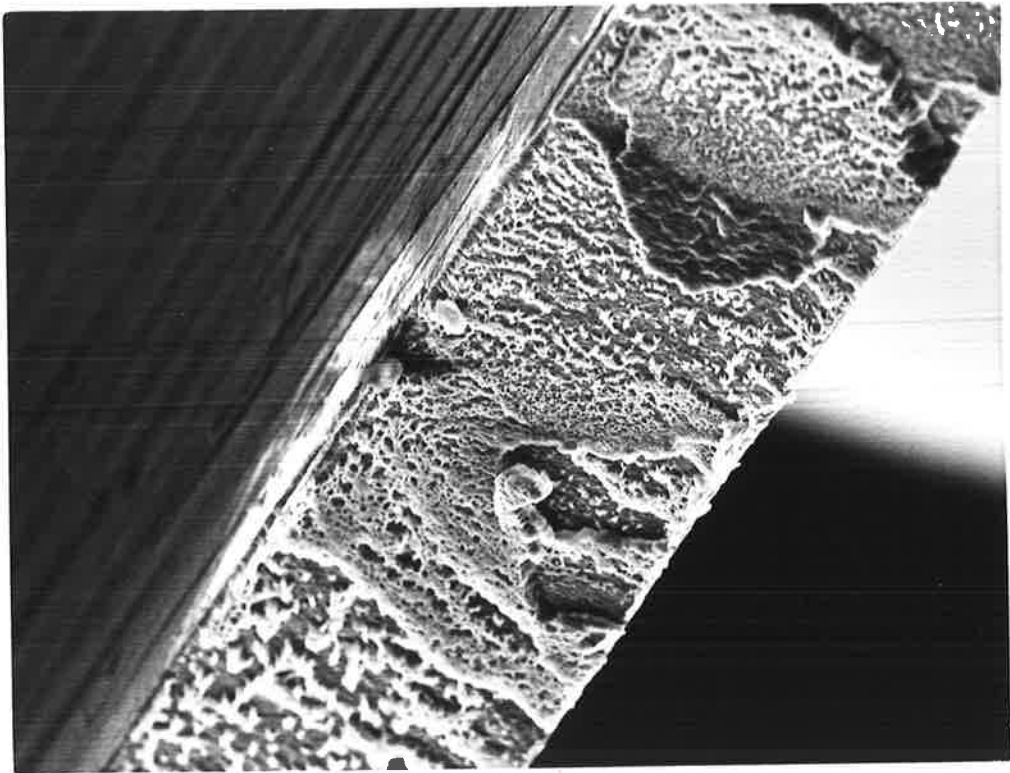
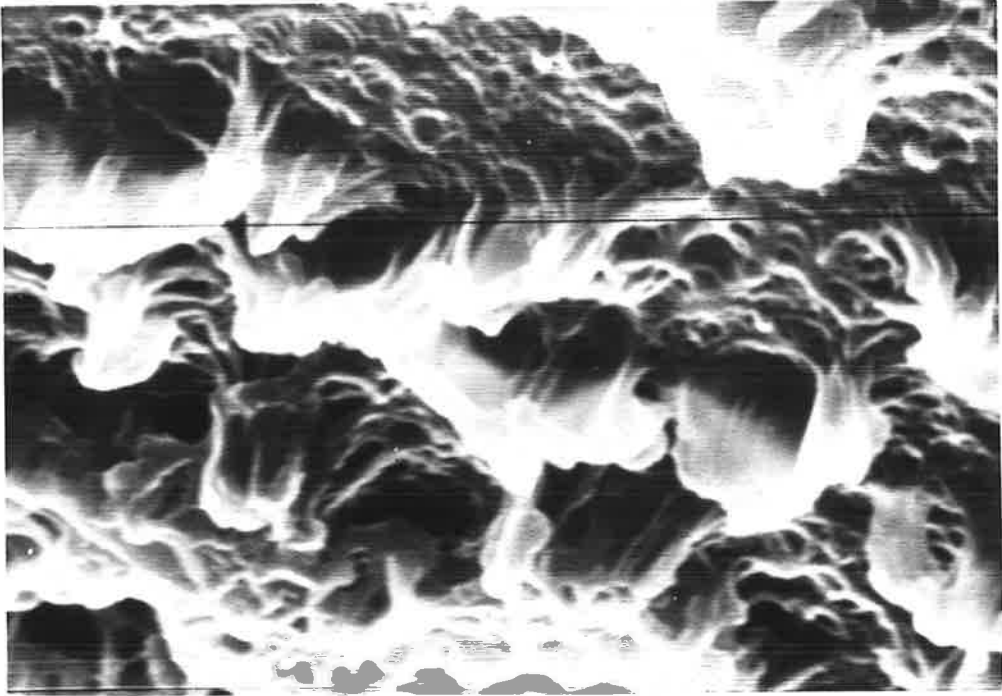


Fig. 4.2.53. Porous craze layer characteristic of region C. Magn. = 156x

Fig. 4.2.54. Edge of test-piece showing where craze-adduct has separated from bulk (uncrazed) polymer. Magn. = 206x

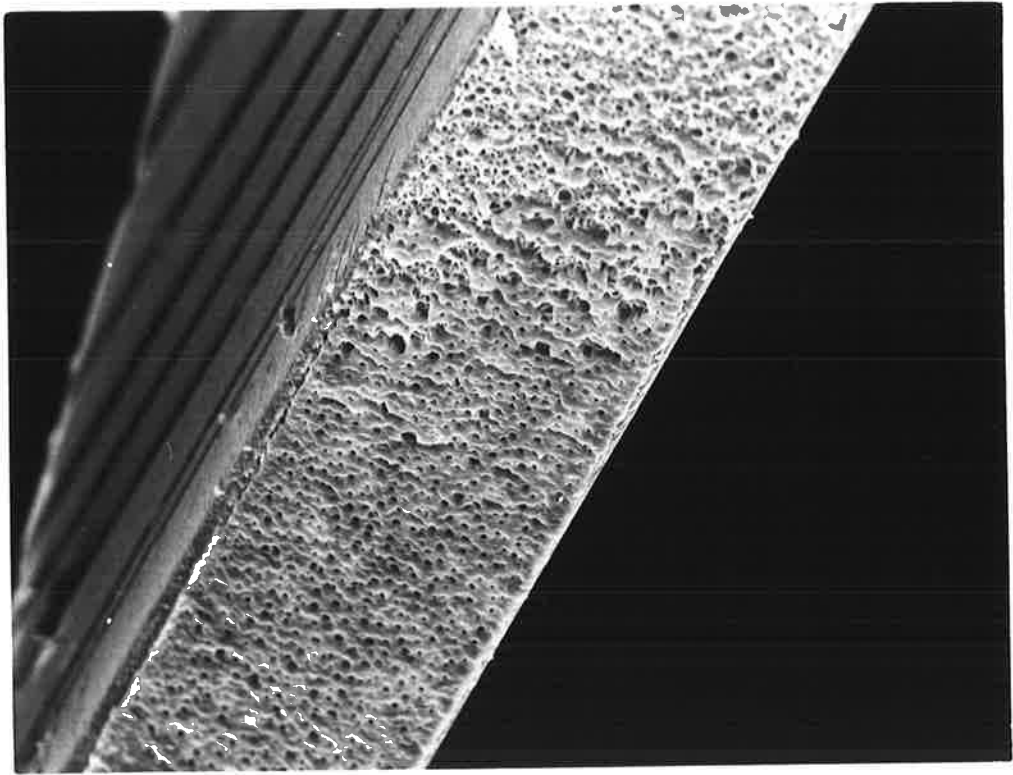
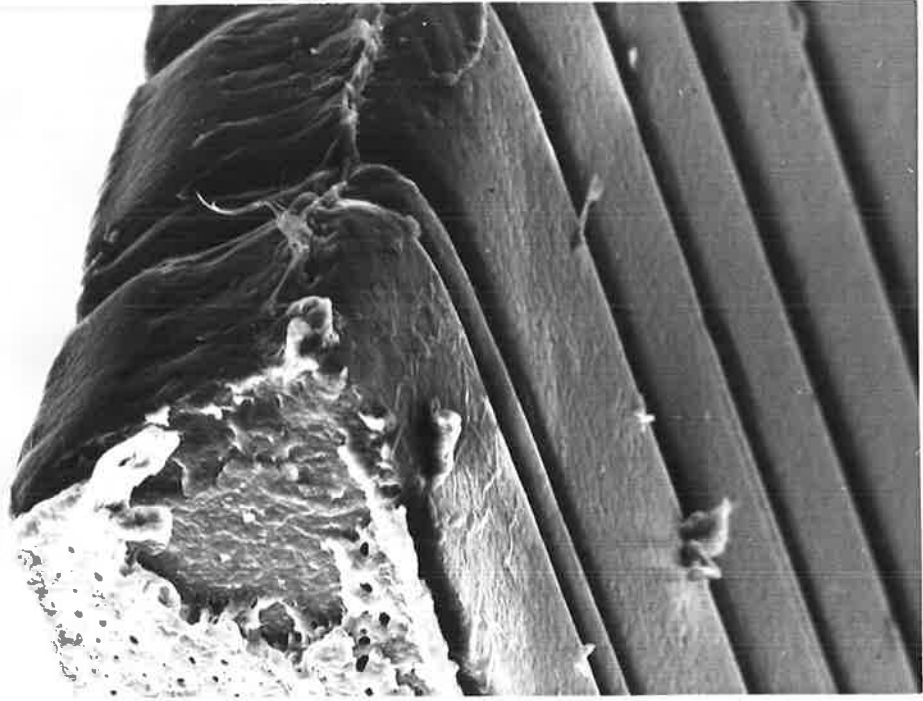
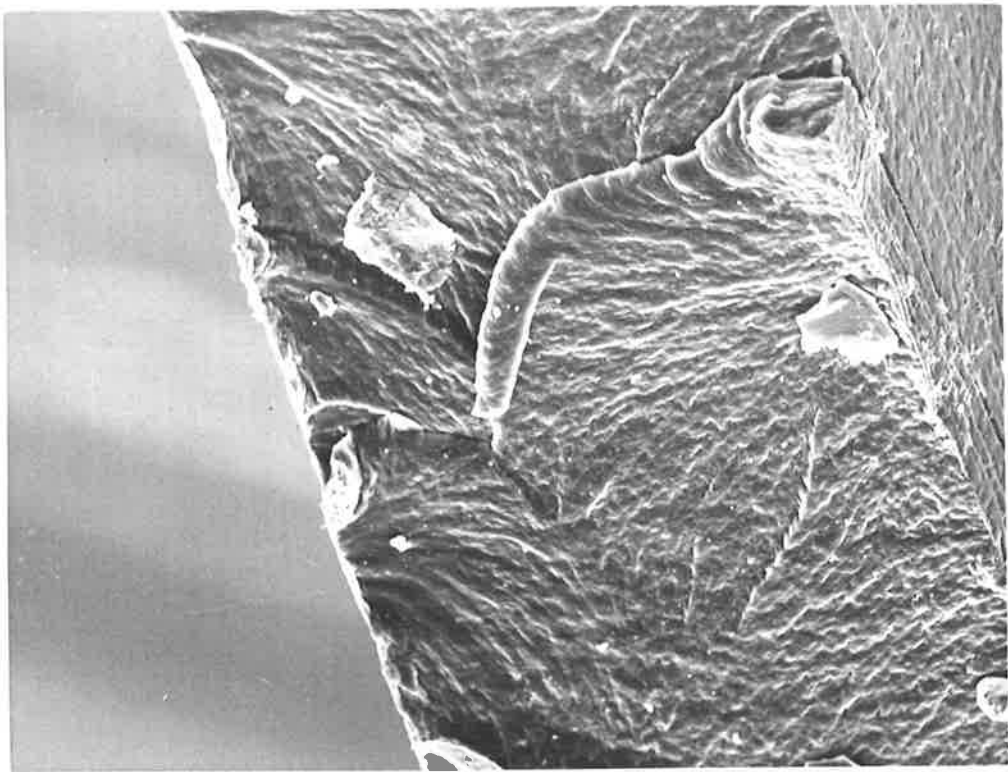


Fig. 4.2.55. Denuded fracture face of nylon 66 after straining with lithium bromide and subsequent wash. Magn. = 535x

Fig. 4.2.56. Fine pores which can be resolved on same fracture surface. Magn. = 2,680x



failure is ascertained.

Nylon 6

Nylon 6 was found to be particularly susceptible to crazing and cracking when stressed with saturated aqueous lithium bromide solution. When initial testing was conducted under the stereomicroscope, craze propagation and breakdown ensued so quickly after craze initiation that observation of large, stable crazes was difficult. Instead, extensively cracked regions were obtained (as shown, for example, in Fig. 4.2.57). The crack walls are smooth, and almost devoid of craze remnants (Fig. 4.2.58). A small number of highly strained filaments bridge the walls; they represent polymer which has been able to resist gross weakening by the salt, and probably indicate the presence of heterogeneities.

At higher magnification (Fig. 4.2.59), the swollen porous specimen surface is evident. In addition, the crack wall (which corresponds to region 1) is again shown to be nearly featureless. The base of a craze filament appears to taper gradually from the bulk polymer.

A more prominent craze filament is shown in Fig. 4.2.60. The highly oriented fine structure of the polymer can be readily seen as well as separation of some of the fibrous elements perpendicular to the draw direction (as observed in macroscopic necking of many crystalline polymers). At the tip of a crack, away from the treated region, a profusion of filamental craze matter is seen, indicating that the conditions of stress and absorbed salt levels are lower. Near the surface the crack wall is still relatively smooth, however, suggesting that high concentrations of agent have

Fig. 4.2.57. Nylon 6 extensively cracked by aqueous lithium bromide. Magn. = 22x

Fig. 4.2.58. Same specimen tilted to reveal interior of cracks almost devoid of craze matter. Magn. = 86x

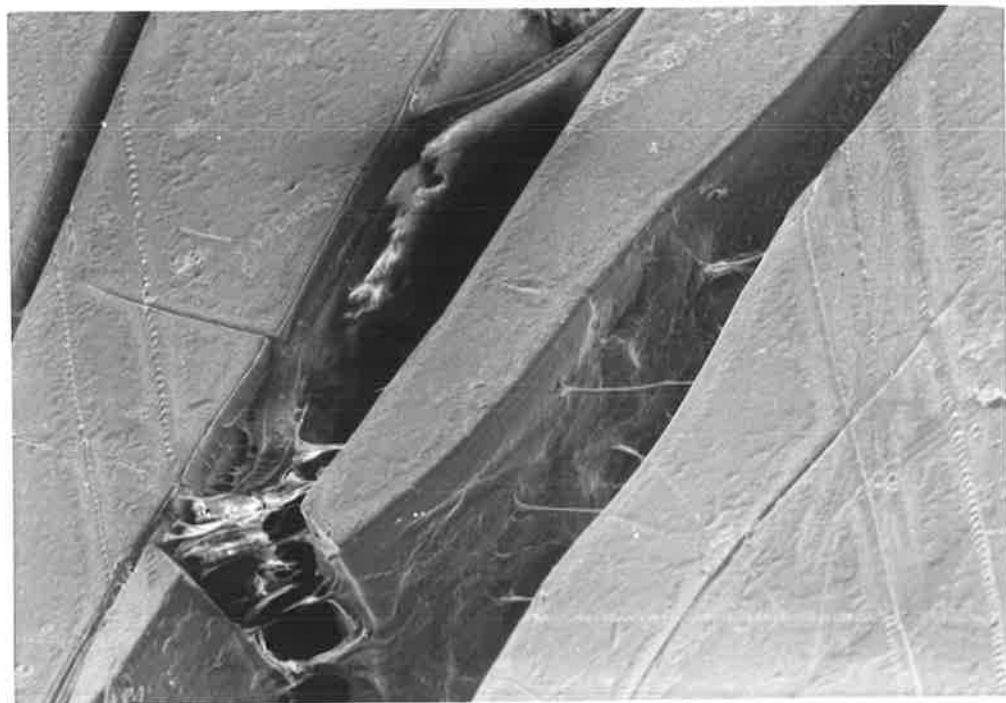
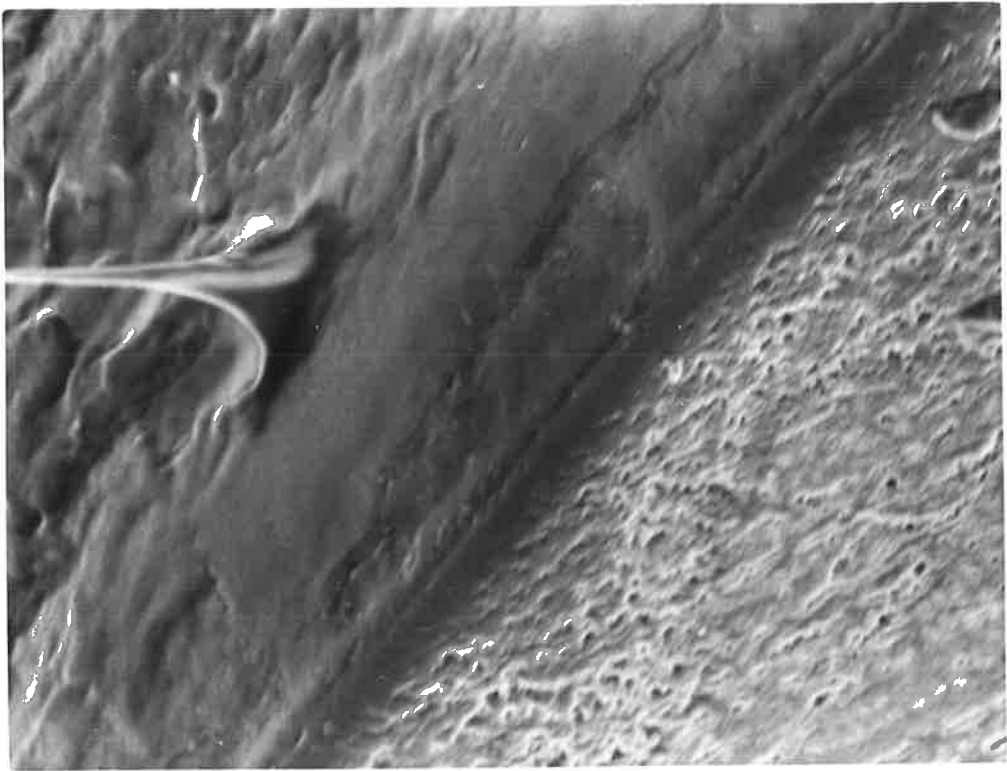
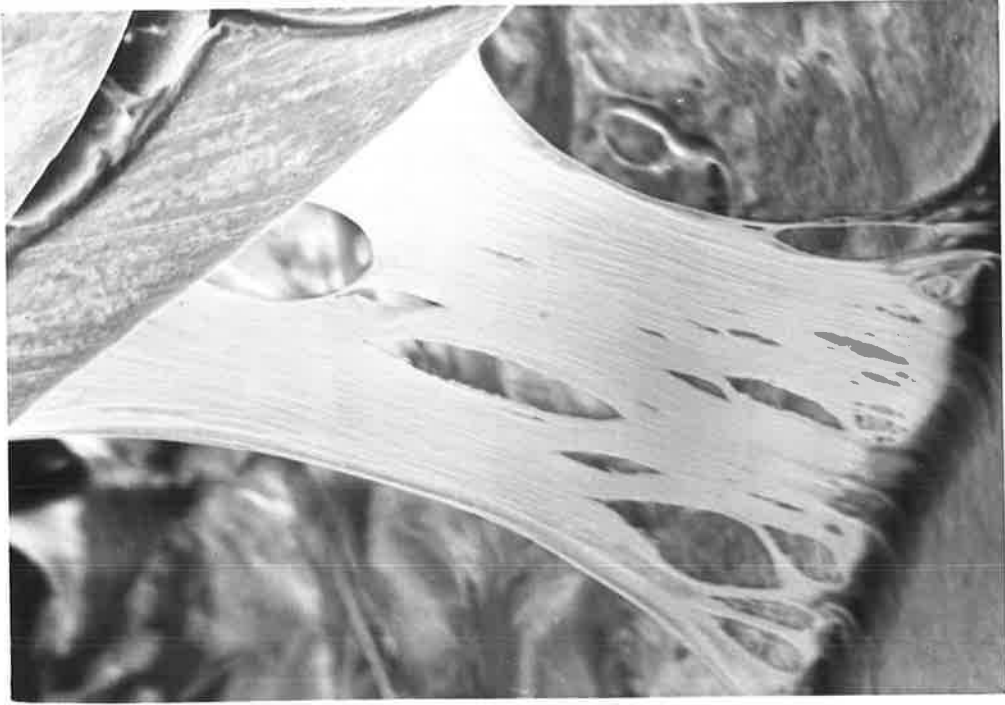


Fig. 4.2.59. Lithium bromide cracked nylon 6. Porous test-piece surface at top left and smooth crack face are shown. Magn. = 860x

Fig. 4.2.60. Highly oriented "bridge" linking crack faces. Magn. = 430x



followed the craze tip away from the treated zone.

Cellulose Acetate

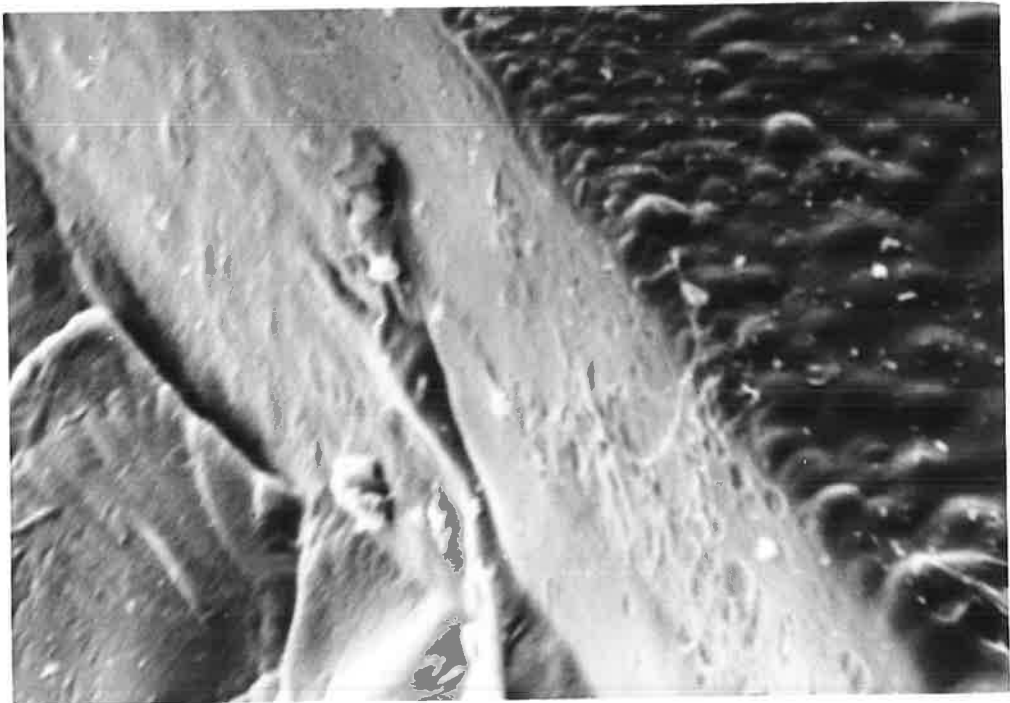
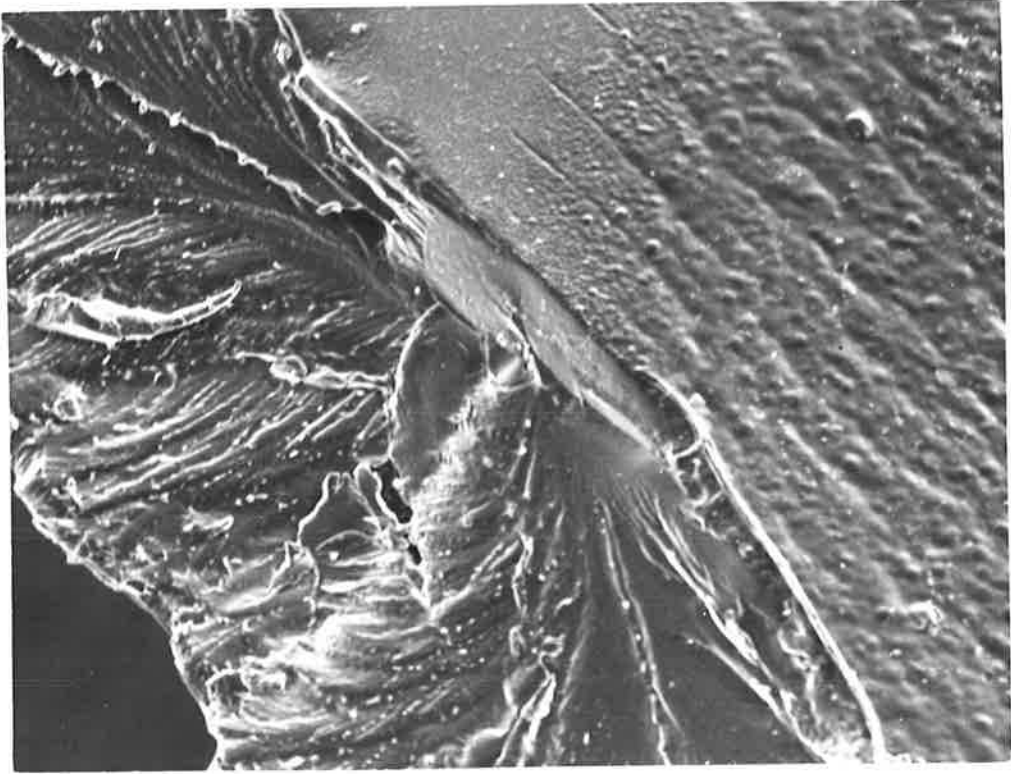
When a drop of saturated aqueous lithium bromide was applied to a cellulose acetate test-piece (A.S.T.M. Type IV) and strained slowly, small crazes were produced at the perimeter of the droplet. Two cracks initiated from the craze region, with one propagating very rapidly. Swelling occurred under the droplet.

The swollen morphology of the treated region is shown at right in Fig. 4.2.61, with small crazes at the edge. The crack has clearly initiated at a craze, but has then grown rapidly, with no apparent craze formation.

At higher magnification (Fig. 4.2.62) the almost featureless initiation region can be seen to contain a small amount of porous substance. It was not possible to determine unambiguously whether it was a trace of residual agent, or (more likely) remnants of craze matter.

Fig. 4.2.61. Cellulose acetate fractured in the presence of aqueous lithium bromide. Small crazes above and parallel to fracture face can be seen emanating from swollen region at right of photograph. Magn. = 300x

Fig. 4.2.62. Same specimen, showing fracture initiation zone and possible craze matter.
Magn. = 2,570x



4.2.4.2. Crazing in Nylons Induced by Lithium Iodide

Lithium iodide was shown by Dunn and Sansom [4] to bind to nylons in the same way as lithium bromide and magnesium perchlorate (Type II salt). Lithium iodide was found in this study to be the most active crazing and cracking agent and was used extensively in experiments designed to clarify the mechanism of agent-induced crazing in nylons (as described in Chapter 5). The salt differs from others used in this work in that only the anion can be detected using energy dispersive X-ray analysis, so that monitoring of salt levels assumed that, at the resolution used, cations were essentially localised adjacent to anions.

Nylon 66

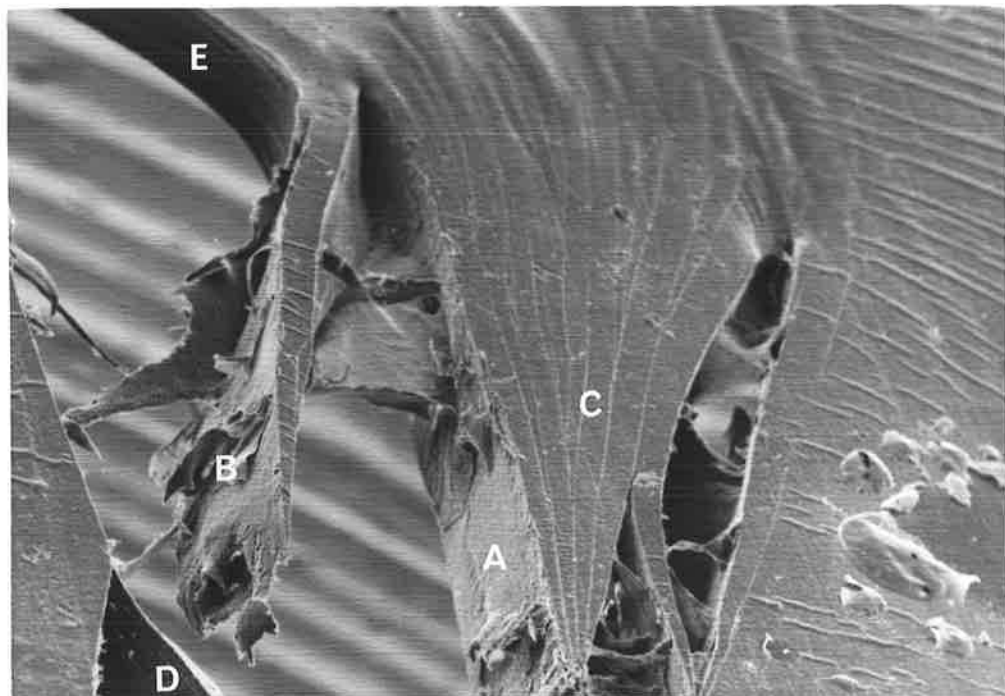
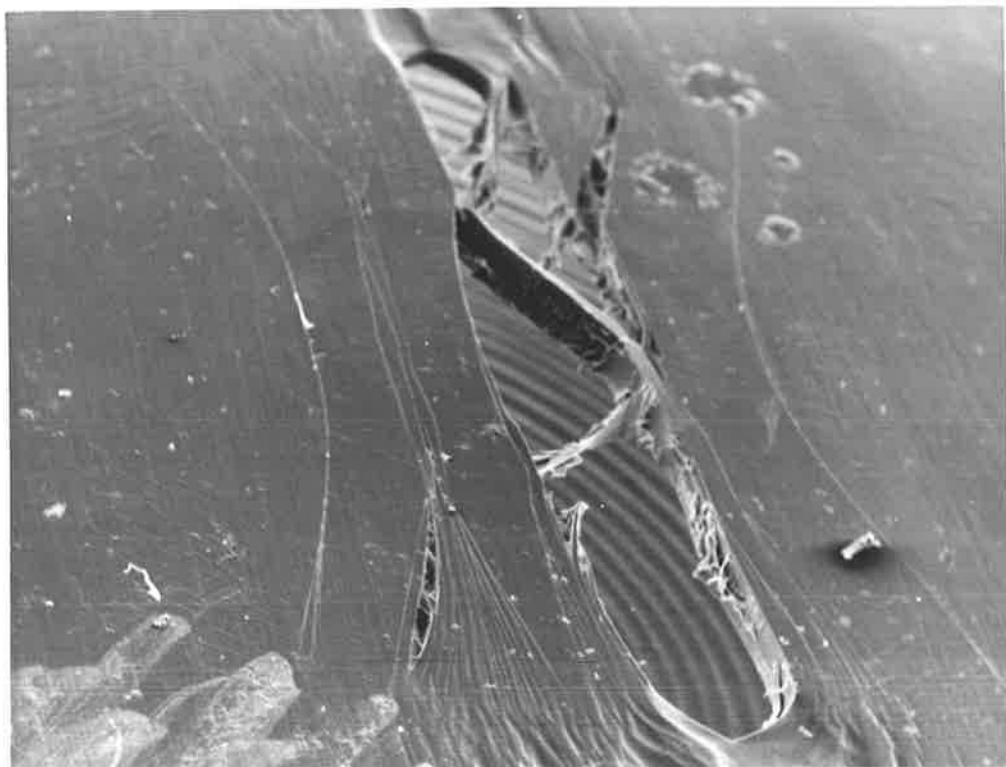
The morphology of stress-crazes in nylon 66 induced by lithium iodide is typical of those induced in other polymers by the same agent. Crazing and fracture of the polymer under three different conditions will be discussed. They show the influence of strain rate and the amount of agent applied to the specimen upon morphology, to give an insight into the mechanism of environmental stress crazing.

(a) Relatively high strain rate in the presence of large quantities of saturated aqueous lithium iodide.

Under these conditions extensive cracking, with only limited viscoelastic deformation of polymer occurred (Fig. 4.2.63). In this specimen the morphology resembles that found for nylons affected by other Type II salts under similar test conditions. Highly elongated matter is essentially absent, and bifurcation of cracks is evident.

Fig. 4.2.63. Nylon 66 stress cracked by lithium iodide under high strain rate conditions. Both bifurcation of a craze and cold drawing at the crack tip can be seen.
Magn. = 25x

Fig. 4.2.64. Five distinct regions can be distinguished
Region A = smooth fracture face
Region B = thin lamellae protruding from fracture face
Region C = narrow radiating crazes
Region D = craze remnants
Region E = "ductile" fracture zone.
Magn. = 76x



Upon closer inspection, five regions can be distinguished (labelled A to E in Fig. 4.2.64). The relatively smooth fracture face (A), from which thin laminae (B) protrude, is evident. Very little craze matter has been produced, as reflected by the very narrow radiating crazes in region C. It is apparent from the morphology of the specimen that crack formation follows close behind the craze tip. Some fracture faces contain craze remnants (for example, region D) and commonly occur where the stress distribution has changed with retardation of crack growth. Where the geometry of the craze tip changes and the level of agent becomes insignificant, "ductile fracture" and microdrawing predominate (region E).

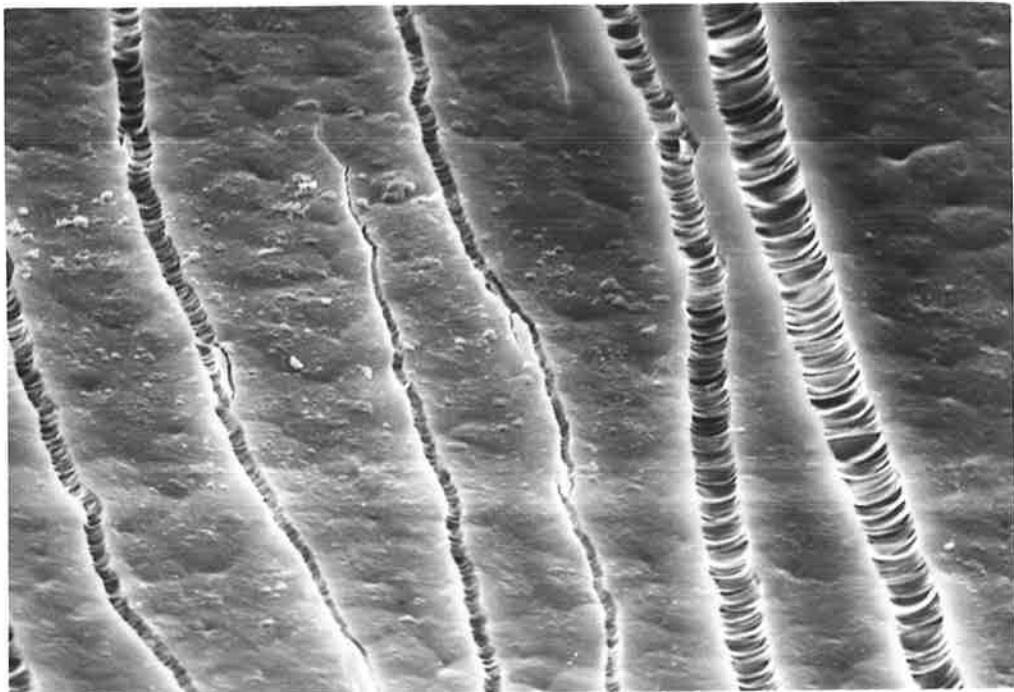
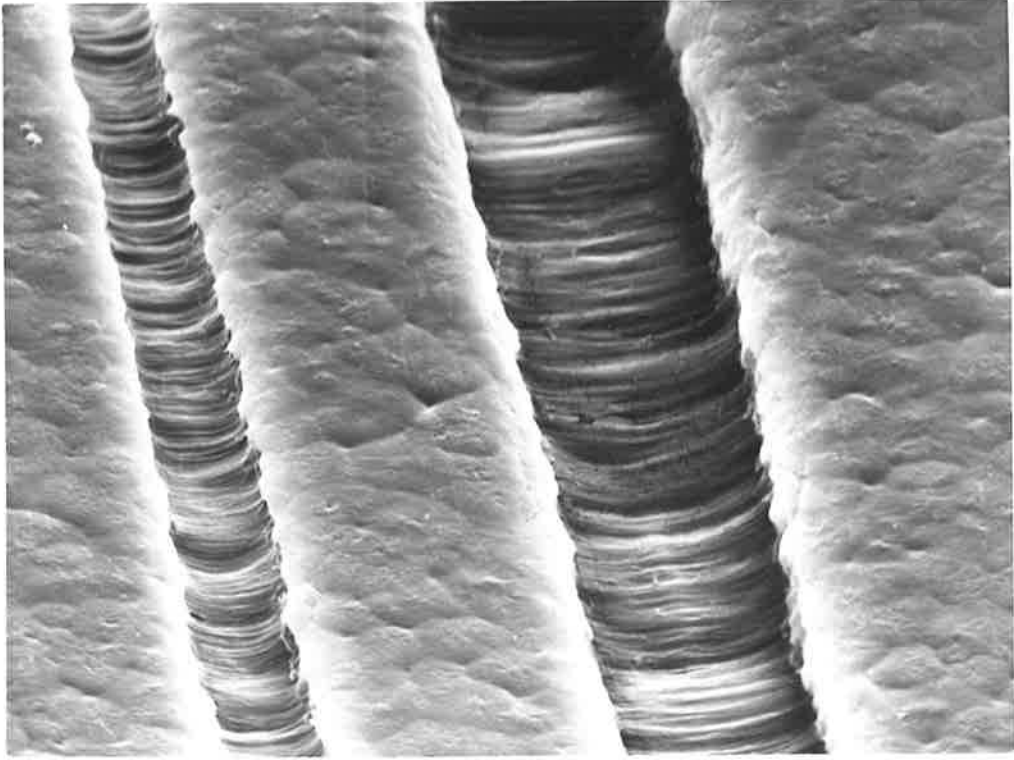
(b) Slow strain rate with large quantities of saturated aqueous lithium iodide.

When a nylon 66 test-piece (for example, A.S.T.M. Type IV) is carefully and slowly strained in the presence of saturated aqueous lithium iodide, it is possible to isolate (by thorough washing with water) well-developed, stable crazes. Of interest are the differences found between crazes in the treated region from those outside.

Broad, parallel-sided crazes passing through spherulitic, untreated bulk nylon 66 are shown in Fig. 4.2.65. Whilst the walls of the craze are not perfectly straight (in particular there are discontinuities dimensionally comparable with the diameter of spherulites) the overall direction of the craze has not been influenced by the presence of spherulites. Of interest, however, is interspherulitic micronecking near

Fig. 4.2.65. Broad lithium iodide induced crazes extending into untreated spherulitic nylon 66. Minor cold drawing at spherulite boundaries (near craze) can be resolved.
Magn. = 1,400x

Fig. 4.2.66. Narrow crazes in treated region of same sample. Note magnification is same as for Fig. 4.2.65. Magn. = 1,400x



the walls of the craze, which suggest that stresses near the normal yield stress of the nylon exist at the craze-bulk polymer interface. In addition, the onset of voids at the centre of the larger craze can be perceived.

In contrast, crazes in the treated region are much more narrow (they are shown in Fig. 4.2.66 using the same magnification as Fig. 4.2.65). In addition, their path is much more irregular, suggesting that the stresses at the craze tip are lower, and so the direction of craze propagation may now be influenced by irregularities in the microstructure of the nylon.

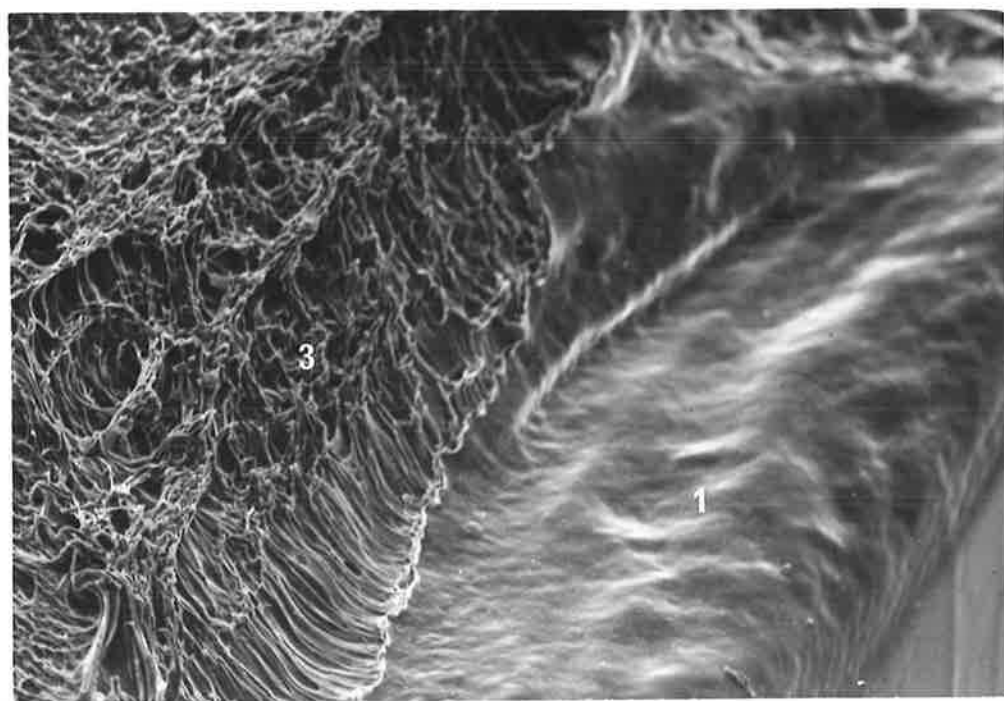
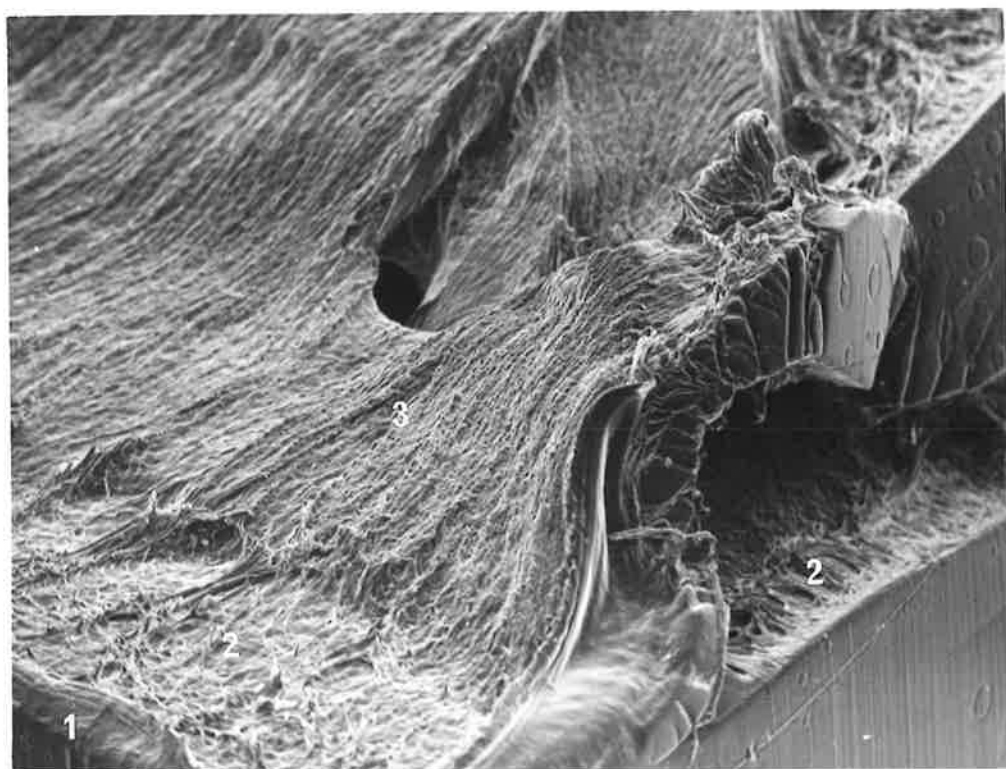
(c) Limited Application of Lithium Iodide to Prestressed Nylon 66.

When a nylon 66 test-piece (A.S.T.M. Type I) was prestressed to approximately $0.8 \sigma_y$, and a drop of saturated aqueous lithium iodide was applied, crazing and cracking rapidly occurred at the surface. Before extensive agent-induced crazing could occur, the specimen ruptured.

The fracture surface cannot be as readily subdivided into regions 1 to 4 as was done for other specimens. However, in Fig. 4.2.67, regions 1, 2 and 3 can be identified, although the region designated type 2 is considerably different to that usually encountered. Region 1 is smooth and has a swollen appearance. At higher magnifications (Fig. 4.2.68) the surface of this region remains featureless. A sharp transition to region 2 exists, which reflects a sudden change in the stress conditions at the craze tip. Region 2

Fig. 4.2.67. Complex fracture surface resulting from application of lithium iodide to prestressed nylon 66. Regions 1 to 3 are initiation, induced-craze and ductile fracture zones. Magn. = 75x

Fig. 4.2.68. Different area of same specimen, showing abrupt change from 1 to region 3. Magn. = 169x



can contain many discrete peaks, as shown in Fig. 4.2.67, as well as polymer oriented more completely away from the edge of the specimen. The texture of this region is distinct from that of region 3 (Fig. 4.2.67), where the crack has not passed through agent-induced crazes, and in which the surface is smoother.

4.2.4.3. The Effect of Solvent Upon Stress-Crazing Activity of Lithium Iodide in Nylons - Morphological Aspects

a) Dimethyl Sulphoxide

Only weak stress-crazing activity was observed when a saturated solution of lithium iodide in dimethyl sulphoxide (DMSO) was used with nylon 66 (containing approximately 2% water).

When a nylon 66 test-piece (ASTM Type I) was strained at a crosshead speed of 0.5 cm/min with a droplet of the agent applied, small crazes were produced subsequent to macroscopic necking. A formvar replica of the surface near the necked-unnecked polymer interface was prepared from which very small crazes would be resolved in the S.E.M. (Fig. 4.2.69). Larger crazes which degenerated into cold drawn regions were observed when anhydrous nylon 66 was used. The morphology was similar to that shown in Fig. 4.2.72.

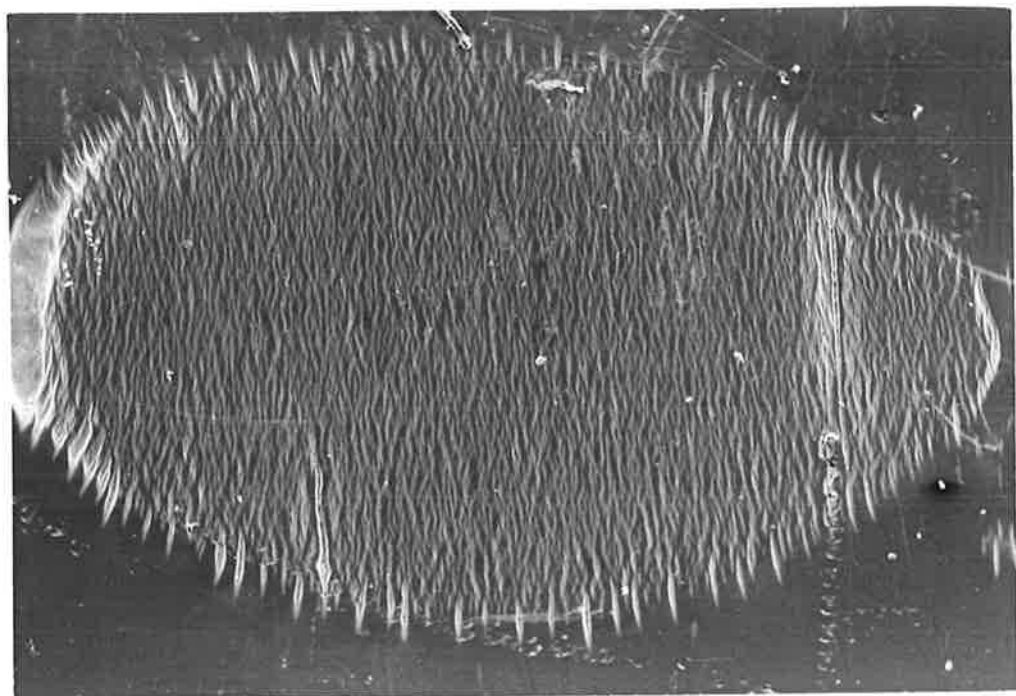
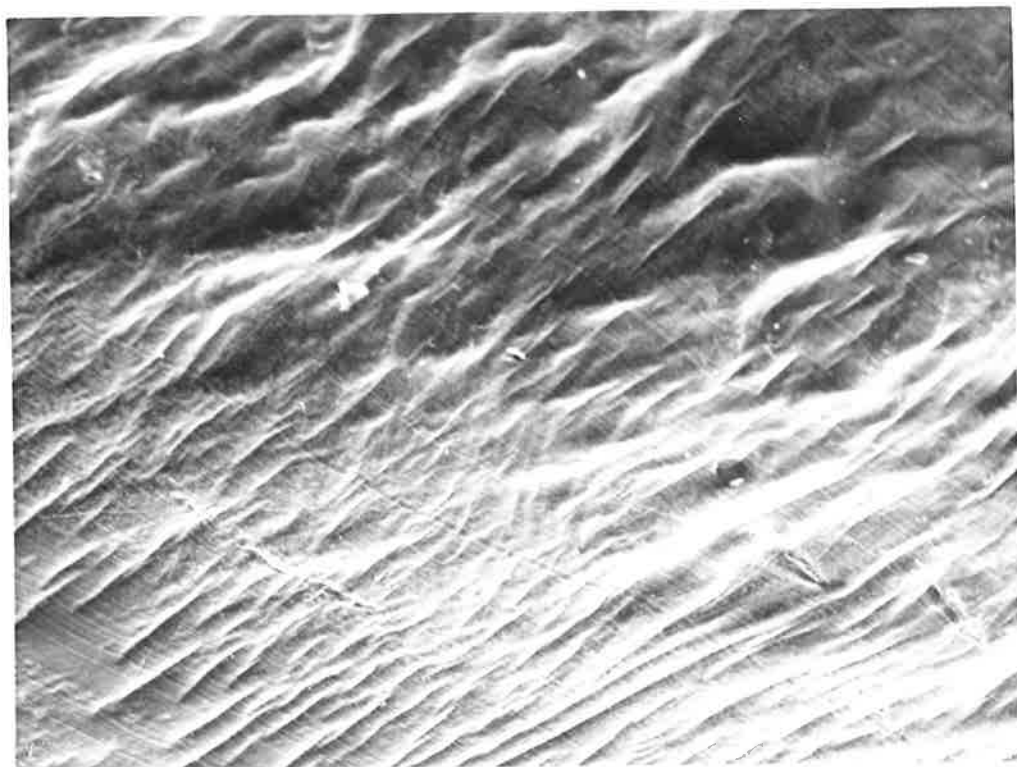
b) 1,2 dihydroxyethane

When a nylon 66 test-piece (A.S.T.M. Type I) was tested under the same conditions as in a), but using a saturated solution of lithium iodide in 1,2 dihydroxyethane, well-defined crazes were produced in the treated region, but stresses near the untreated yield stress were required. Regions 2 and 3 only could be perceived.

When nylon 66 (A.S.T.M. Type IV) was strained very slowly with a drop of the same agent applied, many short, broad crazes formed in the treated region (Fig. 4.2.70). Particularly wide crazes can be seen near the perimeter, but unlike experiments with highly active crazing agents, these crazes did not extend into untreated polymer. The path of

Fig. 4.2.69. Small crazes in nylon 66 induced by a solution of lithium iodide in DMSO. Formvar replica. Magn. = 167x

Fig. 4.2.70. Extensively crazed nylon 66. Agent is lithium iodide/dihydroxyethane. Magn. = 44x



craze propagation appears to be influenced by the spherulitic texture of the bulk polymer (Fig. 4.2.71). At the ends of the treated region (Fig. 4.2.70), so much crazing has occurred that undrawn polymer appear as "islands in a sea" of craze matter (Fig. 4.2.72), although no correlation with spherulitic texture was observed.

From the high incidence of well-developed crazes seen in this specimen, it can be deduced that crazes initiate and propagate at lower stresses than required for craze rupture (crack initiation). The stress-crazing agent has modified the mechanical behaviour of the of the nylon, as shown in Fig. 5.4 (Section 5.1.3). Qualitatively similar results were obtained when anhydrous nylon 66 test-pieces were used.

c) Methyl cyanide

A saturated solution of lithium iodide in methyl cyanide exhibited very high stress-crazing activity, as indicated by the mechanical results obtained for nylon 66 and shown in Fig. 5.4 (Section 5.1.3).

The initiation zone (Region 1) dominates the fracture surface (Fig. 4.2.73) and reflects the very high activity of the agent. An enlargement of this area (Fig. 4.2.74) reveals the fractureless texture of the edge of the fracture face towards the centre of the specimen (at left of Fig. 4.2.74) fine pores are revealed.

There appears to be no region 2 present, indicating that no highly elongated craze matter preceded rupture. There is a rapid transition from region 1 to region 3, which is interpreted as being the result of a crack passing from very weak, iodide-rich region into polymer where no modification by salt has occurred. The sharp boundary between

Fig. 4.2.71. Narrow, well-defined crazes passing through spherulitic nylon 66 in the treated zone. Same specimen as for Fig. 4.2.70. Magn. = 2,360x

Fig. 4.2.72. Degeneration of stable crazes with further elongation to a near-cold drawn state. (Observed at left, right of Fig. 4.2.70). Magn. = 9,220x

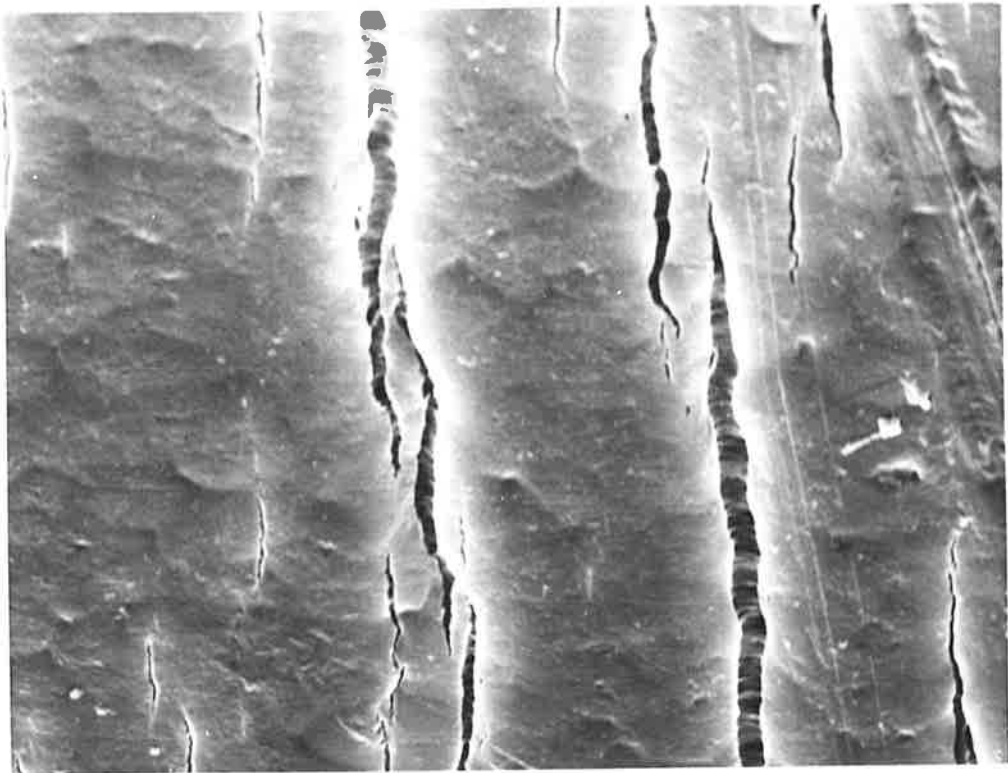
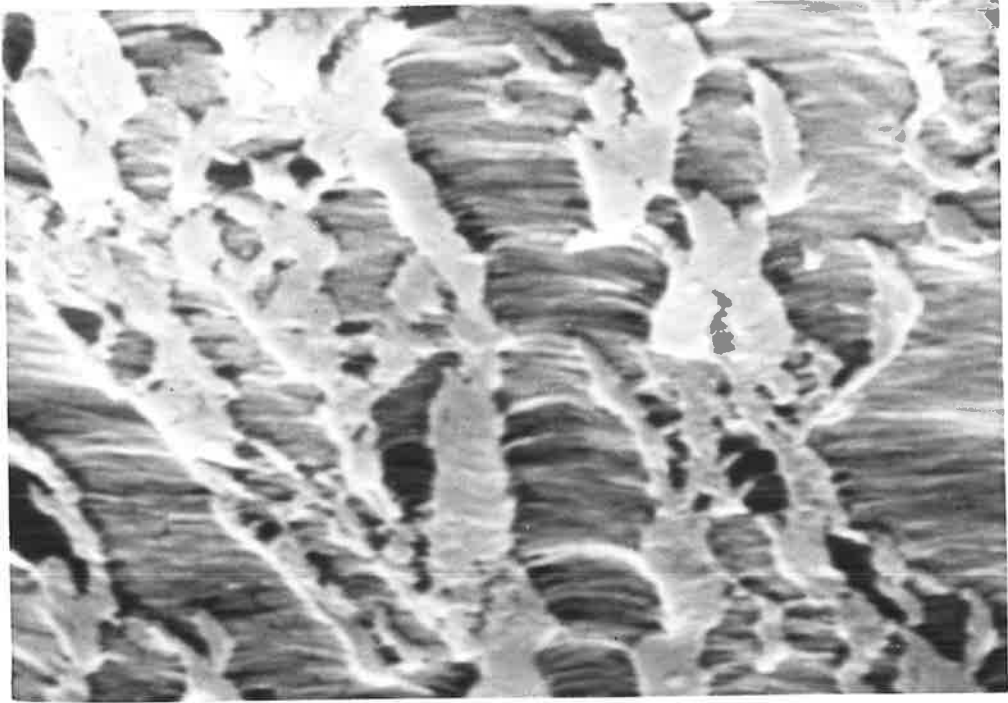
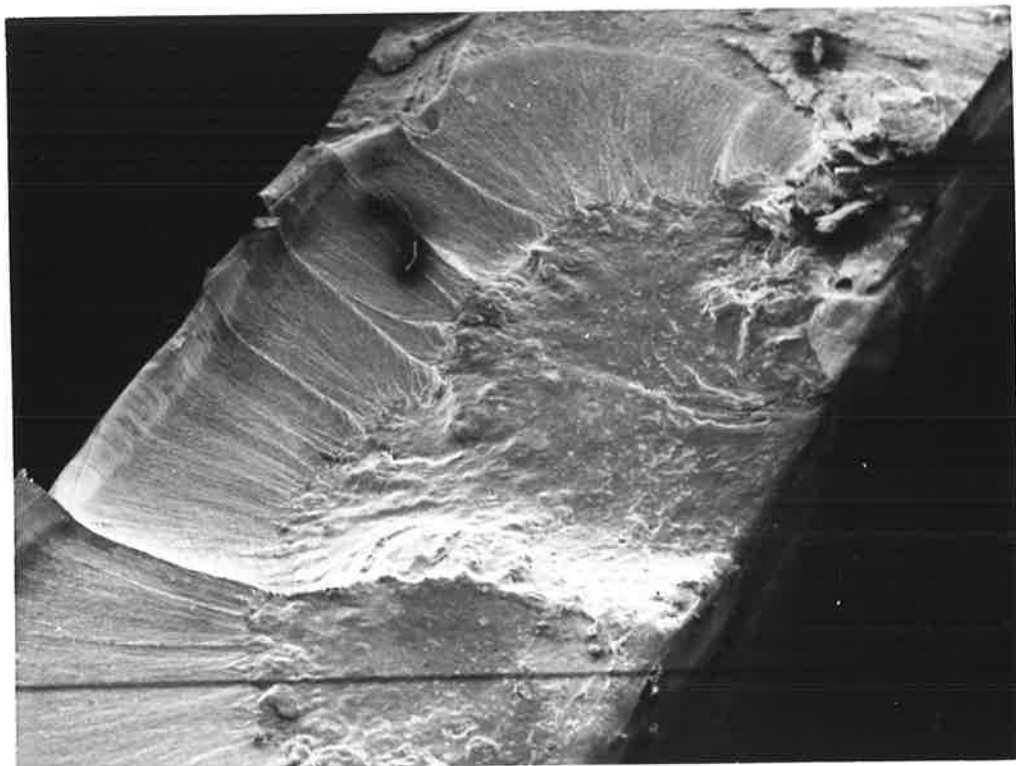


Fig. 4.2.73. Fracture surface of nylon 66 resulting from lithium iodide-methyl cyanide treatment. The initiation zone is prominent. Magn. = 21x

Fig. 4.2.74. Flat terrain characteristic of initiation zone. Magn. = 182x



regions 1 and 3 is shown in Fig. 4.2.75.

The crack propagates through bulk polymer to produce fracture regions 3 and 4 (seen in Fig. 4.2.73), as described in the introduction to Chapter 4.

To establish if the presence of water has an influence upon the fracture mechanism, anhydrous nylon 66 was tested under the same conditions. It was discovered that no "ductile fracture" region 3 was produced. The initiation zone (region 1) was morphologically similar (Fig. 4.2.76) to that obtained in as-received nylon 66, again having a smooth, featureless appearance. Rupture of the polymer in this region provides a notch from which brittle fracture can initiate (Fig. 4.2.77).

Experiments in which nylon 66 (A.S.T.M. Type IV specimens) and 1.00mm thick nylon 6 test-pieces were strained with the same reagent confirmed the very high activity of lithium iodide in methyl cyanide. In particular, nylon 6 was extensively cracked, with the smooth, deep crack walls, devoid of craze matter, being prominent (Fig. 4.2.78). Secondary cracks were common in the treated region, but only isolated evidence for microdrawing was obtained. Where cracks were absent in the treated region, the polymer swelled, to give a porous material.

Fig. 4.2.77. Brittle fracture surface, with initiation zone (in foreground) behaving like a notch. Anhydrous nylon 66 with lithium iodide-methyl cyanide treatment. Magn. = 28x

Fig. 4.2.75. Sharp transition from Region 1 to Region 3 in lithium iodide-methyl cyanide fractured nylon 66. Magn. = 310x

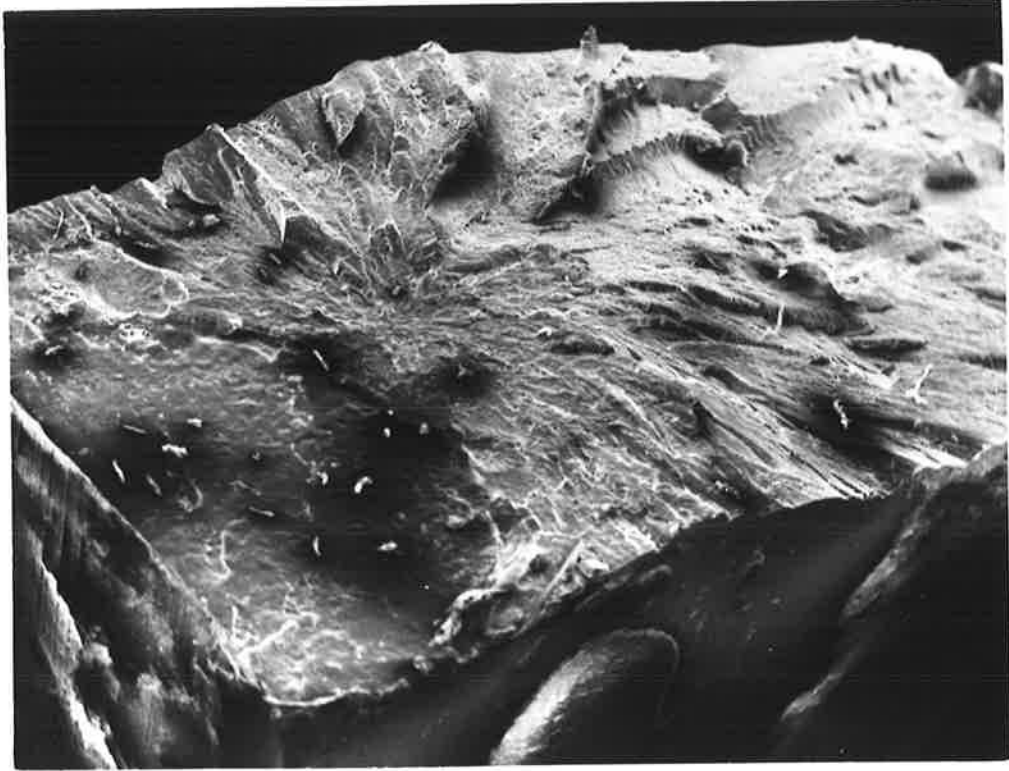
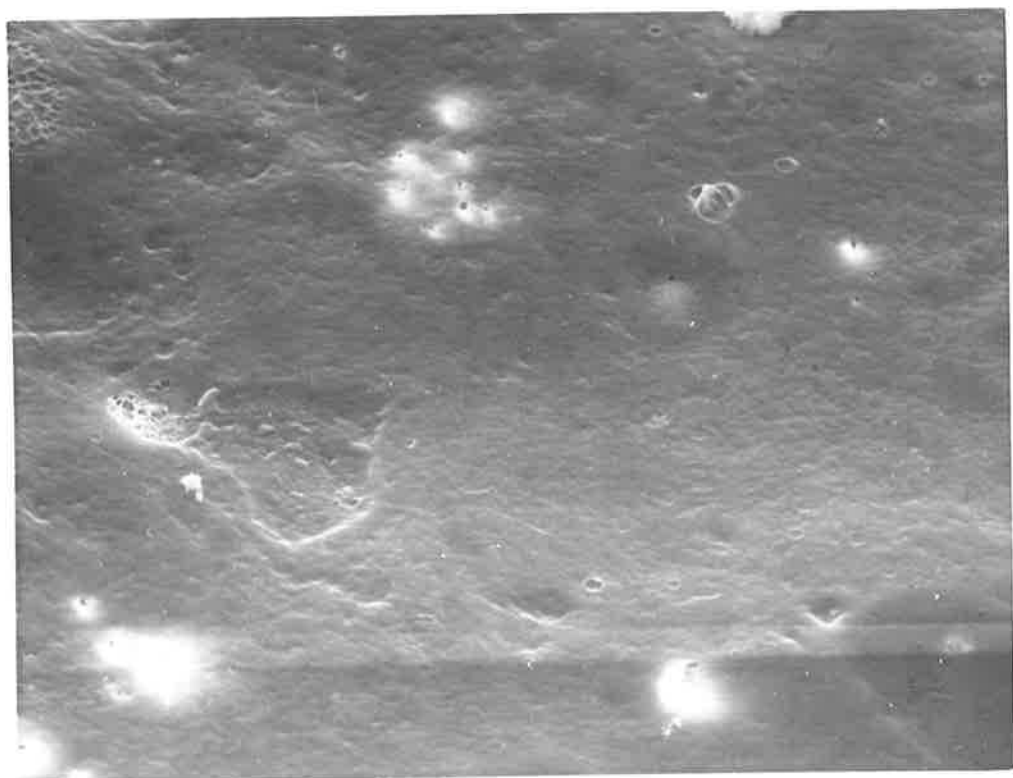


Fig. 4.2.76. Texture of initiation zone of anhydrous nylon 66 is similar to that shown in Fig. 4.2.74. Magn. = 1,200x

Fig. 4.2.78. Extensively cracked nylon 6. Reagent is lithium iodide-methyl cyanide. Magn. = 99x



4.2.5. The Effect of Water Content and Annealing of Nylon 6 Upon Stress Crazing.

The influence of crystallinity and water content upon the morphology of crazes is expected to be large for a variety of reasons. The uptake of agent which is proposed as a precursor to craze initiation, is expected to be much slower in a highly crystalline sample than in one which is amorphous, because of the very low solubility of crystalline polymer in liquids at temperatures much lower than the melting point [142]. The time and stress required for craze initiation is predicted to change with crystalline content. It was found by Lasoski and Cobbs [145] using the data of Starkweather [141] that at 50 and 100% R.H., water sorption in nylon 610 decreased linearly as the percentage crystallinity increased the water vapour permeability increased linearly as the square of the amorphous volume fraction increased [145].

The influence of texture and orientation might also influence the developing craze and this could be reflected in a different craze morphology. For example, a higher amorphous content at interspherulitic boundaries because of rejected impurity build-up could conceivably modify the craze path.

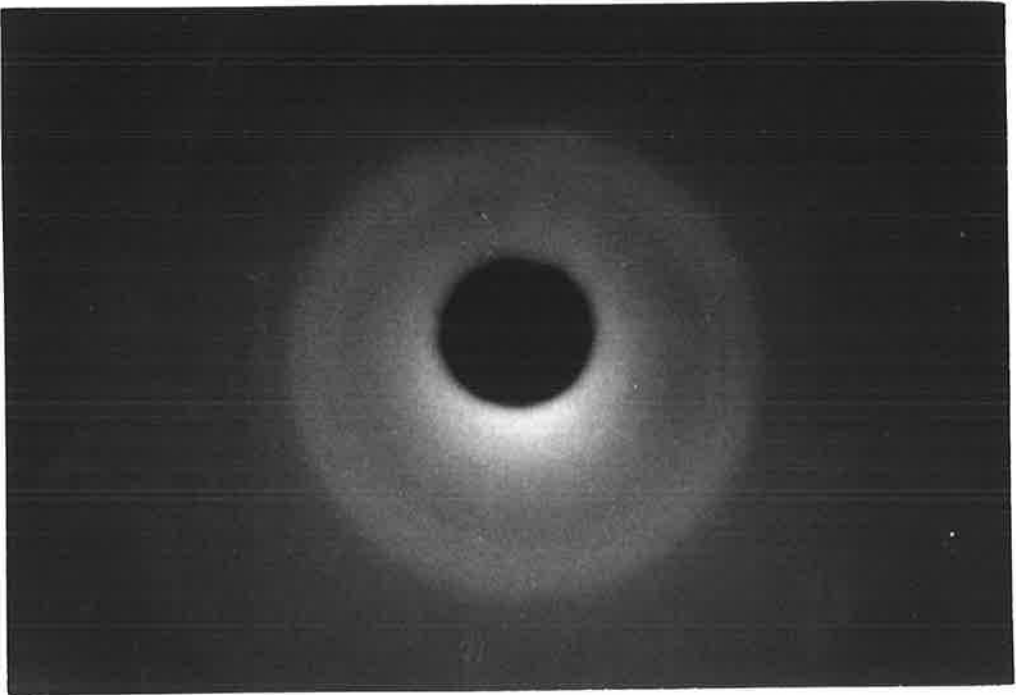
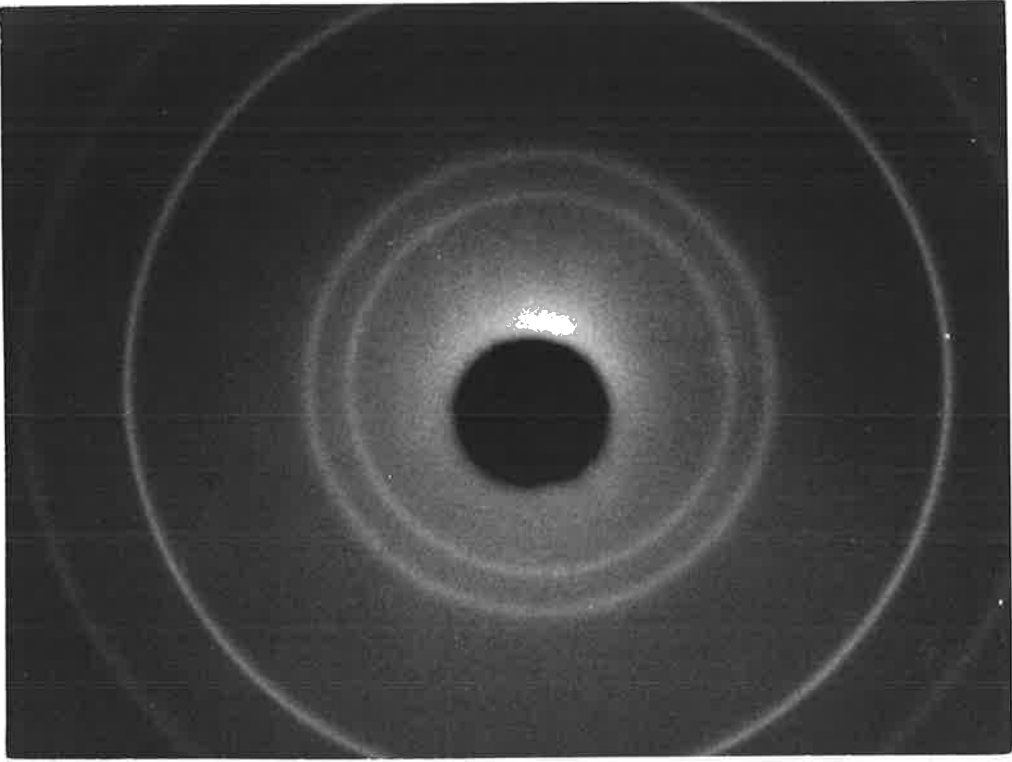
An indication of the dependence of craze morphology upon crystallinity was gained using the following procedure. Nylon 6 films were quenched in air from the melt, or allowed to anneal and cool slowly. These films will be referred to as "quenched" and "annealed" films, and an indication of the difference in crystallinity between them is given in Fig.

4.2.79a,b.

Fig. 4.2.79a Flat plate X-ray diffraction photograph
of annealed nylon 6.

o))))
 d_{200} d_{002} $\bar{}$
 $\bar{}$
 nylon 6 Au

Fig. 4.2.79b Diffraction photograph of quenched nylon
6 (uncoated).



The annealed films gave a pattern, shown in Fig. 4.2.79a; the nine sharp rings correspond to spacings of 0.44nm (d_{002} plane) and 0.37nm (d_{200} plane). The two outer rings are produced by diffraction from the gold coating used for calibration. Irradiation of the quenched sample gave only faint rings (Fig. 4.2.79b) and random scattering from the amorphous region was more evident.

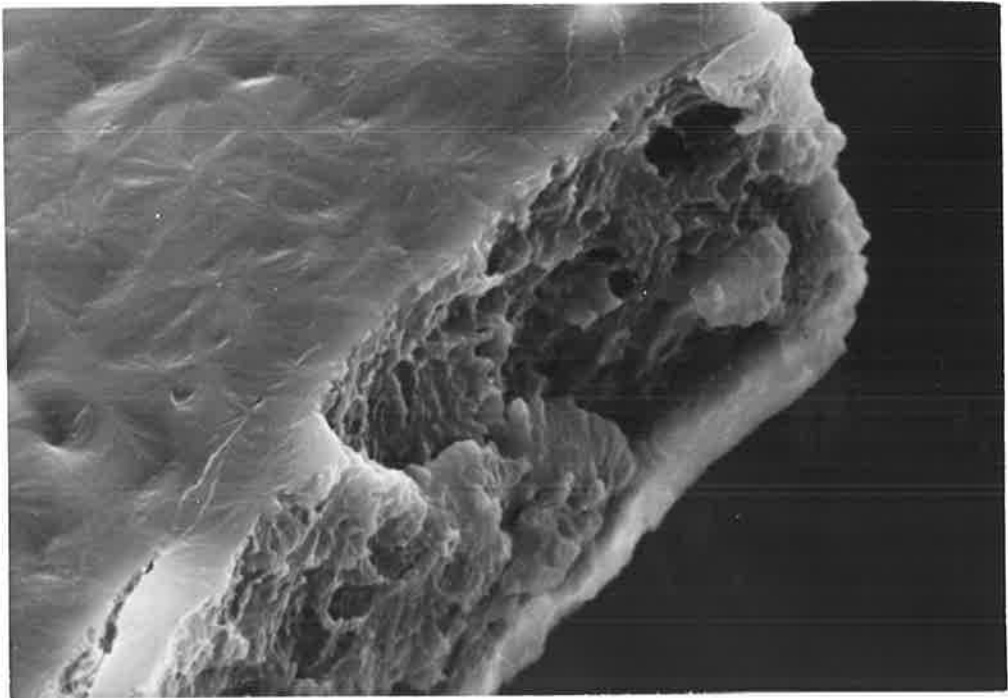
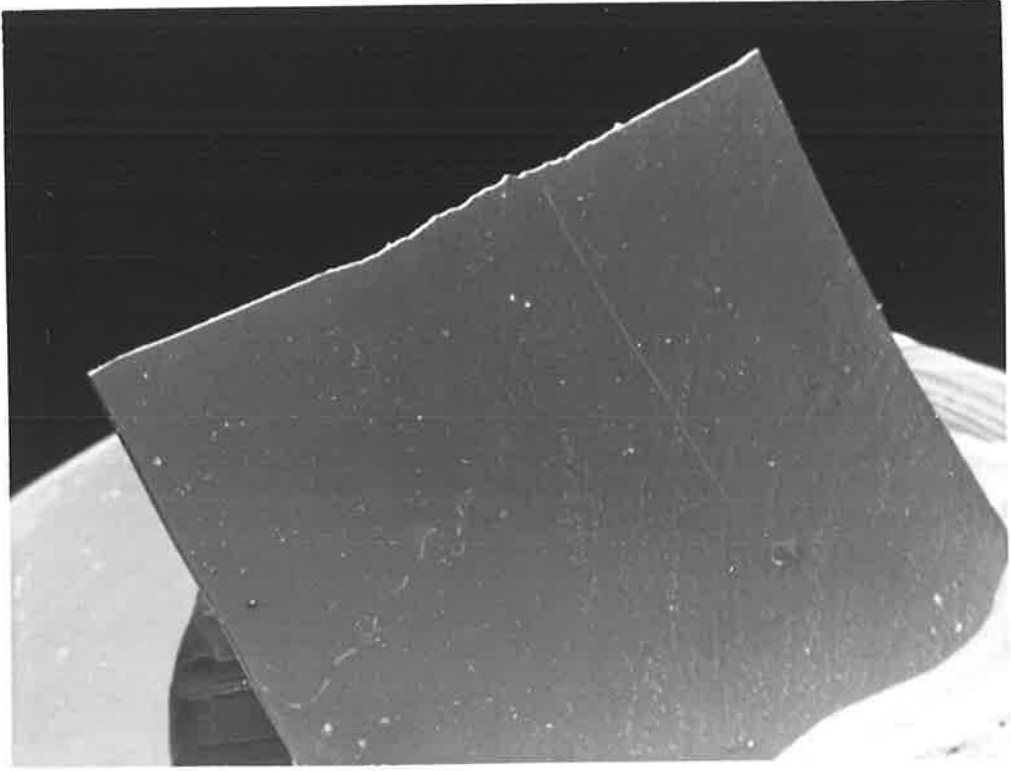
The level of water in the polymer is also predicted to be of consequence to the mechanism of agent uptake in the polymer and this may in turn influence the distribution and morphology of crazes. Both annealed and quenched samples were either maintained in anhydrous condition (by storing in a dessiccator) or were immersed in boiling water to produce water saturated specimens. The latter films are referred to as water-pretreated films. The morphology of crazes and cracks induced in each type of nylon by aqueous zinc chloride (4M) and saturated aqueous lithium iodide is described.

(i) Annealed, anhydrous nylon 6 film

Specimens fractured cleanly at very low (unmeasured) strains in the presence of either salt. The fracture surface depicted in Fig. 4.2.80 (lithium iodide treatment), for example, contains no evidence for crazing or nylon-salt complex production. The texture of a typical fracture face from either salt treatment is shown in Fig. 4.2.81. It is a brittle fracture region (Type 4); thus behaviour is expected when the brittle nature of untreated anhydrous nylon 6 and is discussed later in this section with reference to a mechanism proposed by Boukal [131].

Fig. 4.2.80. Annealed, anhydrous nylon 6 fractured
with aqueous lithium iodide solution.
Magn. = 28x

Fig. 4.2.81. Brittle fracture face of above specimen.
Magn. = 1,830x



(ii) Annealed, water pretreated nylon 6 film

There was a similarity in the results obtained when films were treated with the two different salt types. The dominant texture appears at low magnification to be brittle (Fig. 4.2.82) but at higher magnification (Fig. 4.2.83) small pores and evidence of very limited deformation can be perceived. No distinction could be made between the morphology of films treated with zinc chloride from those treated with lithium iodide. The introduction of water into annealed films appears to have no observable effect upon the failure mode when active stress-crazing agents are present. It is possible that uptake of solvent from the agent into thin films is extremely rapid and so differences in the behaviour between anhydrous and water pretreated films will be difficult to observe. When salt is absent, however, large elongations to break (>20%) were achieved.

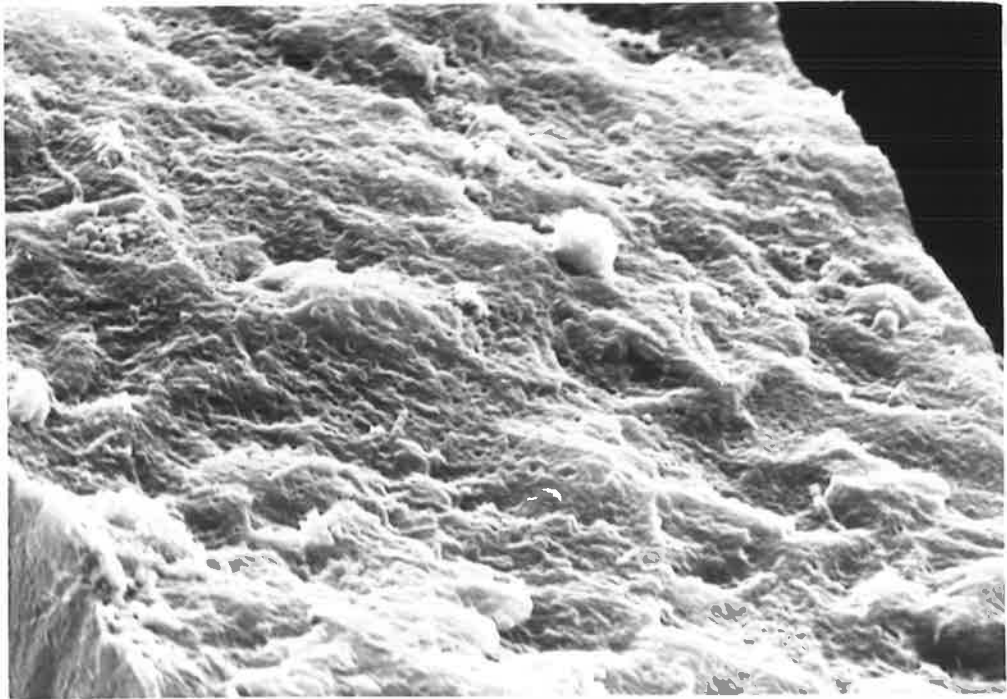
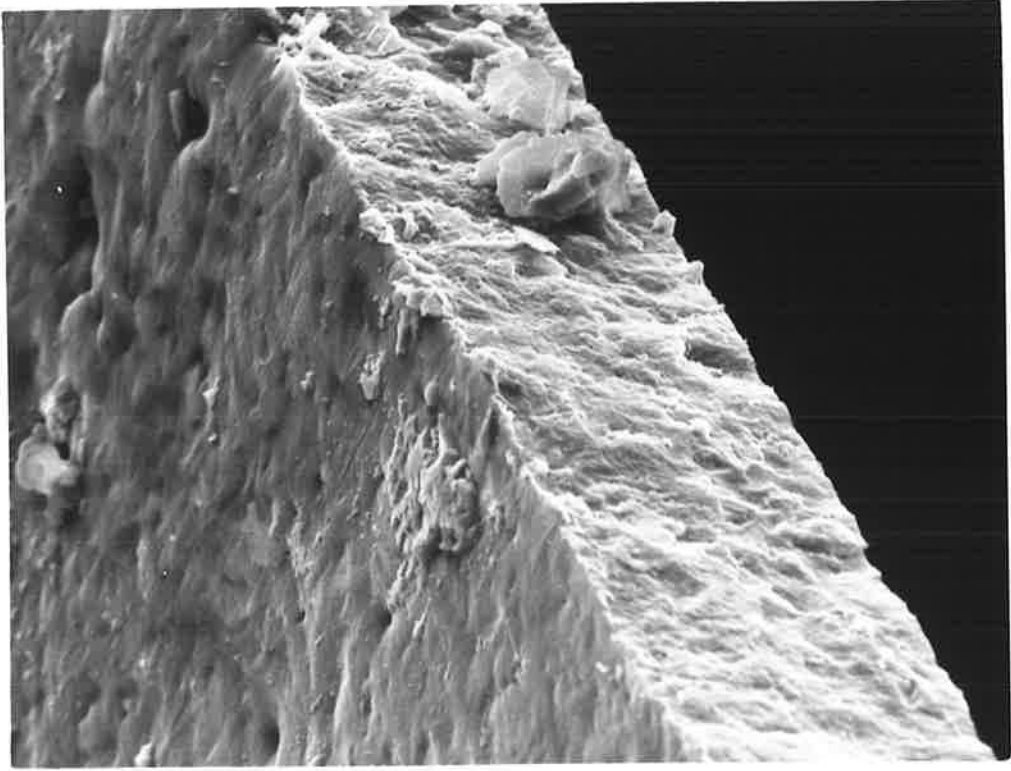
(iii) Air-quenched anhydrous nylon 6 films

Crazing occurred when the films were stressed with either agent, but there was a noticeable difference in the fracture face morphology. Multiple craze initiation occurred when zinc chloride was present, but not with lithium iodide. The nylon in each instance showed no spherulitic texture at the surface, which is consistent with the thermal history of the film.

The zinc chloride treated film is shown in Fig. 4.2.84. Patches of flat, swollen craze matter can be seen, and small pores can just be resolved. It appears that after crazing, the crack has propagated along the craze - bulk polymer

Fig. 4.2.82. Annealed, water pretreated nylon 6 cracked with aqueous lithium iodide. Fracture surface appears brittle. Note spherulitic texture on side of specimen.
Magn. = 940x

Fig. 4.2.83. Fracture surface of above specimen contains very fine pores. Magn. = 3,230x



interface, leaving areas of denuded polymer alternating with patches, covered with craze material. Other crazes can be seen below the fracture surface.

The lithium iodide treated nylon has a fracture surface with a very different morphology. In Fig. 4.2.85, the flat type 1 region is seen at left, followed by a region where craze formation and breakdown has occurred. This second region, which has also been observed in other experiments (see Chapter 4.2.3, for example) comprises a salt-rich phase (a network of small white patches) which overlays the uncomplexed nylon. Precisely why the craze material aggregates in this way is not clear.

The width of the smooth type 1 zone varies along the length of the fracture face, ranging from approximately 20% to 90% of the total thickness of the specimen. Craze formation and subsequent crack development both ensue rapidly. The fracture morphologies of these films are similar to those observed in other experiments using bulk nylon 6 and 66.

(iv) Air-quenched, water pretreated nylon 6 films

When these films were stressed with each agent, noticeable craze formation again preceded fracture. The zinc chloride treated films were extensively cracked and crazes could only be seen at the crack tips (Fig. 4.2.86). The paler region at the top of the photograph shows where the agent was applied. The narrow crazes which can be seen radiating from the fracture surface (top right of photograph) are similar to those seen previously in bulk nylon 66, when stress-crazed with magnesium perchlorate or zinc chloride

Fig. 4.2.84. Quenched anhydrous nylon 6 crazed with aqueous zinc chloride. Patchy craze layer is prominent. Magn. = 2,500x

Fig. 4.2.85. Quenched anhydrous nylon 6 crazed with lithium iodide. Flat region 1 (at far left) and region 2 with white complex can be seen. Magn. = 2,600x

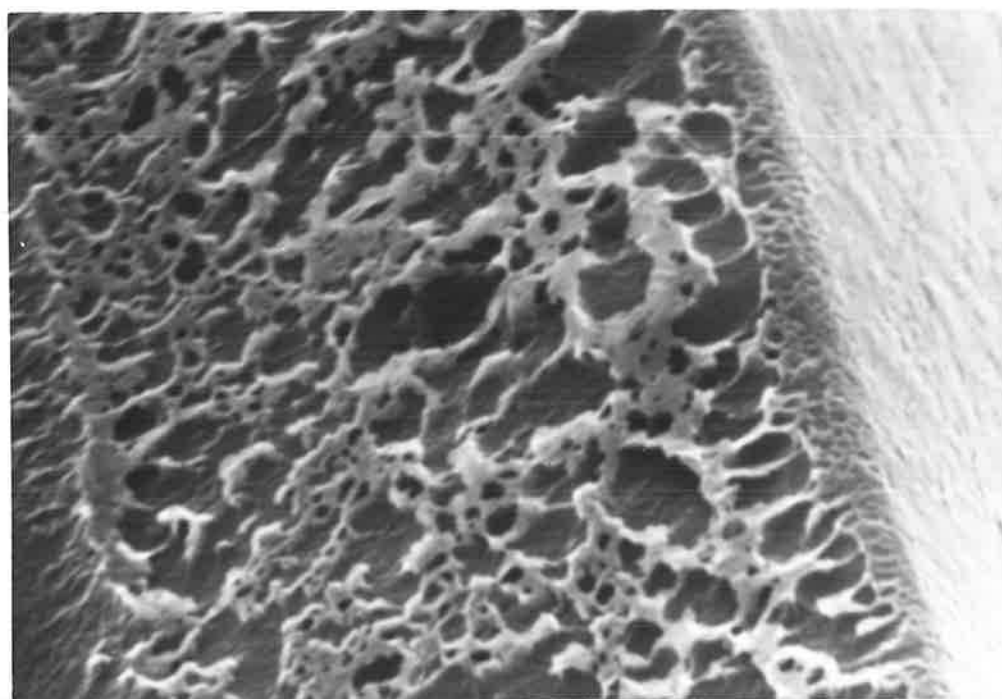
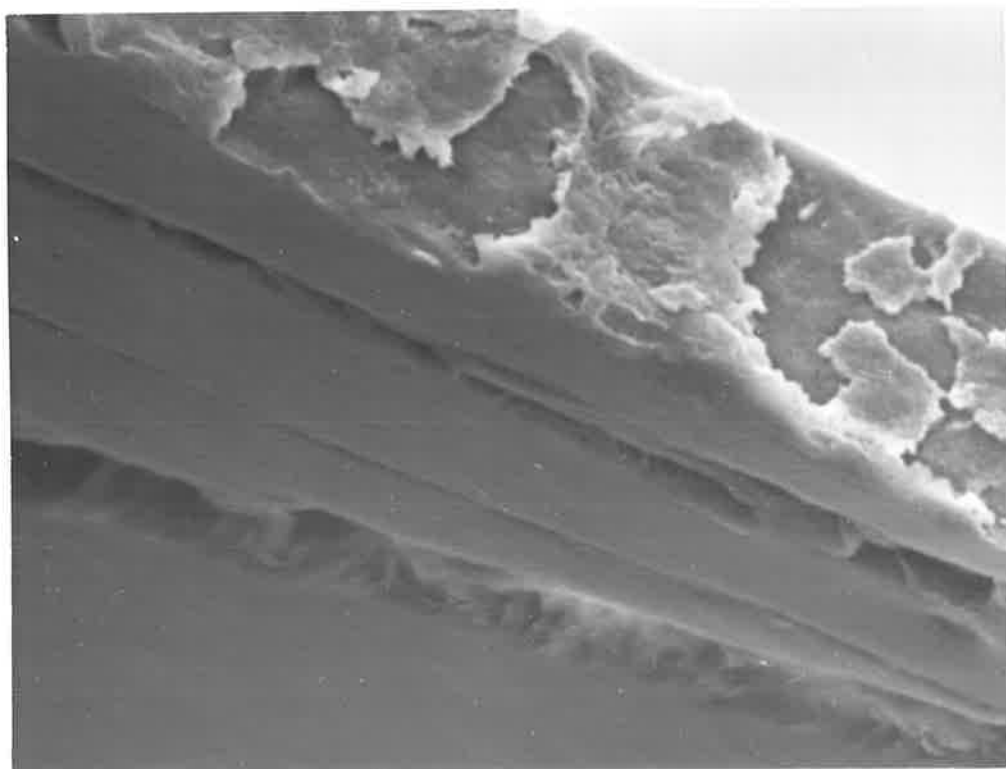
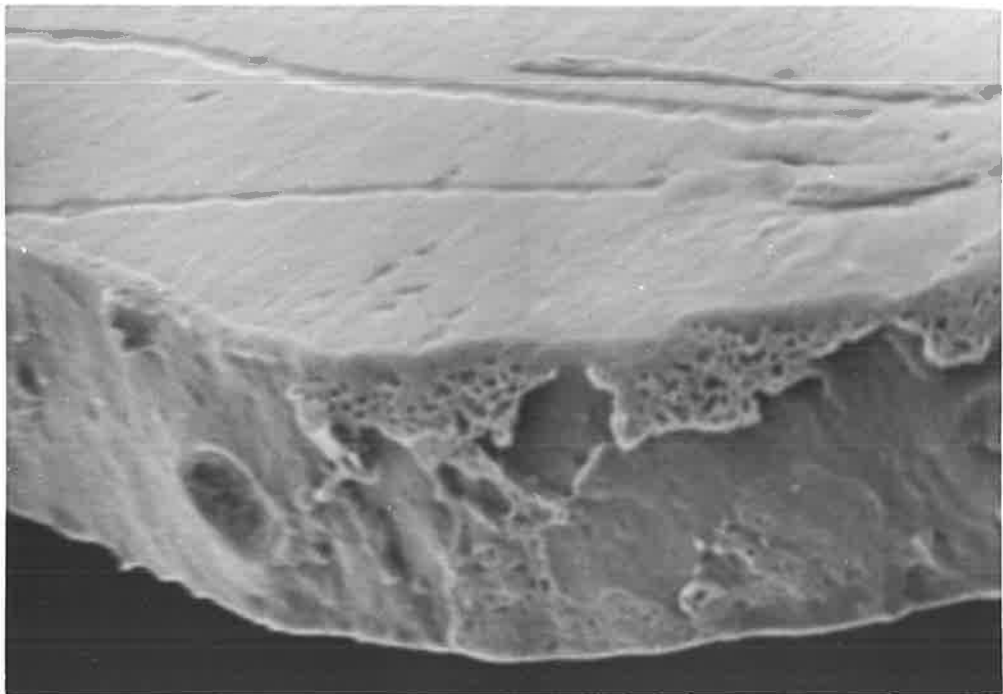
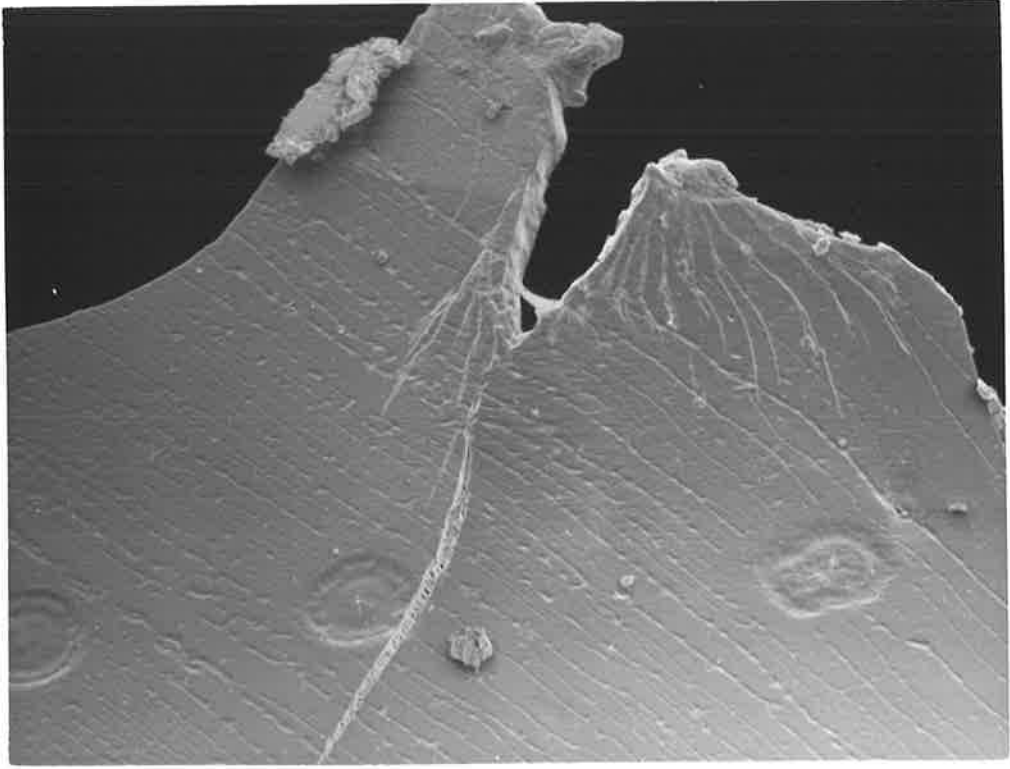


Fig. 4.2.86. Quenched, water pretreated nylon 6 crazed with zinc chloride. Radiating crazes can be seen emanating from treated region at top. Magn. = 260x

Fig. 4.2.87. Fracture surface of above specimen showing craze layer. Magn. = 1,875x



(described in Chapters 4.2.1 and 4.2.3). The striations and depressions on the main surface of the specimen are artifacts resulting from specimen preparation.

The fracture surface shows little evidence of ductile deformation. Patches of porous craze matter (Fig. 4.2.87) are occasionally encountered, but at low magnifications the surface appears to have resulted from brittle fracture. Although crazing has initiated, subsequent elongation before rupture is small. The zinc chloride treated nylon behaves in the same way as proposed for lithium iodide and other type II agent stress-crazed nylons. The similarity between the fracture morphology of nylon films with each treatment is illustrated by comparing Fig. 4.2.88 (zinc chloride treatment) with Fig. 4.2.89 (lithium iodide treatment). The surfaces are morphologically indistinguishable. The mechanism of failure in these specimens is not readily apparent.

The two results which justify comment are:

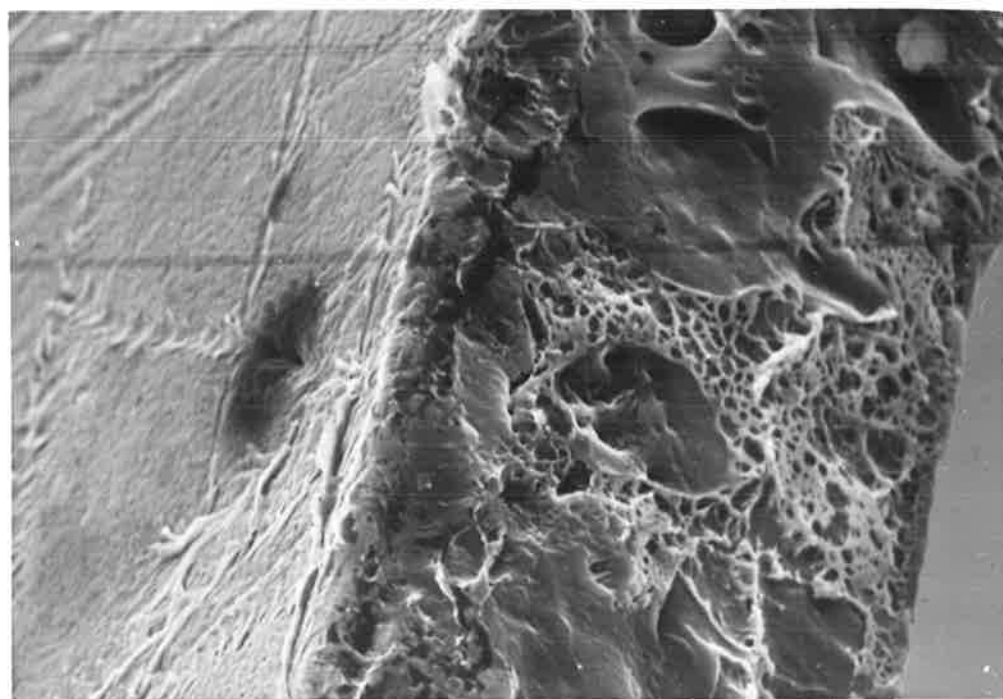
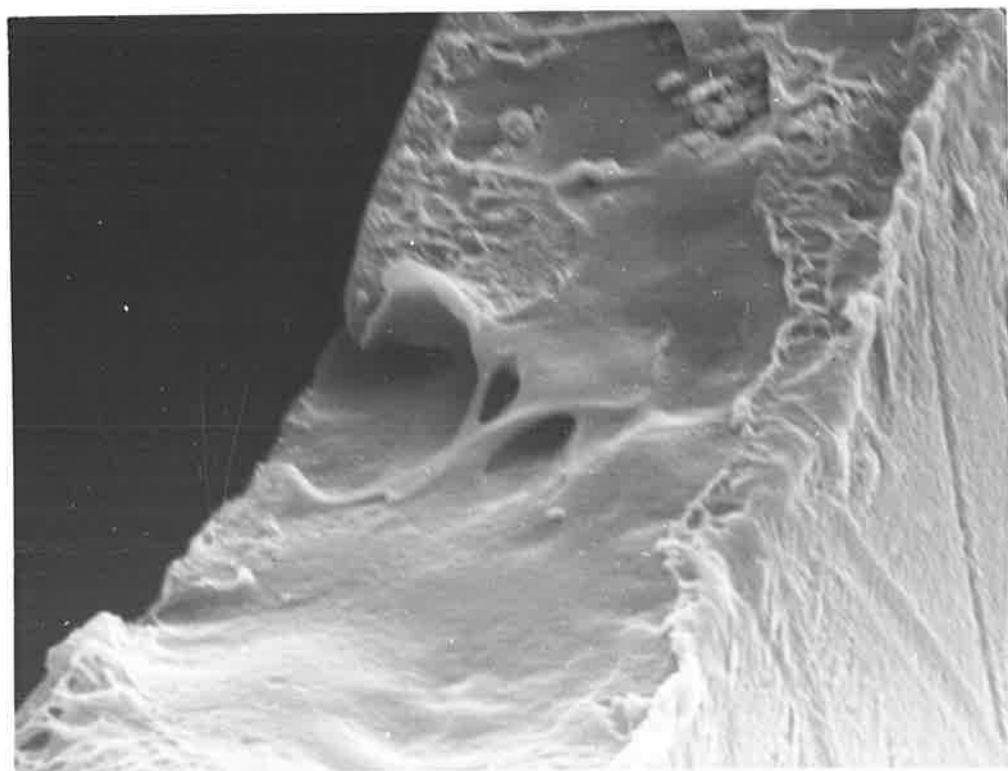
(a) that the water content of nylon 6 does not appear to influence strongly the morphology of crazing and fracture induced by lithium iodide and zinc chloride,

and (b) that the crystallinity and texture of the nylon has an important bearing upon the mechanism of failure under stress.

In the absence of a crazing agent, high water levels cause nylon to have a low modulus of elasticity, and a high elongation to break (as shown in Chapter 5.1 and [131,132]. Boukal [131] proposes that two mechanisms operate. The

Fig. 4.2.88. Quenched, water pretreated nylon 6 treated with aqueous zinc chloride. Compare with fracture morphology below. Magn. = 2,250x

Fig. 4.2.89. Quenched, water pretreated nylon 6 treated with aqueous lithium iodide. Magn. = 2,500x



lattice deforms with orientation of the molecular chains perpendicular to the stress direction, and changes in the lattice parameters arise from increased hydrogen bond length. The first mechanism (called "delayed elasticity") only occurs in the amorphous regions above T_g , and so water is considered to act as a plasticizer enabling the T_g of nylon 6 to fall below 20°C (also shown for nylon 66 by Starkweather [132]). Conformational changes may now occur facilitating reorientation of the lamellae. The absence of a major modification to the mechanism of crazing when agent is present, by water within the matrix, suggests that the energy requirement for sliding and separation of chains in the presence of an active salt, is significantly lower than that required for flow when water alone is the plasticizer.

The factors which regulate the uptake of agent into dry or wet nylon are many. It appears that the solvent in the agent would be able to rapidly penetrate a thin anhydrous nylon film; in addition, no simple correlation between pure solvent and "contaminated" solvent (as a component of a crazing agent associated with salts) uptake into nylons.

The free volume of nylons is a consequence of the specimen's thermal history (as discussed in Chapter 2). The transport of agent increases with increasing free volume, so that a stage may be reached where the relative dimensions of agent and of the space through which it passes may favour rapid diffusion. When this occurs (for example in the dye CI Acid Red 18 and nylon 66 system reported by Peters [134], sorption behaviour becomes "relatively insensitive" to

physical variations in the nylon. It is possible that if nylons are subjected to the appropriate thermal treatment, small molecules (such as water) may pass unhindered through wide corridors in the polymer matrix.

The inter-relation between small molecule uptake and polymer structure is discussed further in Chapter 6.

4.3. Transmission Electron Microscopy of Nylons Strained in the Absence and Presence of Stress-Crazing Agents

The observation of crazing and other deformation modes in nylons at high magnifications could only be performed using transmission electron microscopy (T.E.M.) until a scanning electron microscope (S.E.M.) became available. Results were obtained with thin ($\approx 0.1 \mu\text{m} - 0.5 \mu\text{m}$) nylon films and by using replicas of thicker specimens.

This section is divided into three parts;

- (a) Direct observation of thin films, both coated and uncoated.
- (b) Observation of thin films using direct replicas.
- and (c) One and two stage replica studies of specimens greater than $10 \mu\text{m}$ thick.

The aim of the thin film work was to try to determine whether metal ions were preferentially absorbed into a particular region of the nylon. For example, with highly crystalline films it was thought possible that cations might segregate into the boundaries of spherulites under certain conditions.

Later, work with thicker nylon films ($> 1 \mu\text{m}$ thick) was conducted to determine how the structure changes with stress, both with and without salts present. Finally, T.E.M. was used to complement the research being conducted with the S.E.M. In particular, replicas of bulk specimens which had been stress-crazed were produced, both to substantiate results from the S.E.M. and to obtain higher resolution than that possible from the S.E.M.

4.3.1. Direct Observation of Thin Films

Uncoated

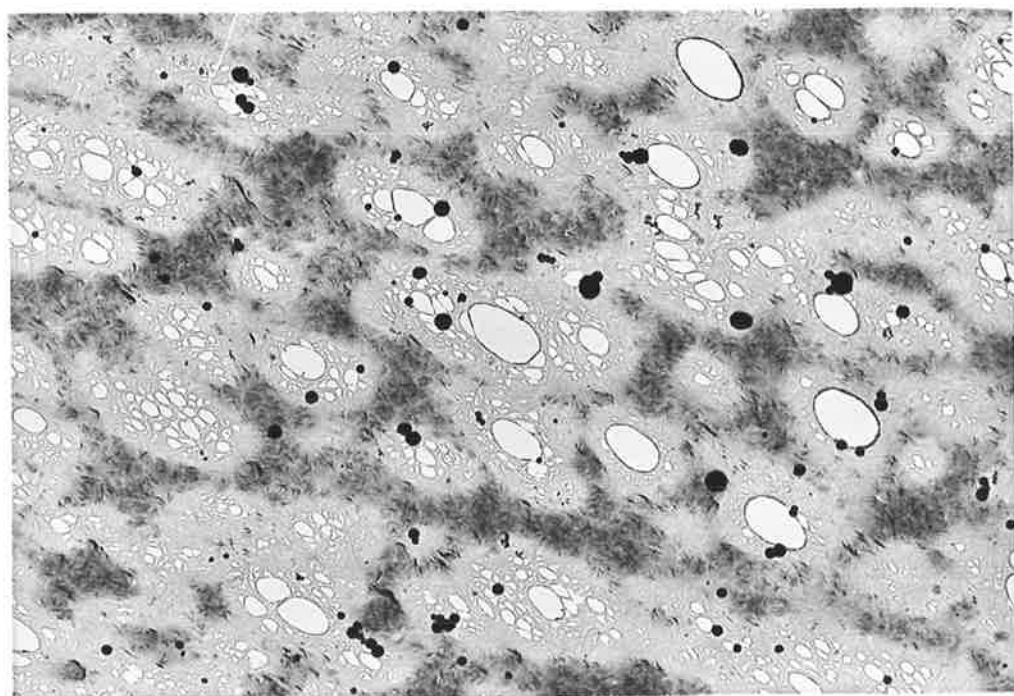
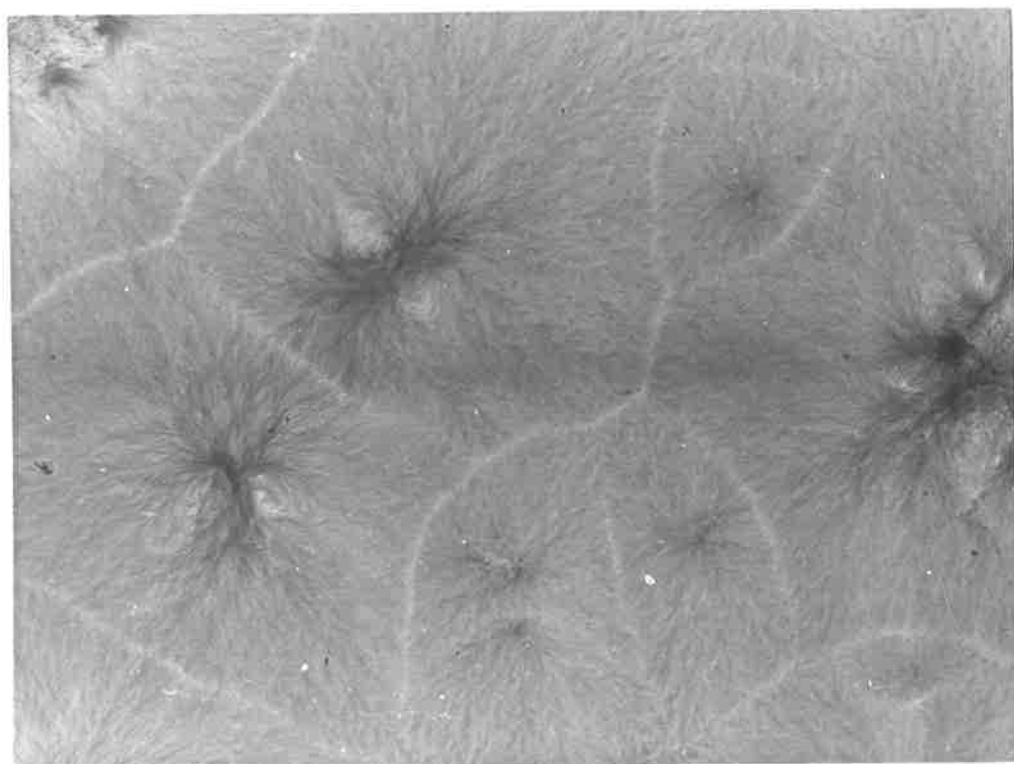
Nylon films less than 1 μm thick can be cast from dilute formic acid and phenolic solutions. When carefully washed and dried, they may be observed intact, with the T.E.M. A nylon 6 film is pictured in Fig. 4.3.1. The film is spherulitic, and no voids or other spurious discontinuities can be seen.

When similar films were exposed to aqueous cupric chloride solutions (0.001 to 1.0 M) for times up to 96 hrs., and observed either washed or unwashed, many developed voids and darker needle-like regions away from the voids (Fig. 4.3.2.). There was no clear relationship between concentration and time of exposure to salt, with the incidence and size of the voids, and further-more, electron diffraction studies indicated that no salt was present. The results were not very conclusive, and analysis was complicated by the effects of shrinkage stresses (as the films dried on the grids) which caused the integrity of the films to be destroyed.

Two additional problems which arose in this work were the inherent lack of contrast of the thin films, and the breakdown of the original structure, either during sample preparation or in the microscope column. Despite efforts to reduce damage, the films were found to disintegrate in the electron beam, especially at high magnifications. An extreme example of a specimen which has transformed finally into a three-dimensional "spider-web" is shown in Fig. 4.3.3.: it had contracted when drying on the grid.

Fig. 4.3.1. Nylon 6 film cast from dilute formic acid solution. Magn. = 14,700x

Fig. 4.3.2. Thin nylon 6 film modified by aqueous cupric chloride. Magn. = 6,400x



Coated Films

One way of overcoming both problems is to coat the films with a carbon support film and to shadow with gold or platinum. The film becomes much stronger in the electron beam, the contrast is improved, and so surface details are enhanced. Unavoidable consequences are a loss of information about the composition of the film, because the interior structure is masked, and an increase in the complexity of the electron diffraction images. The microstructure of a thin nylon 6 film which has been exposed to 0.1M cupric chloride for 4 hrs., dried (with subsequent shrinkage) and shadowed with gold, is shown in Fig. 4.3.4.

Nylon films cast from phenol were thicker ($\approx 1-5 \mu\text{m}$), uniform in thickness and highly spherulitic. An uncoated film which was strained on the surface of water is shown in Fig. 4.3.5. Localised deformation which may be thought of as crazing has in this instance occurred at, and parallel to, the spherulite boundary.

4.3.2. Observation of Thin Films using Replicas

Once uniform, spherulitic films (such as that shown in Fig. 4.3.6) could be routinely prepared, investigation of the tensile deformation characteristics could be undertaken. A special instrument (described in Chapter 3) was constructed to stretch nylon films on the surface of water, or on aqueous solutions of stress crazing agents. Only a brief outline of the work will be given here, because only deformation studies in the absence of agent were very successful, and because thin films do not necessarily exhibit mechanical properties which relate directly to the bulk specimens.

Fig. 4.3.3. "Spider web" produced by disintegration and contraction of nylon 6 film upon drying. Magn. = 8,700x

Fig. 4.3.4. Micronecking in gold-coated nylon 6 film, previously exposed to cupric chloride solution. Magn. = 8,700x

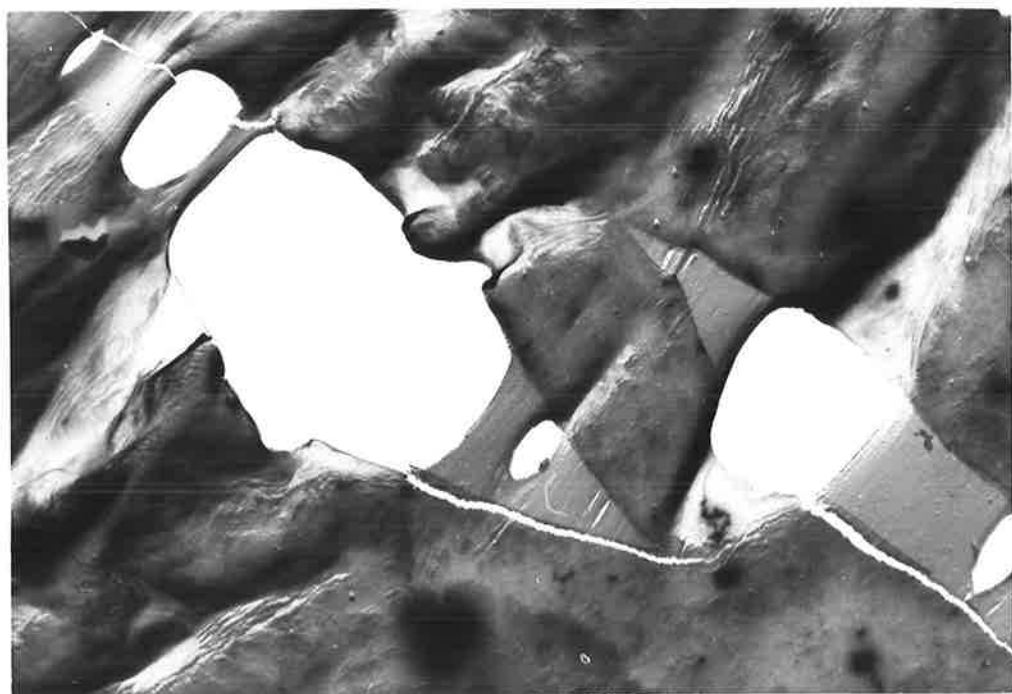
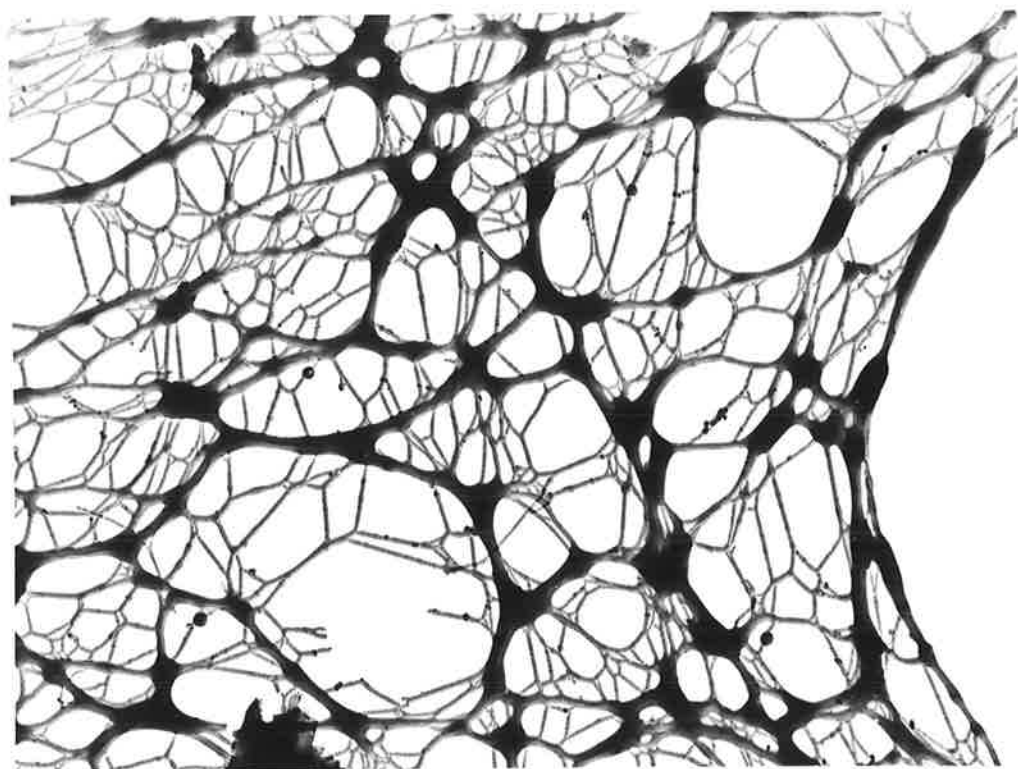
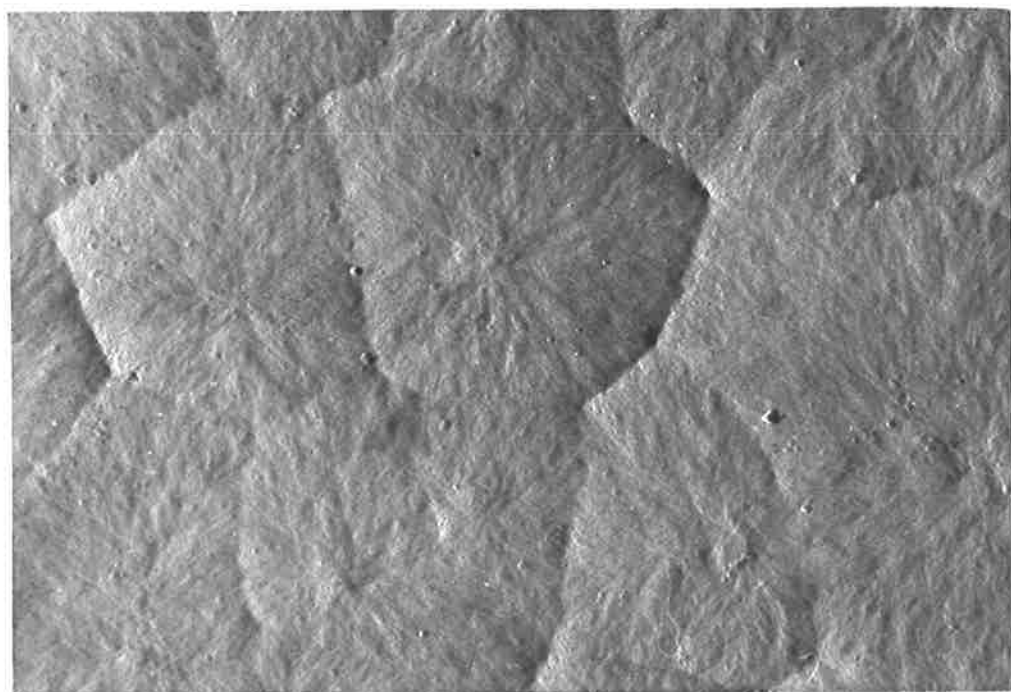
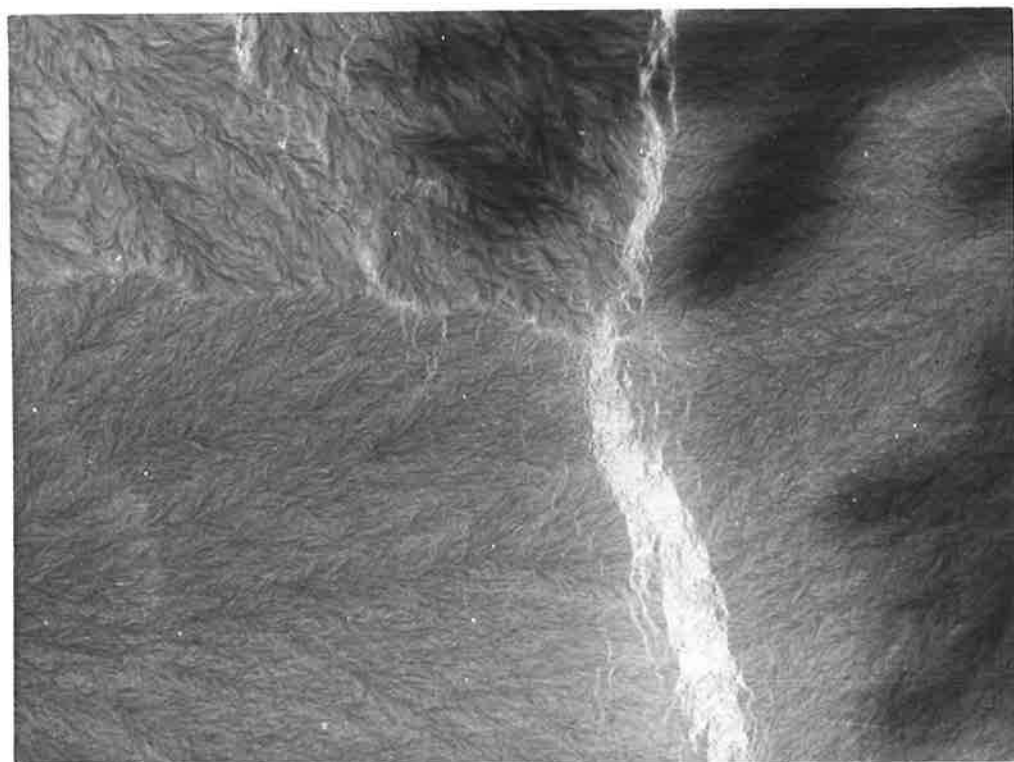


Fig. 4.3.5. Deformation at spherulitic boundaries
of a strained nylon film $\sim 1\mu\text{m}$ thick.
Magn. = 11,500x

Fig. 4.3.6. Carbon-platinum replica of spherulitic
nylon 6 film cast from phenol onto water.
Magn. = 18,500x



Some of the problems which arose and which were overcome by using S.E.M. are also given.

Deformation of Nylon 6 films in the absence of stress-crazing agent

Thin (0.1 to 1.0 μm) films of nylon 6 were cast on water from a phenolic solution and strained up to 50% using the special stretching device. The films were then coated with carbon and shadowed with gold or platinum, and the nylon finally was dissolved using formic acid. The most common and prominent type of yielding which occurred was micro-drawing of the nylon at the spherulite boundaries. An example, where the overall strain was 18%, is shown in Fig. 4.3.7. Other instances of localised yielding can be seen within the spherulite, normal to the applied stress direction. Less commonly, intraspherulitic drawing and indistinct cross-hatching may also occur, as shown in Fig. 4.3.8. In contrast similarly prepared films which were not strained contained no micronecked regions.

Morphology of Thin Nylon Films in the Presence of Agent - Using Replicas

The results of this work were not very satisfactory. Sometimes the poor images obtained were a direct consequence of the practical realities of trying to replicate a highly swollen, deformed substance heavily loaded with a deliquescent salt (a consequence of thin nylon films exposed to zinc chloride solutions). The example shown in Fig. 4.3.9. is given merely to show the extremely poor results which were obtained.

Fig. 4.3.8. Intraspherulitic micronecking and cross-hatching in strained nylon 6 film - Pt/C replica. Applied stress direction shown by arrow. Magn. = 18,500x

Fig. 4.3.7. Microdrawing of spherulite boundaries during straining of phenol cast nylon 6. Direction of applied stress given by arrow. Pt/C replica. Magn. = 18,500x

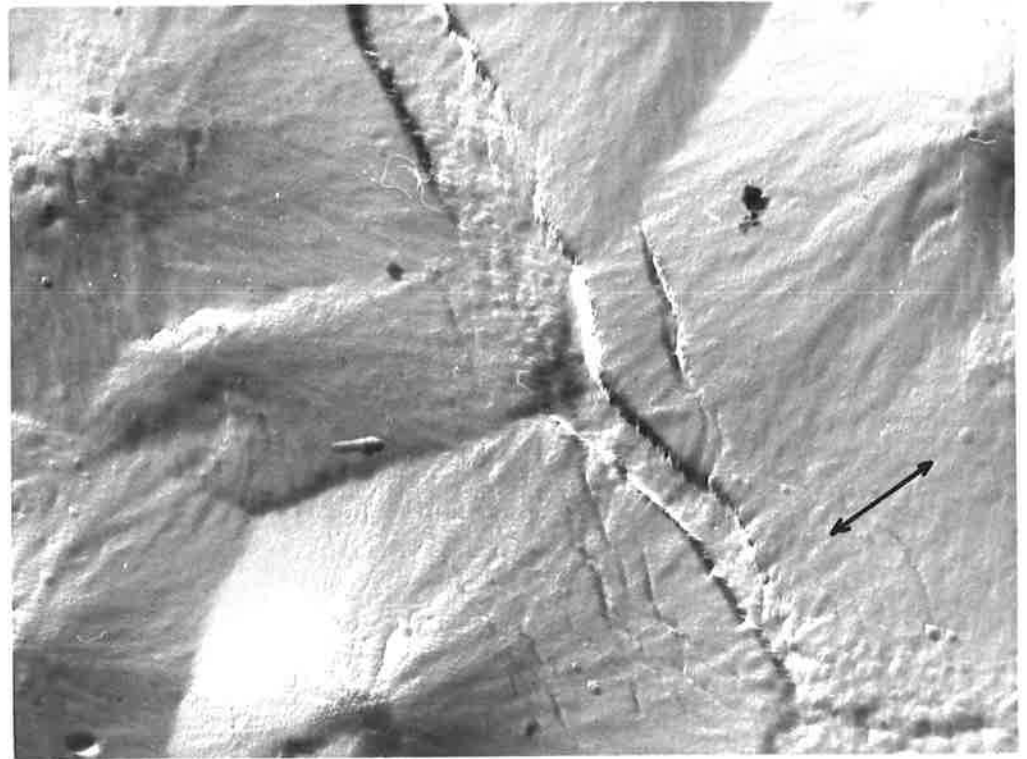
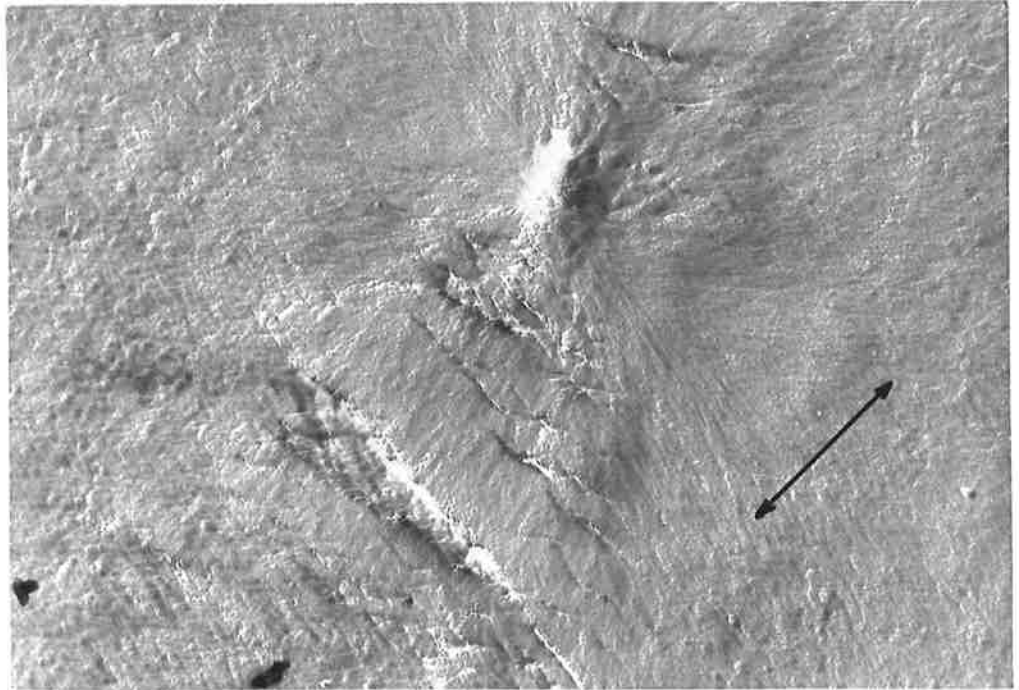
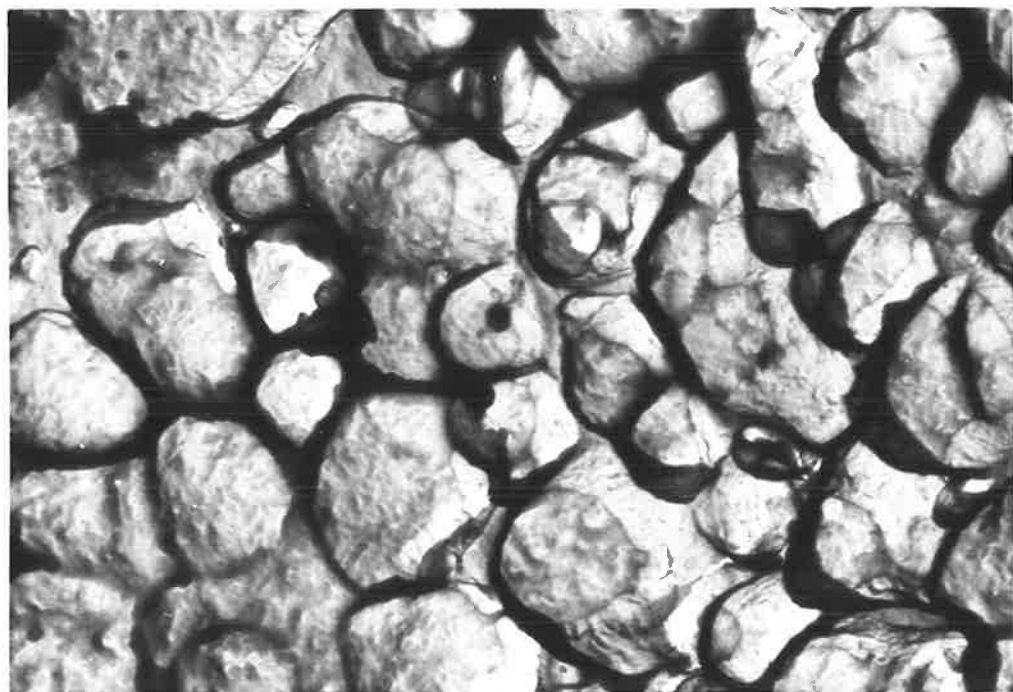
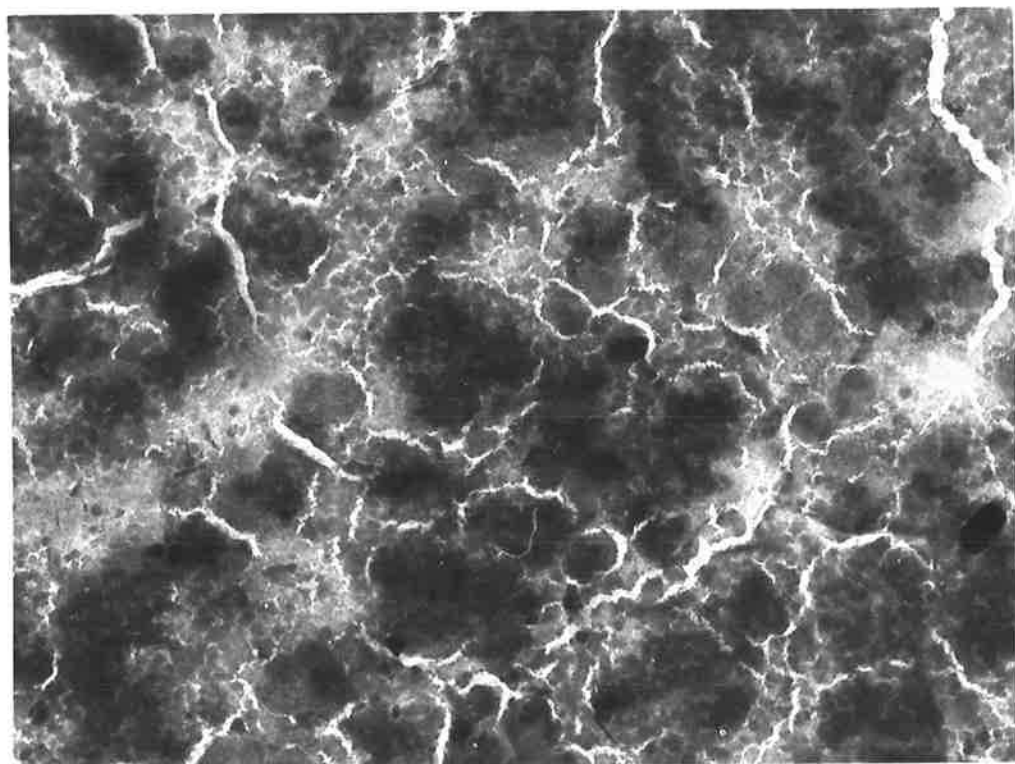


Fig. 4.3.9. Thin nylon 6 film degraded by 5M zinc chloride solution; photograph illustrates typical poor resolution. Magn. = 18,500x

Fig. 4.3.10. Voided fracture surface, revealed by a Pt/C replica with a dimpled appearance. Magn. = 14,700x



The other complication which arises is that voids and other changes to the thin nylon film structure can be faithfully and efficiently recorded, but the intrinsic nature of two dimensional representation can make analysis of the images recorded ambiguous at best. Whilst with hindsight, using the information obtained from S.E.M., it is now possible to interpret the results from the T.E.M., it is otherwise very difficult to relate replicas to three-dimensional surfaces.

Without seeing the fracture surface in three dimensions, the only way of interpreting the pattern in Fig. 4.3.10 would be by using stereopairs, and even then ambiguity would persist as to which part of the fracture region it refers to. However, it does bear a striking resemblance to the "dimples" seen in the plastic fracture of metals and described by Regoux [130]. In metals they are thought to form by the coalescence of microvoids, aided by forces generated as a consequence of the inequality of plastic and elastic stress components.

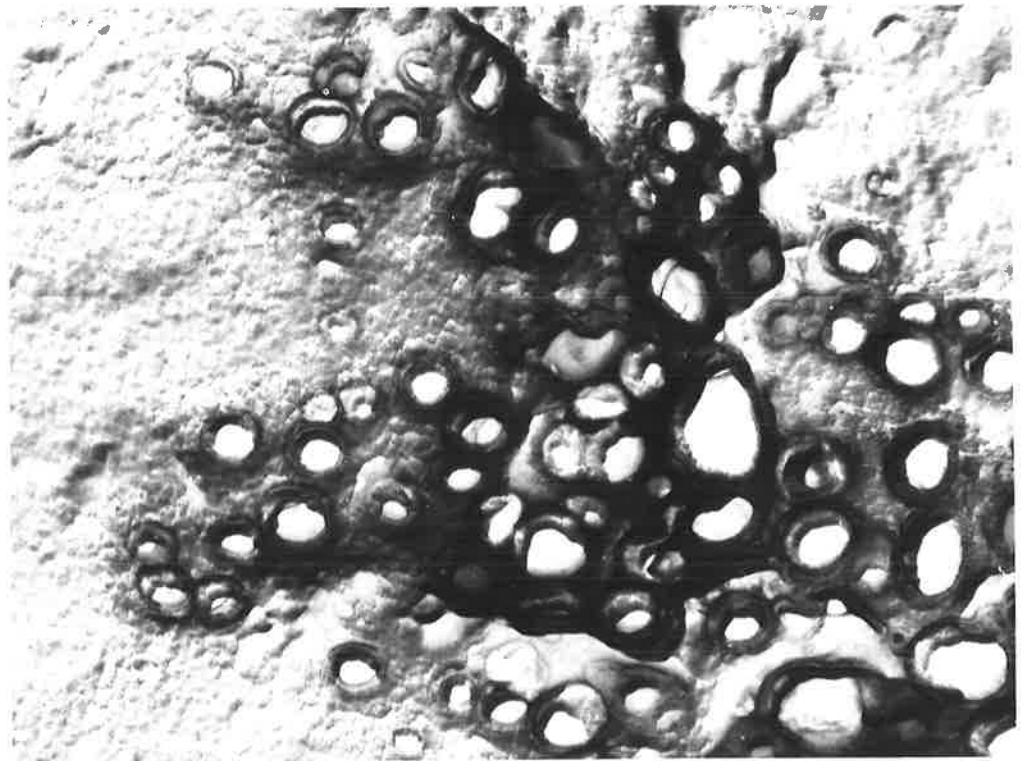
Films in which limited swelling and pore formation occurs are easier to study. Fig. 4.3.11 shows small holes which have developed in thin nylon 66 film (2 μm) strained 5% on the surface of 5M aqueous zinc chloride.

4.3.3. Studies of Thick (> 10 μm) Nylon Samples, using Replicas

The preparation of replicas of very rough fracture surfaces was very difficult and so was only occasionally attempted in this work. Work in which treated and untreated specimens were replicated will be discussed separately.

Fig. 4.3.12. Ductile fracture morphology of bulk nylon
6. C/Pt replica. Magn. = 14,700x

Fig. 4.3.11. C/Pt replica of a nylon 66 film swollen
by zinc chloride. Pores and evidence of
swelling can be seen. Magn. = 19,400x



Untreated Specimens

When a notched, bulk nylon 6 testpiece was strained at 1 cm/min., slow and rapid crack velocity fracture regions could be discerned. Replicas of each are shown in Figs. 4.3.12 and 4.3.13 and they correspond with the results obtained using the S.E.M.

The replication of the surface of unfractured specimens can be routinely achieved when they are not very rough. For example, the structure of homogeneously deformed polymer corp. nylon 66 film is shown in Fig. 4.3.14. The specimen was strained slowly to 12%, and then replicated by coating with carbon and platinum, and dissolving the nylon using formic acid. The spherulites have deformed uniformly in the strain direction (shown by the arrow).

Nylons Treated with Stress Crazeing Agents

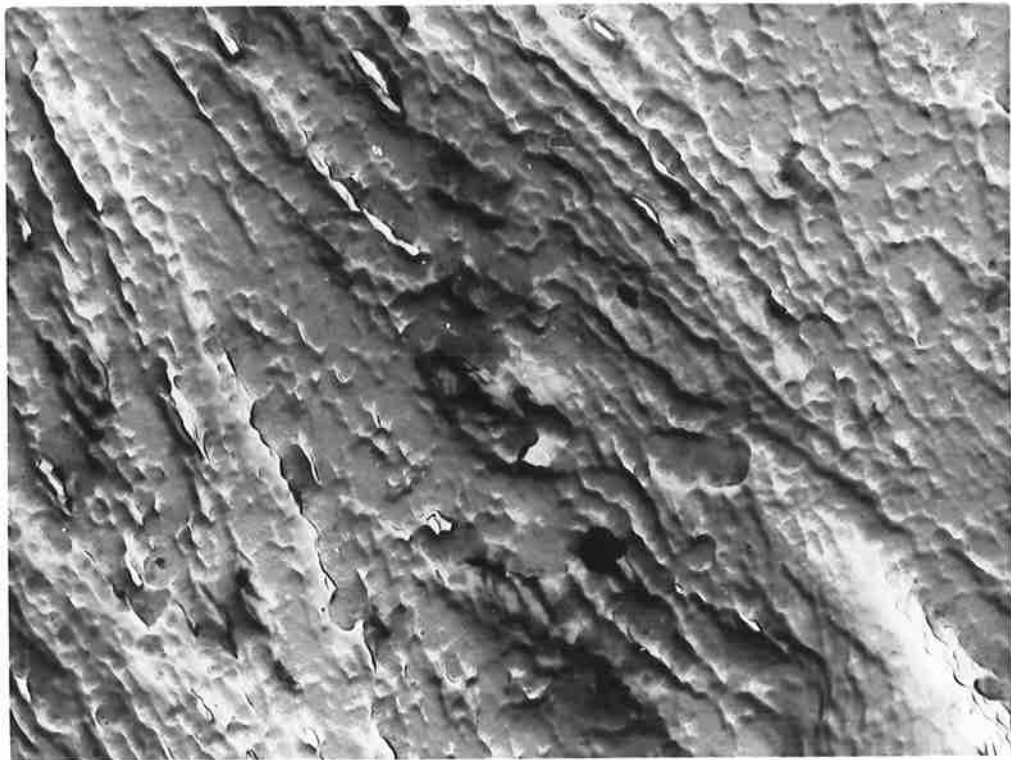
Transmission electron microscopy has not been used extensively because of the problems of replicating deep, complex cracks and crazes, and because of the limitations of representing a three-dimensional profile with a two dimensional replica. However, two examples of the results which can be obtained are given.

The porous texture of films treated with stress crazeing agent and lying between the crazes of a stressed specimen appear highly porous in the S.E.M. The same porous morphology can be seen in Fig. 4.3.15, which shows a nylon 6 film strained in the presence of zinc chloride.

When the same nylon 6 film is strained to break in 5M aqueous zinc chloride solution, and part of the crazed region (which has been washed and dried) replicated, crazes appear as shown in Fig. 4.3.16. Crazes induced in nylons by other

Fig. 4.3.13. Fracture surface of bulk nylon 6 resulting from rapid crack propagation. Pt/C replica. Magn. = 18,500x

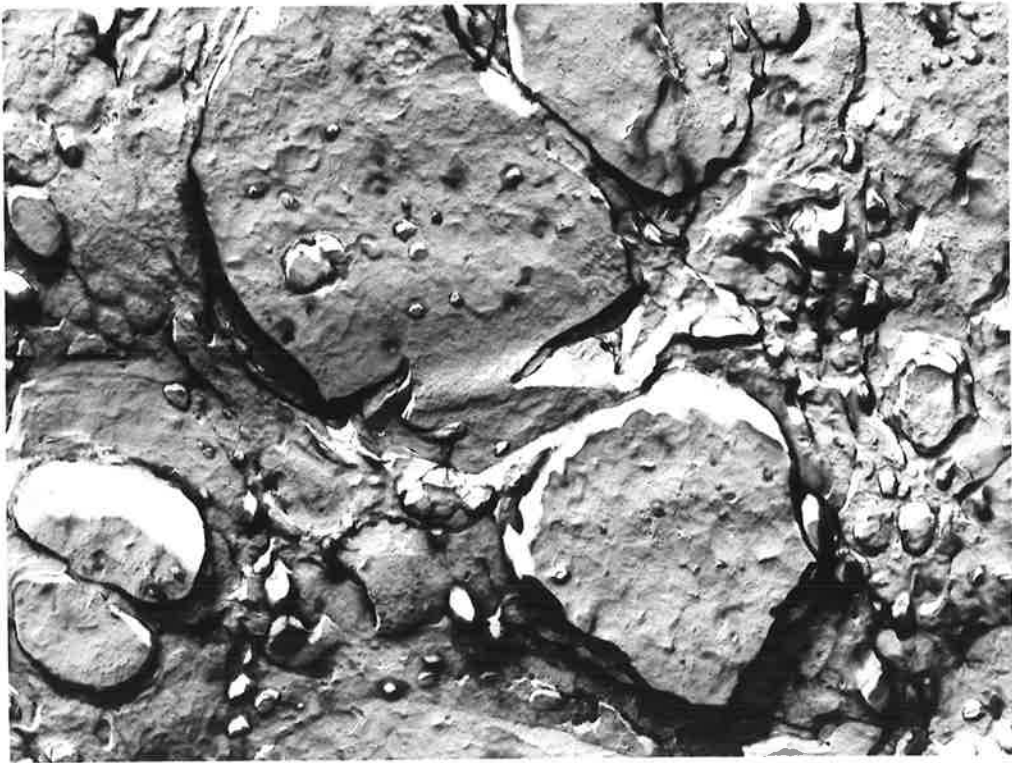
Fig. 4.3.14. Uniform deformation of spherulitic nylon 66. Pt/C replica of bulk sample. Applied stress direction indicated by arrow. Magn. = 6,400x



agents also have a similar morphology. The appearance of the material within the craze has been modified because the shadowing angle used in the replication process was very acute. Although the edges of the craze matter appear discontinuous, this is a consequence of the replication technique. The smooth texture of the surface of the craze contrasts with the more granular uncrazed polymer.

Fig. 4.3.15. Porous texture of nylon 6 film strained in presence of zinc chloride. Pt/C replica. Magn. = 11,500x

Fig. 4.3.16. Replica of zinc chloride crazed nylon 6, showing inadequate detail, compared with SEM results. Magn. = 4,500x



CHAPTER 5.5.1. Mechanical Testing of Polymers

Two approaches were used to examine the tensile behaviour of polymers in the presence of salts. In the first method, tensile testing of nylon specimens which had been allowed to equilibrate to give particular levels of water and/or zinc chloride over the entire test-piece was performed and the results are given in Section 5.1.1. The aim of this type of experiment was to determine the overall mechanical behaviour of homogeneous material.

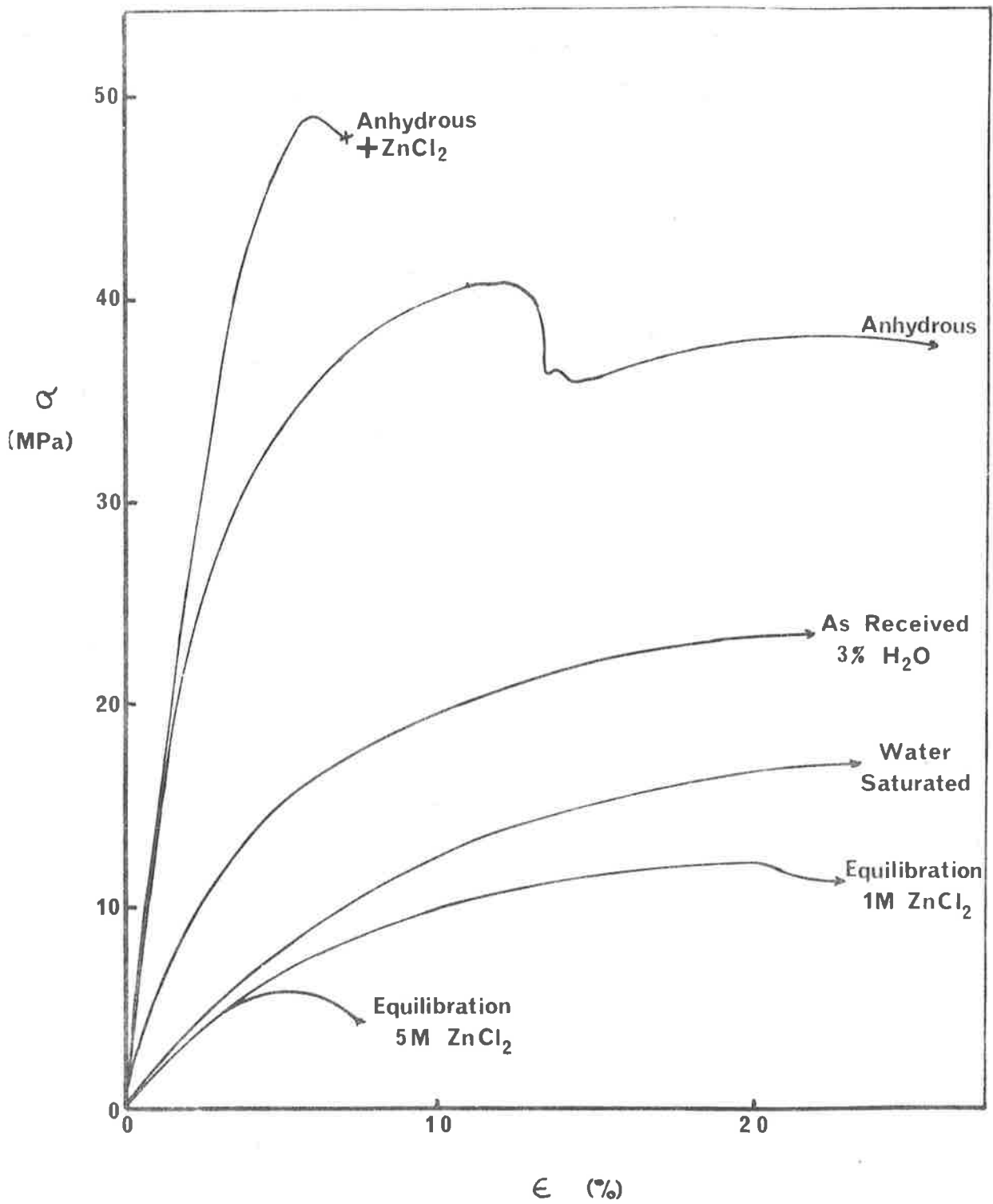
The second method entailed application of a solution of the salt to the test-piece during tensile testing. The tests were carried out under a variety of conditions and are discussed in Sections 5.1.2-4.

5.1.1. Effect of Water and Salt Content upon the Properties of Nylon 6 - Equilibrium Studies

Nylon 6 test-pieces were soaked for long periods of time (>72h) in water and 1 and 2M aqueous zinc chloride solutions, and for a shorter time (2h) in 5M zinc chloride solution. From atomic absorption and X-ray analyses it was found that the nylon had equilibrated with the salt in all except the last case (5M for 2h). Test-pieces were removed from each liquid and the surface of each was wiped dry. Some test-pieces were then dried in a vacuum oven at 120°C until constant weight was obtained. All specimens were then strained at 20°C using a crosshead speed of 10mm min⁻¹. The results of the tests are shown in Fig. 5.1.

When the zinc chloride and water content of the polymer is "moderate" (after equilibration with 1M ZnCl₂),

Fig. 5.1. Tensile behaviour of nylon 6 - effect
of water and salt content.



extensive deformation occurred at low stresses, with high elongation before break (also observed to a lesser extent in nylons with a high water content). The salt and water combined with the polymer in the polar amide regions, causing partial interference of interchain hydrogen bonding and a reduction of the resistance to molecular flow.

When very high levels of zinc chloride and water are contained in the polymer, different tensile results were recorded. The nylon treated with 5M zinc chloride was found to break at low elongation, and the maximum stress recorded was also very low. It is meaningless to try to discuss qualitatively this result; if the nylon had been allowed to equilibrate further with the zinc chloride, severe swelling would have occurred and a meaningful tensile test difficult to reproduce. As the content of water and zinc chloride become very high, the whole physical state of the nylon undergoes a drastic change. The molecular structure of the complex can be imagined as nylon chains surrounded by large amounts of partially and fully solvated ions and water molecules (rather like a gel). No rigid interchain forces remain and so not only relative displacement of chain segments, but total separation of chains can now readily occur. This is reflected by the mechanical data obtained.

When "as received" nylon 6 film, containing about 3% w/w water, is dehydrated (as described previously) and then tensile tested, the yield stress increases markedly. This is because there are no water molecules present to facilitate the displacement of one polar polymer segment relative to that adjacent, and the result is that the yield stress is markedly increased.

5.1.2.1. Comparison of Mechanical Behaviour of Nylons Stressed with Type I and II Salts

Under similar applied stress conditions, lithium iodide-induced crazing and cracking was found to be more extensive than with zinc chloride, and this was confirmed when fracture surfaces were examined (saturated aqueous zinc chloride and lithium iodide solutions were taken to represent very active Type I and II agents respectively).

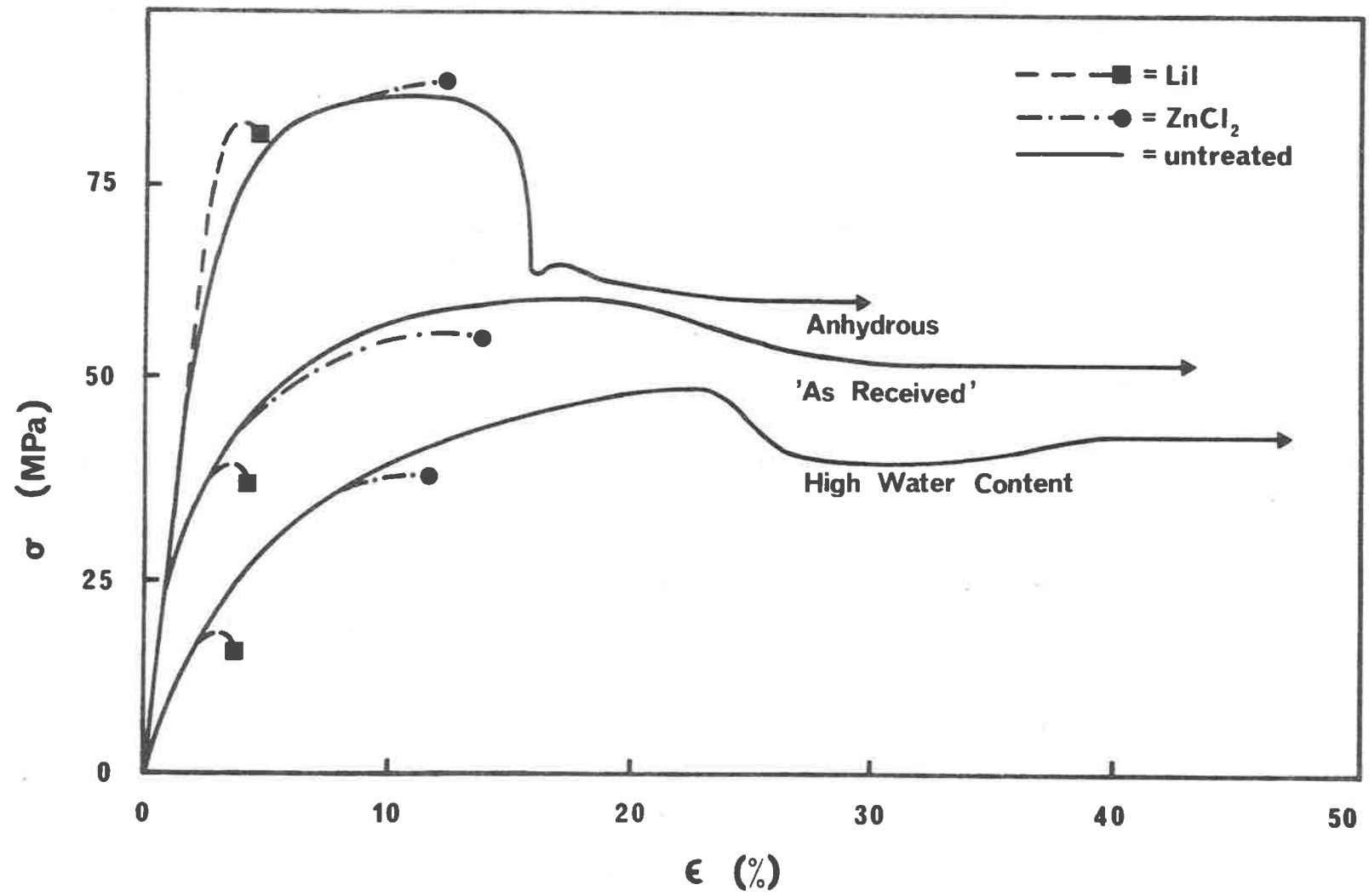
At low stresses, lithium iodide rapidly penetrates the nylon and once crazing has initiated, is absorbed into the polymer near the craze tip. This mechanism can be deduced from other information in Chapters 4 and 5. From evidence also presented elsewhere, a somewhat different mechanism for zinc chloride induced crazing can be proposed.

Mechanisms for each type of crazing, which account for the difference in stress dependence, and which explain the difference in mechanical behaviour, will be provided in Chapter 6.

5.1.2.2. The Effect of Water Content in Nylon 66 Upon Stress-Crazing

Nylon 66 test-pieces (ASTM D638, Type I) containing no water, "as received" levels ($\sim 2.0\%$ w/w) and saturated with water ($\sim 10\%$) were each tensile tested at a crosshead speed of 10mm min^{-1} at room temperature. The mechanical behaviour of the nylons is shown in Fig. 5.2, both in the absence and presence of saturated aqueous solutions of zinc chloride (Type I salt) and lithium iodide (Type II salt).

Fig. 5.2. The influence of Type I (ZnCl_2) and Type II (LiI) solutions upon the mechanical behaviour of nylon 66 containing different levels of water (~ 0.01 , 2 and 10%).



The nylon shows the characteristic yield stress dependence on water content (also indicated in [131,132], with a low yield stress (<50MPa) at high water levels and a high yield stress (~ 85 MPa) under anhydrous conditions. The as received nylon gave a yield stress of approximately 60MPa. The graph shows that at both high and low absorbed water levels, lithium iodide has caused fracture at low strains. Whilst water was present in the nylon, only low stresses were required; however, in the anhydrous nylon, a yield stress nearly the same as the untreated σ_y was reached. The trend which appears for lithium iodide treated samples as the water content of the nylon is reduced is the ratio of σ_y (untreated) to σ_y (treated) decreases markedly, and the elongation to break gradually increases.

As the water content in the nylon is reduced, only slight changes in the ratio of σ_y (untreated) to σ_y (treated) are observed for the zinc chloride experiments. The stresses and strains which can be attained with zinc chloride are greater than for lithium iodide at each water level.

In summary, the effect of water content in nylons appears to be less significant for specimens strained with zinc chloride, than for those tested in the presence of lithium iodide. This result is compatible with a mechanism for crazing based upon the role of solvent in salt-nylon interactions. As stress-crazing for a particular salt has occurred at approximately the same strain for all water levels, a critical strain criterion for crazing is suggested.

Anhydrous nylon films in which zinc chloride has been incorporated ($\approx 25\%$ w/v) sustain higher stresses than untreated nylon. With solvent absent, interchain secondary forces are maintained. Boukal [131] considers the "lattice elastic modules" in directions both parallel and perpendicular to the molecular axes, and concludes (from X-ray results) that in dry nylons the elastic modules approaches the theoretical value in the latter direction. In moist nylons rotation about the molecular axis results from plasticization. Starkweather [132] showed for oriented nylons that anisotropic swelling occurs during water uptake which results in unequal modulus values for different sample directions.

5.1.3. Influence of Solvent Type Upon Stress-Crazing Activity

The crazing activity of Type II salts was tested in a variety of solvents and the mechanical aspects are briefly described in this section (the morphology of crazes is described in Section 4.2.4). The results shown in Fig. 5.3 refer to nylon 66 (ASTM D638 Type I) specimens strained using a crosshead speed of 50mm min^{-1} in the presence of saturated lithium iodide in solvents shown in Table 5.1. The results for the highly active methanolic solution are not included in Fig. 5.3 because of the complications resulting from hydrogen iodide and iodine production.

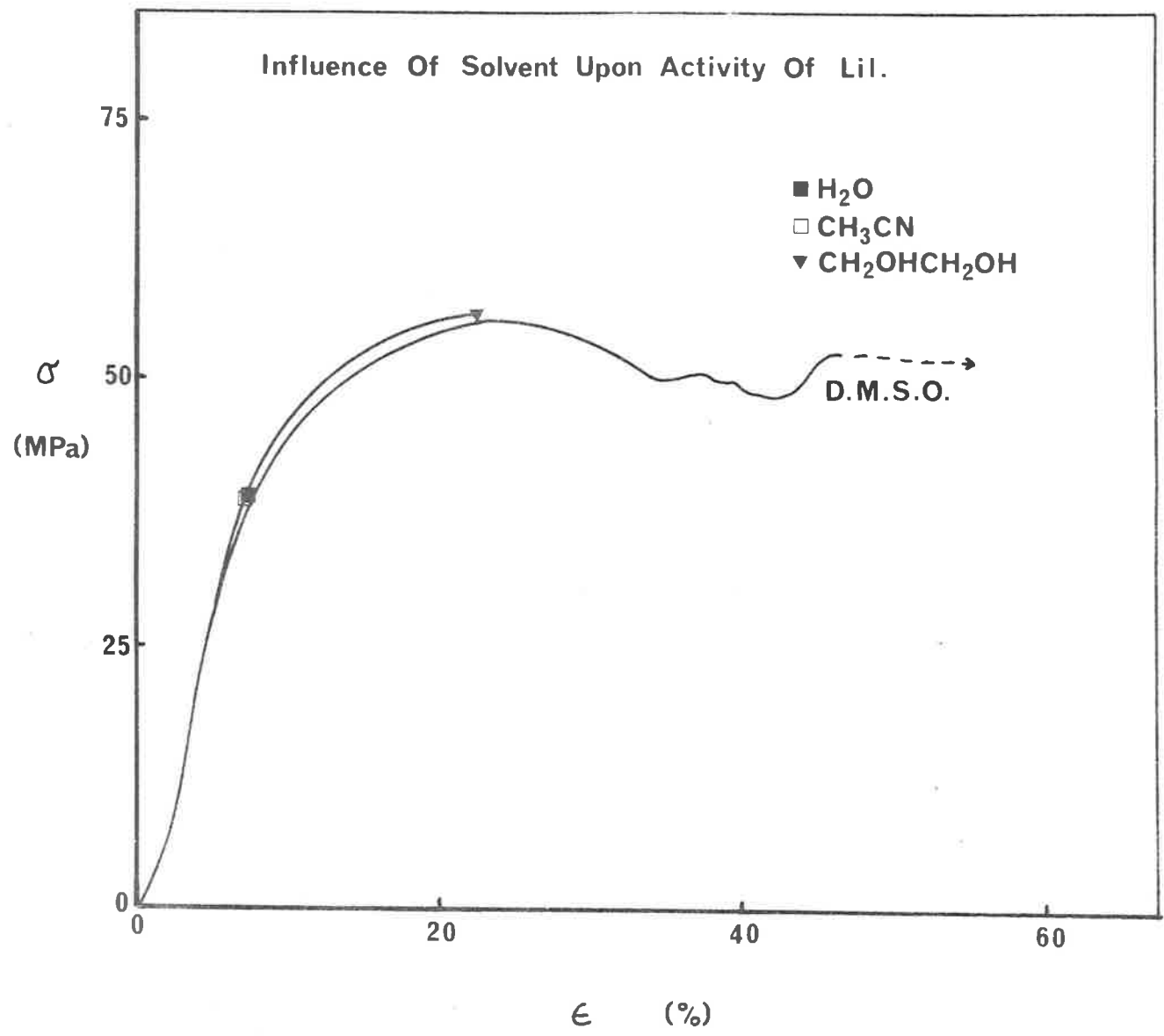
Solvent
water
methyl alcohol
methyl cyanide
1,2 dihydroxyethane
dimethyl sulphoxide (DMSO)

Table 5.1.

The results show that lithium iodide in methyl cyanide is very active, but is less active in DMSO and 1,2 dihydroxyethane. When water, methanol or methyl cyanide are solvents low stresses are required for craze initiation and subsequent craze and crack propagation are rapid. They can all interact with hydrogen bonds and possess a small molecular size.

Dimethyl sulphoxide (DMSO) and 1,2 dihydroxyethane are both good ligands for cations, which may inhibit

Fig. 5.3. Tensile behaviour of nylon 66 tested in the presence of lithium iodide and a variety of solvents.



the crazing activity of the lithium iodide. As DMSO is a dipolar aprotic solvent, iodide ions are not solvated and so would potentially be able to bind strongly to the amide moiety. The inactivity of lithium iodide in DMSO might suggest that cations, rather than anions have the more dominant role in the crazing process. A lithium-DMSO complex is aprotic and so is unable to hydrogen bond to the amide oxygen, with the result that weaker interactions arise (secondary forces which are possible are too weak to disrupt the secondary structure of the nylon). Bidentate liganding of the 1,2 dihydroxyethane with lithium cations may produce large aggregates in which only a low concentration of actively modified protons can arise, compared with hydrated lithium ions. In addition, their size would make penetration into the polymer matrix more difficult than water and methyl alcohol. The reduced rate of uptake of agents with large solvent molecules into the nylon matrix is probably the rate determining factor for craze initiation.

5.1.4. Stress-Crazing Activity of Metal Salts with Polar Polymers

In addition to the detailed study of stress-crazing in nylon 6 and nylon 66, tests were also performed to determine the activity of both Type I and II salts upon the activity of other polar polymers. If, as occurs for these nylons, secondary bonds are disrupted in other polar polymers, crazing may be observed.

Small test-pieces of each polymer were strained very slowly in the presence of the agent, under a stereomicroscope. For the purposes of this qualitative work, activity is indicated using the following simplified index.

- ++ indicates extensive craze and/or crack development, usually at low strains,
- + indicates some evidence of craze formation or swelling,
- indicates no visible effect under the conditions of the test.

A blank indicates that no test was performed.

The results of the tests are summarised in Table 5.2., and a brief description for each type of polymer follows. Where polymers were found to be resistant to both zinc chloride and lithium iodide solutions (which are active Type I and II agents for nylons 6 and 66) no further testing was considered justified.

Polyurethane

The susceptibility of polyurethanes to environmental stress-crazing merited investigation because they are known [135] to form inter-molecular hydrogen bonds between urethane

Polymer	salt =	Type I Agent					Type II Agent			
		-	ZnCl ₂	CoCl ₂	ZnCl ₂	CoCl ₂	LiI	LiBr	Mg(ClO ₄) ₂	LiI
		solvent = water	water	water	CH ₃ OH	CH ₃ OH	water	water	water	CH ₃ OH
Nylon 6	-	++	+	++	++	++	++	++	++	++
66	-	++	+	++	++	++	++	++	++	++
11	-	-					-			
12	-	+?								
Trogamid T.	-	+?					+?			
Polyurethane	-	-					-			
Cellulose Nitrate	-	-								
Cellulose Acetate Butyrate	-	-						-		
Cellophane	+(swell)	+						-	++	
Cellulose Acetate	-	+	-	+			+	+	+	-
Silk	-	++					++			

TABLE 5.2.

groups and so could be vulnerable to disruption of these bonds under conditions similar to those which promote crazing in polyamides.

The sample tested showed mechanical behaviour intermediate between a rubber and a hard thermoplastic, and did not stress craze in the presence of either agent.

Cellulose Derivatives

The susceptibility of four cellulosic polymers towards agent-induced crazing was determined. Cellulose acetate was unaffected by water, but was found to craze and swell in the presence of zinc and lithium halides, and magnesium perchlorate (Table 5.1). Cellophane was rapidly swollen by water and mechanical results could not therefore be interpreted directly in terms of salt activity. Morphological results for cellophane and cellulose acetate are provided in Section 4.2.4.

The tensile behaviour of both cellulose acetate butyrate and cellulose nitrate was uninfluenced by water or salt solutions. It is not possible to determine why the four cellulosic polymers show such wide variance in their susceptibility towards crazing, although there is some correlation to water uptake levels (discussed later in this section). Solvent and salt both need to be absorbed before crazes can initiate, and the resistant cellulose derivatives appeared (from X-ray analysis) not to absorb agent. The uptake of aqueous solutions in cellulose derivatives will be generally retarded by the presence of plasticisers (such as camphor) necessary for commercial use.

Polyamides

The range of polyamides tested was extended by using nylon 11, nylon 12, and a terephthalic acid - N-alkylated hexamethylene diamene ("Trogamid T", a product of O. Bayer, Ltd.). Nylon 11 was found to be resistant to both zinc chloride and lithium iodide, but there was some evidence of agent induced crazing in the fracture surface of nylon 12. These two polymers contained a high hydrophobic content and consequently only absorb relatively low levels of hydroxylic solvents so that modification by the polar agents is not expected. It was found that although the yield stress was not markedly affected by the agent, it appears that from analysis of the fracture surface limited agent-induced crazing had preceded fracture.

Silk

Silk was shown by Barmby and King [136] to dissolve without chemical degradation in arsenic and antimony trichlorides in much the same way as nylons and so was chosen as a naturally occurring polyamide for testing with Type I and II salts. Fracture was found to occur in the presence of either salt type at stresses well below σ_y .

Quantitative Results

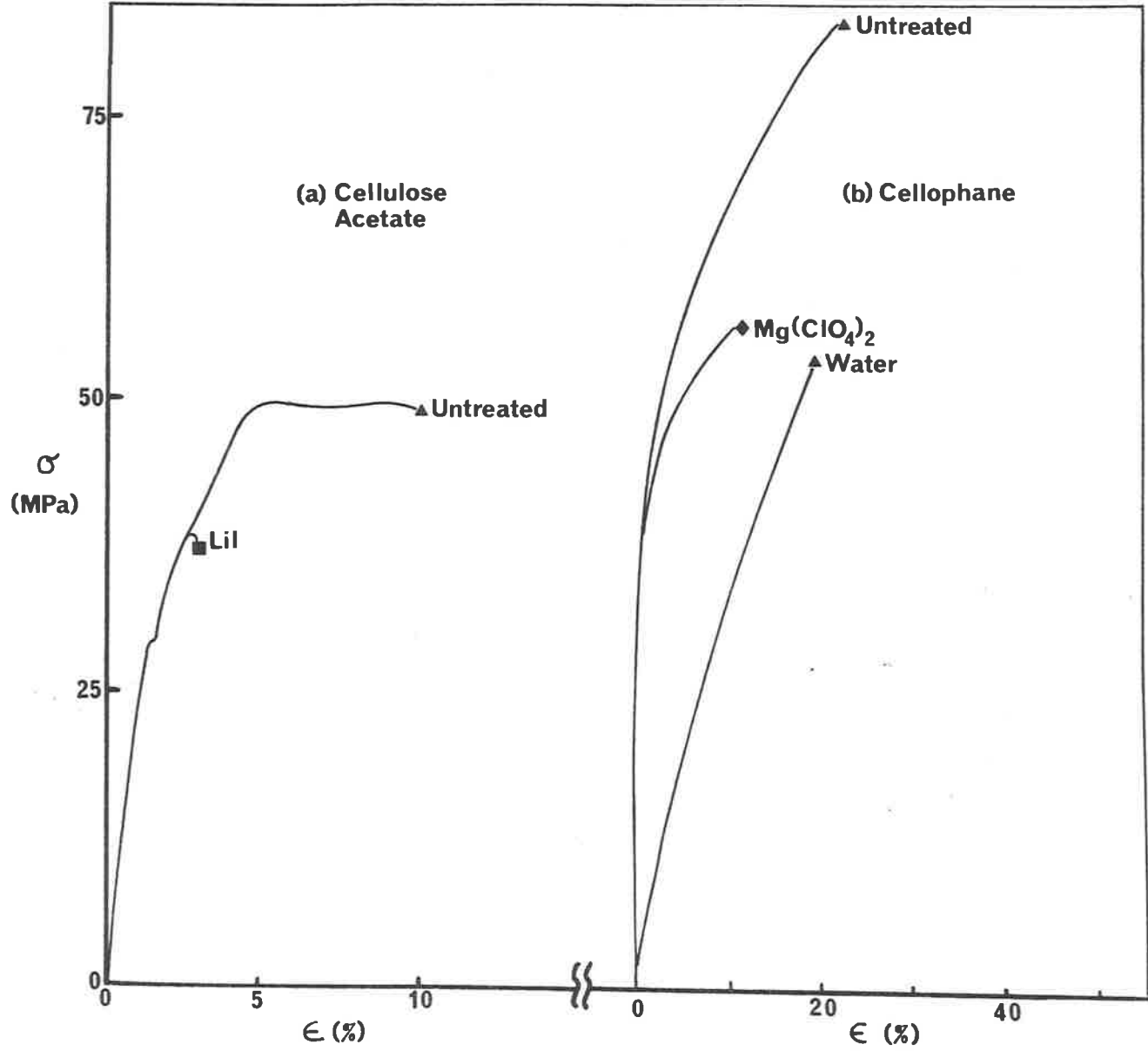
Preliminary studies of the stress-crazing activity of salt solutions with a variety of polar polymers were conducted. Although not enough information has been obtained to make any generalisations, there is evidence that certain cellulose-derived polymers, and polymers containing amide groups (such as proteins) stress-craze in the presence of some salt solutions.

The tensile results for cellulose acetate which has been strained using a crosshead speed of 0.05 cm/min. in the absence and presence of lithium iodide is shown in Fig.

5.4.(a). Fracture at low elongation and stress observed at the low strain rate was accompanied by swelling of the polymer in the treated zone, and small crazes at the treated-untreated boundary. When water only was used instead of lithium bromide, no swelling was observed under similar test conditions. The mechanism of crazing appears from morphological evidence to be similar to that operating in polyamides.

Some tensile tests were performed with cellophane film (regenerated cellulose). The results given in Fig. 5.4.(b) indicate that water has a dominant effect, causing swelling and premature failure of the film. Most salts have only a minor effect and is generally insignificant by comparison. However, cellophane was found to fracture at a lower strain when magnesium perchlorate was present, although the stress reached was similar to when water alone was present. The reason for the activity of this particular salt (compared with other salts) to cellophane, is unclear.

- Fig. 5.4.a. Tensile behaviour of cellulose acetate
in absence and presence of lithium iodide.
- b. Tensile behaviour of cellophane untreated
and with water, salt solutions.



It is appropriate to discuss two aspects of e.s.c. in polar polymers. First, the influence of water (or other hydroxylic solvent) content upon the mechanical behaviour of nylons is relevant, for a variety of reasons. Changes in the tensile and dynamic mechanical behaviour are related to the amount of water present, and the temperature and orientation of the polymer. Secondly, the capacity of all polymers to take up water above a certain critical level appears to determine whether the polymer will craze when aqueous agents are present, and may have a fundamental significance.

Nylons

From the considerable volume of literature which exists concerning the effect of water upon nylons, there are two observations which appear to be beyond dispute. The first is that for nylons having 6 or less methylene groups between each amide moiety, water is taken up in two ways [137-139]. Starkweather [137] showed from sorption isotherms that the first water molecules bound to nylon 66 in a different way to those absorbed near saturation. Similar experiments, supplemented by nuclear magnetic resonance data, led Kawasaki and Sekita [138] to consider that water in nylon 6 with a moisture content of less than 2% by weight, was tightly bound, but at moisture content above 4% mobile water molecules were contained within the polymer matrix. Puffr and Sebenda [75] found using isotherms for both amorphous and crystalline nylons as well as model low molecular weight amides, that those nylons with two to six methylene segments between polar groups could accommodate three water molecules

in accessible regions for each pair of amide segments (one water bound "hard" to two carbonyl oxygen atoms, and two "loose" water molecules binding to amine hydrogens as well as carbonyl oxygens).

The second observation is that water absorption in all nylons causes the appearance of a β relaxation peak for many nylons at approximately -60°C (frequency = 1Hz [132,139,140]. The peak increases as the mole ratio of water to amide unit increases from zero to 0.5, but remains unchanged at higher levels of moisture [140]. The peak is believed to be a result strengthening of interamide bonds when water is present, but unambiguous interpretation was hindered by the presence of significant levels ($\sim 10\%$ w/w) of low molecular weight amides in the samples under investigation [139]. Migasaka [140] observed that at temperatures less than -60°C , water increases the activation energy for the $\gamma \rightarrow \alpha$ crystallographic transition in nylon 6, by binding to the amide groups and acting as a "cohesive agent". In contrast, at temperatures higher than -60°C , water facilitates the $\gamma \rightarrow \alpha$ transition. It appears that there is some correlation between the temperature at which this inversion occurs and the β relaxation process. Starkweather [132] relates the lower modulus of nylons with high moisture contents with a shift in the α peak, which for nylon 66 decreases from 60° in the dry, oriented state, to 50°C at 50% relative humidity, to -5°C at saturation. The binding mechanism is similar to that proposed by Puffr and Sebenda [75], with water molecules "fixed" at temperatures less than the α transition temperature, but

labile above. The significance of the β relaxation is not elaborated upon. Starkweather [141] also reported that as the density and crystallinity of nylons increased, the amount of "accessible" regions decreased, resulting in lower water absorption. This concept of accessible regions is relevant to the changing molecular texture of nylons prior to and during the craze process.

A mechanism which explains crazing in nylons is only satisfactory if it can be used with some validity with other polymers. It was mentioned in Chapter 2 that for polar polymers the prediction of crazing and cracking was less certain than for non-polar polymers, and that a number of factors had a bearing upon the solubility parameter. At the present stage the concepts of hydrogen bonding parameters and solvation abilities are at a primitive stage of development and whilst useful, are only qualitatively successful. For example, the explanation of crazing and cracking in PMMA, PVC and polysulphone by Vincent and Raha [110] places emphasis upon hydrogen bonding between polymer and solvent. In PVC it is necessary to assume that the hydrogen α to the chlorine atom was behaving as a proton donor - a tenuous basis upon which to establish a mechanism.

A simple and perhaps naive exercise is to relate the capacity of all the polar polymers under investigation to take up water, with their vulnerability to stress-crazing with aqueous salt solutions. The pattern which emerges from Table 5.3 is that polymers which can absorb more than approximately 2% water appear to be more susceptible to crazing and cracking than those which take up less. When it is

remembered that the first 2% of water is tightly bound, it seems that it is a fundamental requirement for solvent to behave as a labile carrier for the salt within the polymer matrix, as well as an active participant in the modification of the secondary forces between the polymer chains. If the solvent were simply an inert, non-participating carrier of ions, then no changes in the crazing activity of salts would be expected as the nature of the solvent is changed. Instead, it is clear that by suitable selection of solvent, the activity of the salt may be enhanced or reduced. The fundamental properties of the solvent which determine their influence upon crazing remain to be identified.

Further amplification of the proposed mechanism of the role of the solvent in crazing is more appropriately given in Chapter 6.

Polymer	Water Uptake	E.S.C.?
Nylon 6	11	✓
Nylon 66	8	✓
Nylon 11	2	x
Nylon 12	2	✓?
Trogamid T ^R	3	✓?
Polyurethane	0.6	-
Cellulose Nitrate	0.6	-
Cellulose Acetate	1 - 3	✓?
Cellulose Acetate Butyrate	0.9 - 2.4	x
Cellophane	High	✓
Silk	11 at 65% RH.	✓

TABLE 5.3.

5.2. Chemical Analysis using Energy-Dispersive X-rays

As mentioned in Chapter 3.3.3, energy-dispersive X-ray analysis is a powerful and convenient technique for the correlation of specimen surface morphology with elemental analysis.

The approach followed in this study has been to determine the absorption characteristics of zinc chloride in unstressed nylon 6 and 66 (Chapter 5.2.1). These results have then been examined and considered relevant to the early uptake processes which occur in stressed nylon films. The distribution of cations in fracture surfaces of nylons crazed with either Type I or II salts is then determined (Chapter 5.2.2), from which significant differences in the mechanism of stress-crazing can be identified.

5.2.1. Energy Dispersive X-ray Analysis of Unstressed Nylon Films

Long-term absorption of zinc chloride was examined in nylon 6 and 66 using samples of different thicknesses. The morphology and dimensions of the zinc-rich zones for each sample were essentially identical so only one need be described in detail.

In addition, a study of the influence of time and salt concentration upon the zinc uptake in unstressed nylon 6 films was also made.

Long-term Absorption

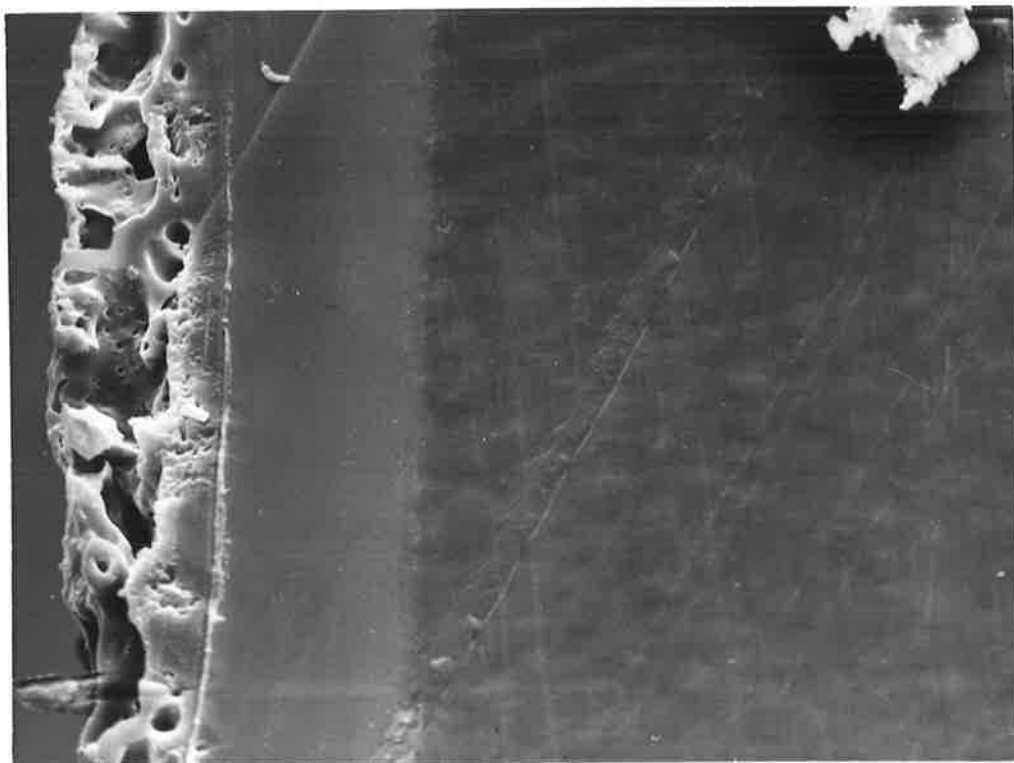
Nylon 6 and 66 samples were immersed in 5M zinc chloride solutions for 28 days and were then washed briefly in water and allowed to dry. Each specimen was cut with a sharp blade, and mounted on S.E.M. stubs so that the cross-section could be seen.

During the wash with distilled water, a white opaque layer was produced which was observed in the S.E.M. It is a porous, zinc-rich material, and is the result of interaction between the zinc chloride-nylon mixture and water. This can be recognised in Fig. 5.6, as the highly porous outer layer. The composition of this zone is uncertain, but presumably some insoluble zinc oxide is present in the layer.

The second, featureless region (pale), is shown by X-ray analysis to also have high levels of zinc chloride. The zinc distribution is shown in Fig. 5.7 to be confined to the outer two zones. At higher resolution it was shown that the zinc chloride concentration was highest in the non-

Fig. 5.6. Cross-section of nylon 6 showing three distinct regions. Only the dark region at right is zinc-deficient.
Magn. = 650x

Fig. 5.7. Corresponding X-ray map. Same magnification as Fig. 5.6.



porous zone, but the outermost porous zone would have a lower overall density, and hence the X-ray emission per unit area will be lower.

The third region (to the right in Fig. 5.6), corresponds to the unaffected central core of the polymer. A line scan for zinc indicates that there is a very abrupt fall-off in zinc levels across the boundary from the zinc-rich zones to the central core.

In the case of zinc chloride absorption by unstressed nylons it appears that Case II uptake [99] is occurring. Case II transport in amorphous polymers is associated with conditions of high penetrant activity, and with temperatures well below the glass transition of the polymer. In polystyrene it was found that there was a linear increase in the weight gain of the polymer with time, and that a sharp boundary existed between an outer, swollen shell of uniform concentration, and an inner core having no penetrant. (Fickian diffusion, which precedes this "relaxation controlled uptake" is often hard to detect because the concentrations attributed to this mechanism are very small by comparison.)

The requirements of a penetrant of high activity, and of temperatures below T_g , are met; a uniform concentration is present in the zinc-rich zone, and a sudden decrease to negligible levels in the central core is observed. No experiments have been performed to confirm the relationship between weight gain and time, or to measure the velocity of the advancement of the boundary, however.

Samples of nylon 6 and 66 which were treated under the same conditions were shown by S.E.M. to have zinc-rich zones

of the same thickness, suggesting that the mechanism of uptake of zinc chloride by each polymer type is similar. By measuring the thickness of the specimens before and after treatment (using the S.E.M.), and by assuming that the central zone is unswollen, it is possible to estimate the approximate degree of swelling which occurs in the zinc-rich zone. The maximum figure is $\approx 80\%$ in both nylon 6 and 66, but the alteration of the outer zone subsequent to washing must be taken into account. This may contribute, say 25%; nevertheless, substantial swelling has occurred in the zinc-rich regions of the polymer.

From the essentially morphological study carried out, it is not possible to predict the molecular changes occurring in the polymer, but one might surmise that the increase in the volume of the zinc-rich zone is caused by chain separation as the zinc chloride and solvent are interspersed between polyamide chain segments.

Uptake of Zinc Ions in Unstressed Nylon 6 Films

Small strips of "as received" nylon 6 film (0.04mm thick) were immersed in 1.0 and 3.0M aqueous zinc chloride for 0.5, 2.25 and 18.0 hrs. at room temperature. Each strip was washed, dried and examined in the S.E.M. as described previously. It was necessary to use magnifications greater than 1000X, and this caused difficulties in obtaining clear results. Problems inherent in the observation of the edges of these poorly conducting films were charging, poor resolution and contrast. When high voltages and low condenser currents were used (to enable X-ray analysis) specimen damage also occurred.

By direct observation and from X-ray maps, only low levels of zinc could be detected in all specimens, and distinctive zinc-rich zones (which were present in specimens exposed to 5M zinc chloride for long periods of time) were absent. A representative surface (nylon 6 soaked in 3M zinc chloride for 18 hours) is shown in Fig. 5.8.

Line scans (as described in Chapter 3) were used as well as X-ray maps, because they proved under these conditions to be more sensitive. Scans for zinc are shown for each sample in Fig. 5.9. Low levels were found for all but one sample which contained moderate levels at the left hand edge (shown in Fig. 5.8). A line scan is also shown for a nylon 6 specimen treated with 5M zinc chloride for 28 days.

From these results it appears that uptake of even concentrated zinc chloride solutions is relatively slow in unstressed nylons. When long exposure times and 5M zinc chloride are used, however, extensive uptake can occur, giving rise to a sharply defined, dilated, zinc-rich phase ("Case II Transport"). When washed with water, the zinc chloride-nylon outer layer precipitates (with opaque zinc oxide production) to give a highly voided, amorphous complex. This material is similar to that observed in many stress-crazing experiments. The exposure times in the latter experiments are very small, so that the presence of complex indicates that during stress-crazing, uptake of salt into the nylon is accelerated. Proposed mechanisms for stress-crazing must take this into account. Further studies of the levels of salt in stressed nylon films are given in Section 5.

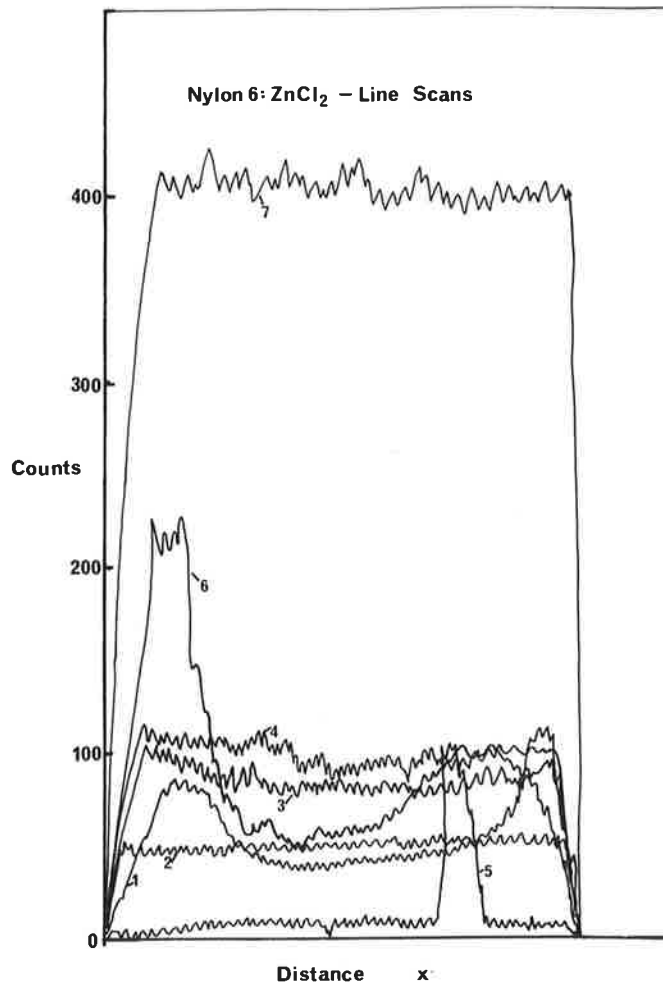
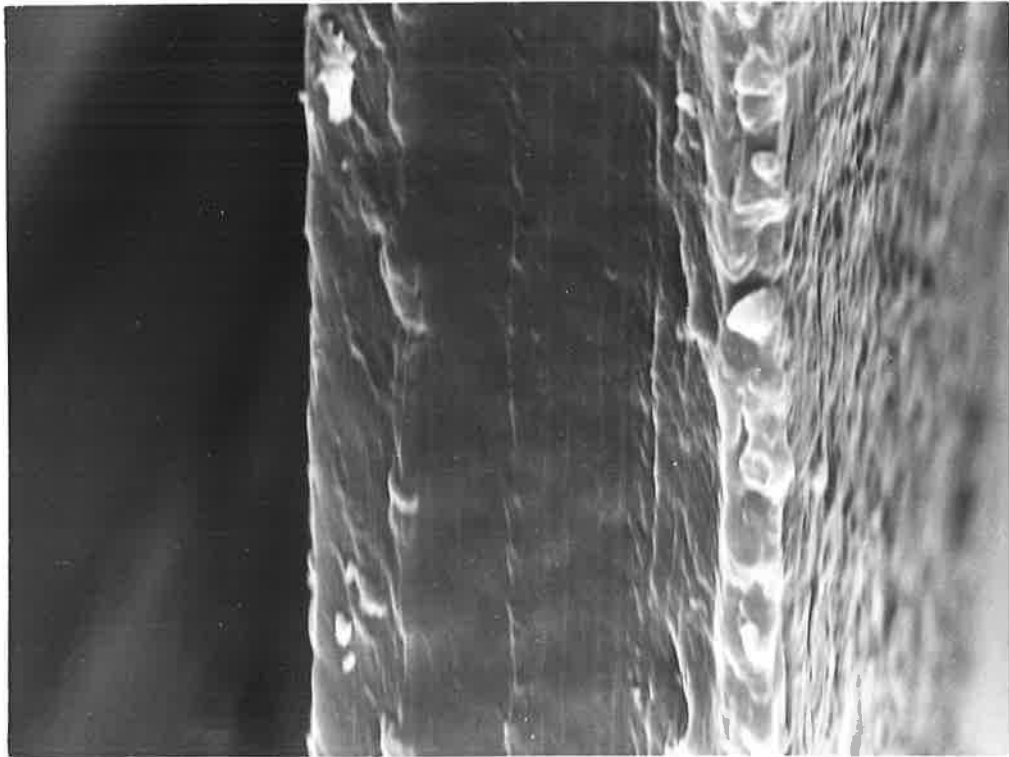
Fig. 5.8. Nylon 6 film immersed in 3M zinc chloride solution for 18 hrs; low levels of zinc were detected, except at edge.
Magn. = 2,670x

Fig. 5.9. Line scans recorded for a number of nylon films immersed in zinc chloride solutions.

1.0M $ZnCl_2$ treatment for 0.5, 2.25, 18.0h are numbered 1, 2, 3 respectively.

3.0M " " " " " " " 4, 5, 6 respectively.

5.0M $ZnCl_2$ treatment for >100h is numbered 7.



5.2.2. The Distribution of Cations in Stress-Crazed Nylons

The morphology of fracture surfaces produced from stress-crazed nylons has been described in detail in Chapter 4. In this section the distribution of stress-crazing agent will be discussed, and will be shown to be in accord with the general mechanism of environmental stress-crazing proposed for nylons.

It was considered necessary only to select a few examples from the vast number of samples obtained, to illustrate the mechanism proposed. Many more samples were examined using energy dispersive X-ray analysis (henceforth abbreviated to X-ray analysis), and the results of all measurements have been considered when making any generalisations.

One problem is the possibility of misleading results, caused by the mechanical transfer of agent during the rupture, rather than the craze-formation and growth process. As well, washing the specimens with distilled water before coating with gold in preparation for scanning electron microscopy can lead to fallacious conclusions. From experience, it is often possible to determine when these spurious alterations have occurred, and where possible, unwashed and washed fracture faces can be compared.

In this section the analysis of ASTM type 1 nylon 66 specimens, ultimately fractured in the presence of aqueous lithium iodide and zinc chloride are described. Single line scans and X-ray maps are given which correspond to each morphological zone (regions 1, 2, 3 and 4 in Chapter 4), for both washed and unwashed specimens.

Type I salts - zinc chloride crazed nylon 66.Washed Specimen

A fracture surface from unnotched anhydrous nylon 66, strained 1 cm/min. in the presence of 5M aqueous zinc chloride, and washed after fracture, is shown in Fig. 5.10. The craze, ductile fracture and brittle fracture regions are readily identifiable. Superimposed upon the photograph is a zinc line-scan, corresponding to the levels of zinc ions across A-A'.

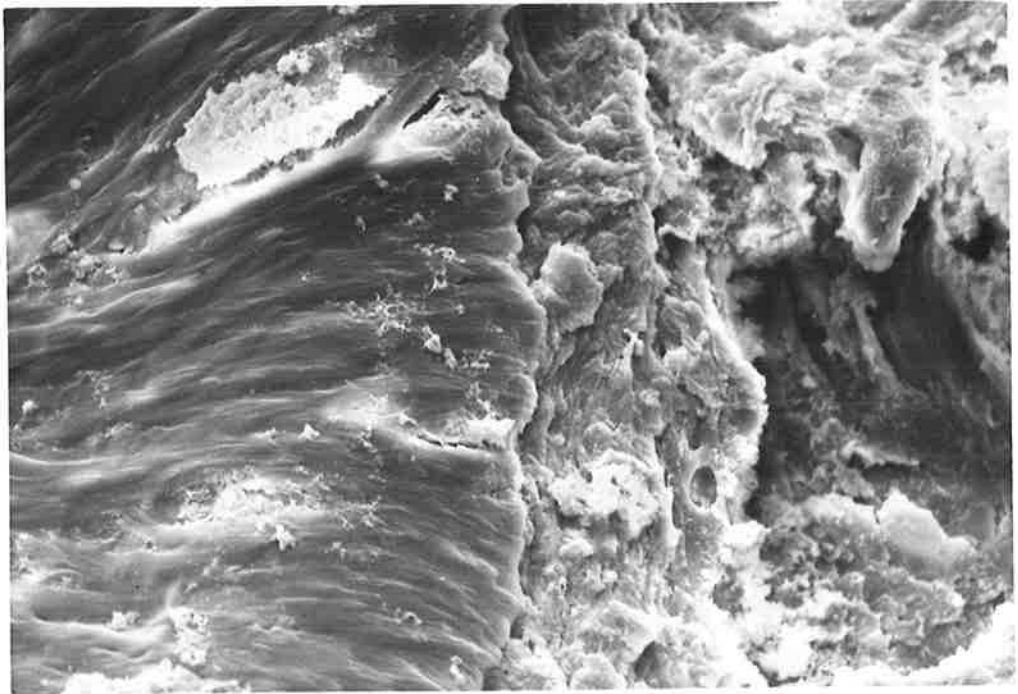
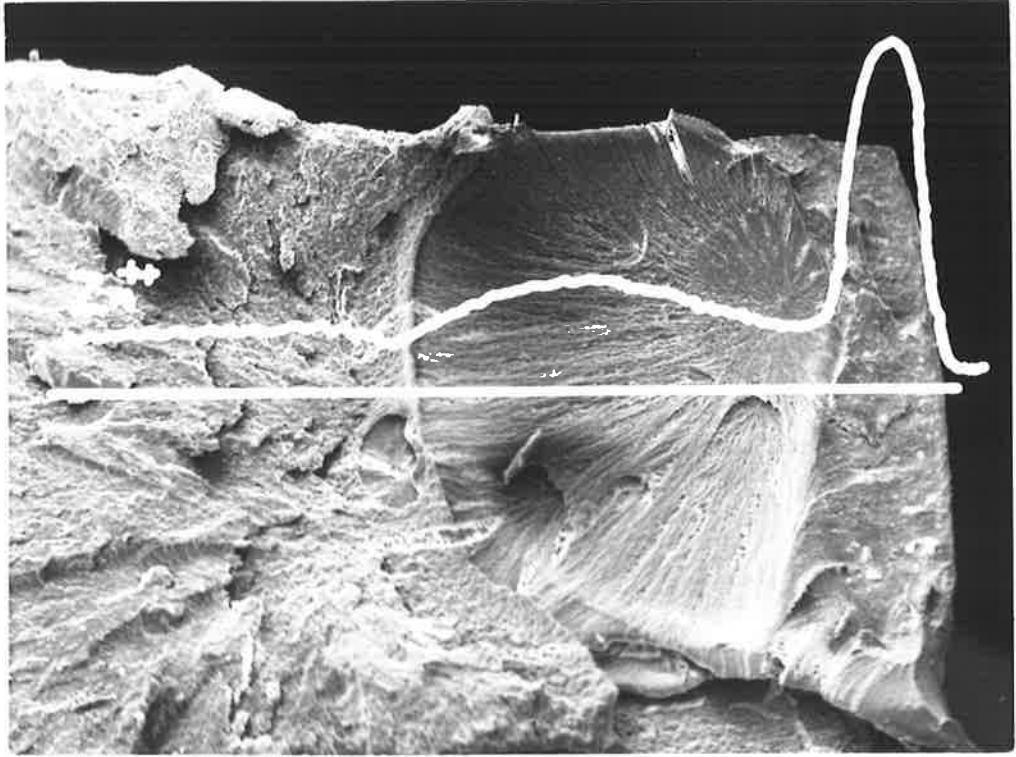
In the craze area (regions 1, 2) there are very high levels of zinc, indicating strong binding to the nylon (the specimen was washed thoroughly in water). However, across the interface between the craze region and the ductile fracture zone (region 3), there is a sharp decrease in the level of zinc ions. Fig. 5.11 shows the abrupt change in morphology from region 2 to region 3, and it is accompanied by a rapid decrease in zinc concentration from right to left. "Maps" of zinc concentration have been produced for each of the regional types, at high magnification; and they confirm the pattern indicated by the line-scans.

The mechanism of crazing in this type of test can be linked with the zinc ion profile.

When high concentrations of zinc are associated directly with the nylon (and so are not washed away with water), then the nylon is able to yield at stresses less than the normal yield stress. As the concentration of zinc diminishes, the modulus of the polymer increases. This results in a change in the mechanical behaviour, from crazing with rapid rupture, to ductile yielding.

Fig. 5.10. Fracture surface of zinc chloride treated, anhydrous nylon 66, with distribution of zinc ions superimposed. (Levels relate to region under straight line.) Magn. = 29x

Fig. 5.11. Abrupt change in morphology from region 2 to region 3 (right to left). The zinc concentration falls rapidly across the boundary. Magn. = 225x



Unwashed Specimen

When the corresponding, unwashed fracture face is analysed for zinc, it is discovered that large amounts have carried over into the ductile and brittle zones (regions 3 and 4). Fig. 5.12 gives the zinc "profile" across the centre of the specimen, and indicates that the level of zinc in region 3 is comparable to that in the craze region. This is confirmed by the corresponding X-ray map which shows a uniform distribution of zinc over most of the area.

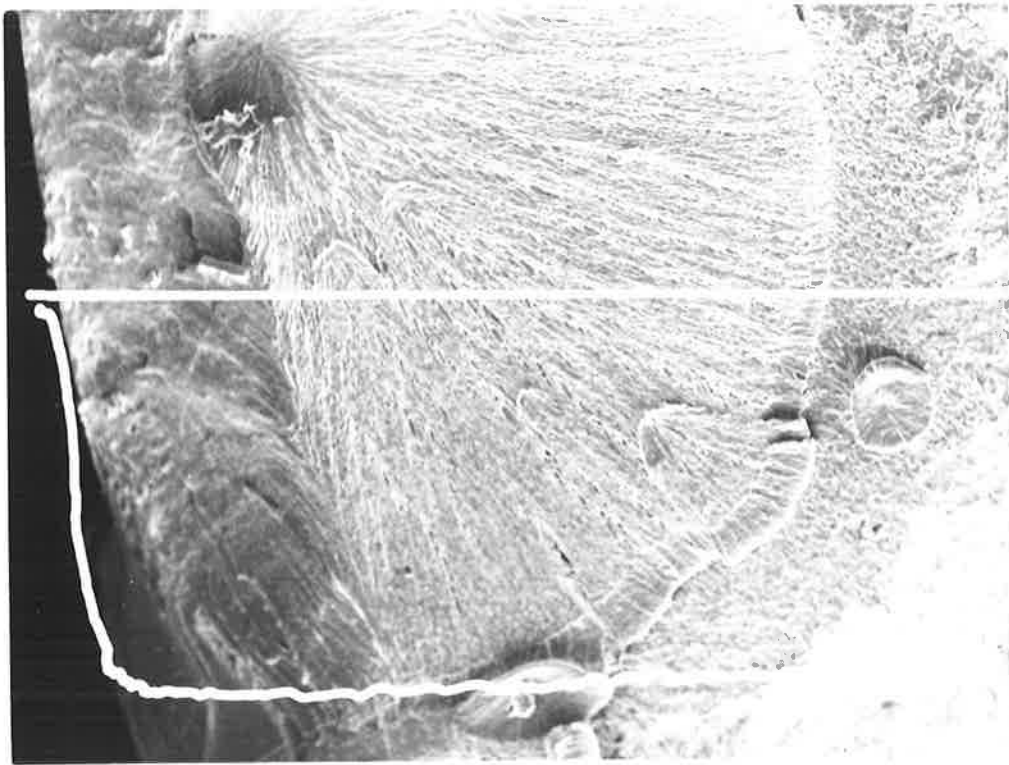
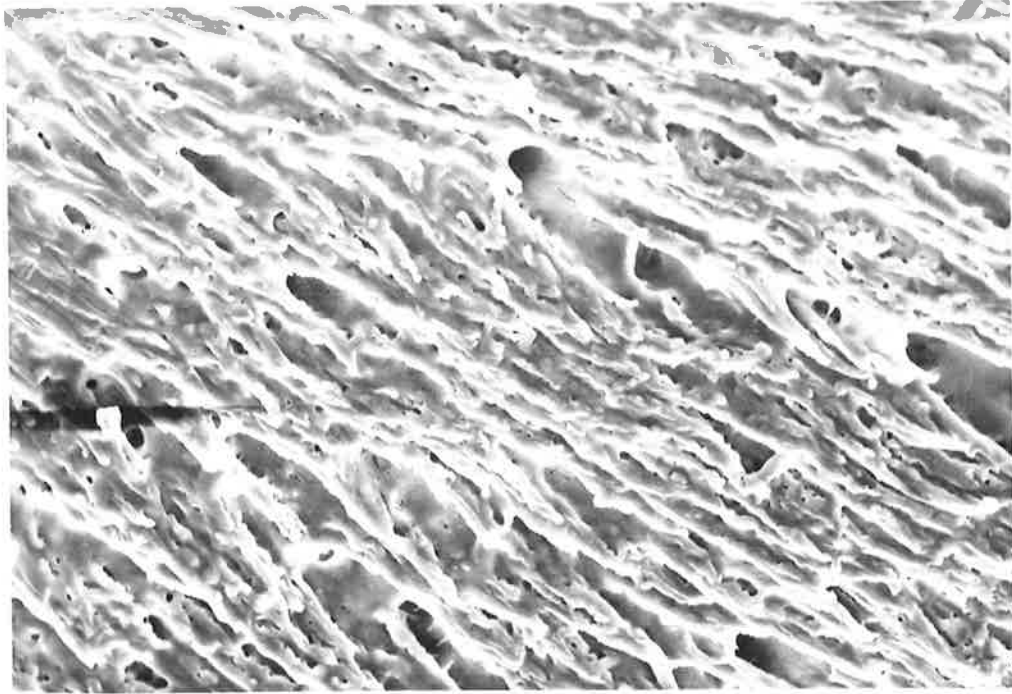
The involvement of the zinc chloride solution appears to be two-fold. During the crazing process, zinc binds strongly to the nylon and remains fixed during subsequent washing with water. During fracture of the specimen, the solution will follow close to the crack front, lowering the free surface energy and so facilitating fracture. In this case, the zinc is not binding directly to the nylon, but is left as a residue on the fracture surface. The unbound zinc chloride is therefore easily washed from the surface with distilled water. (Uptake of zinc chloride into the nylon in region 3 would be very slow, even when high levels of zinc remain, because of the nylon being highly oriented (Fig. 5.13).

Type II salts - Lithium iodide crazed nylon 66.Washed Specimen

A Hounsfield nylon 66 test-piece was preconditioned by boiling it in distilled water for 3 hrs. before testing. The dried specimen was strained at room temperature at 1.0 cm/min., in the presence of a drop of saturated aqueous lithium iodide, applied at the edge. Extensive crazing occurred at low stresses; rapid crack growth beginning at

Fig. 5.12. Unwashed fracture surface of zinc chloride treated nylon 66, with zinc line scan superimposed. Salt has been carried over into region 3. Magn. = 46x

Fig. 5.13. Highly oriented morphology of region 3 of above specimen. Magn. = 375x



the treated region occurred across most of the specimen. When the supply of agent was exhausted, ductile failure occurred before complete fracture of the specimen. In contrast to the tensile test using anhydrous nylon 66 and zinc chloride, in this test there was extensive participation of the agent in the complete fracture of the specimen.

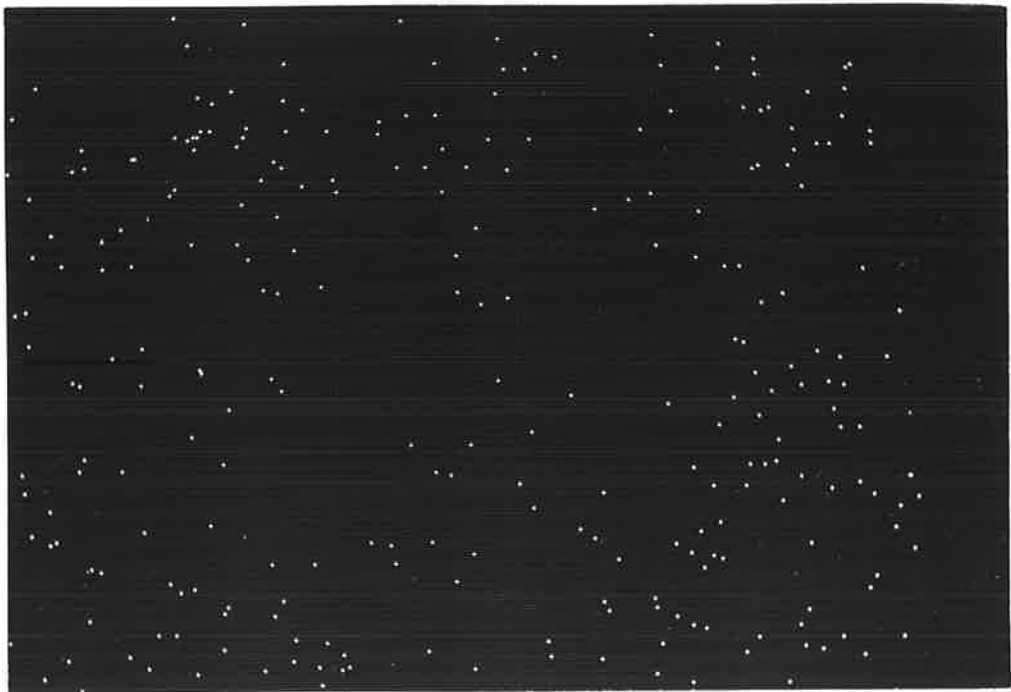
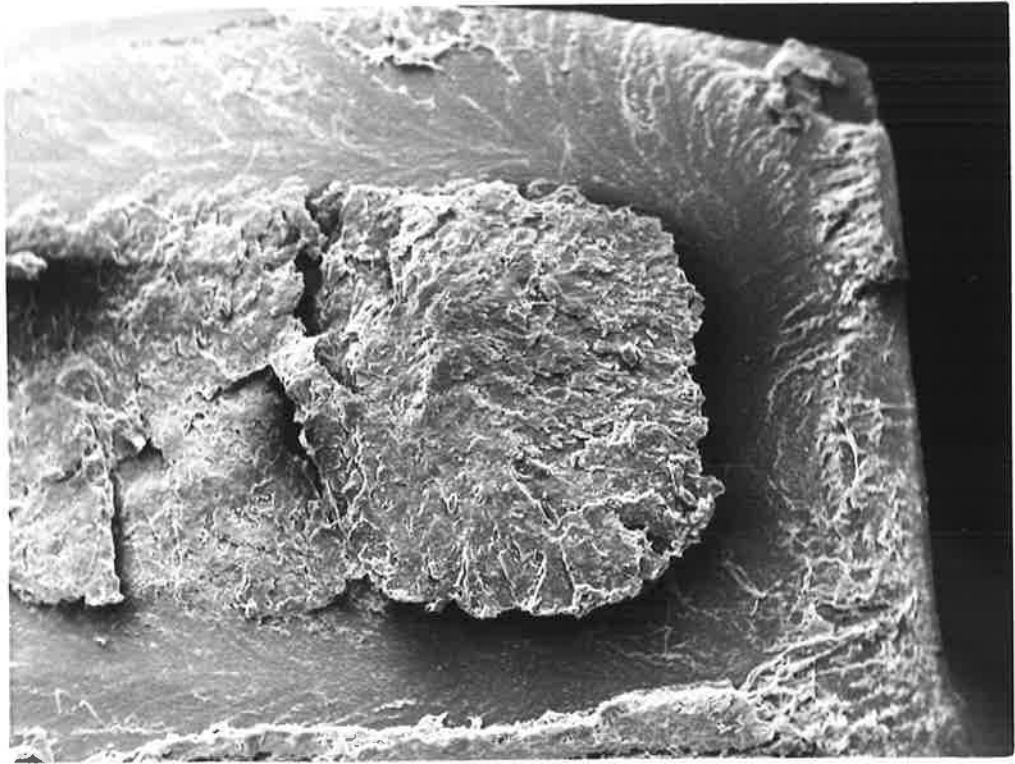
The initiation zone is shown in Fig. 5.14. There is a flat region which extends along the edges of the fracture face, and continues almost to the other end of the specimen. In the centre of the specimen is a rough topology; there has been more extensive deformation before fracture in this region. The two regions correspond to regions 1 and 2 proposed in the general mechanism proposed for stress crazing.

When an X-ray map is produced (discriminating for iodide anions because the atomic mass of lithium is too small), very low levels of iodide are indicated (Fig. 5.15). It appears that when the specimen is washed, the lithium iodide is removed from the fracture face. It is suggested that the lithium iodide is reversibly bonded to the nylon, and this is compatible with the infra-red evidence for hydrogen bonded solvent molecules connecting lithium ions with the nylon. (It is assumed that low levels of iodide ions also indicate low levels of lithium cations.)

X-ray analysis along the fracture face reveals low levels of iodide ions everywhere. The levels of iodine in region 2, near the ductile yield region (region 4) are so low that it is not possible to determine whether any substantial decrease occurs across the interface.

Fig. 5.14. Fracture morphology of lithium iodide treated nylon 66, and subsequently washed with water. Regions 1 and 2. Magn. = 31x

Fig. 5.15. X-ray map showing low levels of iodide ions in fracture surface. Compare with Figs. 5.16,17. Magn. 31x



Unwashed Specimen

High levels of iodide ions were recorded throughout the crazed zone (regions 1, 2). The initiation zone (corresponding to the washed area in Fig. 5.14), with the appropriate X-ray map for iodide ions, is shown in Fig. 5.16, 17. The high density of counts contrasts strongly with the small number obtained for the washed specimen.

High levels of iodide ions were recorded along the fracture surface until the ductile fracture zone (region 3) was reached. A rapid fall-off in counts was observed, indicating that in this unwashed specimen no agent had been carried over. This is expected because much of the lithium iodide solution applied to the testpiece has been carried over a large area of the polymer surface before ductile fracture has occurred. Only a relatively small amount of crazing preceded fracture in the zinc chloride treated nylon 66, so that carry-over of excess agent is much more likely.

The transition from region 2 to 3 is shown in Figs. 5.18, 19 with corresponding line-scans and X-ray map (for iodide ions). There are few counts for both the region at left-centre of the photo, and at the right, where the characteristic ductile fracture morphology is seen. The level of counts for iodide decreases sharply, as was also observed for the washed, zinc chloride treated nylon 66.

Both Type I and Type II stress-crazing agents are implicated in the processes of craze formation and breakdown. It can be concluded from the above observations that in nylons in which water is either absent or present before

Fig. 5.16. Similar specimen to that shown in Fig. 5.14 (lithium iodide treated nylon 66), but unwashed. Regions 1 and 2. Magn. = 29x

Fig. 5.17. X-ray map corresponding to specimen above, indicating high uniform distribution of iodide ions. Experimental conditions for analysis of each specimen were similar. Magn. = 29x

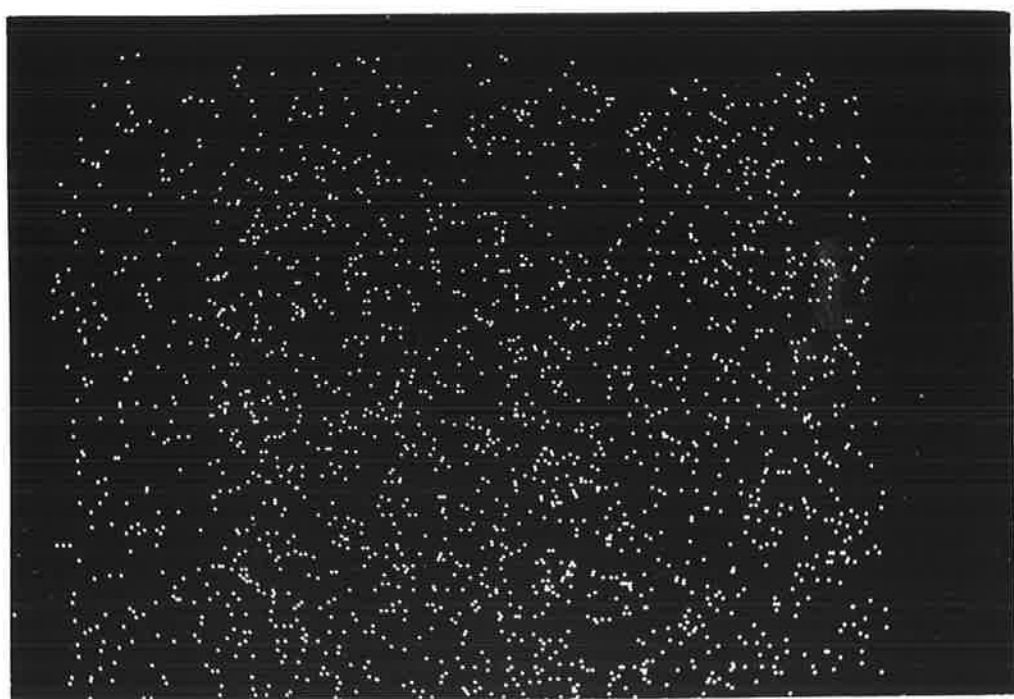
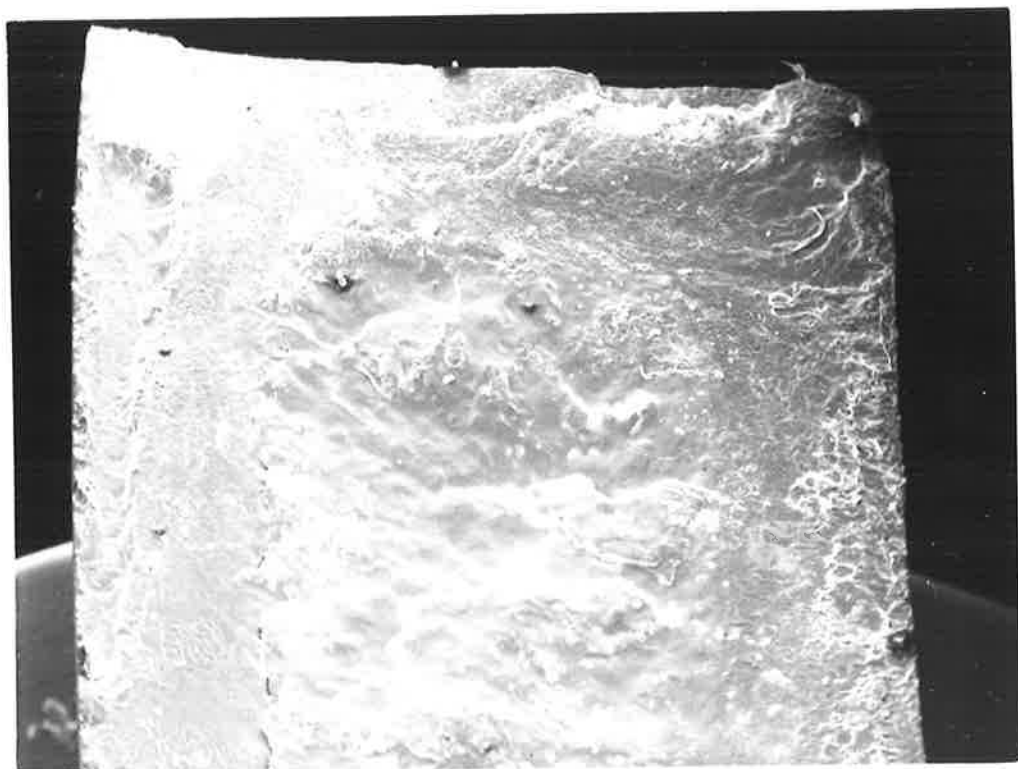
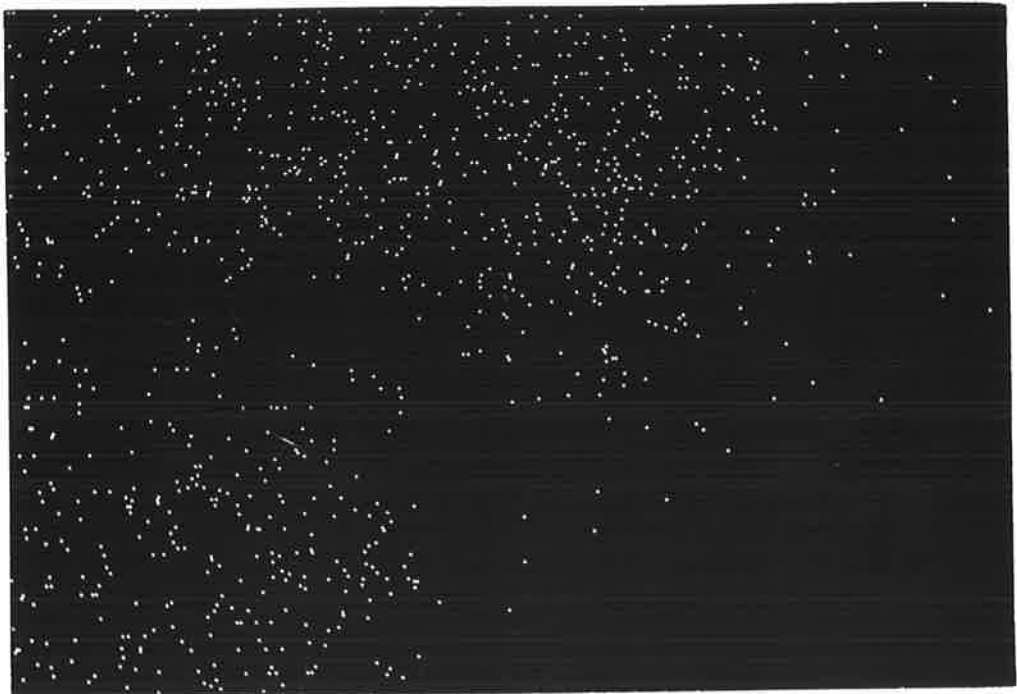
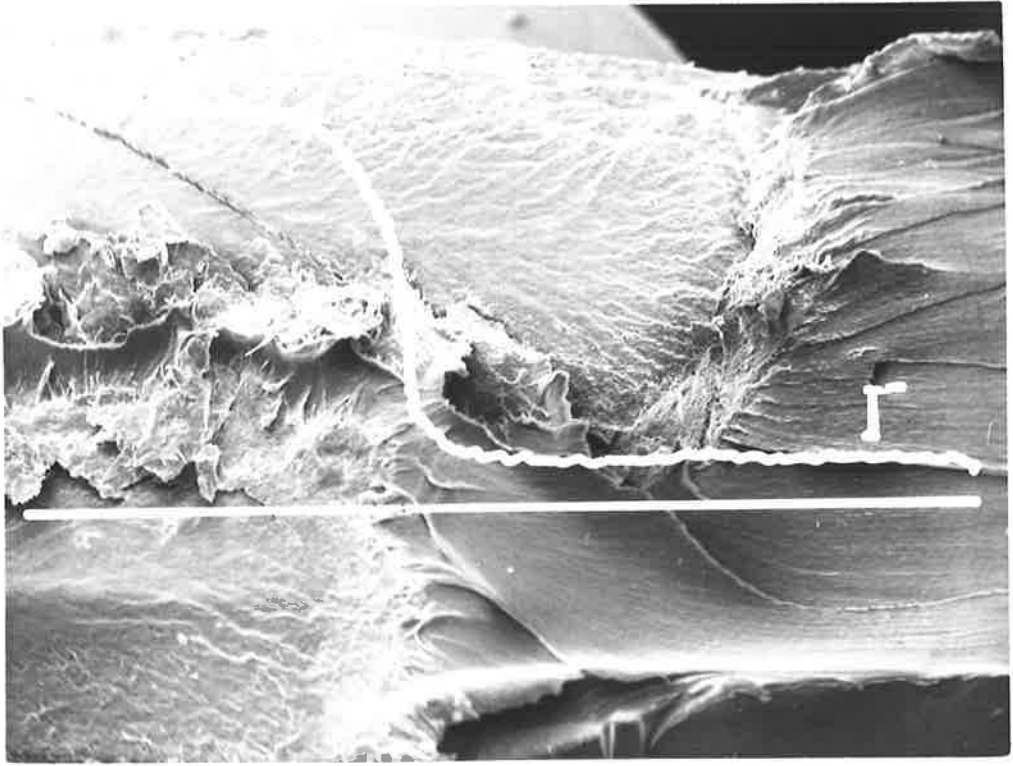


Fig. 5.18. Fracture surface of unwashed nylon 66 specimen treated with lithium iodide. Transition from region 2 to region 3 (left to right) is accompanied by a rapid decline in iodide ions. Magn. = 33x

Fig. 5.19. Corresponding X-ray map showing low levels of iodide ions in region 3. Magn. = 33x



testing, that the agents are not intimately involved in the ductile or brittle fracture processes. The latter processes appear to occur when suitable stress concentrations are reached subsequent to craze formation.

When washed and unwashed specimens are compared, it can be concluded that zinc ions from water-soluble bonds with the nylon, but iodide ions (and so presumably lithium ions) do not. This is in accord with the mechanism of binding suggested from infra-red evidence.

5.3 Solution Studies

5.3.1. The Influence of Salts Upon the Solution

Viscosity of Polyamides

The morphology of salt-induced crazes has been thoroughly described in preceding sections of this thesis and in the review (Chapter 2) reference has been made to the work of Dunn and Sansom [4] and others which provides evidence for the type of interaction which occurs between salt solutions and polar polymers.

Because of their special biological importance, the interactions of biopolymers with salts in aqueous media have been extensively studied, and the current state of development of this complicated subject is revealed in a recent review by Lewin [146]. The study of synthetic polymers with salts has not quite reached the same level of sophistication at present; solution studies of polyamides have been confined largely to determination of physical parameters, such as viscosity-average molecular weight.

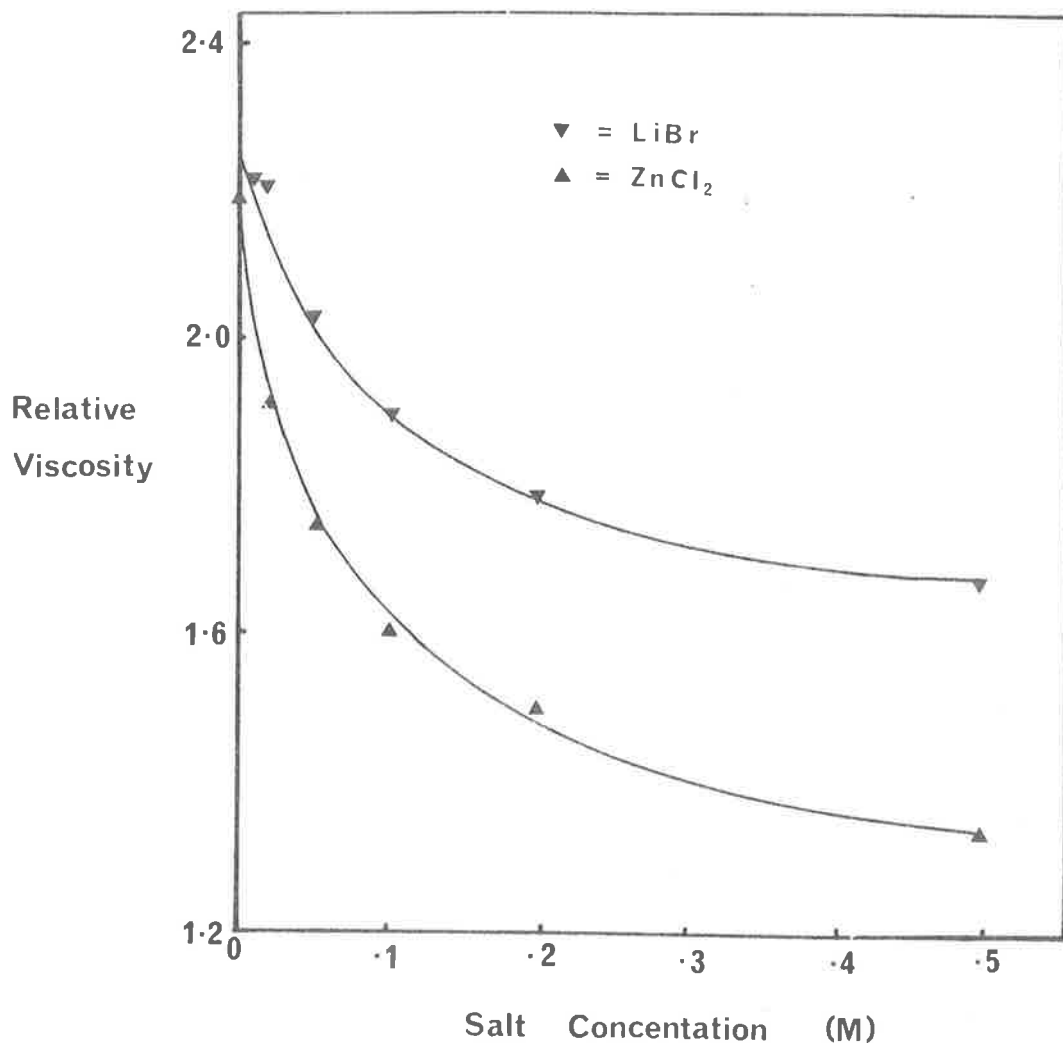
One of the problems which arises in trying to understand salt-polyamide interactions is that experiments need to be confined to a relatively narrow range of solvents. The polyelectrolyte behaviour of polyamides has been measured in formic and sulphuric acid [147,148] and constants have been established for molecular weight determination. Of particular interest were the discoveries that water repressed polyelectrolyte behaviour of nylons in formic acid solution [147] and that for the same molecular weight, branching decreases intrinsic viscosity by forming more compact structures in solution [148].

The effect of added electrolytes to polyamide solutions in formic acid was studied by Saunders [149], and it was found by using refractive index, intrinsic viscosity and light scattering techniques, that polyelectrolyte effects can be swamped when excess potassium chloride is added, making determination of a weight-average molecular weight more reliable. The ionic interamide forces which contribute to the viscosity of charged polyamides in formic acid are suppressed by the counterion effect of the added salt.

When the viscosity of nylons 6 and 66 in aqueous formic acid (90 and 95%w/w respectively) were measured in the presence of type I and II salts, a decrease in the apparent viscosity of the polymer was observed (Fig. 5.20), which is basically in agreement with the results obtained with other salts by Saunders [149]. Although a difference in the viscosity values was obtained between the two salt types (lithium bromide and zinc chloride) it is impossible to substantiate in the media used, whether the difference in binding proposed in the solid state between the salt and polymer persists in solution.

The measurement of solution viscosities of polyamides in m-cresol in the absence and presence of salts should reveal information more amenable to interpretation, as the acidity of m-cresol ($pK = 10.01$ at 25°) is many orders of magnitude less than that of formic acid ($pK = 3.75$ at $20^{\circ}C$) [150].

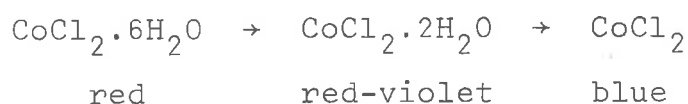
Fig. 5.20. The effect of concentration of lithium bromide and zinc chloride of 0.5% nylon 66 in 90% (w/w) aqueous formic acid.



It was found that no homogeneous mixture of polymer, m-cresol and lithium iodide (or zinc chloride) could be obtained, primarily because of the low solubility of the salt in m-cresol. It appears that no system of solvent, salt and polyamide can be selected which will provide unambiguous information (by viscosity measurement) about the interaction of salts upon polymer proton donor (i.e. another polymer segment or salt-solvent entity) hydrogen bonding. Consequently no further viscometry was undertaken.

5.3.2. Changes in the Nature of Chelates in the Co-ordination Shell of Cobalt Salts

Many hydrated salts of cobalt are pink because of the presence of two or more water molecules surrounding the cation. The colour changes which occur as water molecules are lost from cobalt chloride, for example, are shown in the equation below:



When pale blue anhydrous cobalt chloride is dissolved in methyl alcohol or acetone, for example, deep blue solutions are produced; the cobalt chloride is solvated, but not with water molecules. The color change from pale pink to deep blue is striking, and is often seen when concentrated aqueous cobalt chloride solutions are applied to a nylon which is then strained. The crazed nylon has a blue colour in the treated region, which suggests that a change in the coordination shell of the cobalt has occurred. The hexahydrated cobalt ion transmits at 507nm and 603nm. These wavelengths are in the visible region of the spectrum, so that visible spectrophotometry was used.

The first experiment was to determine what concentration of nonaqueous solvent could, in the presence of water, produce absorption at 663nm. Acetone was chosen as the non-aqueous solvent, because it is miscible with water in all proportions, and because it contained a carbonyl group, which is the active binding group in nylons. Although it

could be suggested that a simple amide would provide a better analogy with polyamides, as a competing solvent, it was not used because of mixing problems, and because it was not considered necessary to limit the results to polyamides. Solutions containing a low concentration of cobalt chloride (usually 0.005M) in acetone: water mixtures ranging in molar percentage of from 0 through to 100% acetone were measured in the spectrophotometer. The appearance of the blue transmission peak was found to occur at a molar % of 57% acetone. The pink peak at 507 nm persists until a molar level of 75% acetone is reached.

It may be concluded from the results, that for cobalt cations which are in the presence of a large excess of both acetone and water, that below 57% acetone, no cobalt ions solvated with less than two water molecules exist, and that above 73% acetone, most cobalt ions are solvated with less than two water molecules.

Quantitative experiments were not undertaken, and the practical problem of assessing relative concentrations of each ion from comparing two peaks of very different magnitude is acknowledged. Nevertheless, it can be concluded from these experiments that:

(a) the binding energies of water and acetone are of the same order. If this were not so reversible exchange of one solvent for the other in the coordination shell would not occur whilst both solvents are in large excess compared with the concentration of the cobalt ion;

(b) the molar ratio of acetone to water which appears to be required for all cobalt ions to be solvated with less

than two water molecules is of the order of 2.5 moles acetone: 1 mole water. This figure is in qualitative agreement with the transformation



Although a characteristic blue colour was always produced during the stress-crazing of nylons with cobalt salts, difficulty was experienced in producing visible spectra. Films of nylon 66 (0.16 mm thick) and nylon 6 (0.025 mm thick) which had been strained the same amount both in the presence and absence of cobalt chloride were compared, but clear and unambiguous results were not obtained. The low absorption by the relatively small amount of cobalt complex, compared with the high absorption of light by the nylon film, lead to differences in substrate absorptions masking the expected results.

CHAPTER 6DISCUSSION

Despite the widespread acceptance of crazing as an important mode of deformation in glassy polymers and the extensive research (as reviewed in Chapter 2) carried out to investigate crazes, much controversy remains concerning the molecular processes involved.

In this study of the rather novel crazing of polyamides induced by inorganic or ionic agents, the objective was to show that craze formation occurs in semicrystalline polar polymers (particularly nylon) and that it is a necessary precursor to polymer rupture. It was hoped that by extensive investigation of the morphology of such crazes, new information about the mechanism of crazing could be obtained which might be valid for polymers in general. An additional objective was to substantiate the chemical mechanism of salt-induced crazing, because the primary cause of craze formation in polyamides is the chemical disruption of hydrogen bonds. It is convenient to divide this chapter so that "physical" and "chemical" aspects can be considered separately.

6.1. The Morphology of Agent-Induced Crazes in
Polyamides

The initial objective was to establish that under certain conditions (the application of certain concentrated salt solutions to stressed polyamides), crazing was a prominent model of failure. From changes in the craze morphology, further information was gained about the conditions which influence crazing.

Various test parameters such as identity and concentration of salt were used. Salts having high stress-crazing activity (lithium, magnesium, zinc and cobalt halides or perchlorates) were extensively used with water and methyl alcohol as solvents. Craze consequential to any of these salt solutions will, in the general sense, be referred to simply as "agent-induced crazes".

When agent-induced crazes in nylons are stabilized by the removal of excess agent or applied stress, examination "in situ" leads to the discovery that they are, like those in polystyrene and polycarbonate, highly elliptical in the surface plane of the test-piece, and the depth of penetration into the specimen was much greater than the breadth of the craze parallel to the principal applied stress. Moreover, the interface between craze matter and bulk, uncrazed polymer was also sharply delineated in crazed nylons. The essential difference between agent-induced crazes in nylons from those in amorphous polymers was found to be one not of type, but rather of scale. (Similarities in morphology are particularly evident with fracture surfaces of polystyrene recently reported by Earl [151].) In nylons, crazes may be larger by an order of magnitude or more and the craze matter can be readily resolved as consisting of filaments separated by voids up to $10\mu\text{m}$ in diameter. Voids in polystyrene rarely exceed $1\mu\text{m}$ in diameter [33,155] and so cannot readily be resolved by optical microscopy.

Large crazes appear to be a consequence of initiation at a small number of sites and of matter near the craze tip being able to undergo high strains without rupture. A

stable craze-bulk polymer interface must be maintained away from the craze tip to avoid degeneration of large crazes by "coalescence" into a uniformly elongated sample indistinguishable from a cold-drawn specimen. The flow behaviour of craze material away from the craze tip may be considerably modified by a change in temperature or level of plasticizer, for example, resulting in rupture before a large craze can form.

It was proposed in Chapter 4 that the stages of craze initiation, development and breakdown are reflected by the fracture surface morphology caused by spontaneous specimen rupture. If appearance is used as a basis for delineating different stages in the craze process, then four distinct steps are involved. The extent to which each of the four regions characteristic of each stage are represented can be used to deduce the mode of failure itself. When test conditions, including type and activity of agent and physical state of the polymer are altered, variations in fracture morphology occur and a number of examples are given in Chapter 4.

The first step in the nylon - "active agent" system (preceeding craze initiation) is the active uptake of agent into the polymer matrix. Energy-dispersive X-ray analysis (Chapter 5.2) revealed that active crazing agents were taken up, even in unstressed nylons, by a "Case II" type [99] mechanism. This is substantiated by morphological evidence, including swelling and the formation of a phase readily distinguishable from unaffected polymer. In the context of

this discussion, it suffices to mention that where agent is abundant (such as at the surface of the specimen where craze initiation occurs) it can be assumed that there is a gross alteration in the mechanical and physical properties of the polymer. The chemical nature of agent-polymer interaction will be referred to later.

In fracture surfaces of nylons with agent induced crazes, the region at the surface where crazes initiate has been designated Region 1. This region is characterized by a swollen, relatively featureless texture, the result of premature rupture of greatly weakened polymer. There was a large variation in the extent to which this region occurred, and it was found that the type and activity of agent, and the conditions under which the test was performed had a profound effect upon not only the initiation of crazes, but also upon subsequent craze processes.

For example, when a low strain rate ($\sim 0.02 \text{ min}^{-1}$) and an agent capable of rapid penetration into the polymer, such as lithium iodide, were used, region 1 can be extensively represented. When more rapid strain rates ($> 0.2 \text{ min}^{-1}$) and less "mobile" agents were used, however, competing failure modes including rapid crack propagation through essentially untreated polymer may occur, pre-empting further agent uptake.

The geometry of the initial craze and also the fissure caused by craze rupture were both found to have a greater influence upon the extent of stable craze growth (and consequently upon the overall mechanical behaviour of the

specimen) than would be suggested by results obtained using single edge notched (S.E.N.) specimens. In the latter specimens, extensive craze growth and fracture often occurred away from the prenotch, when abundant agent was applied. Whilst an analysis of the relationship between notch size and specimen geometry and toughness has not been carried out in nylons, reference can be made to the work of Marshall and Williams [33,115,152,158], Foot and Ward [153], and Doyle [154], when PMMA, polystyrene (PS) and polyethylene terephthalate (PET) were studied.

Williams and Marshall [33] showed that craze initiation and growth were controlled not by the applied stress, but rather by the initial stress intensity factor, K_0 . When fracture toughness was measured as a function of crack velocity [115] or under impact conditions with S.E.N. specimens [152] it was found that the energy absorbed per unit area, w , was dependent upon notch size and not specimen geometry. The stress intensity factor for S.E.N. PMMA was measured at different strain rates and over a range of temperatures, to investigate the adiabatic-isothermal transition proposed to exist at the craze tip [158]. It was found that the value of the critical stress intensity factor, K_C , was rate dependent.

The basic theories for crack and craze initiation evolve from those used for brittle fracture in metals by Griffiths [165] and Inglis [166]. Doyle [154], for example, recognises that the resistance to propagation of a crack is controlled by the sliding of "molecular bundles" in the craze,

a viscous process which makes the Griffiths-Inglis treatment inapplicable. The production of secondary crazes in advance of the craze tip, for example, cannot be explained by "inertial" effects. In contrast, the theories of Van der Boogaart [156] and Andrews and Bevan [157] have evolved from the Griffiths-Inglis treatment. At present it appears necessary to compromise by accepting craze and crack initiation as "brittle" modes of failure, and kinetic craze-crack growth processes as viscous modes. Theories which attempt to explain the fundamental processes of crack and crack initiation in polymers are still evolving.

Although it is not possible to ascertain the exact mechanism of craze initiation from a study of the morphology of the craze, it is apparent that the agent causes gross and rapid modification of the polymer. The effect of stresses acting upon the surface of a test-piece containing inherent flaws, coupled with modification by the agent, is essentially that of high, localised stress concentrations operating at regions of weakened material. Crazing rather than cold-drawing initiates because of localisation of regions particularly susceptible to viscous molecular rearrangement (a material property dependent upon the condition of the specimen) and importantly, because areal craze growth is able to continue with no further molecular slippage or reorientation at the craze-bulk interface. The stress requirements for the second condition can be computed for an isotropic, amorphous polymer more easily than for an isotropic semi-crystalline polymer, but qualitatively it appears that

similar stress conditions are reached for the nylon-salt solution system as for glassy polymers with or without stress-crazing agent, because the geometry and configuration of crazes in both systems are similar.

The agent induced craze growth region (Region 2) in nylons is characterized by having a coarse texture and residual, highly drawn filament peaks or networks. The level of agent present before, during and after the substantiation of the craze were compared for two types of agents by energy-dispersive X-ray analysis; the semiquantitative measurements which were obtained are discussed elsewhere in this chapter.

It was necessary to describe a large range of specimens in Chapter 4 because the morphology of Region 2 changed greatly with experimental conditions. It is emphasized that the mechanism and morphology of crazing is complicated and depends upon the interplay of a number of sometimes subtle processes, making it difficult to predict pragmatically the structural features of a crazed nylon sample resulting from any (arbitrary) test conditions.

Nevertheless, distinctions can be made between the action of Type I and Type II salts from the morphological evidence presented in Chapter 4. With Type II salts, the agent-induced craze region is more extensive, and is often accompanied by a polymer-agent adduct which appears as a separate phase, making it easily distinguishable from the unaffected polymer. The mechanical properties of the adduct differ from that of the polymer alone, and so the interface between the two materials is particularly susceptible to rupture. Fracture may thus proceed along the craze

matter-bulk polymer interface, in a manner akin to rapid fracture in some amorphous polymers (reviewed in Chapter 2), having one surface smooth and denuded.

The fracture of nylons in the presence of Type I salts occurs in a different way. The quite high levels of salt present in Region 2 can rarely be detected by visual inspection because there is no obvious morphological manifestation (such as an adduct). In addition, the craze-bulk polymer interface is stronger and more continuous than for Type I salt-crazed nylons, and consequently rupture may occur preferentially in the highly voided mature craze. This results in a fracture surface with highly drawn craze filaments remaining. Region 2 generally forms to a lesser extent than with Type II agents because of the different mechanism.

When the local concentration of agent at or near the craze tip is insufficient to cause significant reduction of the resistance of the polymer to flow (i.e., when the polymer is no longer plasticized by the agent) a transition to "ductile yielding" (as defined in Chapter 4) occurs. In the absence of agent the stress concentration at the tip of the craze may still promote craze propagation, but the nature of the craze structure will be unlike that observed in Region 2. It is identified as Region 3.

When fracture surfaces of S.E.N. specimens strained in both the absence and presence of agent are compared, it can be deduced that Region 3 represents ruptured fine craze matter which precedes the crack front in untreated polymer.

It seems that at ambient temperature microscopic crazing in polyamides through viscoelastic rearrangement of polymer chains always precedes the crack tip for controlled crack growth conditions.

As the crack velocity increases there may be a transition from "ductile" to "brittle" yielding which is unrelated to agent-induced craze processes and so is not discussed further.

Transmission electron microscopy (T.E.M.) was also used to observe crazing and other deformation modes in nylons. It was found that in addition to the difficulties inherent in specimen preparation and the limitations imposed by using a "two-dimensional technique" to determine the structure of a three-dimensional subject, even faithful replicas revealed little unambiguous information about the fine structure of crazes in polyamides. Secondary effects including the swelling of polymer by the agent, and localised microdrawing of nylons in the absence of agent were found. When high levels of agent were present, it was not possible to obtain advantages in resolution using replication procedures. For these reasons T.E.M. was more valuable as a method by which the dimensions and fine structure of crazes revealed by S.E.M. could be confirmed.

When solvent studies were carried out it was found that:

(a) Solvents behave not merely as passive carriers of salt, but instead actively participate in salt-polymer binding. When a suitable solvent is selected, the polymer

can form more stable mature crazes (for example, when the salt is lithium iodide and solvent is 1,2 dihydroxyethane,) or fracture may ensue so rapidly that viscoelastic deformation is restricted (for example when water or methyl cyanide is used as solvent).

(b) There are size and polarity requirements for solvent with respect to polymer type. In general, small highly polar molecules capable of participating in hydrogen bonding can best penetrate the polyamide matrix. As the binding properties of the solvent molecule are modified by the close proximity of cations (and anions) it is convenient to consider the salt-solvent "cell" as a single entity, especially when a solubility parameter type approach is used. It was found that only solvents capable of being absorbed to greater than 2.0% (w/w) could cause plasticization and consequently stress crazing; this can be related to the type of chemical interactions between polymer and solvent and may be useful in predicting the possibility of agent-induced stress crazing in other polymers.

(c) The levels of solvent present in the polymer before testing, and the relative concentrations of salt and solvent profoundly affect the mechanism, and ultimately the stress requirements for polymer failure.

Energy dispersive X-ray analysis was used to obtain information about (a) the transport of ions in unstressed polyamides, and (b) the relationship between absorbed ion levels and fracture morphology of crazed nylons.

Transport in Unstressed Nylons

It was found that zinc chloride was taken up by unstressed nylon 6 and 66 by a "Case II" transport [100,101] mechanism. The level of agent was high at the surface and remained essentially constant until a sharp interface between salt-absent and salt-present polymer. Whilst the variation in thickness of the zinc-rich zone with absorption time was not measured, it was found that only a very narrow zinc rich zone was produced in unstressed nylons over a time-span several decades longer than that used in tensile testing.

Distribution of Ions in the Fracture Surfaces of Crazed Nylons

When the fracture surfaces of nylons crazed with Type I and II salts were examined by X-ray analysis, additional evidence for differences in the crazing mechanism were obtained. Whilst the overall sequence of events was superficially similar for each salt, it was found that the nature of the interaction between agent and polymer differed from Type I to Type II salts.

Zinc chloride was used as an example of a Type I salt and by analysing a number of fracture surfaces, (some of which were subsequently washed with water) the following pattern emerged. High levels of zinc ions were detected in Regions 1 and 2, both in washed and unwashed specimens, and low levels were detected in Region 3. The zinc had bound to the nylon with solvent-stable bonds (which agreed with the infra-red results of Dunn and Sansom [4] indicating direct cation-carbonyl oxygen binding) in the first two regions;

presumably some agent has carried over into Region 3 subsequent to the creation of fracture surfaces. The level of zinc ions across Region 2 (from Region 1 to Region 3) did not decrease markedly, indicating that under the conditions of short exposure time and relatively high strain rates ($> 0.05 \text{ min}^{-1}$) crazing was only able to occur where high concentrations of zinc were present. The non-reversible binding of zinc to the polymer matrix either prior to or during craze formation and rupture makes it a "static" or "immobile" agent.

The results of analyses of lithium iodide crazed nylons were quite different. Salt levels which were high in both Regions 1 and 2 in the unwashed samples were greatly reduced in washed specimens. Two conclusions which can be made are that the binding of this salt with nylon is reversible and is disrupted by increasing the concentration of solvent and that the agent can more readily leave one polymer matrix region and be carried on to another. As a consequence of rapid transport, the labile agent remains at high levels at or near the craze tip. Salt-solvent is always available to plasticize or facilitate polymer chain flow so that more extensive crazing can occur at lower strains than for Type I agents. Nylons 6 and 66 fracture at both lower stresses and strains with Type II agents than under similar test conditions with Type I agents. The results provided in Chapters 5.1.2.1, 2 indicate that the strain at which fracture occurs is constant and low for Type II salts, and higher (but also constant) for Type I salts, although the fracture

stress changes with water content in the polymer. This suggests that a strain rather than stress criterion exists for crazing and fracture, although it is acknowledged that the method of testing "bulk" polymers would, as outlined in Chapter 3.4.3, inherently give that impression. No measurements have been made of local strains within the treated, or craze zone itself, and so it is only possible to estimate qualitatively the strain existing in the specimen before craze initiation.

6.2. Chemical Mechanism of Salt-Induced Crazing in Polyamides

From the evidence now available it appears that the fundamental process responsible for the alteration in mechanical behaviour of nylons during crazing is the interference with interchain hydrogen bonding. To fully understand the molecular changes which occur and to be able to predict whether polymer modification is going to occur at all, one must know

(a) the chemical and physical properties of the polymer itself,

(b) the mechanism of uptake of one substance (usually with a low molecular weight and size) into another (which has a high molecular weight and in this instance, is a linear polymer),

and (c) the nature of the interactions between low molecular weight substances (or "agent") and polymer which could occur, should the two types of substance be in close proximity.

The approach adopted in this section is to discuss each point separately and then proceed to present a molecular picture of salt-induced crazing in nylons.

6.2.1. Polymer Properties

The first obvious idfference between polyamides and other polymers is that the primary structure comprises polar amide groups capable of inter-chain hydrogen bonding, separated by non-polar, non-hydrogen bonding methylene segments. The chemical and physical properties of polyamides are both dependent upon the spacing of the amide groups, and as indicated in Chapter 2, as the number of methylene groups increases from six, a gradual transition in thermal and other physical properties reflecting lower overall polarity in the polymer can be observed.

The high incidence of hydrogen bonding in nylon 6 and 66 account for the desirable properties of good thermal stability and high tensile strength, making them common engineering thermoplastics. The polymers with larger spacings between amide groups in the chain (nylon 11, nylon 610) have inferior mechanical and thermal properties because of the lower "density" of interchain hydrogen bonds and the inherent higher flexibility of the polymer chain, but absorb lower levels of water and other polar liquids than nylon 6 or 66. The paradox is that the very same hydrogen bonding crosslinks in nylons are responsible for both strong mechanical properties and also the capacity of the nylons to absorb liquids including water and aqueous salt solutions.

Strong polyamides (for example nylon 6) with a high density of hydrogen bond crosslinks are inherently more susceptible to environmental stress crazing than weaker polyamides (for example, nylon 11).

In addition to the primary and secondary structure, there remains to be considered the tertiary or conformational structure of polyamide chains. Much work has been carried out to determine the structure of semicrystalline polymers (for example, by Keller [159,160], Harris [161] and Fischer [162] which emphasize chain folding) and procedures are available for calculating crystalline content and chain spacing parameters. Two-phase models have been used to show the inter-relation of amorphous and crystalline regions, but processes such as dissolution of the crystalline phase are still not understood. Until this handicap is overcome, it will be difficult to devise a dynamic molecular theory which can predict the passage of small molecules through the polymer matrix.

6.2.2. Sorption Mechanisms

Two approaches have found widespread acceptance for describing uptake of small substances into polymer. They are based upon sorption studies and upon "solvent" - polymer compatibility.

Sorption measurements have been carried out extensively for polyamides with either relatively large dye molecules [163,164], or small molecules comparable in size with water (for example [75,133,138]) as penetrants. (The sorption behaviour of nylons towards both types of molecule is of obvious commercial importance.) One of the problems which

always accompanies such studies is the uncertainty of knowing when equilibrium conditions between polymer and penetrant have been reached.

The subject of solvent-polymer compatibility has been reviewed in Chapter 2 but the inclusion of a brief discussion of the work of Van Krevelen [142] and others is justified for two reasons. They attempt to predict solubility parameters for systems in which polar and hydrogen bonding interactions exist, and a new approach is made to assign from the primary structure of the polymer alone, a theoretical solubility parameter value. The latter procedure evolves from the results of Scatchard [167], which showed that there was a linear relationship between the number of carbon atoms and the attraction forces as measured from vapour pressure or heat of vapourization, for a homologous series of hydrocarbons. It was possible to assign values to each group in the "mer" of the polymer and so "molar attraction constants" were tabulated [168]. Van Krevelen has given each group constants for a range of properties. In theory it should be possible to construct a polymer with an arbitrary number of methylene groups, acid groups, amide groups, etc., and from the constants provided, be able to predict a wide variety of physical and thermal properties for that polymer.

The solubility parameters of polar solvents and polar polymers are both large and the absolute difference between the parameter values is often sufficient to make the enthalpy of mixing large and positive (i.e. unfavorable). Van Krevelen considers that there is an additional negative enthalpy contribution brought about by polar attractive

forces which overcomes the unsatisfactory adhesive energy factors. The specificity of highly polar polymers (including polyamides) towards solvents is a direct consequence of the favorable polar attraction requirement.

The specificity which polyamides show towards particular salt solutions may superficially be accepted as agreeing with the rationale given above. If it is accepted that lithium cations merely modify the properties of solvent [86] then it follows that the polar attractive forces between the lithium ligands (water) and the amide moiety of the polyamide are now sufficiently strong to give a negative free energy of mixing. Partial dissolution into the polymer, and reduction of interamide crosslinks can occur causing plasticisation. Water molecules have a somewhat different role when participating in Type I agent modification of polymer, but similar reasoning can be applied.

The concept is not without flaws, however. It is difficult to explain the specificity which polyamides show towards some salts. For example, it is surprising that cupric chloride should be a much weaker stress crazing agent than zinc chloride, when the charge density of each cation is not greatly different. Certainly coordination and other more subtle requirements must be taken into account when predicting binding strengths, modification of solvent molecules and ultimately stress crazing activity.

There also appears to be a limitation to the procedure of dissecting polymer molecules and then attributing properties using the collective sum of the component group values.

For example, nylon 6 and 66 should by this procedure, have identical thermal and mechanical behaviour, but instead nylon 6 has a lower melting point, tensile modulus and is more susceptible to environmental stress crazing than nylon 66. Van Krevelen's concepts could benefit by making allowance for the position of each group in the polymer chain, relative to its neighbour.

6.2.3. Salt-Solvent-Polymer Interactions

The chemical interactions which have been observed between salts, solvents and polymers have been reviewed in Chapter 2 and it was concluded that there are principally two types of salt interaction with the amide oxygen involving solvent participation to a greater or lesser degree [4]. Whilst the bonds between cation, solvent and polyamide can be identified by infra-red and nuclear magnetic resonance spectroscopy, no intensive study has been made of the interrelation of polymer conformation (except to show how cis and trans geometries can be accommodated by the binding mechanism proposed) and salt/solvent concentration.

The physical picture of polar polymer chains surrounded by ions and small molecules has not been considered by materials scientists; the attention of workers in the natural sciences has centred upon a variation of this system and consequently a high level of understanding has now been reached. The biopolymer (protein, nucleic acid, etc.) salt-water system is one of fundamental biological importance, and is analogous to the polyamide salt-solvent system under discussion because both classes of polymers contain highly

polar, hydrogen bonding groups separated by non-hydrogen bonding groups of low polarity. It is convenient to designate the first type of groups hydrophilic and the second hydrophobic.

Whilst it is acknowledged that the primary structure of synthetic polyamides differs from that of biopolymers such as proteins, for example, and although the physical constraints of solid state polyamide contrast with the mobility of biopolymers in solution, it is nevertheless valid to apply the arguments of one system to the other. The review of Lewin [146] summarises the current level of understanding in biological systems, and some of the information relevant to polyamides is given below.

The distribution of non-polar or hydrophobic groups are considered of great significance in determining the tertiary structure of the biopolymer. The area of contact between water and hydrophobic regions is minimized by the polymer chain undergoing conformational changes; hydrophobic-hydrophobic and hydrophilic-hydrophilic interactions are maximized. For water molecules to associate with hydrophilic chain segments in solution, interchain hydrophilic interactions must be overcome. This is analogous to the binding of polar agent with amide groups in nylons requiring breakage of interamide bonds as a precursor step. When hydrophobic groups are adjacent to hydrophilic groups in the polymer chain, repulsions between water and the hydrophobic centre need to be overcome for polymer-water binding to occur. Solvent-polymer interactions can only be predicted

by the summation of binding energies between hydrophilic groups, hydrophobic groups, and water molecules.

With electrolytes present, a variety of ion-solvent entities may be formed, depending upon concentration, ionic strength, etc. Lewin gives examples of hydrated ion pairs with water molecules bridging chain carbonyl groups - an arrangement possible in polyamide-salt solution systems. The conformation of the polymer chains which optimises hydrophilic-hydrophilic attractive forces may not be suitable for solvent or salt binding, particularly if the conformation adopted causes hydrophobic centres to be exposed to the solvent.

Steric factors which can be important in polymer solutions are predicted to be even more significant in solid polyamides. For sorption into, or transport of molecules through the polymer matrix there appears [95,133] to be a correlation between the molecular dimensions of the invading species and the dimensions and distribution of voids in the polymer. The nature of such voids in amorphous regions of the polymer is poorly understood.

From the results obtained with biopolymers, and from evidence cited elsewhere, a possible mechanism of agent uptake must satisfy the following requirements.

(a) The salt-solvent system must be compatible with the polyamide. The sum of polar and hydrogen bonding attractions between the polymer and the solution must make the energy of mixing favorable.

(b) The agent must be able to penetrate the polymer and so there are steric requirements. The polymer must have voids or be able to produce voids which can accommodate the invading species. This requirement appears to be met (from evidence which slows active transport in unstressed films). The nature of voids in amorphous regions is not fully understood.

(c) Interchain forces in the polymer, in particular interamide hydrogen bonding, must be modified or broken for agent-polymer association. In addition, formation of agent-polymer bonds must be energetically favorable. It appears that cation-water-polyamide bonds are reversible whereas water-cation-polyamide bonds are irreversible. The energy of binding for each category may differ, but is presumably sufficiently great to disrupt interchain hydrogen bonding.

(d) For crazing to result from agent association with polymer, polymer flow must be facilitated. The degree to which polymer segments can flow under a given stress will depend upon the degree to which interchain forces remain, and to temperature conditions.

CHAPTER 7.SUGGESTIONS FOR FURTHER WORK.

There were a number of questions posed during this work, for which the investigation of any one would justify extensive research.

Despite the reservations outlined in the study, it is accepted that some information could be obtained by using a fracture mechanics approach. The results obtained with nylons could be compared with those already known for glassy polymers, and variations to the existing theories of craze and crack propagation could be determined.

A more intensive study of the fundamental forces between polyamides, salts, and solvent is necessary before an understanding comparable with that existing for biological systems is reached. One of the first steps could be to examine the kinetic aspects of salt-polyamide interaction with various solvent levels.

There remains much scope in developing theories related to the solubility parameter approach. It should be emphasized, however, that compatibility between polar, hydrogen-bonding solvents and polymers is unlikely to ever be reliably predicted unless new attractive parameters are established. The polyamide-salt solution system may be a potential vehicle for which an improved theory could be based, particularly if fine distinctions between various salt-modified solvents can be measured accurately.

It was proposed in Chapter 6 that certain polyamides will, because of their hydrogen bond content, be inherently susceptible to environmental stress crazing and cracking.

Other polar polymers, both semi-crystalline and amorphous, should be examined for stress-crazing resistance against polar, secondary bond modifiers and ultimately an attempt should be made towards engineering polymers so that they can cope with any hostile environment.

Bibliography

- [1]. Gent, A.N., J. Materials Sci., 5, 925 (1970).
- [2]. Gent, A.N., J. Macromol. Sci.-Phys., B8, 597 (1973).
- [3]. Dunn, P. and Sansom, G.P., J. Appl. Polymer Sci., 13, 1641 (1969).
- [4]. Dunn, P. and Sansom, G.F., J. Appl. Polymer Sci., 13, 1657 (1969).
- [5]. Dunn, P. and Sansom, G.F., J. Appl. Polymer Sci., 13, 1673 (1969).
- [6]. Dunn, P. and Sansom, G.F., J. Appl. Polymer Sci., 14, 1799 (1970).
- [7]. Kambour, R.P. and Robertson, R.E., "The Mechanical Properties of Plastics," in Polymer Science, a Materials Science Handbook, A.D. Jenkins, ed., North Holland Publishing Company, Amsterdam, Chapt. 11., p 803 (1972).
- [8]. Haward, R.N., Int. Symp. Phys. of Non-Cryst. Solids, Sheffield, Sept. (1970).
- [8a]. Haward, R.N. and Owen, D.R.J., J. Materials Sci., 8, 1136 (1973).
- [9]. Andrews, E.H. and Bevan, L., Polymer, 13, 337 (1972).
- [10]. Bueche, F., "Physical Properties of Polymers," Interscience, New York, (1962).
- [11]. Sternstein, S.S. and Ongchin, L., Polymer Preprints, Am. Chem. Soc., Div. Polymer Chem., 10, 1117 (1969).
- [12]. Bowden, P.B. and Oxborough, R.J., "A Critical Strain Criterion for Craze Formation in Polystyrene," from meeting of the British Plastics Inst.; "The Role of Craze in Fracture," Univ. of Liverpool, Liverpool, England (1972).
- [13]. Knight, A.C., J. Polymer Sci., A, 3, 1845 (1965).
- [14]. Knight, A.C., Polymer Eng. Sci., 14, 687 (1974).
- [15]. Matsuo, M., Wang, T.T. and Kwei, T.K., J. Polymer Sci., A-2, 10, 1085 (1972).
- [16]. Wang, T.T., Matsuo, M. and Kwei, T.K., J. Appl. Phys., 42, 4188 (1971).
- [17]. Kambour, R.P., Polymer, 5, 143 (1964).
- [18]. Doyle, M.J., J. Materials Sci., 8, 1185 (1973).
- [19]. Kambour, R.P. and Holik, A.S., J. Polymer Sci., A-2 7, 1393 (1969).

- [20]. Regel, V.R., J. Tech. Phys. (U.S.S.R.) 26, 359 (1956).
[Eng. Trans; Tech. Phys. (U.S.S.R.), 1 353 (1956-57)].
- [21]. Higuchi, M., Proc. First. Int. Conf. Fract., Sendai,
Japan, Vol. 2., 1211 (1966).
- [22]. Sternstein, S.S. and Sims, K.J., Polymer Preprints,
Am. Chem. Soc., Div. Polymer Chem., 5 (2), 422 (1964).
- [23]. Kastelic, J.R. and Baer, E., J. Macromol. Sci.-Phys.,
B7, 679 (1973).
- [24]. Murray, J. and Hull, D., Polymer, 10, 451 (1969).
- [25]. Murray, J. and Hull, D., J. Polymer Sci., A-2, 8, 583
(1970).
- [26]. Murray, J. and Hull, D., J. Polymer Sci., A-2, 8, 1521
(1970).
- [27]. Murray, J. and Hull, D., J. Materials Sci., 8,
- [28]. Kambour, R.P., Appl. Polymer Symp., 7, 215 (1968).
- [29]. Kambour, R.P. and Kopp, R.W., J. Polymer Sci., A-2, 7,
183 (1969).
- [30]. Natarajan, R. and Reed, P.E., J. Polymer Sci., A-2, 10,
585 (1972).
- [31]. Rabinowitz, S. and Beardmore, P., C.R.C. Critical
Reviews in Macromolecular Science, 1, 1 (1972).
- [32]. Murray, J. and Hull, D., J. Materials Sci., 6, 1277 (1971).
- [33]. Marshall, G.P., Culver, L.E. and Williams, J.G., Proc.
Roy. Soc., London, A319, 165 (1970).
- [34]. Burdekin, F.M. and Stone, D.E.W., J. Strain. Analysis
1, 145 (1966).
- [35]. Berry, J.P., J. Polymer Sci., 50, 107, 313 (1961).
- [36]. Rivlin, R.S. and Thomas, A.G., J. Polymer Sci., 10,
291 (1953).
- [37]. Beardmore, P. and Johnson, T.L., Phil. Mag., 23, 1119
(1971).
- [38]. Cessna, L.C., Jr. and Sternstein, S.S., in "Fundamental
Phenomena in the Materials Sciences," Vol. 4 (1966),
45, Plenum Press, New York (1967).
- [39]. Graham, I.D., Marshall, G.P. and Williams, J.G.,
"The Fracture Mechanics of Crazes," paper presented
at Int. Conf. Dynamic Crack Propagation, Lehigh
Univ., (July 1972).
- [40]. Kambour, R.P., J. Polymer Sci., A-2, 4, 349 (1966).

- [41]. Bevis, M. and Hull, D., J. Materials Sci., 5, 983 (1970).
- [42]. Kireenko, O. Ph., Marichin, V.A. and Miasnikova, L.P.,
Seventh Int. Congress of E.M., Grenoble, 369 (1970).
- [43]. Thomas, D.P. and Hagan, R.S., Polymer Eng. Sci., 9,
164 (1969).
- [44]. Kambour, R.P., Polymer Eng. Sci., 8, 281 (1968).
- [45]. Murray, J. and Hull, D., J. Polymer Sci., B, 8, 159 (1970).
- [46]. Berry, J.P., Nature, 185, 91 (1960).
- [47]. Legrand, D.G., Kambour, R.P. and Haaf, W.R., J. Polymer
Sci., A-2, 10, 1565 (1972).
- [48]. Kambour, R.P., J. Polymer Sci., A, 3, 1713 (1965).
- [49]. Berry, J.P., in "Fracture Processes in Polymeric Solids",
B. Rosen, ed., Interscience, New York, Chapt.II, (1964).
- [50]. Bird, R.J., Mann, J., Pogany, G. and Rooney, G.,
Polymer, 7, 307 (1966).
- [51]. Haward, R.N. and Brough, I., Polymer, 10, 724 (1969).
- [52]. Bird, R.J., Rooney, G. and Mann, J., Polymer, 12, 742
(1971).
- [53]. Kambour, R.P., J. Polymer Sci., A-2, 4, 17 (1966).
- [54]. Beardmore, P., Phil. Mag., 19, 389 (1969).
- [55]. Kambour, R.P., "A Review of Crazing and Fracture in
Thermoplastics," G.E. Report, No. 72 CRD285 (1972).
- [56]. Sauer, J.A., Marin, J. and Hsiao, C.C., J. Appl. Phys.,
20, 507 (1949).
- [57]. Hsiao, C.C., and Sauer, J.A., J. Appl. Phys., 21, 1071
(1950).
- [58]. Bernier, A.G. and Kambour, R.P., Macromolecules, 1,
393 (1968).
- [59]. Spurr, O.K., Jr. and Niegisch, W.D., J. Appl. Polymer
Sci., 6, 585 (1962).
- [60]. Bessonov, M.I. and Kurshinskii, E.V., Soviet Phys.
Solid State, 3, 950 (1961).
- [61]. Kambour, R.P. and Russell, R.R., Polymer, 12, 237 (1971).
- [62]. Beahan, P., Bevis, M. and Hull, D., Phil. Mag., 24, 1267
(1971).
- [63]. Kambour, R.P., J. Polymer Sci., A, 2, 4159 (1964).

- [64]. Beahan, P., Bevis, M. and Hull, D., J. Materials Sci., 8, 162 (1972).
- [65]. Rehage, G. and Goldback, G., Angew. Makromol. Chem., 1, 125 (1967).
- [66]. Newman, S.B. and Wolock, I., J. Res. Natl. Bur. Stds. 58, (6), 339, (1957).
- [67]. Beardmore, P. and Rabinowitz, S., J. Materials Sci., 6, 80 (1971).
- [68]. Marsh, D.M., "Fracture of Solids," Interscience, New York, p.119 (1963).
- [69]. Bannerman, D.G. and Magat, E.E., "Polyamides and Polyesters," L.E. Schildknecht, ed., "Polymer Processes", Chapt. VII, Interscience, New York (1956).
- [70]. Pauling, L. and Corey, R.B., Proc. Intern. Wool. Textile Research Conf., B. 249 (1955).
- [71]. Bamford, C.H., Elliott, A. and Hanby, W.E., "Polypeptides," Academic Press, New York (1956).
- [72]. Hildebrand, J. and Scott, R.L., "The Solubility of Non-Electrolytes," 3rd ed., Reinhold Publishing Corp., New York, pp.129, 427. (1949).
- [73]. Hansen, C.M., J. Paint Technology, 39, 104 (1967).
- [74]. Hansen, C.M., J. Paint Technology, 39, 505 (1967).
- [75]. Puffr, R. and Sebenda, J., J. Polymer Sci., C, 16, 79 (1967).
- [76]. Weiske, C.D., Kunststoffe, 54, 626 (1964).
- [77]. Lindquist, I., "Inorganic Adduct Molecules of Oxo-Compounds," Springer-Verlag O.H.G., Berlin (1963).
- [78]. Penland, R.B., Mizushima, S., Curran, C. and Quagliano, J.V., J. Am. Chem. Soc., 79, 1575 (1957).
- [79]. Diorio, A.F., Lippincott, E. and Mandelkern, L., Nature, 195, 1296 (1962).
- [80]. Bello, J. and Bello, H.R., Nature, 194, 682 (1962).
- [81]. Bello, J., Haas, D. and Bello, H.R., Biochemistry, 5, 2539 (1966).
- [82]. Robinson, D.R. and Jencks, W.P., J. Am. Chem. Soc., 87, 2462, 2470 (1965).
- [83]. Balasubramanian, D. and Shaikh, R., Biopolymers, 12, 1639 (1973).
- [84]. Klotz, I.M. and Franzen, J.S., J. Am. Chem. Soc., 84, 3461 (1962).

- [85]. Bull, W.E., Madan, S.K. and Willis, J.E., J. Inorg. Chem. 2, 303 (1963).
- [86]. Kurtz, J. and Harrington, W.F., J. Mol. Biol., 17, 440 (1966).
- [87]. Lotan, N., J. Phys. Chem., 77, 242 (1973).
- [88]. Hamoud, M.R., Vert, M. and Selegny, E., J. Polymer Sci., B, 10, 361 (1972).
- [89]. Hamoud, M.R., Vert, M. and Selegny, E., J. Polymer Sci., Polymer Chem. ed., 12, 851 (1974).
- [90]. Valenti, B., Bianchi, E., Greppi, G., Tealdi, A. and Ciferri, A., J. Phys. Chem., 77, 389 (1973).
- [91]. Bianchi, E., Ciferri, A., Tealdi, A., Torre, R. and Valenti, B., Macromolecules, 7, 495 (1974).
- [92]. Ciferri, A., Bianchi, E., Marchese, F. and Tealdi, A., Makromol. Chem., 150, 265 (1971).
- [93]. Kaplan, M.L. and Kelleher, P.G., Polymer Lett. 9, 561 (1971).
- [94]. Kargin, V.A., Sogolova, T.I., Rapoport, N. Ya., Vorotnikova, V.A. and Slovokhotova, N.A., Polymer Sci. U.S.S.R. (English Trans.), 13, 1998 (1971).
- [95]. Addy, J.K. and Andrews, R.D., Macromolecules, 6, 791 (1973).
- [96]. Andrews, R.D., Proc. of Second Int. Conf. on Yield, Deformation and Fracture of Polymers, Cambridge, (March 1973).
- [97]. Sarda, G. and Peacock, N., Nature, 200, 67 (1963).
- [98]. Crank, J. and Park, G.S., "Diffusion in Polymers," Academic Press, London and New York, (1968).
- [99]. Hopfenberg, H.B. and Stannett, V., "The Physics of Glassy Polymers," Chapt. 9, Haward, R.N. ed. Applied Science Publishers, London (1973).
- [100]. Alfrey, T., Chem. and Eng. News, 43, 64 (1965).
- [101]. Frisch, H.L., J. Polymer Sci., B, 3, 13 (1965).
- [102]. Olf, H.G. and Peterlin, A., J. Polymer Sci., Polymer Phys. ed., 12, 2209 (1974).
- [103]. Hopfenberg, H.B. and Frisch, H.L., J. Polymer Sci., B, 7, 405 (1969).
- [104]. Peterlin, A., Makromol. Chemie, 124, 136 (1969).

- [105]. Robertson, R.E., J. Phys. Chem., 69, 1575 (1965).
- [106]. Nielsen, L.E., J. Polymer Sci., 27, 1 (1959).
- [107]. Rosen, B.J., J. Polymer Sci., 49, 177 (1961).
- [108]. Karasz, F.E. and Kambour, R.P., J. Polymer Sci.,
A-2, 4, 327 (1966).
- [109]. Miller, G.W., Visser, S.A.D. and Morecraft, A.S.,
Polymer Eng. Sci., 11, 73 (1971).
- [110]. Vincent, P.I. and Raha, S., Polymer, 13, 283 (1972).
- [111]. Henry, L.F., Polymer Eng. Sci., 14, 167 (1974).
- [112]. Andrews, E.H. and Bevan, L., Polymer, 13, 337 (1972).
- [113]. Andrews, E.H.; Levy, G.M. and Willis, J., J. Materials
Sci., 8, 1000 (1973).
- [114]. Andrews, E.H. and Levy, G.M., Polymer, 15, 599 (1974).
- [115]. Marshall, P.G., Culver, L.E. and Williams, J.G.,
Plastics and Polymers, April 1970, 75.
- [116]. Narisawa, I., J. Polymer Sci., A-2, 10, 1789 (1972).
- [117]. Miller, R.L., Enc. Polymer Sci. and Tech., 4, 449,
Interscience Publishers, New York (1966).
- [118]. Bennewitz, R., Faserforsch. Textiltech., 5, 155 (1954).
- [119]. Taylor, G.B., J. Am. Chem. Soc., 69, 635 (1947).
- [120]. Mark, H., Der Feste Körper, Leipzig (1938).
- [121]. Houwink, R., J. Prakt. Chem., 157, 15 (1940).
- [122]. Geil, P.H., "Polymer Single Crystals," Interscience,
New York, P.69 (1963).
- [123]. Way, J.L., Atkinson, J.R. and Nutting, J., J. Materials
Sci., 9, 293 (1974).
- [124]. Breedon, J.E., Jackson, J.F., Marcinkowski, M.J. and
Taylor, M.E., Jr., J. Materials Sci., 8, 1071 (1973).
- [125]. Grubb, D.T. and Keller, A., J. Materials Sci., 7, 822
(1972).
- [126]. Johari, O., Research/Development, 25, 16 (1974).
- [127]. Hull, D., and Owen, T.W., J. Polymer Sci., Polymer
Phys. ed., 11, 2039 (1973).
- [128]. Mann, J., Chem. and Ind., p.643 (1966).

- [129]. Haward, R.N., Br. Polymer. J., 4, 159 (1972).
- [130]. Pelloux, R.M.N., Metals Eng. Quart., p.26 (Nov. 1965).
- [131]. Boukal, I., J. Applied Polymer Sci., 11, 1483 (1967).
- [132]. Starkweather, H.W., Jr., J. Macromol. Sci.-Phys., B-3,
727 (1969).
- [133]. Skirrow, G. and Young, K.R., Polymer, 15, 771 (1974).
- [134]. Peters, H.W. and Turner, J.C., J. Soc. Dyers Colour,
74, 252 (1958).
- [135]. Trifan, D.S. and Terenzi, J.F., J. Polymer Sci.,
Polymer Letters ed., 28, 443 (1958).
- [136]. Barmby, D.S. and King, G., Proc. Int. Tax. Res. Conf.
(Australia), B-139 (1955).
- [137]. Starkweather, H.W., Jr., J. Applied Polymer Sci.,
2, 129 (1959).
- [138]. Kawasaki, K. and Sekita, Y., J. Polymer Sci., A, 2,
2437 (1964).
- [139]. Kolarik, J. and Janacek, J., J. Polymer Sci., C16,
441 (1967).
- [140]. Miyasaka, K. and Ishikawa, K., J. Polymer Sci., A-2,
6, 1317 (1968).
- [141]. Starkweather, H.W., Jr., Moore, G.E., Hansen, J.E.,
Roder, T.M., and Brooks, R.E., J. Polymer Sci.,
21, 189 (1956).
- [142]. Van Krevelen, D.W. and Hoftyzer, P.J., "Properties
of Polymers, Correlations with Chemical
Structure", Elsevier Publishing Co.,
Amsterdam, Chapt. 8 (1972).
- [143]. Cornes, P.L. and Haward, R.N., Polymer, 15, 149 (1974).
- [144]. Marshall, G.P., Culver, L.E. and Williams, L.E.,
Plastics and Polymers, Feb. 1969, 75.
- [145]. Lasoski, S.W., Jr. and Cobbs, W.H., Jr., J. Polymer
Sci., 36, 21 (1959).
- [146]. Lewin, S., "Displacement of Water and its Control
of Biochemical Reactions", Academic Press,
London and New York, 1974.
- [147]. Schaeffgen, J.R. and Trivisonno, C.F., J. Am. Chem.
Soc., 73, 4580 (1951).

- [148]. Schaeffgen, J.R. and Trivisonno, C.F., J. Am. Chem. Soc., 74, 2715 (1952).
- [149]. Saunders, P.R., J. Polymer Sci., 57, 131 (1962).
- [150]. "Handbook of Chemistry and Physics", The Chemical Rubber Co., 47th ed., 1966.
- [151]. Earl, B.L., Loneragan, R.J., Markham, J. and Crook, M., J. Applied Polymer Sci., 18, 245 (1974).
- [152]. Marshall, G.P., Williams, J.G. and Turner, C.E., J. Materials Sci., 8, 949 (1973).
- [153]. Foot, J.S. and Ward, I.M., J. Materials Sci., 7, 367 (1972).
- [154]. Doyle, M.J., Maranci, A., Orowan, E. and Stork, S.T., Proc. R. Soc. Lond. A. 329, 137 (1972).
- [155]. Zhurkov, S.N., Kuksenko, V.S. and Slutsker, A.I., Proc. 2nd Int. Conf. on Fracture, Brighton, 531 (1969).
- [156]. Van der Boogaart, A. and Turner, C.E., Trans. J. Plastics Inst., 31, 109 (1963).
- [157]. Andrews, F.H. and Bevan, L., Inst. Phys. Conf., Oxford, Sept. 1966.
- [158]. Marshall, G.P., Coutts, L.H. and Williams, J.G., J. Materials Sci., 9, 1409 (1974).
- [159]. Keller, A., J. Polymer Sci., 36, 361 (1959).
- [160]. Dreyfuss, P. and Keller, A., J. Macromol. Sci.-Phys., B4, 811 (1970).
- [161]. Cannon, C.G. and Harris, P.H., J. Macromol. Sci.-Phys., B3, 357 (1969).
- [162]. Fischer, E.W., Pure Appl. Chem., 31, 113 (1972).
- [163]. Chantrey, G. and Rattee, I.D., J. Applied Polymer Sci., 18, 93 (1974).
- [164]. Chantrey, G. and Rattee, I.D., J. Applied Polymer Sci., 18, 105 (1974).
- [165]. Griffiths, A.A., Phil. Trans. Roy. Soc. Lond., A221, 143 (1921).
- [166]. Inglis, C.E., Trans. Instn. Nav. Archit., Lond., 55, 219 (1913).
- [167]. Scatchard, G., Chem. Rev., 44, 7 (1949).
- [168]. Small, P.A., J. Appl. Chem., 3, 71 (1953).